How *Pseudomonas aeruginosa* adaptations during chronic Cystic Fibrosis lung infections modulate host-microbe interactions

Lisa C. Hennemann

Department of Microbiology & Immunology

McGill University, Montreal

January 2023

A thesis submitted to McGill University in partial fulfillment

of the requirements for the degree of Doctor of Philosophy

Abstract

Chronic *Pseudomonas aeruginosa* (*P.a.*) lung infections occur in over 50% of adult Cystic Fibrosis (CF) patients and are associated with excessive lung inflammation and accelerated lung function decline. Once it has established chronic infections, *P.a.* evolves within the host over time and shows evidence of both genotypic and phenotypic adaptations to the CF lung. While virulence factors may play an important role in early infection stages, many factors appear dispensable during chronic infection, where *P.a.* isolates commonly become deficient in virulence factor production. Surprisingly, infections with LasR-deficient mutants have been associated with worse patient outcomes. While *P.a.* is traditionally considered an extracellular pathogen, a number of past studies suggest that *P.a.* can invade different epithelial cell types. Although the implications of intracellular *P.a.* to infection pathogenesis remain unclear, recent findings from the Nguyen lab demonstrate the presence of intracellular *P.a.* within airway epithelial cells (AEC) of lung explants, suggesting a potential bacterial reservoir inside the airway epithelium. Here, we sought to characterize how *P.a.* adaptations modulate host-microbe interactions and potentially contribute to the pathogenesis of CF lung infections. We hypothesized that phenotypic adaptations commonly observed in *P.a.* isolates from chronic CF infections, namely loss of LasR and Type 3 secretion system (T3SS) function, contribute to CF lung disease by causing deleterious neutrophilic inflammation and by promoting intracellular *P.a.* survival, respectively.

In chapter 2, we studied how the loss of LasR function alters the expression of ICAM-1 and neutrophil adhesion in AEC. Our findings suggest that ICAM-1 expression and neutrophil adhesion are increased in AEC-stimulated with *lasR* mutant filtrates *in vitro*, a process likely attributable to the loss of LasR-dependent secreted proteolytic activity. We further demonstrated that multiple LasR-regulated proteases are capable of degrading ICAM-1. In a subacute *P.a.* murine infection model, we observed an increased airway epithelial ICAM-1 expression and enhanced neutrophilic lung inflammation in *lasR* mutant-infected mice compared to wild-type *P.a.* infected ones.

In the third chapter, we developed a model of long-term intracellular *P.a.* infection within AEC to investigate the ability of different *P.a.* strains to survive intracellularly within AEC. We optimized experimental parameters such as the multiplicity of infection, time points and tobramycin maintenance concentration to allow for intracellular *P.a.* survival for up to 120h. We showed that four clinical CF isolates displayed significant heterogeneity in their ability to

survive intracellularly: the isolate with the highest intracellular survival was non-cytotoxic, while the other isolates caused varying degrees of cytotoxicity.

In our fourth chapter, we sought to investigate the mechanisms underlying the heterogeneity in intracellular survival among CF isolates. We first tested 28 clinical isolates for their intracellular survival within AEC and cytotoxicity induction and found a strong inverse correlation between the two. Given that the T3SS is a major cause of cytotoxicity, we also characterized T3SS secretion and observed that T3SS-deficient clinical isolates were associated with high intracellular survival and low cytotoxicity. We then demonstrated that intracellular survival of T3SS-positive isolates increased significantly when the transcriptional activator ExsA or parts of the T3SS injectisome machinery were knocked out.

In conclusion, we demonstrated how two adaptations commonly observed in chronic CF infection isolates may exacerbate lung inflammation and facilitate the establishment of an intracellular bacterial reservoir inside AEC, respectively. These altered *P.a.*-host interactions may have significant implications for the pathogenesis of chronic *P.a.* infections in the setting of CF lung disease.

Résumé

Des infections pulmonaires chroniques au *Pseudomonas aeruginosa* (*P.a.*) surviennent chez plus de 50 % des patients adultes atteints de fibrose kystique (FK). Elles sont associées à une inflammation pulmonaire excessive, un déclin accéléré de la fonction pulmonaire ainsi qu'une mortalité accrue. Une fois établies comme des infections chroniques qui sont presqu'impossibles à éradiquer, *P.a.* évolue au sein de l'hôte au fil du temps et fait preuve d'adaptations génotypiques et phénotypiques au sein du poumon FK. Les isolats *P.a.* provenant d'infections FK chroniques sont généralement déficients en la production de facteurs de virulence tels que les protéases régulées par LasR et le système de sécrétion de type 3 (T3SS). Étonnamment, les infections par des mutants déficients en LasR ont été associés à une moins bonne santé pulmonaire chez les patients. Malgré que *P.a.* est traditionnellement considéré comme un pathogène extracellulaire, des études antérieures suggèrent que qu'il peut envahir différents types de cellules épithéliales. Des études récentes du laboratoire Nguyen démontrent la présence de *P.a.* intracellulaire dans les cellules épithéliales des voies respiratoires (EVR) d'explants pulmonaires récupérés chez des patients FK en voie des transplantations pulmonaires, suggérant un réservoir bactérien potentiel à l'intérieur de l'épithélium des voies respiratoires. Pour cette thèse, nous avons cherché à caractériser l'impact des adaptations de *P.a.* couramment observées durant les infections chroniques en FK sur interactions hôte-microbe et leur contribution potentielle à la pathogenèse des infections pulmonaires dans le contexte de la FK.

Dans le chapitre 2, nous avons étudié comment la perte de la fonction LasR modifie l'expression d'ICAM-1 et l'adhésion des neutrophiles aux cellules EVR. Nos résultats suggèrent que l'expression d'ICAM-1 et l'adhésion des neutrophiles sont augmentées dans les cellules EVR stimulées avec des filtrats de *P.a.* mutants *lasR in vitro*, un processus lié à la perte d'activité protéolytique sécrétée qui est dépendante de LasR. Nous avons démontré que plusieurs protéases régulées par LasR sont capables de dégrader ICAM-1 et que leurs contributions individuelles peuvent dépendre de la souche *P.a.* Dans un modèle d'infection murin subaiguë au *P.a*, nous avons observé une expression accrue d'ICAM-1 dans les EVR et une inflammation pulmonaire neutrophile accrue chez les souris infectées par le mutant *lasR* comparées à cellules infectées par *P.a.* de type sauvage.

En utilisant le modèle de survie long terme intracellulaire développé au chapitre 3, dans notre quatrième chapitre, nous avons cherché à étudier les mécanismes sous-jacents à l'hétérogénéité

de la survie intracellulaire parmi les isolats clinique *P.a.* provenant des infections FK. Nous avons d'abord testé 28 isolats cliniques pour la survie intracellulaire et la cytotoxicité dans les cellules EVR, et avons trouvé une forte corrélation inverse entre les deux. Étant donné que le T3SS est une cause majeure de cytotoxicité, nous avons également caractérisé la sécrétion de T3SS et observé que les isolats cliniques déficients en T3SS étaient associés à une survie intracellulaire élevée ainsi qu'une faible cytotoxicité. Nous avons ensuite démontré que la survie intracellulaire des isolats positifs pour le T3SS augmentait de manière significative lorsque l'activateur transcriptionnel ExsA ou des parties de la machinerie d'injection T3SS étaient délétés.

En conclusion, nous avons démontré comment deux adaptations couramment observées dans les isolats d'infection chronique peuvent exacerber l'inflammation pulmonaire et faciliter l'établissement d'un réservoir bactérien intracellulaire à l'intérieur de l'EVR, respectivement. Ces interactions *P.a.*-hôte modifiées peuvent avoir des implications importantes pour la pathogenèse des infections chroniques à *P.a.* dans le cadre de la maladie pulmonaire FK.

Acknowledgements

First and foremost, I would like to thank my supervisor Dr. Dao Nguyen for welcoming me into her lab and providing me with such a wonderful opportunity. Thank you for helping me become the independent, critically thinking scientist that I am today and teaching me so many things along the way. I have always appreciated our scientific discussions, your great effort to help me deliver the highest quality work I possibly could and your continued support.

I would further like to thank all Nguyen lab members, past and present, for their help, the fun lab outings and overall supportive and collaborative environment. I would particularly like to thank our lab manager Dr. Geoffrey McKay, a never-ending source of knowledge and wisdom on all things lab-related or not. Thank you for all of your help over the last 5+ years, for your life advice and fun anecdotes, like the time you met Kiefer Sutherland! I would further like to thank everyone who has worked with me on the T3SS and ICAM projects over the years, particularly Dr. Karim Malet, who always spread joy and positive energy in the lab whenever he was around! It was a pleasure supervising multiple undergrads over the years and I would particularly like to highlight my first two undergrads Cedric and Elizabeth, who both left the lab some time ago, but have remained great friends. I enjoyed getting to teach and work with you and enjoyed witnessing your passion for science! To everyone else in the Nguyen lab, particularly Eszter and Jackie, I will miss our Friday afternoon chats and brunches. I hope you manage to add many more memorable quotes to the wall of fame!

I would like to thank my advisory committee members Drs. Simon Rousseau and Marcel Behr for their invaluable advice over the years. Simon, thank you for always being so supportive and positive, your great enthusiasm has always been inspiring. Marcel, I know you might have mostly been there for the annual German Christmas cookies, but you have been a great source of advice and your challenging questions have always pushed me to want to learn more and do better.

To my German support system, Eva and Jannik: thank you for always being such great friends, your friendship felt like a piece of home and made it a lot easier to be away from Germany for so long! Thank you to all of my friends from back home who have kept in touch with me over the years despite the distance and for trying your best to come visit me in Montreal!

To Inga, Severine and all the SPiRE members over the years, I really enjoyed planning parties and organizing little events with you, I hope you manage to go back to the events we used to have before COVID!

Thank you to my partner Jaryd, who has always been a calm, steady presence when research (or life) threw me a curveball. Thank you for always being so kind and incredibly supportive, even when I had to drop off cupcakes for a SPiRE event at 11 PM on a Sunday night and your car window froze halfway open in -10°C weather… Luna and I are extremely lucky to have you and I look forward to following along on your continued academic journey.

Lastly, I would like to thank my family, particularly my sister Julie and my parents, for their continued support and encouragement. Who knows if I would have become a microbiologist without a "biological observation of the day" during vacations or my parents' endless enthusiasm for birds and other animals. Thank you for teaching me the importance of curiosity and moving out of my comfort zone. And thank you to my grandparents Toni and Agi, who were so excited and proud to see me start my journey at McGill, but who unfortunately are no longer able to see me finish my degree. I would not have been able to get to where I am today without all of your support!

Table of Contents

List of Figures and Tables

Chapter 1

Chapter 2

Chapter 3

Chapter 4

List of Abbreviations

ADP – adenosine diphosphate

AEC – airway epithelial cells

ALI – air-liquid interface

ANOVA – analysis of variance

ASL – airway surface liquid

BALF – bronchoalveolar lavage fluid

BMI – body mass index

cAMP - 3',5'-cyclic adenosine monophosphate

c-di-GMP – cyclic di-guanylate

CF – Cystic Fibrosis

CFTR – Cystic Fibrosis transmembrane conductance regulator

CFU – colony forming units

COPD – chronic obstructive pulmonary disorder

CXCL5 – C-X-C motif chemokine 5

DAPI - 4′,6-diamidino-2-phenylindole

DMEM – Dulbecco's modified Eagle medium

DNA – deoxyribonucleic acid

DTT - dithiothreitol

EC – epithelial cells

ECR – elastin-congo red

EDTA - ethylenediaminetetraacetic acid

EGTA – egtazic acid

ENaC – epithelial sodium channel

ER – endoplasmic reticulum

FACS – fluorescence-activated cell sorting

FBS – fetal bovine serum

FEV_1 – forced expiratory volume in the 1^{st} second

FSC – forward scatter

FVD – fixable viability dye

GTPase – guanosine triphosphate hydrolase enzyme

H&E – hematoxylin and eosin

HEK – human embryonic kidney

HSL – homoserine lactone

HRV – human rhinovirus

ICAM-1 – intercellular adhesion molecule 1

IFN – interferon

IL – interleukin

LB – lysogeny broth

LDH – lactate dehydrogenase

LPS – lipopolysaccharide

LTB4 – leukotriene B 4

MCP-1 – monocyte chemoattractant protein 1

MDCK – Madin-Darby canine kidney

MFI – median fluorescence intensity

mICAM-1 – membrane-bound ICAM-1

MOI – multiplicity of infection

mRNA – messenger RNA

MRSA – methicillin-resistant *Staphylococcus aureus*

NETs – neutrophil extracellular traps

NLR – NOD-like receptors

NLRC4 – NLR familu CARD-domain containing protein 4

NTM – non-tuberculous mycobacteria

OD – optical density

P.a. – *Pseudomonas aeruginosa*

PAMP – pathogen associated molecular pattern

PAR-2 – protease-activated receptor 2

PBS – phosphate-buffered saline

PCR – polymerase chain reaction

PFA – paraformaldehyde

pH – potential of hydrogen

PRR – pattern recognition receptor

QS – quorum sensing

rhICAM-1 – recombinant human ICAM-1

RNA – ribonucleic acid

RNF213 – ring finger protein 213

ROI – region of interest

RT – room temperature

SCFM – synthetic CF medium

SD – standard deviation

SDS-PAGE - Sodium dodecyl-sulfate polyacrylamide gel electrophoresis

SEM – standard error of the mean

SSC – side scatter

T3SS – Type three secretion system

T4P – type IV protease

TBS-T – tris-buffered saline supplemented with 0.1% Tween 20

TLR – Toll-like receptor

TNF-α - tumor necrosis factor α

TRITC - tetramethylrhodamine

uPAR – urokinase-type plasminogen activator receptor

UPEC – uropathogenic *Escherichia coli*

UTI – urinary tract infection

VCAM-1 – vascular cell adhesion molecule 1

Wt – wild-type

Contributions of Authors

This doctoral thesis was prepared in accordance with the guidelines stated in the McGill University "Guidelines for Thesis Preparations". The work of this thesis is presented in the "Manuscript-based thesis" format. All studies have been performed under the supervision of Dr. Dao Nguyen. The detailed contributions of the authors are listed below and designated by their initials.

Chapter 1: Literature Review

The literature review was written by LCH and edited by DN. It contains sections of a micro review by LCH and DN that was published in Microbial Cell, which were reprinted in accordance with the Creative Commons Attribution license: **Hennemann LC**, Nguyen D. **LasR-regulated proteases in acute vs. chronic lung infection: a double-edged sword.** Microb Cell. 2021;8(7):161-3.

Chapter 2: **Hennemann LC**, LaFayette SL, Malet JK, Bortolotti P, Yang T, McKay GA, Radzioch D, Rousseau S, Nguyen D. **LasR-deficient *Pseudomonas aeruginosa* variants increase airway epithelial mICAM-1 expression and enhance neutrophilic lung inflammation.** PLOS Pathogens. 2021;17(3):e1009375.

This manuscript was reprinted in its entirety from PLoS Pathogens in accordance with the Creative Commons Attribution license. LCH, SLL and DH performed the experiments. The data was analyzed by LCH, SLL and JKM. LCH, JKM and PB developed the methodology used in this work. TY and GAM generated the protease complementation constructs used to generate the complemented +*lasA*, +*lasB*, +*aprA* and +*prpL* strains. DR provided the resources for the mouse bead infection model. LCH, SR and DN conceptualized this work, wrote and edited the manuscript.

Chapter 3: Malet JK*, **Hennemann LC***, Hua EML, Faure E, Waters V, Rousseau S, Nguyen D. **A Model of Intracellular Persistence of *Pseudomonas aeruginosa* in Airway Epithelial Cells**. Cellular Microbiology. 2022;2022:5431666.

This manuscript was reprinted in its entirety from Cellular Microbiology in accordance with the Creative Commons Attribution license. JKM, LCH, EF, SR, and DN conceived the study. JKM, LCH, and EMLH performed the experimental work. VW provided data and bacterial strains. JKM, LCH, and DN analyzed the data. JKM, LCH, SR, VW, and DN wrote and revised the manuscript. *JKM and LCH contributed equally to this work.

Chapter 4: Loss of T3SS function facilitates intracellular *Pseudomonas aeruginosa* survival and proliferation within airway epithelial cells. **Hennemann LC**, Malet JK, Hua EML, Jusab S, Nelson A, Adam D, Brochiero E, Waters V, Rousseau S, Nguyen D. *Manuscript in preparation*.

LCH, JKM and DN conceived the study. LCH, JKM, EMLH and SJ performed the experimental work and analyzed the data. AN generated the C2 and C3 *exoS* mutants. DA and EB provided human primary AEC. VW provided clinical strain data and bacterial strains. LCH, JKM and DN wrote the manuscript. LCH, JKM and DN revised the manuscript.

Chapter 5: Discussion

The discussion was written by LCH and edited by DN. It contains sections of a micro review by LCH and DN that was published in Microbial Cell, which were reprinted in accordance with the Creative Commons Attribution license: **Hennemann LC**, Nguyen D. **LasR-regulated proteases in acute vs. chronic lung infection: a double-edged sword.** Microb Cell. 2021;8(7):161-3.

Original Contribution to Knowledge

The data presented in this thesis in the form of two published manuscripts and one unpublished manuscript contributes original knowledge to the study of the pathological consequences of *Pseudomonas aeruginosa* (*P.a.*) host-adaptation and the field of intracellular *P.a.*

In chapter 2, we described a novel mechanism through which host-adapted, *lasR*-deficient *P.a.* strains may exacerbate CF lung inflammation. Specifically, we demonstrated that*:*

- Both engineered and naturally occurring *lasR*-deficient *P.a.* isolates result in increased ICAM-1 levels on airway epithelial cells (AEC) compared to wild-type *lasR* strains
- LasR-regulated proteases can degrade recombinant human ICAM-1
- Elevated ICAM-1 levels on AEC are associated with increased neutrophil adhesion
- *P.a. lasR* deficiency is associated with increased bronchial ICAM-1 expression and elevated neutrophilic inflammation in a murine bead infection model

In chapter 3, we established a robust long-term survival model of intracellular *P.a.* within AEC, which may be more representative of chronic *P.a.* infections in the CF lung than previously used infection models. Specifically, the model allowed us to:

- Examine intracellular *P.a.* long-term survival up to 120h (5 days) post infection
- Investigate intracellular survival dynamics at the population and single cell level using complimentary techniques (viable colony forming unit counts, lactate dehydrogenase release assay, flow cytometry and confocal imaging)
- Identify a “hyper-proliferator” phenotype in a clinical *P.a.* isolate

In chapter 4, we examined the intracellular survival of the most extensive collection of clinical *P.a.* isolates tested in this context to date. We further identified loss of type 3 secretion (T3SS) function, a common adaptation of *P.a.* to the host lung, as a major driver of intracellular survival among clinical isolates, which may be of therapeutic relevance. Specifically, we demonstrated that:

- There is significant strain heterogeneity in the ability to survive intracellularly within AEC
- T3SS-deficient strains display decreased cytotoxicity and increased intracellular survival within AEC

- T3SS injectisome function suppresses intracellular *P.a.* survival even in the absence of T3SS effector function
- The increased intracellular survival of T3SS-deficient isolates is largely driven by a subpopulation of hyper-proliferating bacteria in a small percentage of infected cells

Together, our results demonstrate that, paradoxically, loss of *P.a.* virulence factors during chronic infection may in fact increase host lung pathology and bacterial survival. Our results offer novel insights into *P.a.* pathogenesis and reveal ICAM-1 as a potential treatment target to limit pulmonary inflammation in the CF lung. Identifying bacterial factors involved in the intracellular *P.a.* lifestyle may uncover additional treatment targets that could improved *P.a.* eradication by removing an intracellular *P.a.* reservoir.

Chapter 1: Introduction

1.1 Cystic Fibrosis

Cystic Fibrosis (CF) is a fatal autosomal recessively inherited disorder that affects approximately 4,300 Canadians (1). It is predominantly observed in Caucasian populations, particularly in individuals of Northern European, Eastern European or Ashkenazi Jewish ancestry, but is also observed at a lower prevalence in non-Caucasian populations (2-5). Within Europe and North America, pockets of communities with a significantly elevated prevalence of CF have been observed, as is the case for people living in certain parts of Northeastern Quebec, where the incidence of CF has been described to be as high as 1 in 900 life births (6).

1.1.1. CFTR dysfunction

In 1989, it was discovered that CF is caused by an underlying dysfunction in the Cystic Fibrosis transmembrane conductance regulator (CFTR) (7), which functions as a 3',5'-cyclic adenosine monophosphate (cAMP)-regulated anion channel in the outer cell membrane (8). CFTR expression is mostly observed on airway, intestinal and exocrine epithelial cells (EC) in the lungs, intestine and other organs such as the pancreas (9). In cells expressing dysfunctional CFTR, the cross-membrane ion efflux is interrupted and anions such as Cl^- and bicarbonate are retained in host cells rather than being secreted into the extracellular milieu (10, 11). Bicarbonate retention within the epithelium has been shown to result in a decrease in airway surface liquid (ASL) pH, which has been linked to a number of adverse effects (12). While CFTR regulates the epithelial sodium channel (ENaC) under normal conditions, dysregulated ENaC in the CF lung leads to an increased Na^+ influx into EC (13). The resulting high intracellular salt concentration is followed by an increased water influx into cells and a depletion of the ASL (14-17), resulting in a thick mucus layer and a number of other deleterious downstream effects. Mucus plugging is potentially further exacerbated by conformational changes in the mucin proteins under low pH conditions in the CF ASL, resulting in an increased mucus viscosity (18). The extent of CFTR dysfunction, disease severity and treatment options are dependent on the nature of the underlying CFTR mutation, which is typically grouped into six major groups, with a seventh group recently suggested by De Boeck et al. (19). As shown in Table 1.1, the groups are defined by the type of CFTR protein dysfunction and the resulting phenotype.

Group	Phenotype	Cause	Genotypic examples
I	Severely truncated or absent protein	Introduction of frameshift or stop codon close to the beginning of the gene	G542X (20)
II	Severely reduced protein abundance at the cell surface	Protein misfolding results in degradation by the endoplasmic reticulum (ER) quality-control system	ΔF508 (7)
III	CFTR gating defect	Mutations affect channel regulation, resulting in a gating defect and reduced probability of the channel being open	G551D (21)
IV	CFTR conductance defect	Mutations affect channel ion conductance, resulting in a reduced ion current	R117H (22)
V	Decreased protein abundance	Mutations do not cause structural or functional protein changes, but affect protein abundance through abnormal splicing or promoter activity	2789+5 G->A (23)
VI	Increased protein turnover	C-terminal truncations result in reduced protein stability at the plasma membrane or during post-ER processing steps	Q1412X (24)
VII	No protein expression	Mutations that result in a lack of mRNA transcription	1717-1 G->A (25)

Table 1.1: CFTR dysfunction classification.

Typically, patients homozygous for alleles in groups 1, 2, 3 and 7 tend to present with more severe disease than patients homozygous or heterozygous for alleles in groups 4-6 (19, 26). Out of more than 2000 CFTR mutations described to date, more than 400 of which have been established to cause CF (27), the ΔF508 mutation is by far the most prevalent allele, accounting for almost 70% of mutant CFTR alleles observed in CF patients (28). However, the exact frequency of certain mutations within different patient populations is highly dependent on geographical factors and patient ancestry (28).

1.1.2. Impaired pulmonary host defenses

CFTR dysfunction facilitates bacterial lung colonization in different manners, and recurrent/chronic bacterial infections as well as the resulting lung tissue damage are key factors in CF lung pathology. Firstly, depletion of the ASL results in dysfunctional mucociliary clearance, which would normally clear inhaled pathogens and debris (15, 17). Secondly, the

lack of bicarbonate secretion into the extracellular space results in a drop in pH within the remaining ASL, rendering antimicrobial peptides less effective or non-functional (12, 29).

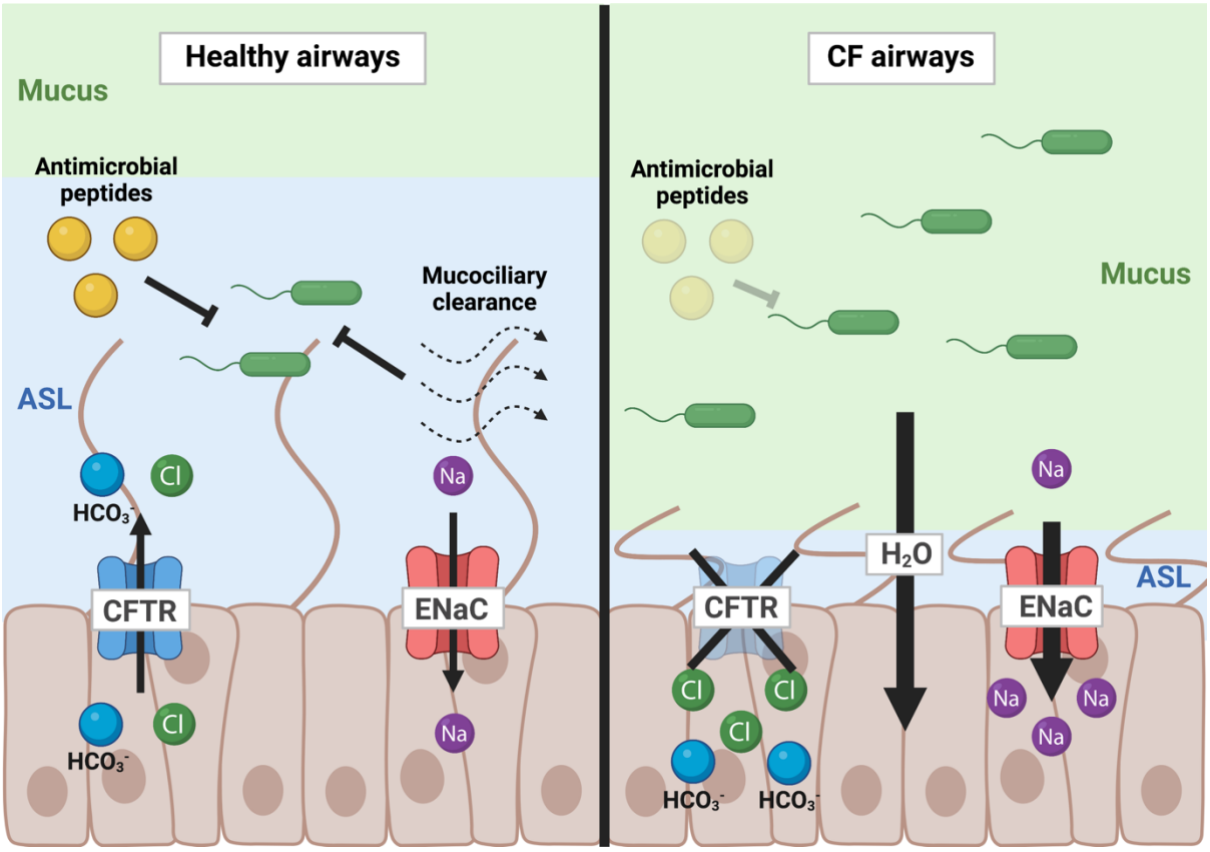

Figure 1.1: Mucociliary clearance and antimicrobial peptides in healthy vs CF airways. Created in Biorender.

Mucociliary clearance is a key component of the innate host defenses that allow the lungs to remain infection-free despite being a mucosal site. In healthy lungs, cilia on the apical side of airway epithelial cells (AEC) beat in a coordinated effort to transport mucus, microbes and debris across the respiratory tract where they can be cleared through coughing (30, 31). In the CF lung, on the other hand, ciliary beating is impaired due to the depletion of the ASL and increased mucus viscosity, resulting in ciliary collapse (15, 18) and impaired pathogen clearance.

Another important innate defense mechanism that appears to be defective in the CF lung as a direct consequence of CFTR dysfunction on AEC are antimicrobial peptides. A variety of antimicrobial peptides, which are primarily secreted by AEC and neutrophils, are relevant to pulmonary infections (32-36). The cationic nature of many antimicrobial peptides allows these

short polypeptides to integrate into negatively charged bacterial membranes and induce bacterial lysis, while leaving neutral eukaryotic membranes unharmed (37). Widely studied examples of antimicrobial peptides produced and secreted by human cells in the airways include LL-37, human β-defensin-3 and lysozyme (38). Antimicrobial peptide activity has been shown to be diminished in the CF airways due to the acidic ASL pH caused by a lack of CFTR-mediated bicarbonate secretion, as antimicrobial peptides have greater activity at a basic pH (12). As a result, antimicrobial peptide-mediated bacterial killing is ineffective in the CF airways.

Innate immune cell functions are also affected by CFTR dysfunction, either through direct or indirect mechanisms. Pulmonary bacterial challenge of mice expressing CFTR-inactivated myeloid cells resulted in increased inflammatory markers and death, indicating that CFTR dysfunction may result in myeloid cell dysfunction (39, 40). However, studies of CF neutrophil function revealed conflicting results. While some studies indicated that CF neutrophils displayed reduced intracellular bacterial killing and degranulation compared to wild-type neutrophils (40-42), others failed to identify any defects in CF neutrophil function (43). Whether the functional impairment of CF neutrophils is due to an intrinsic CFTR-dependent defect or acquired from the inflammatory milieu of the CF airways remains unresolved.

Together, dysfunctional mucociliary clearance and ineffective antimicrobial peptide-mediated bacterial killing, among several host defense defects, allow for the colonization of the CF airways by a number of opportunistic pathogens whose growth would be kept in check under normal conditions.

1.1.3. Cystic Fibrosis lung microbiology

Facilitated by the aforementioned host defense defects, CF airways are susceptible to colonization by a number of different microorganisms, including well established opportunistic pathogens, and often harboring multiple organisms at once. While the clinical significance of certain microorganisms, such as *S. maltophilia* and different *Achromobacter* species, remains to be fully established, *Burkholderia cepacia* complex and *Pseudomonas aeruginosa* (*P.a.*) in particular have been linked to increased lung pathology (44-49). While comparatively rare, *B. cepacia* complex infections are associated with poor patient outcomes, can progress rapidly and result in fatal respiratory failure (44-46). *P.a.* infections, on the other hand, are frequently

observed in CF patients and are associated with an increased lung function decline and elevated pulmonary inflammatory markers (47-49).

In comparison, the clinical significance of *S. aureus* infections remains ambiguous. In CF children, among whom >70% may be infected by *S. aureus* depending on the age group, *S. aureus* infections are associated with poor lung function and increased inflammation (48, 50). Conversely, *S. aureus* infections in adults appear to be somewhat protective, seeing as they are associated with decreased mortality and higher lung function (51, 52). Adding an additional layer of complexity, certain strain phenotypes such as small colony variants and methicillin-resistant *Staphylococcus aureus* (MRSA) are associated with worse patient outcomes (53-55).

As shown in Figure 1.2, patient age is a major determinant of which microorganisms are most prevalent in the CF lungs. While some organisms, such as *S. aureus* and *H. influenzae* appear to be more prevalent in children and adolescents, the prevalence of *P.a.* and the fungus *A. fumigatus* rises significantly starting in early adulthood and *P.a.* becomes the predominant pathogen in patients starting in the age group from 25-34 years of age (1).

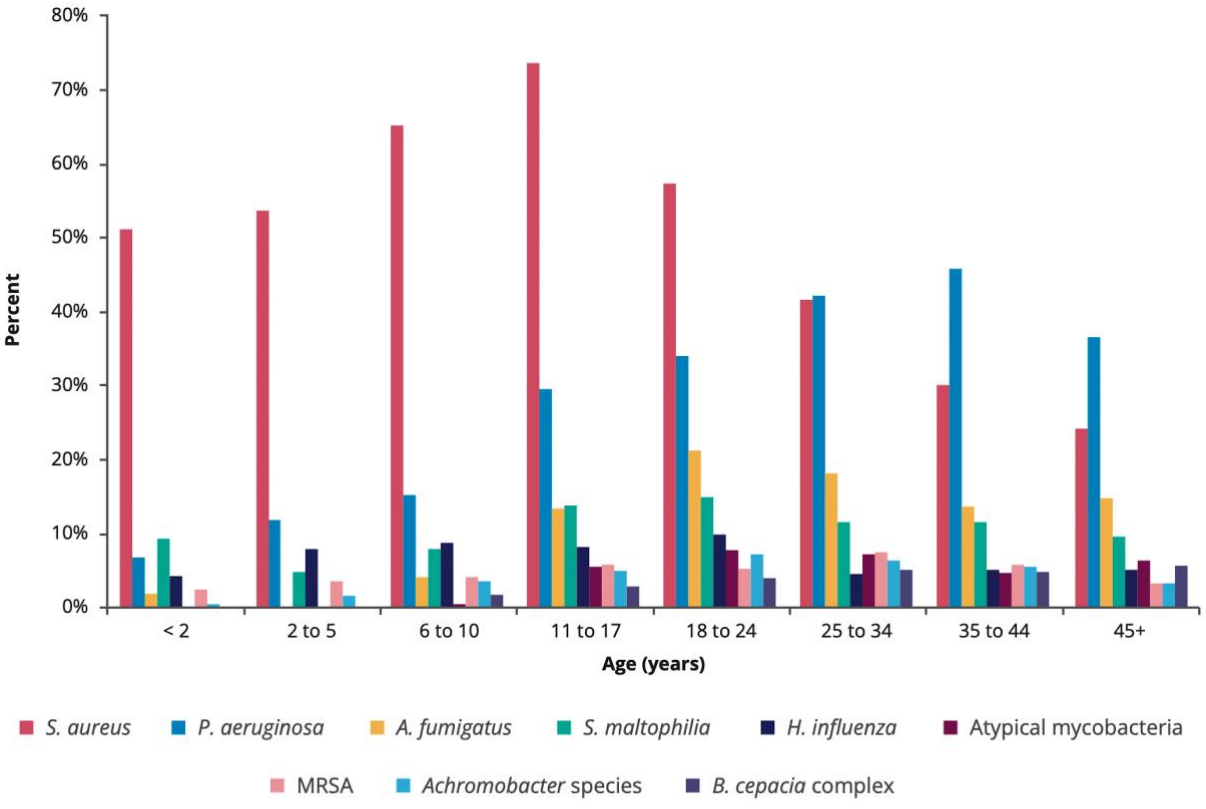

Figure 1.2: Age-specific prevalence of respiratory infections in individuals with CF in Canada, 2020. Adapted from (1).

The sequential infection of *S. aureus*/*H. influenza* and *P.a.* has been the topic of many inquiries and a number of possible explanations have been raised: Firstly, unlike most other CF pathogens, *P.a.* infections are typically aggressively treated with antibiotic eradication therapy in order to clear the bacterium as soon as it is detected (56). As a consequence, chronic *P.a.* infections may simply be delayed for a longer time than *S. aureus* infections due to antibiotic use. Another hypothesis is that *P.a.* is only able to establish a chronic infection in airways that have already sustained considerable damage and are thus more susceptible to *P.a.* infection (57). It has further been observed that the onset of chronic *P.a.* infections tends to coincide with a loss of bacterial community diversity in older CF patients (58). However, it remains to be elucidated whether a lack of bacterial diversity is a predisposing factor for *P.a.* colonization or whether *P.a.* infection directly reduces bacterial diversity. The reason for the delayed onset of chronic *P.a.* infections compared to other CF pathogens is likely multifactorial and highly complex.

P.a. infections in the CF lung also tend to be highly dynamic: patients can sequentially be infected with different strains, with repeated cycles of infection and bacterial clearance, either spontaneously or following antibiotic eradication therapy given at the time of new onset infection. Furthermore, it is not uncommon to recover multiple isolates of the same species from patient sputum, which can be the result of regional diversification of one original strain or of two or more distinct infecting strains (59, 60).

1.1.4. Excessive lung inflammation

Along with recurrent (bacterial) infections, excessive, non-resolving inflammation is a key feature of CF lung disease. This inflammatory response is largely dominated by neutrophils, but other cell types such as AEC also contribute to the pro-inflammatory environment through the secretion of pro-inflammatory cytokines and chemokines like interleukin (IL)-6 and IL-8 (61-63). The inflammation appears to be caused by a combination of an intrinsic hyperinflammatory state linked to the loss of CFTR function as well as a consequence of (chronic) bacterial infections which trigger a sustained inflammatory response. While the exact link between CFTR dysfunction and a hyperinflammatory state remains to be established, a number of studies suggest that lung inflammation may precede infection with typical CF pathogens. Studies in young CF children and in a CF ferret model have demonstrated sterile inflammation and mucus plugging even in the absence of infection (64, 65). An intrinsic hyperinflammatory state is further supported by data generated using human CF AEC, which

displayed a significantly greater inflammatory response to a given stimulus when compared to cells from healthy donors (66-68).

Further exacerbating the intrinsic inflammation, recurrent or chronic bacterial infections are potent inducers of inflammation via pathogen-associated molecular patterns (PAMPs) such as lipopolysaccharide (LPS), lipoteichoic acid, flagellin and peptidoglycan (69). Of note, pathogen clearance in the CF lung is generally ineffective due to a number of barrier defense and innate immune defects as well as bacterial evasion mechanisms (70-73). As a consequence, bacterial proliferation is largely uncontrolled and can reach $>10^9$ colony forming units (CFU)/mL in patient sputum samples (74). The bacterial abundance in turn triggers additional neutrophil recruitment to the lung, resulting in the excessive inflammation typically observed in the CF lung.

The inflammatory response in the CF lung is not only excessive, but also deleterious to the host. Neutrophils recruited to the airways secrete both reactive oxygen and nitrogen species as well as proteases including neutrophil elastase, cathepsin G and matrix metalloproteases, all of which have been demonstrated to damage surrounding host tissues (61, 75, 76). Neutrophil secreted proteases may even further exacerbate the effect of CFTR dysfunction by degrading CFTR and activating ENaC (77, 78). In fact, sputum levels of pro-inflammatory cytokines and secreted neutrophil proteases show a strong negative correlation with lung function, further indicating that neutrophilic lung inflammation is a major driver of lung function decline (52, 62, 79).

1.1.5. Other associated morbidities

Although CF lung pathology causes the most morbidity and mortality, CF is in fact a multi-organ disease that can affect numerous organs, ranging from the pancreas to the intestine (80). CFTR is most highly expressed on epithelia (9). Due to the presence of a variety of EC across different organs, the effect of CFTR dysfunction can result in an array of symptoms. Particularly small (exocrine) ducts tend to get blocked by mucus due to mucus dehydration, resulting in pancreatic insufficiency, liver disease and male infertility. Other commonly encountered symptoms include intestinal blockage, nutrient deficits, below-average height, low body mass index (BMI), depression and anxiety (81).

Pancreatic insufficiency is observed in about 85% of CF patients and is more commonly observed in patients homozygous for “severe” CFTR mutations (82, 83). Pancreatic insufficiency typically stems from a bicarbonate/water imbalance in the EC lining the pancreatic ducts, which results in a decreased bicarbonate concentration of the pancreatic secretions, a lower pH and lower volume due to dehydration (84). These thickened secretions can block the pancreatic ducts, resulting in the impaired absorption of nutrients such as proteins, fat and starch in the intestine, necessitating the life-long supplementation of pancreatic enzymes and fat-soluble vitamins in CF patients (83, 84).

Another part of the digestive system that is frequently affected in CF is the intestinal tract, whose epithelial lining shows similar ion exchange defects to the lung epithelium. Excessive water absorption by the intestinal epithelium and the consequent dehydration of intestinal contents results in meconium ileus in CF infants and distal bowel obstruction in CF adults (85). Treatment options include laxative drugs, enemas and, in severe cases, surgery (86).

CF liver disease is the third leading cause of death in CF patients and is mainly traced back to ion exchange defects in the epithelial lining of the gall bladder and the bile duct (87). Decreased bicarbonate secretion of the epithelium and increased water influx into the epithelium result in a drop in bile pH and increased bile viscosity, respectively. Because of the increased viscosity, coupled with an increased mucin secretion, bile stagnates in the biliary tree and may block the bile duct (87, 88).

1.2 Treatments of Cystic Fibrosis lung disease

1.2.1. CFTR modulators

Arguably the biggest advance in the management of CF has been the development of CFTR modulators, which are aimed at aiding proper protein folding/function and increasing protein levels at the cell surface (89). There are currently four categories of CFTR modulators: potentiators, correctors, amplifiers and stabilizers, the efficacy of which in rescuing proper CFTR function is highly dependent on the patient mutation class (90). However, to date, only corrector and potentiator therapies have been approved for therapy in patients. As shown in Fig. 1.3, correctors may be used to improve CFTR processing and trafficking defects observed in classes II and V, while potentiators may be used to improve CFTR function defects in classes III and IV. However, there is currently no approved modulator treatment for classes I, VI and

VII. Even within classes II-V, treatment is not automatically accessible to all patients, particularly if patients have an uncommon CFTR mutation that is not well-defined and even if treatment is initiated, treatment success within a given mutation class is not uniform (91). In some cases, patient-derived organoids have been used as predictors of treatment success or to investigate whether patients with rare mutations would benefit from treatment with existing modulators (92).

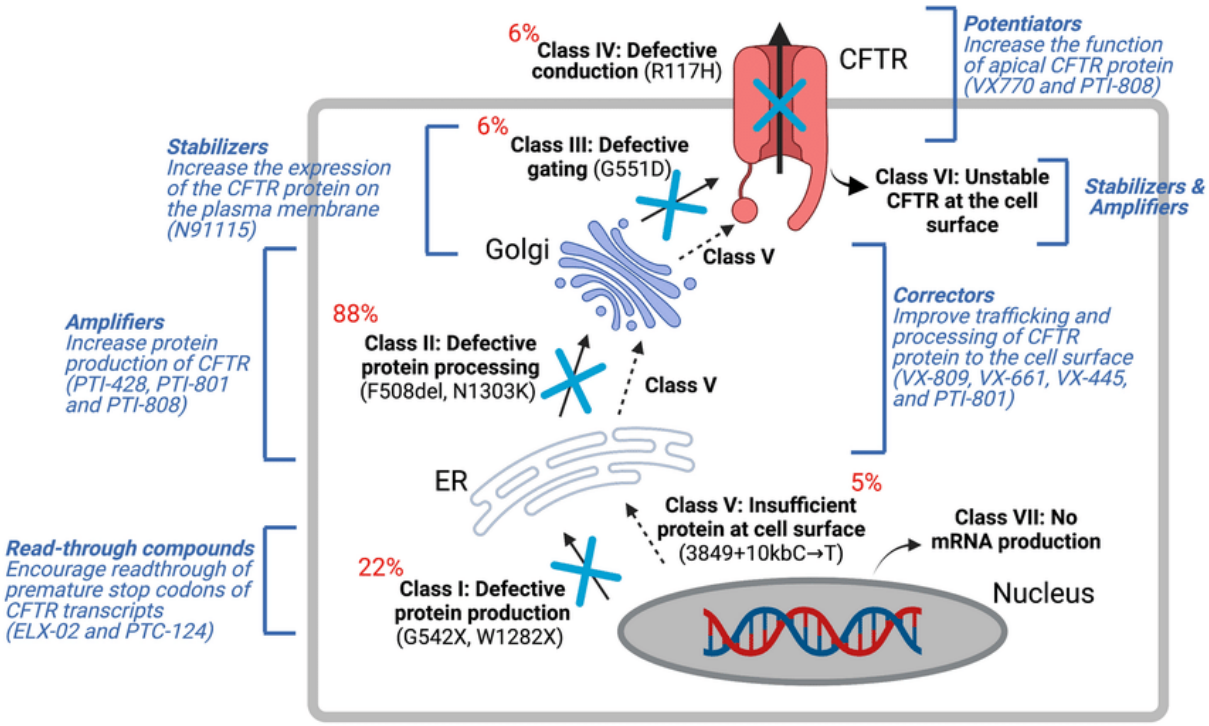

Figure 1.3: Approved modulators or modulators under investigation for the different CFTR dysfunction classes. Adapted from (90).

CFTR modulator therapy has been linked to improvements in several clinical parameters including sweat chloride levels (indicating successful improvement or restoration of CFTR function), the forced expiratory volume in the 1st second (FEV_1), BMI and the frequency of exacerbations requiring hospitalization (93). Treatment success is however variable, in part depending on the degree of prior lung tissue damage, where patients with advanced lung pathology may not respond as well to modulator therapy as patients with mild lung disease. Additionally, multiple studies reported a decrease in the bacterial abundance of certain CF pathogens, a reduced risk of new-onset infections, as well as a reduction in pulmonary inflammatory markers upon modulator treatment (94-96). However, chronic infections typically failed to be cleared and one study even observed a rebound in bacterial abundance

after prolonged modulator treatment, suggesting that CFTR restoration may not be sufficient to clear already established chronic infections (95).

Given the limited availability of current modulator therapies for patients with uncommon alleles, treatment success that can vary depending on the exact mutation and other factors, the high cost and need for life-long treatment, there is a continued need for novel therapies. The advent of gene-editing techniques like CRISPR-Cas offers new potential avenues for treatment (90).

1.2.2. Antimicrobials

There are four primary uses for antibiotics in the treatment of CF patients: eradication treatment (particularly of initial *P.a.* infections), chronic intermittent treatment of chronic *P.a.* infection, short-term treatment of acute pulmonary exacerbations and therapy to combat specific infections such as non-tuberculous mycobacterial (NTM) pulmonary infections. These therapies can consist of a single drug or a combination of antibiotics that are administered as oral, systemic or inhaled antibiotics. Antibiotic therapy is typically challenging in CF patients due to increasing rates of antimicrobial resistance and decreased antimicrobial activity under conditions frequently observed in the CF lung (such as low oxygen) (97). Furthermore, chronic infections are typically refractory to antibiotic killings due to factors such as slow bacterial growth and bacteria growing as biofilms in the CF mucus, among others.

1.2.2.1. *Pseudomonas aeruginosa* eradication therapy and management of chronic infections

When CF children acquire *P.a.* and have an initial positive sputum culture, they are typically treated with antibiotic regimens of inhaled tobramycin and/or colistin or ciprofloxacin to eradicate *P.a.* and prevent progression to chronic infection (98). Successful eradication therapy has been associated with decreased inflammatory markers in bronchoalveolar lavage fluid (BALF) for 12 months post eradication (99). However, eradication therapies have a relatively high failure rate of 10-40%, meaning that many patients will eventually fail to clear the *P.a.* infection and become chronically infected (100-102).

Several studies have investigated the potential determinants of eradication treatment failure, both in terms of host factors and bacterial factors. To date, none identified any significant association between host factors and eradication therapy outcomes, indicating that host factors

such as CFTR phenotype, age or lung function may not be a driving factor of eradication therapy failure (102, 103). Consequently, this raises the possibility that the infecting *P.a.* strain is an important determinant of eradication treatment failure. A recent study of CF children in Canada identified "chronic infection-like" bacterial phenotypes as potential risk factors for eradication therapy failure (102). Strain characteristics that were statistically overrepresented in isolates from persistent infections vs eradicated infections included low twitching motility, overproduction of the exopolysaccharide alginate and resistance to tobramycin, all of which are more frequently observed in chronic infection isolates compared to new-onset infection isolates (102). A subsequent study of these strains found that persistent isolates displayed resistance to phagocytosis and intracellular killing by neutrophils, the predominant immune cell found in the CF lung (104). This increased resistance to neutrophil killing is likely multi-factorial and appears to be (partly) driven by the differences in alginate production and twitching motility mentioned above. These recent findings open new avenues to improving eradication therapies, but there are clearly still considerable gaps in our understanding of the underlying factors of eradication therapy failure.

Even if eradication fails, long-term inhaled antibiotics are still commonly administered during chronic infection stages to minimize the effects of *P.a.* infection on lung function decline, pulmonary inflammation and exacerbation frequency (105).

1.2.2.2. Antimicrobial therapy during pulmonary exacerbations

Periods of pulmonary exacerbations are typically characterized by a drop in lung function, shortness of breath, fever and increased sputum production that require treatment with systemic antibiotics and occasionally hospitalization (106). Inflammatory markers such as IL-6, IL-8 and neutrophil elastase are often elevated compared to the patient's baseline during stable disease phases (107). Antibiotics are typically not administered to eradicate an existing infection, but rather aim to decrease the bacterial load and consequently lung inflammation. While symptoms typically improve upon treatment, some patients' lung function never fully recovers to the pre-exacerbation baseline (108, 109).

While the cause of exacerbations remains poorly understood, some studies suggest that the onset of exacerbations may be triggered by respiratory viral infections, including human rhinovirus, influenza and respiratory syncytial virus (110).

1.2.2.3. Antimicrobial treatment of non-tuberculous mycobacterial infections

While mycobacterial infections remain rare compared to *P.a.* and *S. aureus*, NTM infections are detected in approximately 10% of CF patients, primarily in adults (1). Most NTM infections in CF patients are attributable to either *M. abscessus* complex or *M. avium* complex (111). The clinical significance of NTM infections is still under investigation, as only ~50% of culture-positive patients develop clinically significant NTM lung disease, and poor lung function is primarily associated with *M. abscessus* complex rather than *M. avium* complex infection (111, 112).

The decision to treat NTM infections in CF patients is further complicated by the complex and prolonged treatment protocols required for mycobacterial eradication. Antibiotic treatment is typically administered for over a year and consists of at least three simultaneous antibiotics (111), is associated with significant side effects and thus needs to be carefully considered. However, antibiotic treatment is usually indicated prior to lung transplantation, as post-transplant NTM lung disease may cause significant morbidity (113).

1.2.3. Anti-inflammatory drugs

Treating the deleterious inflammation in the CF lung remains a big treatment challenge, as a certain level of inflammation is required to keep pulmonary infections in check, but excessive inflammation is associated with lung pathology.

Ibuprofen is the only anti-inflammatory treatment currently approved for chronic use in CF patients. Ibuprofen limits neutrophil recruitment to the airways by inhibiting prostaglandin signaling and clinical trial data suggests that ibuprofen treatment is able to slow lung function decline, increase patient body weight and limit the number of hospitalizations (114, 115).

The macrolide antibiotic azithromycin is commonly prescribed for its anti-inflammatory activity. While azithromycin has no significant anti-bacterial effect on *P.a.*, it appears to lower inflammatory cell infiltration and cytokine levels upon bacterial infection in a murine infection models (116). Several studies demonstrated that long-term azithromycin treatment of CF patients was associated with increased body weight and fewer exacerbations compared to a placebo group (117, 118). Patients undergoing chronic azithromycin treatment were also less likely to acquire certain CF-related pathogens, including *B. cepacia* complex and MRSA (119).

Interestingly, azithromycin treatment was associated with increased pulmonary function in patients infected with *P.a.*, but not in mixed study populations with varying infection status or uninfected patients (117, 118, 120, 121).

Lastly, corticosteroids have been investigated as a potential anti-inflammatory treatment in CF patients. However, while improved lung function in patients treated with the corticosteroid prednisone appeared promising, prednisone treatment was also associated with an increased rate of *P.a.* acquisitions, lower height and abnormal glucose metabolism (122). Furthermore, systemic corticosteroids are not recommended for prolonged treatment due to their toxicity (123).

Similarly, a clinical trial investigating the efficacy of a leukotriene B4 (LTB4) inhibitor had to be terminated prematurely due to reports of an increased incidence of pulmonary related serious adverse events and pulmonary exacerbations in patients treated with the LTB4 inhibitor (124). A subsequent study exploring possible causes of treatment failure suggested that treatment with the LTB4 inhibitor resulted in a marked decrease in pulmonary neutrophils and a significant rise in pulmonary bacterial levels and bacteremia in a murine model (125). This failed trial highlights the difficulty in balancing suppression of bacterial growth and limiting inflammation-associated lung tissue damage.

1.3 The opportunistic pathogen *Pseudomonas aeruginosa*

1.3.1. The genus *Pseudomonas*

P.a. is a rod-shaped gram-negative bacterium capable of causing disease in plants, animals and humans. It is frequently isolated from soil and water environments and can colonize a variety of habitats due to its ability to grow under both aerobic and anaerobic conditions and its remarkable metabolic versatility (126-128). The genus *Pseudomonas* currently consists of 144 described species, making it the genus with the largest number of species within gram-negative bacteria (129). Like *P.a.*, other members of the genus such as *P. putida* and *P. fluorescens* are occasionally described as human pathogens, but to a significantly lesser degree than *P.a.* (130, 131). Additionally, some species can cause disease in animals and as both plant pathogens and mutualists, making *Pseudomonas* an agriculturally relevant genus (130).

1.3.2 Genomic organization and environmental adaptability

With a genome size of 5.5-7 Mbp, *P.a.* has a significantly larger genome than other opportunistic pathogens, such as *H. influenzae* and *S. aureus*, whose genome sizes are 1.83 Mbp and 2.8 Mbp, respectively (132-134). A recent study comparing 1311 *P.a.* isolates from various environmental sources showed that only 665 of 54272 identified genes were considered to be core genes, while the vast majority were considered either flexible (26420) or unique (27187) genes (135). Additionally, a total of 3010 fragmented or complete plasmids were identified, of which 12% and 5% encoded for virulence or resistance genes, respectively (135). Together, the sheer number of virulence and metabolic genes encoded by different *P.a.* strains likely accounts for how a single species can colonize such a vast variety of environmental niches.

Another important factor that makes *P.a.* such a versatile opportunistic pathogen is its vast repertoire of regulatory systems, with approximately 9.3% of genes encoding for regulatory proteins (136). This allows the bacterium to rapidly adapt to changing environmental stressors and nutritional availability.

1.3.3. *Pseudomonas aeruginosa* quorum sensing

One such mechanism through which *P.a.* can quickly adapt to changing conditions in a bacterial density-dependent manner are its quorum sensing (QS) systems: the Las, Rhl, and PQS systems, among which the Las and Rhl systems are the best understood (137). The Las and Rhl systems are positive feedback systems in which the autoinducers bind to a transcriptional activator (LasR, RhlR), which in turn binds certain conserved sequences upstream of QS-regulated genes, as shown for the Las system in Fig. 1.4. It is estimated that the Las and Rhl systems together affect the expression of approximately 10% of *P.a.*-encoded genes (138), many of whom encode for virulence factors such as secreted proteases (LasA, LasB, AprA) and phenazines (pyocyanin, phenazine-1-carboxylic acid) (139, 140).

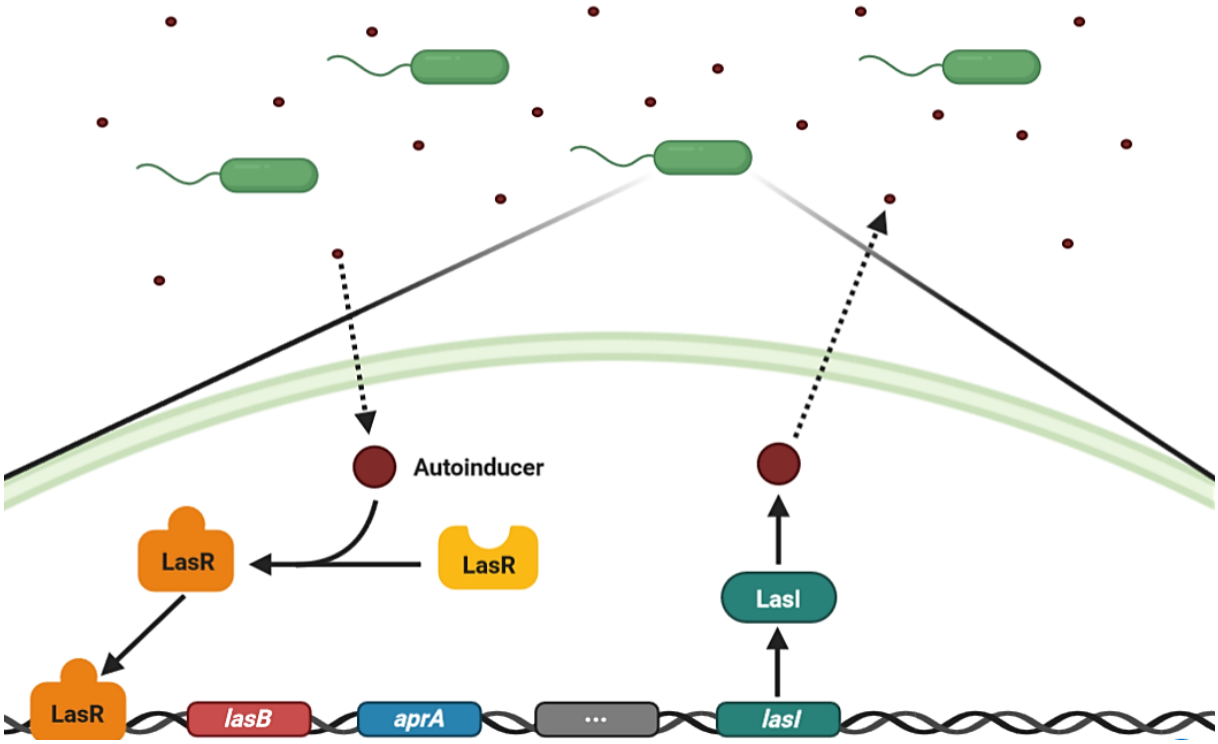

Figure 1.4: Las quorum sensing system in *P.a.* Created in Biorender.

The transcriptional activators further induce genes encoding for proteins responsible for the biosynthesis of the autoinducer, namely LasI and RhlI, resulting in a positive feedback loop (137). Additionally, the autoinducer's ability to cross bacterial membranes results in a bacterial density-dependent accumulation of autoinducer in the bacterial community, allowing bacterial communities to coordinate gene expression. While the homoserine lactone autoinducers for both the Las and Rhl systems display a high degree of similarity, they do not cross-activate the transcriptional activator of the other system (141). However, there is some overlap in gene activation between the two QS systems, such as *lasB*, whose transcription is activated by both LasR and RhlR (137). Interestingly, there are reports of the Rhl system partially compensating for the loss of LasR function in some strains, further complicating the investigation of the exact contribution of one specific QS system to a given phenotype, considering the significant overlap and inter-connectivity of the two systems (142, 143).

LasR function appears to be important for initial infection stages in the CF lung, likely as a mechanism of immune evasion via its associated virulence factors (144, 145). However, it seems to be dispensable during chronic infection stages, as >1/3 of chronic infection isolates display a loss of LasR function (146, 147). Intriguingly, patients infected by *lasR*-deficient mutant isolates were shown to have poorer lung function along with increased plasma IL-8,

indicating increased inflammation (146, 148). These findings are somewhat paradoxical as a loss of virulence factor expression might be expected to result in decreased lung pathology rather than increasing it. The underlying reasons for this surprising observation are still being investigated.

1.4 *Pseudomonas aeruginosa* human infections and models

1.4.1. Human infections

In humans, *P.a.* can cause infections in a range of organs and tissues, including the lung, skin, urinary tract, cornea and blood (149). Skin infections are particularly common in patients with burns and other wounds, and corneal infections are predominantly observed in contact lens wearers (149, 150). Urinary tract infections caused by *P.a.* have been described, but are less frequent than infections caused by uropathogenic *E. coli* (UPEC) (151). *P.a.* infections are also commonly described in the context of catheters in hospital settings, where *P.a.* can grow as a difficult to treat biofilm on catheters, potentially resulting in urine or bloodstream infections and sepsis in immunocompromised patients (149, 152, 153). Among all infection sites, however, lung infections are the most frequently observed and can present both as acute or chronic infections (154-156).

Acute lung infections are usually described in the context of ventilator-associated pneumonia in immunocompromised and critically ill patients, which can escalate to sepsis (156, 157). Chronic infections, on the other hand, are more commonly observed in patients with chronic structural lung disease or barrier function defects, such as CF, chronic obstructive pulmonary disorder (COPD), bronchiectasis or primary ciliary dyskinesia (154, 155, 158).

1.4.2. Animal models

1.4.2.1. Models of CF lung disease

The absence of an easily accessible animal model that fully recapitulates CF lung pathologies has been a significant challenge in CF research. CFTR knockout mice typically only display the intestinal disease associated with CF, but do not exhibit an obstructive airway phenotype similar to what is observed in the CF lung (159). While ENaC knockout mice seem to recapitulate some properties of the CF lung, such as mucus plugging and inflammation, they remain an imperfect model due to the fact that the wild-type CFTR does not allow for studies on the effects of different CFTR mutations or CFTR modulators (160). While recent years have

seen the establishment of two promising CF animal models that closely resemble overall CF patient pathology, the CF pig and the CF ferret (73, 161), working with these animals typically requires specific expertise, is more labor-intensive, time-intensive, expensive and comes with additional ethical considerations for animal experiments (162). While these animal models have offered some important insights on CF lung physiology, they are far from offering the same throughput that mouse experiments do and are inaccessible to most labs.

1.4.2.2. Models of pulmonary *Pseudomonas aeruginosa* infection

Models to investigate pulmonary chronic *P.a.*-host interactions are further complicated by the fact that *P.a.* does not typically establish a chronic infection in the wild-type mouse lung (162). Infections usually range from a few hours to 2-4 days and result either in a complete clearance of the bacteria by the mouse immune system or the death of the mouse due to an overwhelming infection. Transgenic ENaC mutant mice show some promise, where a subset of mutant mice still harbored a low burden of *P.a.* for up to 12 days post infection, but it is unclear for how much longer an infection could be sustained in this model (163). It thus remains challenging to model the non-resolving, non-lethal chronic infections typically observed in the CF lung in a murine model. There has been some success with an intranasal infection of mice, which is believed to result in the continuous re-infection of the murine lung from the nose (164). However, the pulmonary host/microbe interactions are unlikely to reflect those of a chronic, sustained pulmonary infection. Another commonly used model is the bead infection model, where *P.a.* is embedded in agar beads and the beads are consequently instilled intratracheally (148, 165). The advantage of this system is that *P.a.* can secrete factors such as proteases and cytotoxic phenazines into the lung environment, which the host immune system then reacts to over a prolonged amount of time. Additionally, the macrocolonies and microaerobic conditions inside the agar beads closely mirror the *P.a.* growth conditions within biofilms or inside the mucus of the CF lung (162). However, this system does not allow for the study of bacterial factors requiring host cell contact.

1.5 Host-pathogen interactions in initial *Pseudomonas aeruginosa* infection

1.5.1. Host recognition and immune response to *Pseudomonas aeruginosa*

AEC and alveolar macrophages are the first cells to encounter *P.a.* in the CF lung and are thus pivotal in recruiting additional immune cells, such as neutrophils, to the site of infection. *P.a.* expresses an array of PAMPs, resulting in the activation of pattern recognition receptors (PRR)

such as toll like receptors (TLR) and NOD-like receptors (NLR) on these cells (166, 167). While the most prominent PAMPs, flagellin and lipopolysaccharide (LPS), show redundant detection via multiple PRRs, additional PAMPs include ExoS, components of the T3SS injectisome apparatus, the cytotoxic phenazine pyocyanin, peptidoglycan and mannuronic acid, which is a component of the exopolysaccharide alginate (168-172). Detection of these PAMPs via PRR consequently results in the release of pro-inflammatory mediators and immune cell influx to the infected area. While AEC are not considered to be professional immune cells, they are important first responders to inhaled pathogens. Their functions include forming a physical barrier, mucociliary clearance, contributing to bacterial killing through the secretion of antimicrobial peptides and reactive oxygen species, as well as the recruitment and activation of professional immune cells via the secretion of cytokines and chemokines (173).

Briefly, AEC and macrophages secrete chemokines such as IL-8 and LTB4 that form a concentration gradient upon PAMP detection (167, 174, 175). Neutrophils and other immune cells consequently follow the chemokine concentration gradient, which requires rolling adhesion to the capillary endothelium, traversal of the interstitium, binding to the basal membrane of AEC, epithelial transmigration and finally adhesion to the apical side of AEC (61, 176). While some steps of this process, particularly immune cell movement across the interstitium and transepithelial migration, are incompletely understood, some molecules such as the pro-inflammatory adhesion molecule ICAM-1 appear to be involved in multiple steps of this process. ICAM-1 expression on endothelial cells, along with the expression of other adhesion molecules like P-selectin, E-selectin and VCAM-1, is necessary for neutrophil rolling adhesion to capillary endothelial cells (177). At the same time, ICAM-1 expression on AEC appears to be involved in neutrophil transepithelial migration and potentially neutrophil retention within the lung (61, 178-181). As a consequence, chemokine, cytokine and adhesion molecule expression of AEC in response to infectious stimuli are key contributors to initiating and shaping the host immune response to pulmonary infections.

Once in the lung lumen, neutrophils exert their antibacterial functions, which include the secretion of proteases, neutrophil extracellular traps (NETs), as well as bacterial phagocytosis and intracellular killing within neutrophil phagosomes (182). Unfortunately, neutrophilic killing of *P.a.* in the CF lung is often ineffective due to a number of host defects such as dysfunctional antimicrobial peptides and the absence of mucociliary clearance, as well as bacterial immune evasion. An intrinsic dysfunction of neutrophil bacterial killing due to CFTR

dysfunction may also be a possible contributing factor of the ineffective bacterial clearance in CF (183), however this question remains unresolved. Due to the continued proliferation of bacteria, increasing numbers of neutrophils are recruited to the CF lung, resulting in the excessive neutrophilic inflammation frequently observed in CF patients (71). This neutrophilic inflammation in turn directly contributes to lung tissue destruction in the CF lung via the cleavage of host proteins by neutrophil elastase and myeloperoxidase as well as through tissue damage due to the release of reactive oxygen and nitrogen species (61, 184). In fact, neutrophil elastase levels in CF patient sputum are positively correlated with lung disease severity and are an important biomarker of lung disease progression (75). Additionally, extracellular DNA in NETs further increases ASL viscosity, potentially exacerbating CF lung pathology (185).

1.5.2. Major virulence factors required for initial infection and immune evasion

Its arsenal of virulence factors largely accounts for *P.a.*'s ability to successfully infect such a wide variety of different hosts and tissue types. *P.a.* virulence factors range from adhesion factors to injection systems and secreted toxins and exoproducts. Here, we review some of the most important factors that contribute to establishing an initial infection.

1.5.2.1. Secreted proteases

P.a. secretes an abundance of different proteases and expression levels of these proteases are typically regulated by bacterial QS (137). Major QS-regulated proteases include LasA, LasB, AprA and type 4 protease (T4P), most of which are secreted through a type 2 secretion system, with the exception of AprA, which is secreted through a type 1 secretion system (186). Of note, protease secretion patterns by individual strains are not only affected by the complex interplay of QS systems, but also by the fact that co-secretion of certain proteases is required for the activation or potentiation of other proteases (187, 188).

P.a. secreted proteases have been extensively studied for their ability to cause host tissue damage and subvert host immunity during early infection stages. Prominent examples include the elastases LasA and LasB, the alkaline protease AprA and T4P (also referred to as PrpL) (186). Additional proteases have been described, but are less well defined in their function. Numerous *in vitro* studies indicate that *P.a.* secreted proteases, particularly LasB and AprA, can proteolytically degrade a broad range of host molecules (Fig. 1.5). They can degrade cell

junction and extracellular matrix proteins (e.g. occludin, VE-cadherin, elastin, collagen) and surface receptors (e.g uPAR, PAR-2), leading to the breakdown of cellular barriers and direct tissue damage (189-194). Inactivation of chemokines and immune mediators such as IL-8, IL-6 and ENA78 (CXCL5) can suppress host immunity and enable immune evasion, resulting in dampened neutrophil responses to infection (148, 195). Furthermore, degradation of interferon (IFN)-γ suppresses anti-viral responses in AEC, leading to increased viral spreading upon infection with human rhinovirus and respiratory syncytial virus, potentially resulting in further lung pathology and increasing the risk of lung exacerbations (196).

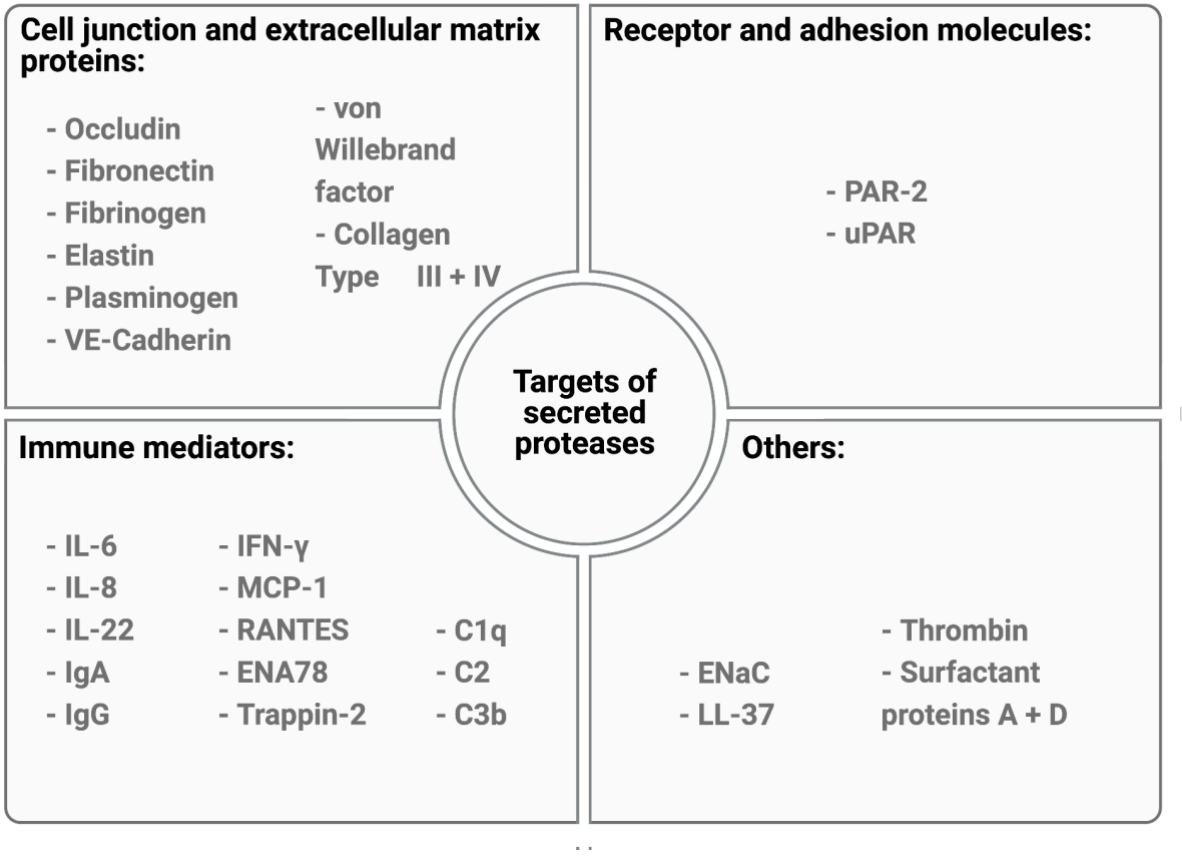

Figure 1.5: Host targets of *P.a.* secreted proteases. Created in Biorender.

Interestingly, immune evasion via secreted proteases is not limited to the degradation of host proteins, as *P.a.* has been observed to cleave components of its own flagellum in order to prevent recognition of the potent PAMP flagellin by host PRR and thus evade immune recognition (197).

1.5.2.2. The type 3 secretion system

T3SS are widely expressed by gram-negative bacteria such as *E. coli*, *S. enterica* and *P.a.* (198). Depending on the bacterium, T3SS can range in complexity from a handful of effector proteins to dozens (198). Additionally, these effectors may be organized in more than one T3SS, as is the case for the two *S. enterica* T3SS which are primarily used during invasion and intracellular survival, respectively (199). Unlike other bacteria, however, *P.a.* only possesses four T3SS effectors: ExoS, ExoT, ExoU and ExoY, out of which ExoS and ExoU are typically mutually exclusive and not encoded by the same strain. ExoS and ExoT both possess an ADP-ribosyltransferase and a GTPase-activating domain, while ExoY is an adenylate cyclase and ExoU is a phospholipase (200). Out of the four effectors, ExoS and ExoU are particularly well-studied and ExoS has been shown to initiate host cell apoptosis, while ExoU causes rapid-onset necrosis in host cells (201, 202), likely as a form of immune evasion.

In an acute pneumonia mouse model, both ExoU or ExoS secretion was associated with increased pulmonary bacterial loads 18h post infection, while ExoT secretion had no effect (203), likely due to the ExoU- or ExoS-mediated killing of immune cells and consequently greater bacterial fitness in the lung (204). Interestingly, ExoU secretion was associated with greater mouse mortality and increased bacterial dissemination to the spleen and liver, despite comparable pulmonary bacterial loads to an isogenic strain expressing ExoS (203). This is likely attributable to the excessive ExoU-mediated cellular damage not only to immune cells, but also to EC, contributing to lung tissue damage and allowing for the dissemination of bacteria and cytokines across damaged epithelial barriers (205, 206). While not associated with a significant increase in either mortality or pulmonary bacterial counts, mice infected with an ExoT-secreting strain displayed greater bacterial dissemination to the spleen and liver compared to mice infected by a secretion-deficient strain. This may be caused by the known effect of ExoT on wound healing, potentially rendering epithelial barriers more susceptible to dissemination (207). Together, the literature suggests that ExoS- and ExoU-expressing strains are associated with greater pulmonary bacterial loads due to immune evasion, increased systemic dissemination and/or increased mortality in acute infection settings (203, 206, 208). These observations mirror findings in patients with acute pneumonia, where T3SS-positive strains were found to be associated with increased morbidity (209).

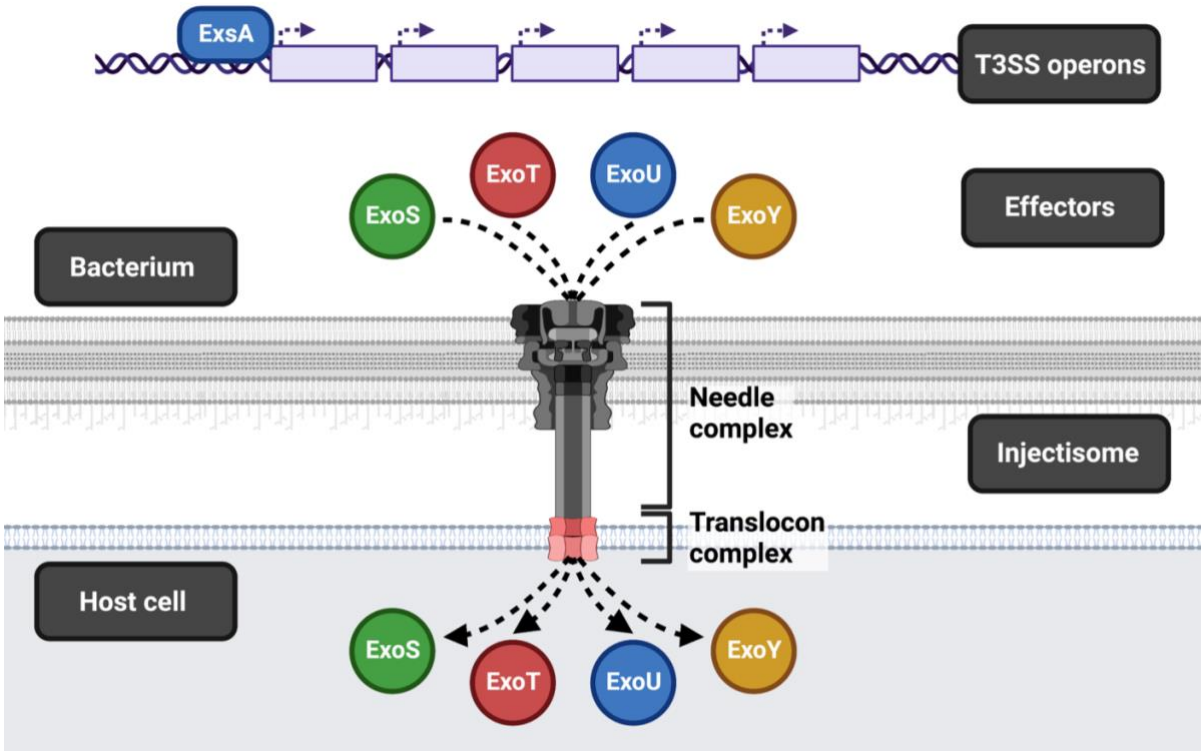

Figure 1.6: The *P.a.* T3SS. Created in Biorender.

In addition to the effectors, the *P.a.* T3SS consists of several regulatory and structural components as shown in Fig. 1.6. The T3SS transcriptional activator ExsA activates the transcription of the T3SS genes, most of whom are organized within 5 operons (210). Transcription and secretion of T3SS effectors is regulated through ExsA, ExsC, ExsD and ExsE, which have varying binding affinities to each other. T3SS secretion can be triggered either through host cell contact or in low Ca2+ conditions (211, 212). In the absence of secretion induction, ExsE binds ExsC and ExsD binds ExsA, preventing T3SS gene transcription. Once secretion is turned on, however, ExsE is secreted, freeing ExsC to bind ExsD and allowing ExsA to transcribe the T3SS genes. Effectors are then injected into the host cell cytosol via the needle complex and the translocon complex, which forms a pore within host membranes (200). Together, the needle and translocon complex are referred to as the injectisome.

While "professional" intracellular pathogens like *S. enterica* and *S. flexneri* typically employ their T3SS to hijack intracellular pathways and optimize their uptake into host cells, *P.a.* T3SS effectors appear to have an opposite effect, where their interaction with intracellular small GTPases inhibits bacterial uptake (213-215). Interestingly, there are reports of components of the bacterial flagellum getting injected into the host cell cytoplasm through the T3SS and

eliciting a host immune response (216). This process is likely due to the high homology between the T3SS needle apparatus and the transmembrane part of the bacterial flagellum, a process that has been demonstrated for multiple gram-negative pathogens (171, 217).

1.5.2.3. Bacterial flagellum and pili

A single flagellum allows *P.a.* to move through liquid with low viscosity, which is referred to as swimming motility. But beyond movement, the flagellum is also necessary for surface adhesion to biotic and abiotic surfaces and is a potent PAMP which gets recognized through host receptors like TLR-2, TLR-5 and NLRC4, inducing a pro-inflammatory response (168, 216, 218, 219). Additionally, *P.a.* encodes for type IV pili which mediate twitching motility and are also involved in surface sensing and adhesion (220).

1.5.2.4. Other acute virulence factors

Besides its T3SS and arsenal of secreted proteases, *P.a.* also encodes for the potent secreted exotoxin A, the cytotoxic and bactericidal phenazine pyocyanin and a type 6 secretion system that is used to intoxicate both competing bacteria and host cells (221-223). Other important bacterial virulence factors include the siderophore pyoverdine, which is an important iron scavenger (224).

1.5.3. Transition from acute to chronic infection

If eradication therapies fail, *P.a.* typically establishes a chronic infection in the CF lung that persists despite antibiotic treatments. Over the course of chronic infections which last years to decades, *P.a.* adapts to the CF lung environment and typically loses expression of many virulence factors, including the T3SS, twitching and swimming motility, protease secretion and secretion of the cytotoxic phenazine pyocyanin (225). In some chronic infection isolates, many of these virulence factors are downregulated at once through mutations in master regulators, such as LasR or RhlR (146). On the other hand, chronic infection isolates typically show increased biofilm formation, mucoidy and antibiotic resistance (225), as shown in Figure 1.7. Numerous longitudinal studies tracking *P.a.* clones over time in the CF lung have revealed common genotypical and phenotypical changes and have investigated the consequences of some of these adaptations for the host and treatment outcomes (226-228). Still, the clinical implications of many of these commonly observed adaptations remain to be elucidated.

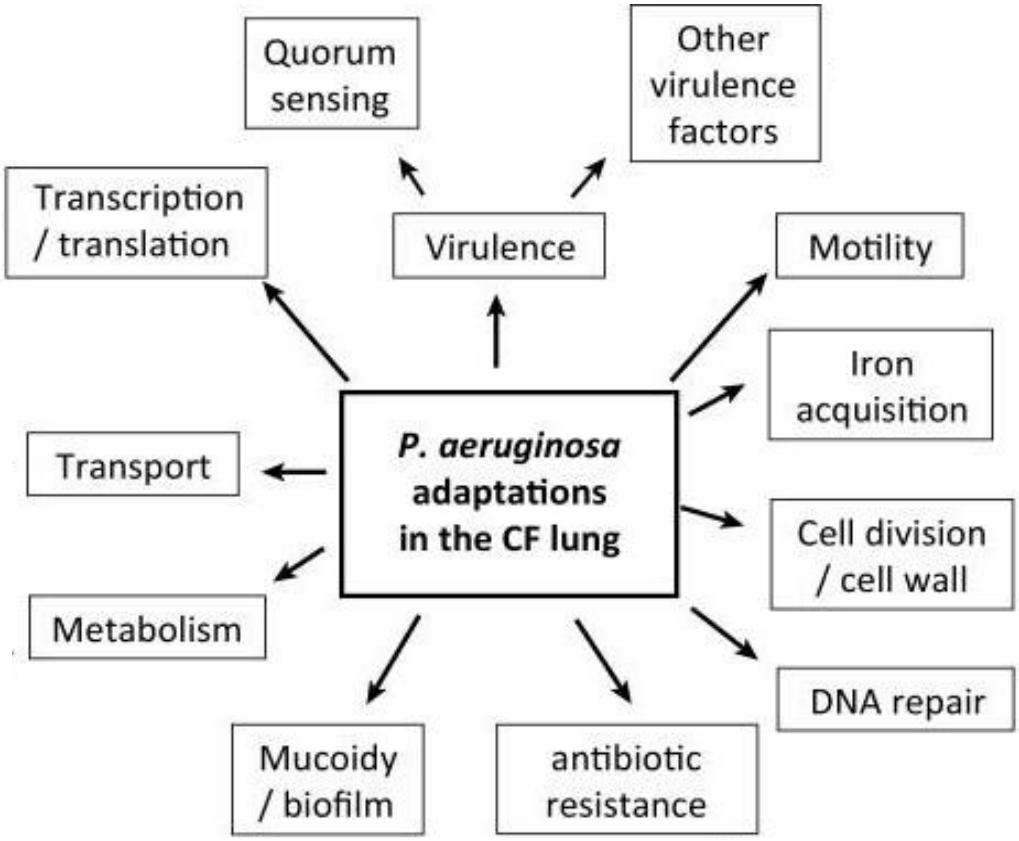

Figure 1.7: Common *P.a.* adaptations in the CF lung. Adapted from (225).

Adaptations observed in *P.a.* isolates from different patients tend to share many similarities, likely due to common selective pressures in the CF lung (229). However, it is important to keep in mind that isolates recovered from the sputum of individual patients may not be representative of the entire *P.a.* population in the CF lung. For instance, it has been demonstrated that *P.a.* genetically and phenotypically diversifies, forming distinct sub-lineages in different lung regions (230). As such, patients may harbor different clonally related isolates that display a wide variety of phenotypic characteristics, such as varying virulence factor expression or antimicrobial resistance phenotypes (230). These characteristics likely reflect differences in bacterial competition, oxygen conditions, nutritional conditions and immune cell presence throughout the lung (225, 231, 232).

1.5.4. Systems mediating the acute-to-chronic switch in *Pseudomonas aeruginosa*

Switching from a motile, highly virulent state to a sessile, biofilm-encased state is a key feature of *P.a.*'s ability to transition between different infection stages in the host. This switch is largely regulated by the second messenger cyclic di-guanylate (c-di-GMP) and the RetS/GacS/LadS regulatory system (233). In *P.a.*, c-di-GMP levels are determined by its production through diguanylate cyclases and its degradation by phosphodiesterases. The balance of production and degradation and the resulting c-di-GMP levels are determined by a range of extracellular cues, such as surface detection (233). High c-di-GMP levels result in a switch towards biofilm formation, which is typically observed in chronic infections, whereas low c-di-GMP levels result in a switch towards motile bacteria and T3SS activity (233).

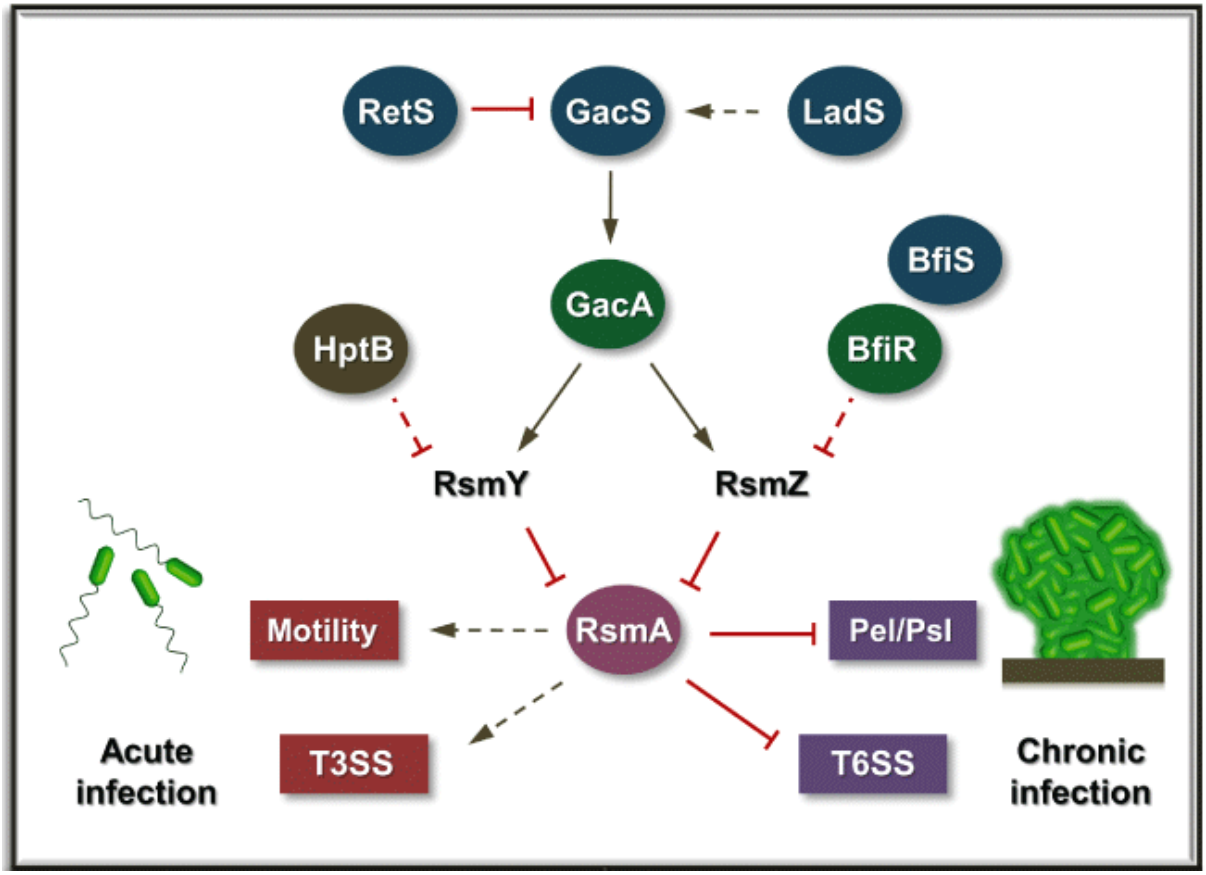

Figure 1.8: The GacS pathway functions as a switch between a motile and sessile bacterial lifestyle. Adapted from (234).

As shown in Fig. 1.8, the histidine kinase GacS signals through the small RNAs RsmY and RsmZ, which inhibit the translational repressor RsmA (234). This inhibition of RsmA results in increased biofilm formation due to derepression of genes such as *pel* and *psl* and decreased

motility due to a lack of induction of these motility-associated genes. The sensor histidine kinases RetS and LadS are upstream of this pathway and tip gene expression towards biofilm formation or a motile lifestyle (234). Interestingly, RsmA also suppresses the expression of the diguanylate cyclase SadC, which synthesizes c-di-GMP (235). Thus, RsmA not only represses biofilm formation through the direct suppression of biofilm genes, but also by suppressing c-di-GMP levels. This switch is considered as one of the major modulators as *P.a.* transitions from an acute to a chronic infection in the context of CF lung infections and mutations in *gacS*, *retS* and *ladS* are occasionally observed in CF isolates, such as the clinical isolate CHA (236).

1.6 Host-adapted *Pseudomonas aeruginosa* phenotypes

1.6.1. Antibiotic resistance and tolerance

While initial infection isolates, which are likely acquired from the environment rather than from patient-to-patient transmission (237), are likely to be sensitive to some antibiotics, chronic infection isolates tend to display multidrug resistance (225). This resistance is likely attributable to repeated antibiotic exposure, particularly during exacerbations, which select for resistant mutants (238). Depending on the antibiotic's mode of action, resistance may be a consequence of efflux pumps that export the antibiotic from the bacterial cell, mutation of the antibiotic target, or active degradation of the antibiotic by bacterial proteins (239, 240). Resistance mechanisms that are of particular relevance to the treatment of *P.a.* infections are listed in Table 1.2.

Antibiotic	Target	Resistance mechanism	Reference
Ciprofloxacin/ levofloxacin	DNA gyrase & topoisomerase IV	Target mutation (*gyrAB, parCE*) and increased efflux pump expression (e.g. *mexCDoprJ*)	(241)
Tobramycin/ amikacin	30S ribosomal subunit	Aminoglycoside-modifying enzymes (e.g. aminoglycoside phosphoryltransferase), increased efflux pump expression, target mutation	(240)
Colistin	LPS fatty acids and phosphates	LPS modifications that limit polymyxin activity (e.g. via phosphoethanolamine transferase MCR-1)	(242)
Aztreonam	Penicillin-binding protein-3	Target mutation (*ftsI*), increased efflux pump expression	(243)

Table 1.2: *P.a.* antibiotic resistance to clinically relevant antibiotics.

Another challenge in treating *P.a.* infections in the CF lung is the fact that *in vitro* antibiotic susceptibility testing of *P.a.* is a poor predictor of treatment outcome (244). This can be partially explained by the fact that susceptibility testing conditions typically do not mirror the conditions in the CF lung. Factors like oxygen conditions, growth rate/stage and biofilm growth have been demonstrated to significantly affect the tolerance of *P.a.* towards antibiotics (245). Importantly, tolerance (also referred to as phenotypic resistance by some) is a transient physiological state that allows the bacterium to survive in the presence of high bactericidal antibiotic concentrations. Unlike genotypic resistance, tolerance is not passed on to the bacterial progeny and can be antibiotic class non-specific. While tolerance mechanisms remain poorly understood, they include bacteria entering a metabolic dormancy state, biofilm growth, activation of stress signaling such as the stringent response and reduced antibiotic penetration (246-248). Antibiotic tolerance not only contributes to drug failure (249), but also increases the likelihood of resistance mutations arising before all bacteria have been neutralized (250).

1.6.2. Biofilm formation

Biofilm formation is the major mechanism conferring antibiotic tolerance to *P.a*. The switch from a motile to a sessile, biofilm-encased lifestyle is typically mediated by differential regulation via altered c-di-GMP levels and the GacS/RetS two-component system, as described above (233). *P.a.* has the ability to form biofilms both on biotic and abiotic surfaces, protecting it from external stresses such as immune cell killing and antibiotics (245, 251). These biofilms are composed of a combination of exopolysaccharides, namely Pel, Psl and alginate for *P.a.*, and extracellular DNA, proteins and lipids, with the exact composition being dependent on the strain background (251).

The antibiotic tolerance conferred by a biofilm-encased lifestyle is likely the result of a combination of factors, such as lower antibiotic penetration rates through the biofilm matrix, which may be partially dependent on the charge of the antibiotic, low oxygen conditions in the biofilm and a low metabolic rate of bacteria in the center of the biofilm (245). Additionally, the low nutrient conditions within the biofilm may activate the stringent response, which has been shown to mediate tolerance to different classes of antibiotics (247). Simultaneously, biofilms also interfere with neutrophil killing through several mechanisms. The biofilm matrix acts as a physical barrier which neutrophils cannot penetrate, while alginate and Psl interfere with complement deposition and neutrophil opsonophagocytosis (252-254). Furthermore, alginate has been shown to scavenge reactive oxygen species and diminish the activity of

antimicrobial peptides (255, 256). Together, the increased antibiotic tolerance and immune evasion of biofilm-encased bacteria explain why *P.a.* biofilms are so difficult to eradicate.

1.6.3. Potential bacterial reservoirs

Following antibiotic treatment and multiple negative sputum cultures, CF patients sometimes test sputum positive for *P.a.* again, and genetic analyses have revealed that these relapsing infections harbor the original strain recovered before eradication treatment (257). Multiple explanations have been proposed for this observation. The negative sputum cultures may not be representative of the entire lung due to imperfect sampling, and *P.a.* might not have been completely eradicated. Alternatively, the patient might have been reinfected by the same environmental source of *P.a.* that they were originally infected by. Another possibility is a reservoir of *P.a.* in the paranasal sinuses that persists during antibiotic treatment due to sinus obstruction and consequent poor antibiotic access to the sinuses (258). The bacteria could then spread from the upper to the lower airways. This notion is supported by the fact that the microbiome of the sinuses is highly similar to that of the lower airways in CF patients, with strains recovered from both sites displaying similar genotypic and phenotypic characteristics (259, 260). However, the direction of spread cannot be definitively established and it is also possible that bacteria spread from the lower to the upper airways and sinuses.

Finally, there is the possibility of a largely understudied reservoir, namely intracellular *P.a.* that may survive within airway EC. Since *P.a.* is traditionally considered an extracellular pathogen, this possibility remains frequently overlooked despite the fact that reports of intracellular *P.a.* within various types of epithelial cells both *in vitro* and in animal models date back three decades (261-263).

1.7 Intracellular *Pseudomonas aeruginosa* in epithelial cells

There is increasing evidence that bacteria traditionally characterized as extracellular bacteria, such as *P.a.*, *E. coli* and *S. aureus*, can also be facultative intracellular bacteria. This intracellular lifestyle may contribute to antibiotic treatment failure, relapsing infections, and facilitate the establishment of a chronic infection (264-267). Intracellular UPEC is widely accepted to have clinical relevance in the setting of UTIs since it has been observed within sloughed epithelial cells in patient urine samples (268, 269), and may explain why certain patients relapse frequently after antibiotic treatment for chronic UTIs (264, 269, 270). The

relevance of intracellular *P.a.* remains however uncertain, as past studies have only been conducted *in vitro* and within non-pulmonary, primarily corneal animal infection models (261, 271-273). It thus remains unclear whether intracellular *P.a.* occurs in lung infections and if so, what role it plays in the pathogenesis of chronic lung infections.

1.7.1. Invasion of (airway) epithelial cells

The internalization process into various types of ECs has been studied by many groups, although there are some discrepant observations (Table 1.3). Several factors, including varying MOI, duration of infection, EC type and whether differences in internalization are distinguished from adherence, make it difficult to directly compare between individual studies.

Factor	Effect	Description	Source
Flagellum	↑/-	Corneal EC: Motile flagellum facilitates internalization Rabbit primary corneal EC: no involvement	(274, 275)
Pilus	↑	Madin-Darby canine kidney cells: Pilus interaction with Asialo-GM1 increases internalization	(276)
LPS outer core	↑	Rabbit primary corneal EC: A complete outer LPS core with a terminal glucose residue facilitates internalization	(275)
LecA	↑	Human lung EC H1299: Binding to Gb3 results in lipid zipper-like uptake	(277, 278)
OprF	↑	Human middle ear EC: OprF facilitates invasion	(279)
ExoS/T	↓/-	Corneal EC: ExoS and ExoT inhibit int. HeLa cells: expression of ExoS and ExoT is negatively correlated with bacterial internalization Human bladder EC: T3SS-deficient strain does not display a difference in internalization	(213, 214, 271)
VgrG2B	↑	HeLa cells: T6SS-delivered VgrG2B increases internalization via interaction with the microtubule network component γTuRC	(280)

Table 1.3: Bacterial factors involved in the *P.a.* internalization process into EC.

P.a. employs several motility appendages, membrane proteins and lipids to bind to host factors in order to initiate its uptake into EC (Table 1.3). The literature suggests that *P.a.* is able to invade EC via a trigger-like process that requires active actin polymerization and can be

inhibited by temporarily culturing cells at 4°C or via incubation with cytochalasin D (281, 282). However, it remains less clear whether this process also involves microtubule filaments as Mittal et al. show decreased internalization into human middle ear ECs upon inhibition of either actin or microtubule filaments, while Fleiszig et al. report that microtubule inhibition via colchicine had no impact on internalization into corneal ECs (279, 281). A second potential mode of internalization, which was uncovered more recently, is a zipper-like process that appears to be triggered by *P.a.* LecA binding to the glycosphingolipid Gb3 on host cells, which results in an actin polymerization-independent uptake of the bacterium (278).

1.7.2. Intracellular survival within (airway) epithelial cells

While there is extensive literature on the initial internalization stages of *P.a.* into EC, data on prolonged intracellular survival is more scarce. Survival is often only tracked for up to 12h, which is likely more reflective of acute stages of infection rather than chronic infections that are typically observed in CF patients (283-285). Even in studies with longer infection time courses, comparisons are difficult due to differences in MOI and epithelial cell type (213, 271, 279, 286).

To date, most investigations of intracellular *P.a.* survival have focused on the role of the T3SS, likely due to the established role of the T3SS in the intracellular lifestyle of other intracellular pathogens, such as *S. enterica* and *S. flexneri* (199, 287). Initial reports by Heimer et al. suggested that unlike wild-type *P.a.*, which are able to escape their compartment and enter the host cytosol via the T3SS effector ExoS, T3SS-negative mutants are unable to escape their vacuole, which consequently acidifies. The authors suggested that this would eventually result in bacterial killing of T3SS-negative, but not T3SS-positive bacteria (285). T3SS-positive bacteria would then be able to disseminate throughout the host cell using pilus-mediated twitching motility (288). Recent findings from the same lab, however, show that their initial hypothesis that T3SS-negative vacuolar bacteria are degraded is in fact incorrect and that bacteria are actually able to survive within the acidified vacuoles, display characteristics associated with biofilm formation and are more tolerant to antibiotics like the cell-permeable ofloxacin compared to cytosolic T3SS-positive bacteria, which are readily killed (286). The authors further hypothesize that this T3SS-negative population of vacuolar bacteria may be clinically relevant in the context of antibiotic eradication therapies and the establishment of chronic *P.a.* infections (286). Similar observations of a biofilm-like phenotype of *P.a.* were previously made by another lab (273), while others substantiate the observation that a

subpopulation of bacteria can escape into the cytosol via co-localization of bacteria with cytosolic septin cages by confocal imaging in HeLa cells (289). However, reports of the intracellular *P.a.* localization vary significantly across studies, with some studies reporting a plasma membrane-adjacent localization in bleb-like vacuoles (284, 290), while others report a perinuclear membrane-surrounded localization (291) or a cytosolic localization (279, 285, 289). Notably, these findings may be highly cell type-, timing- and strain-dependent.

Penaranda et al. also recently observed that in bladder ECs, which are a model of *P.a.* UTIs, mutation of the transcriptional regulator AlgR resulted in a significant decrease in intracellular survival (271). While AlgR regulates a number of bacterial virulence factors such as the T3SS and quorum sensing, none of the tested mutants in downstream genes, including T3SS mutants, recapitulated the difference in intracellular survival observed for the *algR* mutant (271). The authors further demonstrated that the observations in a murine UTI model mirrored those in *in vitro* experiments, suggesting that intracellular *P.a.* may be physiologically relevant in the setting of *P.a.* UTIs and that *in vitro* results translate well to *in vivo* studies in this context (271).

In summary, the literature suggests that *P.a.* is capable of invading various human EC types *in vitro* as well as in certain animal infection models of acute infection. It is thus conceivable that *P.a.* may also invade AEC in the airways of CF patients, which may function as a reservoir. An intracellular lifestyle of a small subpopulation would allow *P.a.* to persist during antibiotic treatments due to poor diffusion rates of antibiotics into eukaryotic cells, which is particularly true for aminoglycosides like tobramycin, the antibiotic of choice during *P.a.* eradication therapy (292). *P.a.* would also be shielded from killing by host immune cells like neutrophils. At the end of antibiotic treatment, even a small persistent intracellular population of *P.a.* may be sufficient to reinfect its surrounding tissues.

1.8 Rationale and research objectives

P.a. is a formidable opportunistic pathogen, which is capable of rapidly adapting to changing environmental conditions. In the context of pulmonary infections in CF patients, genotypic and phenotypic *P.a.* adaptations to the host environment over time are well documented. However, the full impact of many frequent adaptations, including loss of LasR and T3SS function, remains to be elucidated. Here, we sought to examine the impact of common adaptations

observed in chronic infection isolates on two processes important to infection pathogenesis, namely the induction of airway inflammation and bacterial persistence.

The first objective of our work was to examine how *P.a.* loss of LasR function, which occurs in about 1/3 of chronic infection isolates, modulates the levels of the pro-inflammatory adhesion molecule ICAM-1 on AEC. We further sought to examine how these altered ICAM-1 levels might affect neutrophil adhesion to AEC *in vitro* as well as neutrophil recruitment to the airways in an *in vivo* bead infection model. Due to the demonstrated immunosuppressive action of LasR-regulated proteases, we hypothesized that a lack of LasR function may result in elevated levels of ICAM-1 on AEC in conjunction with elevated neutrophil recruitment and/or retention.

Our second objective was to establish a model of long-term intracellular *P.a.* survival within AEC in order to identify bacterial factors facilitating intracellular *P.a.* survival. We hypothesized that a robust long-term survival model would allow us to distinguish between strains capable of intracellular long-term survival and strains that are unable to survive, which would lay the foundation for future in-depth analyses.

The third and final objective of this study was to hone in on the observed heterogeneity in the intracellular survival of CF clinical isolates using our newly established intracellular infection and survival model. In order to identify additional "hyper-proliferator" strains, we screened a clinical *P.a.* collection consisting of 28 isolates for their ability to survive intracellularly within AEC. We hypothesized that the observed survival heterogeneity was driven by T3SS status and that T3SS-deficiency, which is commonly observed during chronic infection stages, may facilitate an intracellular lifestyle.

1.9 References

1. Cystic Fibrosis Canada. (2022). *The Canadian Cystic Fibrosis Registry 2020 Annual Data Report*. Toronto, Canada: Cystic Fibrosis Canada.
2. Kosorok MR, Wei WH, Farrell PM. The incidence of cystic fibrosis. Stat Med. 1996;15(5):449-62.
3. Kerem B, Chiba-Falek O, Kerem E. Cystic fibrosis in Jews: frequency and mutation distribution. Genet Test. 1997;1(1):35-9.

4. Farrell PM. The prevalence of cystic fibrosis in the European Union. J Cyst Fibros. 2008;7(5):450-3.

5. Bobadilla JL, Macek M, Jr., Fine JP, Farrell PM. Cystic fibrosis: a worldwide analysis of CFTR mutations--correlation with incidence data and application to screening. Hum Mutat. 2002;19(6):575-606.

6. Rozen R, De Braekeleer M, Daigneault J, Ferreira-Rajabi L, Gerdes M, Lamoureux L, et al. Cystic fibrosis mutations in French Canadians: three CFTR mutations are relatively frequent in a Quebec population with an elevated incidence of cystic fibrosis. Am J Med Genet. 1992;42(3):360-4.

7. Riordan JR, Rommens JM, Kerem B, Alon N, Rozmahel R, Grzelczak Z, et al. Identification of the cystic fibrosis gene: cloning and characterization of complementary DNA. Science. 1989;245(4922):1066-73.

8. Riordan JR. CFTR function and prospects for therapy. Annu Rev Biochem. 2008;77:701-26.

9. Crawford I, Maloney PC, Zeitlin PL, Guggino WB, Hyde SC, Turley H, et al. Immunocytochemical localization of the cystic fibrosis gene product CFTR. Proc Natl Acad Sci U S A. 1991;88(20):9262-6.

10. Anderson MP, Gregory RJ, Thompson S, Souza DW, Paul S, Mulligan RC, et al. Demonstration that CFTR is a chloride channel by alteration of its anion selectivity. Science. 1991;253(5016):202-5.

11. Smith JJ, Welsh MJ. cAMP stimulates bicarbonate secretion across normal, but not cystic fibrosis airway epithelia. J Clin Invest. 1992;89(4):1148-53.

12. Pezzulo AA, Tang XX, Hoegger MJ, Abou Alaiwa MH, Ramachandran S, Moninger TO, et al. Reduced airway surface pH impairs bacterial killing in the porcine cystic fibrosis lung. Nature. 2012;487(7405):109-13.

13. Stutts MJ, Canessa CM, Olsen JC, Hamrick M, Cohn JA, Rossier BC, et al. CFTR as a cAMP-dependent regulator of sodium channels. Science. 1995;269(5225):847-50.

14. Jiang C, Finkbeiner WE, Widdicombe JH, McCray PB, Jr., Miller SS. Altered fluid transport across airway epithelium in cystic fibrosis. Science. 1993;262(5132):424-7.

15. Matsui H, Grubb BR, Tarran R, Randell SH, Gatzy JT, Davis CW, et al. Evidence for periciliary liquid layer depletion, not abnormal ion composition, in the pathogenesis of cystic fibrosis airways disease. Cell. 1998;95(7):1005-15.

16. Zhou Z, Duerr J, Johannesson B, Schubert SC, Treis D, Harm M, et al. The ENaC-overexpressing mouse as a model of cystic fibrosis lung disease. J Cyst Fibros. 2011;10 Suppl 2:S172-82.

17. Boucher RC. Evidence for airway surface dehydration as the initiating event in CF airway disease. J Intern Med. 2007;261(1):5-16.

18. Tang XX, Ostedgaard LS, Hoegger MJ, Moninger TO, Karp PH, McMenimen JD, et al. Acidic pH increases airway surface liquid viscosity in cystic fibrosis. J Clin Invest. 2016;126(3):879-91.

19. De Boeck K, Amaral MD. Progress in therapies for cystic fibrosis. Lancet Respir Med. 2016;4(8):662-74.

20. Kerem BS, Zielenski J, Markiewicz D, Bozon D, Gazit E, Yahav J, et al. Identification of mutations in regions corresponding to the two putative nucleotide (ATP)-binding folds of the cystic fibrosis gene. Proc Natl Acad Sci U S A. 1990;87(21):8447-51.

21. Cutting GR, Kasch LM, Rosenstein BJ, Zielenski J, Tsui LC, Antonarakis SE, et al. A cluster of cystic fibrosis mutations in the first nucleotide-binding fold of the cystic fibrosis conductance regulator protein. Nature. 1990;346(6282):366-9.

22. Sheppard DN, Rich DP, Ostedgaard LS, Gregory RJ, Smith AE, Welsh MJ. Mutations in CFTR associated with mild-disease-form Cl- channels with altered pore properties. Nature. 1993;362(6416):160-4.

23. Highsmith WE, Jr., Burch LH, Zhou Z, Olsen JC, Strong TV, Smith T, et al. Identification of a splice site mutation (2789 +5 G > A) associated with small amounts of normal CFTR mRNA and mild cystic fibrosis. Hum Mutat. 1997;9(4):332-8.

24. Haardt M, Benharouga M, Lechardeur D, Kartner N, Lukacs GL. C-terminal truncations destabilize the cystic fibrosis transmembrane conductance regulator without impairing its biogenesis. A novel class of mutation. J Biol Chem. 1999;274(31):21873-7.

25. Guillermit H, Fanen P, Ferec C. A 3' splice site consensus sequence mutation in the cystic fibrosis gene. Hum Genet. 1990;85(4):450-3.

26. Marson FAL, Bertuzzo CS, Ribeiro JD. Classification of CFTR mutation classes. Lancet Respir Med. 2016;4(8):e37-e8.

27. The Clinical and Functional TRanslation of CFTR (CFTR2); available at http://cftr2.

28. Estivill X, Bancells C, Ramos C. Geographic distribution and regional origin of 272 cystic fibrosis mutations in European populations. The Biomed CF Mutation Analysis Consortium. Hum Mutat. 1997;10(2):135-54.

29. Abou Alaiwa MH, Reznikov LR, Gansemer ND, Sheets KA, Horswill AR, Stoltz DA, et al. pH modulates the activity and synergism of the airway surface liquid antimicrobials β-defensin-3 and LL-37. Proc Natl Acad Sci U S A. 2014;111(52):18703-8.
30. Knowles MR, Boucher RC. Mucus clearance as a primary innate defense mechanism for mammalian airways. J Clin Invest. 2002;109(5):571-7.
31. Sagel SD, Davis SD, Campisi P, Dell SD. Update of respiratory tract disease in children with primary ciliary dyskinesia. Proc Am Thorac Soc. 2011;8(5):438-43.
32. Soong LB, Ganz T, Ellison A, Caughey GH. Purification and characterization of defensins from cystic fibrosis sputum. Inflamm Res. 1997;46(3):98-102.
33. Harder J, Meyer-Hoffert U, Teran LM, Schwichtenberg L, Bartels J, Maune S, et al. Mucoid Pseudomonas aeruginosa, TNF-alpha, and IL-1beta, but not IL-6, induce human beta-defensin-2 in respiratory epithelia. Am J Respir Cell Mol Biol. 2000;22(6):714-21.
34. Kovach MA, Ballinger MN, Newstead MW, Zeng X, Bhan U, Yu FS, et al. Cathelicidin-related antimicrobial peptide is required for effective lung mucosal immunity in Gram-negative bacterial pneumonia. J Immunol. 2012;189(1):304-11.
35. Barlow PG, Svoboda P, Mackellar A, Nash AA, York IA, Pohl J, et al. Antiviral activity and increased host defense against influenza infection elicited by the human cathelicidin LL-37. PLoS One. 2011;6(10):e25333.
36. Hiemstra PS, Amatngalim GD, van der Does AM, Taube C. Antimicrobial Peptides and Innate Lung Defenses: Role in Infectious and Noninfectious Lung Diseases and Therapeutic Applications. Chest. 2016;149(2):545-51.
37. Matsuzaki K. Why and how are peptide-lipid interactions utilized for self-defense? Magainins and tachyplesins as archetypes. Biochim Biophys Acta. 1999;1462(1-2):1-10.
38. Laube DM, Yim S, Ryan LK, Kisich KO, Diamond G. Antimicrobial peptides in the airway. Curr Top Microbiol Immunol. 2006;306:153-82.
39. Bonfield TL, Hodges CA, Cotton CU, Drumm ML. Absence of the cystic fibrosis transmembrane regulator (Cftr) from myeloid-derived cells slows resolution of inflammation and infection. J Leukoc Biol. 2012;92(5):1111-22.
40. Ng HP, Zhou Y, Song K, Hodges CA, Drumm ML, Wang G. Neutrophil-Mediated Phagocytic Host Defense Defect in Myeloid Cftr-Inactivated Mice. PLOS ONE. 2014;9(9):e106813.
41. Bernut A, Dupont C, Ogryzko NV, Neyret A, Herrmann JL, Floto RA, et al. CFTR Protects against Mycobacterium abscessus Infection by Fine-Tuning Host Oxidative Defenses. Cell Rep. 2019;26(7):1828-40.e4.

42. Pohl K, Hayes E, Keenan J, Henry M, Meleady P, Molloy K, et al. A neutrophil intrinsic impairment affecting Rab27a and degranulation in cystic fibrosis is corrected by CFTR potentiator therapy. Blood. 2014;124(7):999-1009.

43. McKeon DJ, Cadwallader KA, Idris S, Cowburn AS, Pasteur MC, Barker H, et al. Cystic fibrosis neutrophils have normal intrinsic reactive oxygen species generation. European Respiratory Journal. 2010;35(6):1264-72.

44. Muhdi K, Edenborough FP, Gumery L, O'Hickey S, Smith EG, Smith DL, et al. Outcome for patients colonised with Burkholderia cepacia in a Birmingham adult cystic fibrosis clinic and the end of an epidemic. Thorax. 1996;51(4):374-7.

45. Ledson MJ, Gallagher MJ, Jackson M, Hart CA, Walshaw MJ. Outcome of Burkholderia cepacia colonisation in an adult cystic fibrosis centre. Thorax. 2002;57(2):142-5.

46. Isles A, Maclusky I, Corey M, Gold R, Prober C, Fleming P, et al. Pseudomonas cepacia infection in cystic fibrosis: an emerging problem. J Pediatr. 1984;104(2):206-10.

47. Konstan MW, Morgan WJ, Butler SM, Pasta DJ, Craib ML, Silva SJ, et al. Risk factors for rate of decline in forced expiratory volume in one second in children and adolescents with cystic fibrosis. J Pediatr. 2007;151(2):134-9, 9.e1.

48. Sagel SD, Gibson RL, Emerson J, McNamara S, Burns JL, Wagener JS, et al. Impact of Pseudomonas and Staphylococcus infection on inflammation and clinical status in young children with cystic fibrosis. J Pediatr. 2009;154(2):183-8.

49. Emerson J, Rosenfeld M, McNamara S, Ramsey B, Gibson RL. Pseudomonas aeruginosa and other predictors of mortality and morbidity in young children with cystic fibrosis. Pediatr Pulmonol. 2002;34(2):91-100.

50. Cogen J, Emerson J, Sanders DB, Ren C, Schechter MS, Gibson RL, et al. Risk factors for lung function decline in a large cohort of young cystic fibrosis patients. Pediatr Pulmonol. 2015;50(8):763-70.

51. Liou TG, Adler FR, Fitzsimmons SC, Cahill BC, Hibbs JR, Marshall BC. Predictive 5-year survivorship model of cystic fibrosis. Am J Epidemiol. 2001;153(4):345-52.

52. Mayer-Hamblett N, Aitken ML, Accurso FJ, Kronmal RA, Konstan MW, Burns JL, et al. Association between pulmonary function and sputum biomarkers in cystic fibrosis. Am J Respir Crit Care Med. 2007;175(8):822-8.

53. Ren CL, Morgan WJ, Konstan MW, Schechter MS, Wagener JS, Fisher KA, et al. Presence of methicillin resistant Staphylococcus aureus in respiratory cultures from cystic fibrosis patients is associated with lower lung function. Pediatr Pulmonol. 2007;42(6):513-8.

54. Sawicki GS, Rasouliyan L, Pasta DJ, Regelmann WE, Wagener JS, Waltz DA, et al. The impact of incident methicillin resistant Staphylococcus aureus detection on pulmonary function in cystic fibrosis. Pediatr Pulmonol. 2008;43(11):1117-23.

55. Besier S, Smaczny C, von Mallinckrodt C, Krahl A, Ackermann H, Brade V, et al. Prevalence and clinical significance of Staphylococcus aureus small-colony variants in cystic fibrosis lung disease. J Clin Microbiol. 2007;45(1):168-72.

56. Ratjen F, Munck A, Kho P, Angyalosi G. Treatment of early Pseudomonas aeruginosa infection in patients with cystic fibrosis: the ELITE trial. Thorax. 2010;65(4):286-91.

57. de Bentzmann S, Roger P, Puchelle E. Pseudomonas aeruginosa adherence to remodelling respiratory epithelium. Eur Respir J. 1996;9(10):2145-50.

58. Chmiel JF, Aksamit TR, Chotirmall SH, Dasenbrook EC, Elborn JS, LiPuma JJ, et al. Antibiotic management of lung infections in cystic fibrosis. I. The microbiome, methicillin-resistant Staphylococcus aureus, gram-negative bacteria, and multiple infections. Ann Am Thorac Soc. 2014;11(7):1120-9.

59. Lieberman TD, Flett KB, Yelin I, Martin TR, McAdam AJ, Priebe GP, et al. Genetic variation of a bacterial pathogen within individuals with cystic fibrosis provides a record of selective pressures. Nat Genet. 2014;46(1):82-7.

60. Erfanimanesh S, Emaneini M, Modaresi MR, Feizabadi MM, Halimi S, Beigverdi R, et al. Distribution and Characteristics of Bacteria Isolated from Cystic Fibrosis Patients with Pulmonary Exacerbation. Canadian Journal of Infectious Diseases and Medical Microbiology. 2022;2022:5831139.

61. Downey DG, Bell SC, Elborn JS. Neutrophils in cystic fibrosis. Thorax. 2009;64(1):81-8.

62. Sagel SD, Wagner BD, Anthony MM, Emmett P, Zemanick ET. Sputum biomarkers of inflammation and lung function decline in children with cystic fibrosis. Am J Respir Crit Care Med. 2012;186(9):857-65.

63. Parker D, Prince A. Innate immunity in the respiratory epithelium. Am J Respir Cell Mol Biol. 2011;45(2):189-201.

64. Esther CR, Jr., Muhlebach MS, Ehre C, Hill DB, Wolfgang MC, Kesimer M, et al. Mucus accumulation in the lungs precedes structural changes and infection in children with cystic fibrosis. Sci Transl Med. 2019;11(486).

65. Rosen BH, Evans TIA, Moll SR, Gray JS, Liang B, Sun X, et al. Infection Is Not Required for Mucoinflammatory Lung Disease in CFTR-Knockout Ferrets. Am J Respir Crit Care Med. 2018;197(10):1308-18.

66. Kube D, Sontich U, Fletcher D, Davis PB. Proinflammatory cytokine responses to P. aeruginosa infection in human airway epithelial cell lines. Am J Physiol Lung Cell Mol Physiol. 2001;280(3):L493-502.
67. Bérubé J, Roussel L, Nattagh L, Rousseau S. Loss of cystic fibrosis transmembrane conductance regulator function enhances activation of p38 and ERK MAPKs, increasing interleukin-6 synthesis in airway epithelial cells exposed to Pseudomonas aeruginosa. J Biol Chem. 2010;285(29):22299-307.
68. Carrabino S, Carpani D, Livraghi A, Di Cicco M, Costantini D, Copreni E, et al. Dysregulated interleukin-8 secretion and NF-κB activity in human cystic fibrosis nasal epithelial cells. Journal of Cystic Fibrosis. 2006;5(2):113-9.
69. Mogensen TH. Pathogen recognition and inflammatory signaling in innate immune defenses. Clin Microbiol Rev. 2009;22(2):240-73, Table of Contents.
70. Cohen TS, Prince A. Cystic fibrosis: a mucosal immunodeficiency syndrome. Nat Med. 2012;18(4):509-19.
71. Cantin AM, Hartl D, Konstan MW, Chmiel JF. Inflammation in cystic fibrosis lung disease: Pathogenesis and therapy. Journal of Cystic Fibrosis. 2015;14(4):419-30.
72. Malhotra S, Hayes D, Jr., Wozniak DJ. Cystic Fibrosis and Pseudomonas aeruginosa: the Host-Microbe Interface. Clin Microbiol Rev. 2019;32(3).
73. Stoltz DA, Meyerholz DK, Pezzulo AA, Ramachandran S, Rogan MP, Davis GJ, et al. Cystic fibrosis pigs develop lung disease and exhibit defective bacterial eradication at birth. Sci Transl Med. 2010;2(29):29ra31.
74. Le Gall F, Le Berre R, Rosec S, Hardy J, Gouriou S, Boisramé-Gastrin S, et al. Proposal of a quantitative PCR-based protocol for an optimal Pseudomonas aeruginosa detection in patients with cystic fibrosis. BMC Microbiol. 2013;13:143.
75. Dittrich AS, Kühbandner I, Gehrig S, Rickert-Zacharias V, Twigg M, Wege S, et al. Elastase activity on sputum neutrophils correlates with severity of lung disease in cystic fibrosis. European Respiratory Journal. 2018;51(3):1701910.
76. McKelvey MC, Weldon S, McAuley DF, Mall MA, Taggart CC. Targeting Proteases in Cystic Fibrosis Lung Disease. Paradigms, Progress, and Potential. American Journal of Respiratory and Critical Care Medicine. 2020;201(2):141-7.
77. Le Gars M, Descamps D, Roussel D, Saussereau E, Guillot L, Ruffin M, et al. Neutrophil elastase degrades cystic fibrosis transmembrane conductance regulator via calpains and disables channel function in vitro and in vivo. Am J Respir Crit Care Med. 2013;187(2):170-9.

78. Caldwell RA, Boucher RC, Stutts MJ. Neutrophil elastase activates near-silent epithelial Na+ channels and increases airway epithelial Na+ transport. Am J Physiol Lung Cell Mol Physiol. 2005;288(5):L813-9.

79. Reihill J, Moffitt K, Douglas L, Stuart Elborn J, Jones A, Lorraine Martin S. Sputum trypsin-like protease activity relates to clinical outcome in cystic fibrosis. Journal of Cystic Fibrosis. 2020;19(4):647-53.

80. Shteinberg M, Haq IJ, Polineni D, Davies JC. Cystic fibrosis. Lancet. 2021;397(10290):2195-211.

81. Naehrig S, Chao CM, Naehrlich L. Cystic Fibrosis. Dtsch Arztebl Int. 2017;114(33-34):564-74.

82. Kristidis P, Bozon D, Corey M, Markiewicz D, Rommens J, Tsui LC, et al. Genetic determination of exocrine pancreatic function in cystic fibrosis. Am J Hum Genet. 1992;50(6):1178-84.

83. Singh VK, Schwarzenberg SJ. Pancreatic insufficiency in Cystic Fibrosis. J Cyst Fibros. 2017;16 Suppl 2:S70-s8.

84. Taylor CJ, Aswani N. The pancreas in cystic fibrosis. Paediatr Respir Rev. 2002;3(1):77-81.

85. Sabharwal S. Gastrointestinal Manifestations of Cystic Fibrosis. Gastroenterol Hepatol (N Y). 2016;12(1):43-7.

86. van der Doef HP, Kokke FT, van der Ent CK, Houwen RH. Intestinal obstruction syndromes in cystic fibrosis: meconium ileus, distal intestinal obstruction syndrome, and constipation. Curr Gastroenterol Rep. 2011;13(3):265-70.

87. Diwakar V, Pearson L, Beath S. Liver disease in children with cystic fibrosis. Paediatr Respir Rev. 2001;2(4):340-9.

88. Kobelska-Dubiel N, Klincewicz B, Cichy W. Liver disease in cystic fibrosis. Prz Gastroenterol. 2014;9(3):136-41.

89. Lopes-Pacheco M. CFTR Modulators: The Changing Face of Cystic Fibrosis in the Era of Precision Medicine. Front Pharmacol. 2019;10:1662.

90. Lee J-A, Cho A, Huang EN, Xu Y, Quach H, Hu J, et al. Gene therapy for cystic fibrosis: new tools for precision medicine. Journal of Translational Medicine. 2021;19(1):452.

91. Mergiotti M, Murabito A, Prono G, Ghigo A. CFTR Modulator Therapy for Rare CFTR Mutants. Journal of Respiration. 2022;2(2):59-76.

92. Ramalho AS, Fürstová E, Vonk AM, Ferrante M, Verfaillie C, Dupont L, et al. Correction of CFTR function in intestinal organoids to guide treatment of cystic fibrosis. Eur Respir J. 2021;57(1).
93. O'Shea KM, O'Carroll OM, Carroll C, Grogan B, Connolly A, O'Shaughnessy L, et al. Efficacy of elexacaftor/tezacaftor/ivacaftor in patients with cystic fibrosis and advanced lung disease. Eur Respir J. 2021;57(2).
94. Rowe SM, Heltshe SL, Gonska T, Donaldson SH, Borowitz D, Gelfond D, et al. Clinical mechanism of the cystic fibrosis transmembrane conductance regulator potentiator ivacaftor in G551D-mediated cystic fibrosis. Am J Respir Crit Care Med. 2014;190(2):175-84.
95. Hisert KB, Heltshe SL, Pope C, Jorth P, Wu X, Edwards RM, et al. Restoring Cystic Fibrosis Transmembrane Conductance Regulator Function Reduces Airway Bacteria and Inflammation in People with Cystic Fibrosis and Chronic Lung Infections. Am J Respir Crit Care Med. 2017;195(12):1617-28.
96. Ricotta EE, Prevots DR, Olivier KN. CFTR modulator use and risk of nontuberculous mycobacteria positivity in cystic fibrosis, 2011–2018. ERJ Open Research. 2022;8(2):00724-2021.
97. King P, Citron DM, Griffith DC, Lomovskaya O, Dudley MN. Effect of oxygen limitation on the in vitro activity of levofloxacin and other antibiotics administered by the aerosol route against Pseudomonas aeruginosa from cystic fibrosis patients. Diagn Microbiol Infect Dis. 2010;66(2):181-6.
98. Folkesson A, Jelsbak L, Yang L, Johansen HK, Ciofu O, Høiby N, et al. Adaptation of Pseudomonas aeruginosa to the cystic fibrosis airway: an evolutionary perspective. Nat Rev Microbiol. 2012;10(12):841-51.
99. Douglas TA, Brennan S, Gard S, Berry L, Gangell C, Stick SM, et al. Acquisition and eradication of P. aeruginosa in young children with cystic fibrosis. Eur Respir J. 2009;33(2):305-11.
100. Høiby N, Frederiksen B, Pressler T. Eradication of early Pseudomonas aeruginosa infection. J Cyst Fibros. 2005;4 Suppl 2:49-54.
101. Stanojevic S, Waters V, Mathew JL, Taylor L, Ratjen F. Effectiveness of inhaled tobramycin in eradicating Pseudomonas aeruginosa in children with cystic fibrosis. J Cyst Fibros. 2014;13(2):172-8.
102. Vidya P, Smith L, Beaudoin T, Yau YC, Clark S, Coburn B, et al. Chronic infection phenotypes of Pseudomonas aeruginosa are associated with failure of eradication in children with cystic fibrosis. Eur J Clin Microbiol Infect Dis. 2016;35(1):67-74.

103. Tramper-Stranders GA, van der Ent CK, Molin S, Yang L, Hansen SK, Rau MH, et al. Initial Pseudomonas aeruginosa infection in patients with cystic fibrosis: characteristics of eradicated and persistent isolates. Clin Microbiol Infect. 2012;18(6):567-74.
104. Kwong K, Benedetti A, Yau Y, Waters V, Nguyen D. Failed Eradication Therapy of New-Onset Pseudomonas aeruginosa Infections in Children With Cystic Fibrosis Is Associated With Bacterial Resistance to Neutrophil Functions. J Infect Dis. 2022;225(11):1886-95.
105. Ehsan Z, Clancy JP. Management of Pseudomonas aeruginosa infection in cystic fibrosis patients using inhaled antibiotics with a focus on nebulized liposomal amikacin. Future Microbiol. 2015;10(12):1901-12.
106. Bhatt JM. Treatment of pulmonary exacerbations in cystic fibrosis. European Respiratory Review. 2013;22(129):205-16.
107. Goss CH. Acute Pulmonary Exacerbations in Cystic Fibrosis. Semin Respir Crit Care Med. 2019;40(6):792-803.
108. Sanders DB, Bittner RC, Rosenfeld M, Hoffman LR, Redding GJ, Goss CH. Failure to recover to baseline pulmonary function after cystic fibrosis pulmonary exacerbation. Am J Respir Crit Care Med. 2010;182(5):627-32.
109. Sanders DB, Bittner RC, Rosenfeld M, Redding GJ, Goss CH. Pulmonary exacerbations are associated with subsequent FEV1 decline in both adults and children with cystic fibrosis. Pediatr Pulmonol. 2011;46(4):393-400.
110. Asner S, Waters V, Solomon M, Yau Y, Richardson SE, Grasemann H, et al. Role of respiratory viruses in pulmonary exacerbations in children with cystic fibrosis. J Cyst Fibros. 2012;11(5):433-9.
111. Skolnik K, Kirkpatrick G, Quon BS. Nontuberculous Mycobacteria in Cystic Fibrosis. Curr Treat Options Infect Dis. 2016;8(4):259-74.
112. Esther CR, Jr., Esserman DA, Gilligan P, Kerr A, Noone PG. Chronic Mycobacterium abscessus infection and lung function decline in cystic fibrosis. J Cyst Fibros. 2010;9(2):117-23.
113. Chalermskulrat W, Sood N, Neuringer IP, Hecker TM, Chang L, Rivera MP, et al. Non-tuberculous mycobacteria in end stage cystic fibrosis: implications for lung transplantation. Thorax. 2006;61(6):507-13.
114. Konstan MW, Byard PJ, Hoppel CL, Davis PB. Effect of high-dose ibuprofen in patients with cystic fibrosis. N Engl J Med. 1995;332(13):848-54.
115. Lands LC, Milner R, Cantin AM, Manson D, Corey M. High-dose ibuprofen in cystic fibrosis: Canadian safety and effectiveness trial. J Pediatr. 2007;151(3):249-54.

116. Legssyer R, Huaux F, Lebacq J, Delos M, Marbaix E, Lebecque P, et al. Azithromycin reduces spontaneous and induced inflammation in ΔF508 cystic fibrosis mice. Respiratory Research. 2006;7(1):134.
117. Clement A, Tamalet A, Leroux E, Ravilly S, Fauroux B, Jais JP. Long term effects of azithromycin in patients with cystic fibrosis: A double blind, placebo controlled trial. Thorax. 2006;61(10):895-902.
118. Saiman L, Anstead M, Mayer-Hamblett N, Lands LC, Kloster M, Hocevar-Trnka J, et al. Effect of azithromycin on pulmonary function in patients with cystic fibrosis uninfected with Pseudomonas aeruginosa: a randomized controlled trial. Jama. 2010;303(17):1707-15.
119. Cogen JD, Onchiri F, Emerson J, Gibson RL, Hoffman LR, Nichols DP, et al. Chronic Azithromycin Use in Cystic Fibrosis and Risk of Treatment-Emergent Respiratory Pathogens. Ann Am Thorac Soc. 2018;15(6):702-9.
120. Saiman L, Marshall BC, Mayer-Hamblett N, Burns JL, Quittner AL, Cibene DA, et al. Azithromycin in patients with cystic fibrosis chronically infected with Pseudomonas aeruginosa: a randomized controlled trial. Jama. 2003;290(13):1749-56.
121. Nichols DP, Odem-Davis K, Cogen JD, Goss CH, Ren CL, Skalland M, et al. Pulmonary Outcomes Associated with Long-Term Azithromycin Therapy in Cystic Fibrosis. Am J Respir Crit Care Med. 2020;201(4):430-7.
122. Eigen H, Rosenstein BJ, FitzSimmons S, Schidlow DV. A multicenter study of alternate-day prednisone therapy in patients with cystic fibrosis. Cystic Fibrosis Foundation Prednisone Trial Group. J Pediatr. 1995;126(4):515-23.
123. Mogayzel PJ, Jr., Naureckas ET, Robinson KA, Mueller G, Hadjiliadis D, Hoag JB, et al. Cystic fibrosis pulmonary guidelines. Chronic medications for maintenance of lung health. Am J Respir Crit Care Med. 2013;187(7):680-9.
124. Konstan MW, Döring G, Heltshe SL, Lands LC, Hilliard KA, Koker P, et al. A randomized double blind, placebo controlled phase 2 trial of BIIL 284 BS (an LTB4 receptor antagonist) for the treatment of lung disease in children and adults with cystic fibrosis. J Cyst Fibros. 2014;13(2):148-55.
125. Döring G, Bragonzi A, Paroni M, Aktürk FF, Cigana C, Schmidt A, et al. BIIL 284 reduces neutrophil numbers but increases P. aeruginosa bacteremia and inflammation in mouse lungs. J Cyst Fibros. 2014;13(2):156-63.
126. Crone S, Vives-Flórez M, Kvich L, Saunders AM, Malone M, Nicolaisen MH, et al. The environmental occurrence of Pseudomonas aeruginosa. APMIS. 2020;128(3):220-31.

127. Diggle SP, Whiteley M. Microbe Profile: Pseudomonas aeruginosa: opportunistic pathogen and lab rat. Microbiology (Reading). 2020;166(1):30-3.
128. Rojo F. Carbon catabolite repression in Pseudomonas: optimizing metabolic versatility and interactions with the environment. FEMS Microbiology Reviews. 2010;34(5):658-84.
129. Gomila M, Peña A, Mulet M, Lalucat J, García-Valdés E. Phylogenomics and systematics in Pseudomonas. Frontiers in Microbiology. 2015;6.
130. Silby MW, Winstanley C, Godfrey SA, Levy SB, Jackson RW. Pseudomonas genomes: diverse and adaptable. FEMS Microbiol Rev. 2011;35(4):652-80.
131. Scales BS, Dickson RP, LiPuma JJ, Huffnagle GB. Microbiology, genomics, and clinical significance of the Pseudomonas fluorescens species complex, an unappreciated colonizer of humans. Clin Microbiol Rev. 2014;27(4):927-48.
132. Klockgether J, Cramer N, Wiehlmann L, Davenport CF, Tümmler B. Pseudomonas aeruginosa Genomic Structure and Diversity. Front Microbiol. 2011;2:150.
133. Fleischmann RD, Adams MD, White O, Clayton RA, Kirkness EF, Kerlavage AR, et al. Whole-genome random sequencing and assembly of Haemophilus influenzae Rd. Science. 1995;269(5223):496-512.
134. Wang J, Liu Y, Wan D, Fang X, Li T, Guo Y, et al. Whole-Genome Sequence of Staphylococcus aureus Strain LCT-SA112. Journal of Bacteriology. 2012;194(15):4124-.
135. Freschi L, Vincent AT, Jeukens J, Emond-Rheault JG, Kukavica-Ibrulj I, Dupont MJ, et al. The Pseudomonas aeruginosa Pan-Genome Provides New Insights on Its Population Structure, Horizontal Gene Transfer, and Pathogenicity. Genome Biol Evol. 2019;11(1):109-20.
136. Stover CK, Pham XQ, Erwin AL, Mizoguchi SD, Warrener P, Hickey MJ, et al. Complete genome sequence of Pseudomonas aeruginosa PAO1, an opportunistic pathogen. Nature. 2000;406(6799):959-64.
137. Lee J, Zhang L. The hierarchy quorum sensing network in Pseudomonas aeruginosa. Protein Cell. 2015;6(1):26-41.
138. Schuster M, Greenberg EP. A network of networks: quorum-sensing gene regulation in Pseudomonas aeruginosa. Int J Med Microbiol. 2006;296(2-3):73-81.
139. Gambello MJ, Kaye S, Iglewski BH. LasR of Pseudomonas aeruginosa is a transcriptional activator of the alkaline protease gene (apr) and an enhancer of exotoxin A expression. Infect Immun. 1993;61(4):1180-4.

140. Higgins S, Heeb S, Rampioni G, Fletcher MP, Williams P, Cámara M. Differential Regulation of the Phenazine Biosynthetic Operons by Quorum Sensing in Pseudomonas aeruginosa PAO1-N. Frontiers in Cellular and Infection Microbiology. 2018;8.
141. Venturi V. Regulation of quorum sensing in Pseudomonas. FEMS Microbiology Reviews. 2006;30(2):274-91.
142. Dekimpe V, Déziel E. Revisiting the quorum-sensing hierarchy in Pseudomonas aeruginosa: the transcriptional regulator RhlR regulates LasR-specific factors. Microbiology. 2009;155(3):712-23.
143. Feltner JB, Wolter DJ, Pope CE, Groleau M-C, Smalley NE, Greenberg EP, et al. LasR Variant Cystic Fibrosis Isolates Reveal an Adaptable Quorum-Sensing Hierarchy in Pseudomonas aeruginosa. mBio. 2016;7(5):e01513-16.
144. Alcorn JF, Wright JR. Degradation of pulmonary surfactant protein D by Pseudomonas aeruginosa elastase abrogates innate immune function. J Biol Chem. 2004;279(29):30871-9.
145. Laarman AJ, Bardoel BW, Ruyken M, Fernie J, Milder FJ, van Strijp JA, et al. Pseudomonas aeruginosa alkaline protease blocks complement activation via the classical and lectin pathways. J Immunol. 2012;188(1):386-93.
146. Hoffman LR, Kulasekara HD, Emerson J, Houston LS, Burns JL, Ramsey BW, et al. Pseudomonas aeruginosa lasR mutants are associated with cystic fibrosis lung disease progression. J Cyst Fibros. 2009;8(1):66-70.
147. Wilder CN, Allada G, Schuster M. Instantaneous within-patient diversity of Pseudomonas aeruginosa quorum-sensing populations from cystic fibrosis lung infections. Infect Immun. 2009;77(12):5631-9.
148. LaFayette SL, Houle D, Beaudoin T, Wojewodka G, Radzioch D, Hoffman LR, et al. Cystic fibrosis-adapted Pseudomonas aeruginosa quorum sensing lasR mutants cause hyperinflammatory responses. Sci Adv. 2015;1(6).
149. Bassetti M, Vena A, Croxatto A, Righi E, Guery B. How to manage Pseudomonas aeruginosa infections. Drugs Context. 2018;7:212527.
150. Stern GA. Pseudomonas keratitis and contact lens wear: the lens/eye is at fault. Cornea. 1990;9 Suppl 1:S36-8; discussion S9-40.
151. Ronald A. The etiology of urinary tract infection: traditional and emerging pathogens. The American Journal of Medicine. 2002;113(1, Supplement 1):14-9.
152. Trautner BW, Darouiche RO. Catheter-associated infections: pathogenesis affects prevention. Arch Intern Med. 2004;164(8):842-50.

153. Cole SJ, Records AR, Orr MW, Linden SB, Lee VT. Catheter-associated urinary tract infection by Pseudomonas aeruginosa is mediated by exopolysaccharide-independent biofilms. Infect Immun. 2014;82(5):2048-58.
154. Davies JC. Pseudomonas aeruginosa in cystic fibrosis: pathogenesis and persistence. Paediatr Respir Rev. 2002;3(2):128-34.
155. Martínez-Solano L, Macia MD, Fajardo A, Oliver A, Martinez JL. Chronic Pseudomonas aeruginosa infection in chronic obstructive pulmonary disease. Clin Infect Dis. 2008;47(12):1526-33.
156. Fujitani S, Sun HY, Yu VL, Weingarten JA. Pneumonia due to Pseudomonas aeruginosa: part I: epidemiology, clinical diagnosis, and source. Chest. 2011;139(4):909-19.
157. Crouch Brewer S, Wunderink RG, Jones CB, Leeper KV, Jr. Ventilator-associated pneumonia due to Pseudomonas aeruginosa. Chest. 1996;109(4):1019-29.
158. Piatti G, De Santi MM, Farolfi A, Zuccotti GV, D'Auria E, Patria MF, et al. Exacerbations and Pseudomonas aeruginosa colonization are associated with altered lung structure and function in primary ciliary dyskinesia. BMC Pediatrics. 2020;20(1):158.
159. Wilke M, Buijs-Offerman RM, Aarbiou J, Colledge WH, Sheppard DN, Touqui L, et al. Mouse models of cystic fibrosis: phenotypic analysis and research applications. J Cyst Fibros. 2011;10 Suppl 2:S152-71.
160. Mall M, Grubb BR, Harkema JR, O'Neal WK, Boucher RC. Increased airway epithelial Na+ absorption produces cystic fibrosis-like lung disease in mice. Nat Med. 2004;10(5):487-93.
161. Sun X, Sui H, Fisher JT, Yan Z, Liu X, Cho HJ, et al. Disease phenotype of a ferret CFTR-knockout model of cystic fibrosis. J Clin Invest. 2010;120(9):3149-60.
162. Lorenz A, Pawar V, Häussler S, Weiss S. Insights into host–pathogen interactions from state-of-the-art animal models of respiratory Pseudomonas aeruginosa infections. FEBS Letters. 2016;590(21):3941-59.
163. Brao KJ, Wille BP, Lieberman J, Ernst RK, Shirtliff ME, Harro JM. Scnn1b-Transgenic BALB/c Mice as a Model of Pseudomonas aeruginosa Infections of the Cystic Fibrosis Lung. Infection and Immunity. 2020;88(9):e00237-20.
164. Fothergill JL, Neill DR, Loman N, Winstanley C, Kadioglu A. Pseudomonas aeruginosa adaptation in the nasopharyngeal reservoir leads to migration and persistence in the lungs. Nat Commun. 2014;5:4780.
165. van Heeckeren AM, Schluchter MD. Murine models of chronic Pseudomonas aeruginosa lung infection. Lab Anim. 2002;36(3):291-312.

166. Lavoie EG, Wangdi T, Kazmierczak BI. Innate immune responses to Pseudomonas aeruginosa infection. Microbes Infect. 2011;13(14-15):1133-45.
167. DiMango E, Zar HJ, Bryan R, Prince A. Diverse Pseudomonas aeruginosa gene products stimulate respiratory epithelial cells to produce interleukin-8. J Clin Invest. 1995;96(5):2204-10.
168. Adamo R, Sokol S, Soong G, Gomez MI, Prince A. Pseudomonas aeruginosa flagella activate airway epithelial cells through asialoGM1 and toll-like receptor 2 as well as toll-like receptor 5. Am J Respir Cell Mol Biol. 2004;30(5):627-34.
169. Raoust E, Balloy V, Garcia-Verdugo I, Touqui L, Ramphal R, Chignard M. Pseudomonas aeruginosa LPS or flagellin are sufficient to activate TLR-dependent signaling in murine alveolar macrophages and airway epithelial cells. PLoS One. 2009;4(10):e7259.
170. Epelman S, Stack D, Bell C, Wong E, Neely GG, Krutzik S, et al. Different domains of Pseudomonas aeruginosa exoenzyme S activate distinct TLRs. J Immunol. 2004;173(3):2031-40.
171. Zhao Y, Shao F. The NAIP-NLRC4 inflammasome in innate immune detection of bacterial flagellin and type III secretion apparatus. Immunol Rev. 2015;265(1):85-102.
172. Flo TH, Ryan L, Latz E, Takeuchi O, Monks BG, Lien E, et al. Involvement of Toll-like Receptor (TLR) 2 and TLR4 in Cell Activation by Mannuronic Acid Polymers*. Journal of Biological Chemistry. 2002;277(38):35489-95.
173. Hiemstra PS, McCray PB, Jr., Bals R. The innate immune function of airway epithelial cells in inflammatory lung disease. Eur Respir J. 2015;45(4):1150-62.
174. Kooguchi K, Hashimoto S, Kobayashi A, Kitamura Y, Kudoh I, Wiener-Kronish J, et al. Role of alveolar macrophages in initiation and regulation of inflammation in Pseudomonas aeruginosa pneumonia. Infect Immun. 1998;66(7):3164-9.
175. Martin TR, Pistorese BP, Chi EY, Goodman RB, Matthay MA. Effects of leukotriene B4 in the human lung. Recruitment of neutrophils into the alveolar spaces without a change in protein permeability. J Clin Invest. 1989;84(5):1609-19.
176. Adams W, Espicha T, Estipona J. Getting Your Neutrophil: Neutrophil Transepithelial Migration in the Lung. Infection and Immunity. 2021;89(4):e00659-20.
177. Muller WA. Leukocyte-Endothelial Cell Interactions in the Inflammatory Response. Laboratory Investigation. 2002;82(5):521-34.
178. Tosi MF, Stark JM, Smith CW, Hamedani A, Gruenert DC, Infeld MD. Induction of ICAM-1 expression on human airway epithelial cells by inflammatory cytokines: effects on neutrophil-epithelial cell adhesion. Am J Respir Cell Mol Biol. 1992;7(2):214-21.

179. Qin L, Quinlan WM, Doyle NA, Graham L, Sligh JE, Takei F, et al. The roles of CD11/CD18 and ICAM-1 in acute Pseudomonas aeruginosa-induced pneumonia in mice. J Immunol. 1996;157(11):5016-21.

180. Choi H, Fleming NW, Serikov VB. Contact activation via ICAM-1 induces changes in airway epithelial permeability in vitro. Immunol Invest. 2007;36(1):59-72.

181. Lin WC, Fessler MB. Regulatory mechanisms of neutrophil migration from the circulation to the airspace. Cell Mol Life Sci. 2021;78(9):4095-124.

182. Teng TS, Ji AL, Ji XY, Li YZ. Neutrophils and Immunity: From Bactericidal Action to Being Conquered. J Immunol Res. 2017;2017:9671604.

183. Wang G, Nauseef WM. Neutrophil dysfunction in the pathogenesis of cystic fibrosis. Blood. 2022;139(17):2622-31.

184. Galli F, Battistoni A, Gambari R, Pompella A, Bragonzi A, Pilolli F, et al. Oxidative stress and antioxidant therapy in cystic fibrosis. Biochimica et Biophysica Acta (BBA) - Molecular Basis of Disease. 2012;1822(5):690-713.

185. Linssen RS, Chai G, Ma J, Kummarapurugu AB, van Woensel JBM, Bem RA, et al. Neutrophil Extracellular Traps Increase Airway Mucus Viscoelasticity and Slow Mucus Particle Transit. Am J Respir Cell Mol Biol. 2021;64(1):69-78.

186. FILLOUX A. Protein Secretion Systems in Pseudomonas aeruginosa: An Essay on Diversity, Evolution, and Function. Frontiers in Microbiology. 2011;2.

187. Kessler E, Safrin M, Gustin JK, Ohman DE. Elastase and the LasA protease of Pseudomonas aeruginosa are secreted with their propeptides. J Biol Chem. 1998;273(46):30225-31.

188. Oh J, Li XH, Kim SK, Lee JH. Post-secretional activation of Protease IV by quorum sensing in Pseudomonas aeruginosa. Sci Rep. 2017;7(1):4416.

189. Golovkine G, Faudry E, Bouillot S, Voulhoux R, Attrée I, Huber P. VE-cadherin cleavage by LasB protease from Pseudomonas aeruginosa facilitates type III secretion system toxicity in endothelial cells. PLoS Pathog. 2014;10(3):e1003939.

190. Yang J, Zhao H-L, Ran L-Y, Li C-Y, Zhang X-Y, Su H-N, et al. Mechanistic Insights into Elastin Degradation by Pseudolysin, the Major Virulence Factor of the Opportunistic Pathogen Pseudomonas aeruginosa. Scientific Reports. 2015;5(1):9936.

191. Li J, Ramezanpour M, Fong SA, Cooksley C, Murphy J, Suzuki M, et al. Pseudomonas aeruginosa Exoprotein-Induced Barrier Disruption Correlates With Elastase Activity and Marks Chronic Rhinosinusitis Severity. Frontiers in Cellular and Infection Microbiology. 2019;9.

192. Heck LW, Morihara K, McRae WB, Miller EJ. Specific cleavage of human type III and IV collagens by Pseudomonas aeruginosa elastase. Infect Immun. 1986;51(1):115-8.
193. Leduc D, Beaufort N, de Bentzmann S, Rousselle JC, Namane A, Chignard M, et al. The Pseudomonas aeruginosa LasB metalloproteinase regulates the human urokinase-type plasminogen activator receptor through domain-specific endoproteolysis. Infect Immun. 2007;75(8):3848-58.
194. Dulon S, Leduc D, Cottrell GS, D'Alayer J, Hansen KK, Bunnett NW, et al. Pseudomonas aeruginosa elastase disables proteinase-activated receptor 2 in respiratory epithelial cells. Am J Respir Cell Mol Biol. 2005;32(5):411-9.
195. Leidal KG, Munson KL, Johnson MC, Denning GM. Metalloproteases from Pseudomonas aeruginosa degrade human RANTES, MCP-1, and ENA-78. J Interferon Cytokine Res. 2003;23(6):307-18.
196. Sörensen M, Kantorek J, Byrnes L, Boutin S, Mall MA, Lasitschka F, et al. Pseudomonas aeruginosa Modulates the Antiviral Response of Bronchial Epithelial Cells. Frontiers in Immunology. 2020;11.
197. Bardoel BW, van der Ent S, Pel MJ, Tommassen J, Pieterse CM, van Kessel KP, et al. Pseudomonas evades immune recognition of flagellin in both mammals and plants. PLoS Pathog. 2011;7(8):e1002206.
198. Coburn B, Sekirov I, Finlay BB. Type III secretion systems and disease. Clin Microbiol Rev. 2007;20(4):535-49.
199. dos Santos AMP, Ferrari RG, Conte-Junior CA. Type three secretion system in Salmonella Typhimurium: the key to infection. Genes & Genomics. 2020;42(5):495-506.
200. Hauser AR. The type III secretion system of Pseudomonas aeruginosa: infection by injection. Nat Rev Microbiol. 2009;7(9):654-65.
201. Kaminski A, Gupta KH, Goldufsky JW, Lee HW, Gupta V, Shafikhani SH. Pseudomonas aeruginosa ExoS Induces Intrinsic Apoptosis in Target Host Cells in a Manner That is Dependent on its GAP Domain Activity. Scientific Reports. 2018;8(1):14047.
202. Deruelle V, Bouillot S, Job V, Taillebourg E, Fauvarque MO, Attrée I, et al. The bacterial toxin ExoU requires a host trafficking chaperone for transportation and to induce necrosis. Nat Commun. 2021;12(1):4024.
203. Shaver CM, Hauser AR. Relative contributions of Pseudomonas aeruginosa ExoU, ExoS, and ExoT to virulence in the lung. Infect Immun. 2004;72(12):6969-77.

204. Diaz MH, Shaver CM, King JD, Musunuri S, Kazzaz JA, Hauser AR. Pseudomonas aeruginosa induces localized immunosuppression during pneumonia. Infect Immun. 2008;76(10):4414-21.

205. Kudoh I, Wiener-Kronish JP, Hashimoto S, Pittet JF, Frank D. Exoproduct secretions of Pseudomonas aeruginosa strains influence severity of alveolar epithelial injury. Am J Physiol. 1994;267(5 Pt 1):L551-6.

206. Kurahashi K, Kajikawa O, Sawa T, Ohara M, Gropper MA, Frank DW, et al. Pathogenesis of septic shock in Pseudomonas aeruginosa pneumonia. J Clin Invest. 1999;104(6):743-50.

207. Geiser TK, Kazmierczak BI, Garrity-Ryan LK, Matthay MA, Engel JN. Pseudomonas aeruginosa ExoT inhibits in vitro lung epithelial wound repair. Cell Microbiol. 2001;3(4):223-36.

208. Vance RE, Rietsch A, Mekalanos JJ. Role of the type III secreted exoenzymes S, T, and Y in systemic spread of Pseudomonas aeruginosa PAO1 in vivo. Infect Immun. 2005;73(3):1706-13.

209. Hauser AR, Cobb E, Bodi M, Mariscal D, Vallés J, Engel JN, et al. Type III protein secretion is associated with poor clinical outcomes in patients with ventilator-associated pneumonia caused by Pseudomonas aeruginosa. Crit Care Med. 2002;30(3):521-8.

210. Frank DW. The exoenzyme S regulon of Pseudomonas aeruginosa. Mol Microbiol. 1997;26(4):621-9.

211. Vallis AJ, Yahr TL, Barbieri JT, Frank DW. Regulation of ExoS production and secretion by Pseudomonas aeruginosa in response to tissue culture conditions. Infect Immun. 1999;67(2):914-20.

212. Rietsch A, Mekalanos JJ. Metabolic regulation of type III secretion gene expression in Pseudomonas aeruginosa. Mol Microbiol. 2006;59(3):807-20.

213. Ha U, Jin S. Growth phase-dependent invasion of Pseudomonas aeruginosa and its survival within HeLa cells. Infect Immun. 2001;69(7):4398-406.

214. Cowell BA, Chen DY, Frank DW, Vallis AJ, Fleiszig SM. ExoT of cytotoxic Pseudomonas aeruginosa prevents uptake by corneal epithelial cells. Infect Immun. 2000;68(1):403-6.

215. Deng Q, Barbieri JT. Modulation of host cell endocytosis by the type III cytotoxin, Pseudomonas ExoS. Traffic. 2008;9(11):1948-57.

216. Ince D, Sutterwala FS, Yahr TL. Secretion of Flagellar Proteins by the Pseudomonas aeruginosa Type III Secretion-Injectisome System. J Bacteriol. 2015;197(12):2003-11.

217. Reyes Ruiz VM, Ramirez J, Naseer N, Palacio NM, Siddarthan IJ, Yan BM, et al. Broad detection of bacterial type III secretion system and flagellin proteins by the human NAIP/NLRC4 inflammasome. Proc Natl Acad Sci U S A. 2017;114(50):13242-7.
218. Feldman M, Bryan R, Rajan S, Scheffler L, Brunnert S, Tang H, et al. Role of flagella in pathogenesis of Pseudomonas aeruginosa pulmonary infection. Infect Immun. 1998;66(1):43-51.
219. Bruzaud J, Tarrade J, Coudreuse A, Canette A, Herry JM, Taffin de Givenchy E, et al. Flagella but not type IV pili are involved in the initial adhesion of Pseudomonas aeruginosa PAO1 to hydrophobic or superhydrophobic surfaces. Colloids Surf B Biointerfaces. 2015;131:59-66.
220. Jain R, Behrens AJ, Kaever V, Kazmierczak BI. Type IV pilus assembly in Pseudomonas aeruginosa over a broad range of cyclic di-GMP concentrations. J Bacteriol. 2012;194(16):4285-94.
221. Lau GW, Hassett DJ, Ran H, Kong F. The role of pyocyanin in Pseudomonas aeruginosa infection. Trends Mol Med. 2004;10(12):599-606.
222. Michalska M, Wolf P. Pseudomonas Exotoxin A: optimized by evolution for effective killing. Frontiers in Microbiology. 2015;6.
223. Chen L, Zou Y, She P, Wu Y. Composition, function, and regulation of T6SS in Pseudomonas aeruginosa. Microbiol Res. 2015;172:19-25.
224. Bonneau A, Roche B, Schalk IJ. Iron acquisition in Pseudomonas aeruginosa by the siderophore pyoverdine: an intricate interacting network including periplasmic and membrane proteins. Scientific Reports. 2020;10(1):120.
225. Winstanley C, O'Brien S, Brockhurst MA. Pseudomonas aeruginosa Evolutionary Adaptation and Diversification in Cystic Fibrosis Chronic Lung Infections. Trends Microbiol. 2016;24(5):327-37.
226. Smith EE, Buckley DG, Wu Z, Saenphimmachak C, Hoffman LR, D'Argenio DA, et al. Genetic adaptation by Pseudomonas aeruginosa to the airways of cystic fibrosis patients. Proc Natl Acad Sci U S A. 2006;103(22):8487-92.
227. Huse HK, Kwon T, Zlosnik JE, Speert DP, Marcotte EM, Whiteley M. Parallel evolution in Pseudomonas aeruginosa over 39,000 generations in vivo. mBio. 2010;1(4).
228. Bianconi I, D'Arcangelo S, Esposito A, Benedet M, Piffer E, Dinnella G, et al. Persistence and Microevolution of Pseudomonas aeruginosa in the Cystic Fibrosis Lung: A Single-Patient Longitudinal Genomic Study. Frontiers in Microbiology. 2019;9.

229. Marvig RL, Sommer LM, Molin S, Johansen HK. Convergent evolution and adaptation of Pseudomonas aeruginosa within patients with cystic fibrosis. Nat Genet. 2015;47(1):57-64.
230. Jorth P, Staudinger BJ, Wu X, Hisert KB, Hayden H, Garudathri J, et al. Regional Isolation Drives Bacterial Diversification within Cystic Fibrosis Lungs. Cell Host Microbe. 2015;18(3):307-19.
231. Clark ST, Diaz Caballero J, Cheang M, Coburn B, Wang PW, Donaldson SL, et al. Phenotypic diversity within a Pseudomonas aeruginosa population infecting an adult with cystic fibrosis. Sci Rep. 2015;5:10932.
232. Williams D, Evans B, Haldenby S, Walshaw MJ, Brockhurst MA, Winstanley C, et al. Divergent, coexisting Pseudomonas aeruginosa lineages in chronic cystic fibrosis lung infections. Am J Respir Crit Care Med. 2015;191(7):775-85.
233. Valentini M, Filloux A. Biofilms and Cyclic di-GMP (c-di-GMP) Signaling: Lessons from Pseudomonas aeruginosa and Other Bacteria. J Biol Chem. 2016;291(24):12547-55.
234. Mikkelsen H, Sivaneson M, Filloux A. Key two-component regulatory systems that control biofilm formation in Pseudomonas aeruginosa. Environmental Microbiology. 2011;13(7):1666-81.
235. Moscoso JA, Jaeger T, Valentini M, Hui K, Jenal U, Filloux A. The Diguanylate Cyclase SadC Is a Central Player in Gac/Rsm-Mediated Biofilm Formation in Pseudomonas aeruginosa. Journal of Bacteriology. 2014;196(23):4081-8.
236. Sall KM, Casabona MG, Bordi C, Huber P, de Bentzmann S, Attrée I, et al. A gacS deletion in Pseudomonas aeruginosa cystic fibrosis isolate CHA shapes its virulence. PLoS One. 2014;9(4):e95936.
237. Römling U, Wingender J, Müller H, Tümmler B. A major Pseudomonas aeruginosa clone common to patients and aquatic habitats. Appl Environ Microbiol. 1994;60(6):1734-8.
238. Diaz Caballero J, Clark ST, Coburn B, Zhang Y, Wang PW, Donaldson SL, et al. Selective Sweeps and Parallel Pathoadaptation Drive Pseudomonas aeruginosa Evolution in the Cystic Fibrosis Lung. mBio. 2015;6(5):e00981-15.
239. Glen KA, Lamont IL. β-lactam Resistance in Pseudomonas aeruginosa: Current Status, Future Prospects. Pathogens. 2021;10(12).
240. Poole K. Aminoglycoside resistance in Pseudomonas aeruginosa. Antimicrob Agents Chemother. 2005;49(2):479-87.
241. Rehman A, Patrick WM, Lamont IL. Mechanisms of ciprofloxacin resistance in Pseudomonas aeruginosa: new approaches to an old problem. Journal of Medical Microbiology. 2019;68(1):1-10.

242. Dößelmann B, Willmann M, Steglich M, Bunk B, Nübel U, Peter S, et al. Rapid and Consistent Evolution of Colistin Resistance in Extensively Drug-Resistant Pseudomonas aeruginosa during Morbidostat Culture. Antimicrobial Agents and Chemotherapy. 2017;61(9):e00043-17.
243. Jorth P, McLean K, Ratjen A, Secor PR, Bautista GE, Ravishankar S, et al. Evolved Aztreonam Resistance Is Multifactorial and Can Produce Hypervirulence in Pseudomonas aeruginosa. mBio. 2017;8(5):e00517-17.
244. Hurley MN, Ariff AH, Bertenshaw C, Bhatt J, Smyth AR. Results of antibiotic susceptibility testing do not influence clinical outcome in children with cystic fibrosis. J Cyst Fibros. 2012;11(4):288-92.
245. Ciofu O, Tolker-Nielsen T. Tolerance and Resistance of Pseudomonas aeruginosa Biofilms to Antimicrobial Agents—How P. aeruginosa Can Escape Antibiotics. Frontiers in Microbiology. 2019;10.
246. Sulaiman JE, Lam H. Evolution of Bacterial Tolerance Under Antibiotic Treatment and Its Implications on the Development of Resistance. Frontiers in Microbiology. 2021;12.
247. Nguyen D, Joshi-Datar A, Lepine F, Bauerle E, Olakanmi O, Beer K, et al. Active Starvation Responses Mediate Antibiotic Tolerance in Biofilms and Nutrient-Limited Bacteria. Science. 2011;334(6058):982-6.
248. Martins D, McKay G, Sampathkumar G, Khakimova M, English AM, Nguyen D. Superoxide dismutase activity confers (p)ppGpp-mediated antibiotic tolerance to stationary-phase Pseudomonas aeruginosa. Proceedings of the National Academy of Sciences. 2018;115(39):9797-802.
249. Meylan S, Andrews IW, Collins JJ. Targeting Antibiotic Tolerance, Pathogen by Pathogen. Cell. 2018;172(6):1228-38.
250. Levin-Reisman I, Ronin I, Gefen O, Braniss I, Shoresh N, Balaban NQ. Antibiotic tolerance facilitates the evolution of resistance. Science. 2017;355(6327):826-30.
251. Alhede M, Bjarnsholt T, Givskov M, Alhede M. Chapter One - Pseudomonas aeruginosa Biofilms: Mechanisms of Immune Evasion. In: Sariaslani S, Gadd GM, editors. Advances in Applied Microbiology. 86: Academic Press; 2014. p. 1-40.
252. Jesaitis AJ, Franklin MJ, Berglund D, Sasaki M, Lord CI, Bleazard JB, et al. Compromised Host Defense on Pseudomonas aeruginosa Biofilms: Characterization of Neutrophil and Biofilm Interactions. The Journal of Immunology. 2003;171(8):4329-39.

253. Pier GB, Coleman F, Grout M, Franklin M, Ohman DE. Role of alginate O acetylation in resistance of mucoid Pseudomonas aeruginosa to opsonic phagocytosis. Infect Immun. 2001;69(3):1895-901.

254. Mishra M, Byrd MS, Sergeant S, Azad AK, Parsek MR, McPhail L, et al. Pseudomonas aeruginosa Psl polysaccharide reduces neutrophil phagocytosis and the oxidative response by limiting complement-mediated opsonization. Cell Microbiol. 2012;14(1):95-106.

255. Malhotra S, Limoli DH, English AE, Parsek MR, Wozniak DJ. Mixed Communities of Mucoid and Nonmucoid Pseudomonas aeruginosa Exhibit Enhanced Resistance to Host Antimicrobials. mBio. 2018;9(2).

256. Learn DB, Brestel EP, Seetharama S. Hypochlorite scavenging by Pseudomonas aeruginosa alginate. Infect Immun. 1987;55(8):1813-8.

257. Munck A, Bonacorsi S, Mariani-Kurkdjian P, Lebourgeois M, Gérardin M, Brahimi N, et al. Genotypic characterization of Pseudomonas aeruginosa strains recovered from patients with cystic fibrosis after initial and subsequent colonization. Pediatr Pulmonol. 2001;32(4):288-92.

258. Hansen SK, Rau MH, Johansen HK, Ciofu O, Jelsbak L, Yang L, et al. Evolution and diversification of Pseudomonas aeruginosa in the paranasal sinuses of cystic fibrosis children have implications for chronic lung infection. Isme j. 2012;6(1):31-45.

259. Dosanjh A, Lakhani S, Elashoff D, Chin C, Hsu V, Hilman B. A comparison of microbiologic flora of the sinuses and airway among cystic fibrosis patients with maxillary antrostomies. Pediatr Transplant. 2000;4(3):182-5.

260. Mainz JG, Naehrlich L, Schien M, Käding M, Schiller I, Mayr S, et al. Concordant genotype of upper and lower airways P aeruginosa and S aureus isolates in cystic fibrosis. Thorax. 2009;64(6):535-40.

261. Fleiszig SM, Zaidi TS, Fletcher EL, Preston MJ, Pier GB. Pseudomonas aeruginosa invades corneal epithelial cells during experimental infection. Infect Immun. 1994;62(8):3485-93.

262. Fleiszig SM, Zaidi TS, Preston MJ, Grout M, Evans DJ, Pier GB. Relationship between cytotoxicity and corneal epithelial cell invasion by clinical isolates of Pseudomonas aeruginosa. Infect Immun. 1996;64(6):2288-94.

263. Pier GB, Grout M, Zaidi TS, Olsen JC, Johnson LG, Yankaskas JR, et al. Role of mutant CFTR in hypersusceptibility of cystic fibrosis patients to lung infections. Science. 1996;271(5245):64-7.

264. Anderson GG, Dodson KW, Hooton TM, Hultgren SJ. Intracellular bacterial communities of uropathogenic Escherichia coli in urinary tract pathogenesis. Trends Microbiol. 2004;12(9):424-30.
265. Hunstad DA, Justice SS. Intracellular Lifestyles and Immune Evasion Strategies of Uropathogenic Escherichia coli. Annual Review of Microbiology. 2010;64(1):203-21.
266. Mysorekar IU, Hultgren SJ. Mechanisms of uropathogenic Escherichia coli persistence and eradication from the urinary tract. Proceedings of the National Academy of Sciences. 2006;103(38):14170-5.
267. Peyrusson F, Varet H, Nguyen TK, Legendre R, Sismeiro O, Coppée J-Y, et al. Intracellular Staphylococcus aureus persisters upon antibiotic exposure. Nature Communications. 2020;11(1):2200.
268. Martínez-Figueroa C, Cortés-Sarabia K, del Carmen Alarcón-Romero L, Catalán-Nájera HG, Martínez-Alarcón M, Vences-Velázquez A. Observation of intracellular bacterial communities in urinary sediment using brightfield microscopy; a case report. BMC Urology. 2020;20(1):89.
269. Rosen DA, Hooton TM, Stamm WE, Humphrey PA, Hultgren SJ. Detection of intracellular bacterial communities in human urinary tract infection. PLoS Med. 2007;4(12):e329.
270. Scott VC, Haake DA, Churchill BM, Justice SS, Kim JH. Intracellular Bacterial Communities: A Potential Etiology for Chronic Lower Urinary Tract Symptoms. Urology. 2015;86(3):425-31.
271. Penaranda C, Chumbler NM, Hung DT. Dual transcriptional analysis reveals adaptation of host and pathogen to intracellular survival of Pseudomonas aeruginosa associated with urinary tract infection. PLoS Pathog. 2021;17(4):e1009534.
272. Kazmierczak BI, Jou TS, Mostov K, Engel JN. Rho GTPase activity modulates Pseudomonas aeruginosa internalization by epithelial cells. Cellular Microbiology. 2001;3(2):85-98.
273. Garcia-Medina R, Dunne WM, Singh PK, Brody SL. Pseudomonas aeruginosa Acquires Biofilm-Like Properties within Airway Epithelial Cells. Infection and Immunity. 2005;73(12):8298-305.
274. Fleiszig SM, Arora SK, Van R, Ramphal R. FlhA, a component of the flagellum assembly apparatus of Pseudomonas aeruginosa, plays a role in internalization by corneal epithelial cells. Infect Immun. 2001;69(8):4931-7.

275. Zaidi TS, Fleiszig SM, Preston MJ, Goldberg JB, Pier GB. Lipopolysaccharide outer core is a ligand for corneal cell binding and ingestion of Pseudomonas aeruginosa. Invest Ophthalmol Vis Sci. 1996;37(6):976-86.

276. Comolli JC, Waite LL, Mostov KE, Engel JN. Pili binding to asialo-GM1 on epithelial cells can mediate cytotoxicity or bacterial internalization by Pseudomonas aeruginosa. Infect Immun. 1999;67(7):3207-14.

277. Novoa A, Eierhoff T, Topin J, Varrot A, Barluenga S, Imberty A, et al. A LecA ligand identified from a galactoside-conjugate array inhibits host cell invasion by Pseudomonas aeruginosa. Angew Chem Int Ed Engl. 2014;53(34):8885-9.

278. Eierhoff T, Bastian B, Thuenauer R, Madl J, Audfray A, Aigal S, et al. A lipid zipper triggers bacterial invasion. Proceedings of the National Academy of Sciences. 2014;111(35):12895-900.

279. Mittal R, Grati M, Gerring R, Blackwelder P, Yan D, Li JD, et al. In vitro interaction of Pseudomonas aeruginosa with human middle ear epithelial cells. PLoS One. 2014;9(3):e91885.

280. Sana TG, Baumann C, Merdes A, Soscia C, Rattei T, Hachani A, et al. Internalization of Pseudomonas aeruginosa Strain PAO1 into Epithelial Cells Is Promoted by Interaction of a T6SS Effector with the Microtubule Network. mBio. 2015;6(3):e00712-15.

281. Fleiszig SM, Zaidi TS, Pier GB. Pseudomonas aeruginosa invasion of and multiplication within corneal epithelial cells in vitro. Infect Immun. 1995;63(10):4072-7.

282. Darling KE, Dewar A, Evans TJ. Role of the cystic fibrosis transmembrane conductance regulator in internalization of Pseudomonas aeruginosa by polarized respiratory epithelial cells. Cell Microbiol. 2004;6(6):521-33.

283. Evans D, Kuo T, Kwong M, Van R, Fleiszig S. Pseudomonas aeruginosa strains with lipopolysaccharide defects exhibit reduced intracellular viability after invasion of corneal epithelial cells. Exp Eye Res. 2002;75(6):635-43.

284. Hritonenko V, Evans DJ, Fleiszig SM. Translocon-independent intracellular replication by Pseudomonas aeruginosa requires the ADP-ribosylation domain of ExoS. Microbes Infect. 2012;14(15):1366-73.

285. Heimer SR, Evans DJ, Stern ME, Barbieri JT, Yahr T, Fleiszig SM. Pseudomonas aeruginosa utilizes the type III secreted toxin ExoS to avoid acidified compartments within epithelial cells. PLoS One. 2013;8(9):e73111.

286. Kumar NG, Nieto V, Kroken AR, Jedel E, Grosser MR, Hallsten ME, et al. Pseudomonas aeruginosa can diversify after host cell invasion to establish multiple intracellular niches. bioRxiv. 2022:2022.10.07.511388.
287. Bajunaid W, Haidar-Ahmad N, Kottarampatel AH, Ourida Manigat F, Silué N, Tchagang CF, et al. The T3SS of Shigella: Expression, Structure, Function, and Role in Vacuole Escape. Microorganisms. 2020;8(12).
288. Nieto V, Kroken AR, Grosser MR, Smith BE, Metruccio MME, Hagan P, et al. Type IV Pili Can Mediate Bacterial Motility within Epithelial Cells. mBio. 2019;10(4):e02880-18.
289. Krokowski S, Lobato-Márquez D, Chastanet A, Pereira PM, Angelis D, Galea D, et al. Septins Recognize and Entrap Dividing Bacterial Cells for Delivery to Lysosomes. Cell Host Microbe. 2018;24(6):866-74.e4.
290. Jolly AL, Takawira D, Oke OO, Whiteside SA, Chang SW, Wen ER, et al. Pseudomonas aeruginosa-induced bleb-niche formation in epithelial cells is independent of actinomyosin contraction and enhanced by loss of cystic fibrosis transmembrane-conductance regulator osmoregulatory function. mBio. 2015;6(2):e02533.
291. Angus AA, Lee AA, Augustin DK, Lee EJ, Evans DJ, Fleiszig SMJ. Pseudomonas aeruginosa Induces Membrane Blebs in Epithelial Cells, Which Are Utilized as a Niche for Intracellular Replication and Motility. Infection and Immunity. 2008;76(5):1992-2001.
292. Luedtke NW, Carmichael P, Tor Y. Cellular Uptake of Aminoglycosides, Guanidinoglycosides, and Poly-arginine. Journal of the American Chemical Society. 2003;125(41):12374-5.

Preamble to Chapter 2

P.a. loss-of-function *lasR* variants are frequently detected in chronic CF infection isolates and are paradoxically associated with accelerated lung function decline compared to wild-type *lasR* isolates. Previous work by our lab and others has demonstrated that LasR-regulated proteases associated with early infection stages are capable of degrading a wide range of pro-inflammatory immune mediators including cytokines, chemokines and adhesion molecules, which likely facilitates bacterial immune evasion. In a chronic infection setting, on the other hand, loss of LasR-regulated proteases appears to result in overall increased levels of pro-inflammatory chemokines, greater neutrophilic inflammation and lung pathology.

The pro-inflammatory adhesion molecule ICAM-1 has been reported to be elevated on AEC in the CF lung, particularly in the proximity of neutrophils. While the effect of elevated ICAM-1 on AEC in the human lung remains incompletely understood, animal infection models suggest that epithelial ICAM-1 may facilitate neutrophil recruitment and/or retention within the lung during bacterial pulmonary infection. Here, we sought to investigate the interplay of *lasR* wild-type and mutant strains with AEC both *in vitro* and *in vivo* in order to examine whether altered epithelial ICAM-1 may contribute to the observed excessive inflammation triggered by *lasR* mutant strains.

Chapter 2: LasR-deficient *Pseudomonas aeruginosa* variants increase airway epithelial mICAM-1 expression and enhance neutrophilic lung inflammation

Lisa C. Hennemann[1,2], Shantelle L. LaFayette[1,2], Julien K. Malet[2], Perrine Bortolotti[2], Tianxiao Yang[2], Geoffrey A. McKay[2], Daniel Houle[2], Danuta Radzioch[3,4], Simon Rousseau[2,3], Dao Nguyen[1,2,3]

[1]Department of Microbiology and Immunology, McGill University, Montreal, Quebec, Canada.

[2]Meakins-Christie Laboratories, Translational Research in Respiratory Diseases, Research Institute of the McGill University Health Centre, Montreal, Quebec, Canada.

[3]Department of Medicine, McGill University, Montreal, Quebec, Canada.

[4]Department of Human Genetics, Research Institute of the McGill University Health Centre, Infectious Diseases and Immunity in Global Health Program Montreal, Quebec, Canada.

PLoS Pathogens. 2021 Mar 10;17(3):e1009375. doi: 10.1371/journal.ppat.1009375.

2.1 Abstract

Pseudomonas aeruginosa causes chronic airway infections, a major determinant of lung inflammation and damage in cystic fibrosis (CF). Loss-of-function *lasR* mutants commonly arise during chronic CF infections, are associated with accelerated lung function decline in CF patients and induce exaggerated neutrophilic inflammation in model systems. In this study, we investigated how *lasR* mutants modulate airway epithelial membrane bound ICAM-1 (mICAM-1), a surface adhesion molecule, and determined its impact on neutrophilic inflammation *in vitro* and *in vivo*. We demonstrated that LasR-deficient strains induce increased mICAM-1 levels in airway epithelial cells compared to wild-type strains, an effect attributable to the loss of mICAM-1 degradation by LasR-regulated proteases and associated with enhanced neutrophil adhesion. In a subacute airway infection model, we also observed that *lasR* mutant-infected mice displayed greater airway epithelial ICAM-1 expression and increased neutrophilic pulmonary inflammation. Our findings provide new insights into the intricate interplay between *lasR* mutants, LasR-regulated proteases and airway epithelial ICAM-1 expression, and reveal a new mechanism involved in the exaggerated inflammatory response induced by *lasR* mutants.

2.2 Author summary

Cystic fibrosis (CF) patients develop progressive lung disease characterized by chronic airway infections, commonly caused by the opportunistic pathogen *Pseudomonas aeruginosa*, and excessive non-resolving neutrophilic inflammation. Loss of function mutations of the *lasR* quorum sensing transcription regulator gene commonly arise during chronic *P. aeruginosa* infections and are associated with increased lung inflammation. In this study, we demonstrated that loss-of-function *lasR* mutants induced increased mICAM-1 levels on airway epithelial cells compared to wild-type *P. aeruginosa* strains in cell culture and in murine infection models. This effect was caused by the loss of ICAM-1 degradation by LasR-regulated secreted protease, facilitated neutrophil adhesion, and was associated with increased neutrophilic lung inflammation. Our study provides novel insights into the *P. aeruginosa*—airway epithelial–neutrophil interactions, and demonstrates how a common pathoadaptation of *P. aeruginosa* may drive lung disease progression by exacerbating inflammation.

2.3 Introduction

Individuals with the genetic disease Cystic Fibrosis (CF) develop progressive lung disease characterized by chronic airway infections and exuberant neutrophilic inflammation. Mutations

in the Cystic Fibrosis Transmembrane Conductance Regulator (CFTR) gene lead to impaired chloride secretion and poor mucociliary clearance, making CF patients prone to lung infections. Chronic airway infections are major drivers of persistent inflammation in CF lung disease (1). The majority of adult CF patients are infected with *Pseudomonas aeruginosa* for decades, which is associated with increased morbidity and mortality (2–4). Within the airways, *P. aeruginosa* interacts with airway epithelial cells (AEC) to induce expression of pro-inflammatory mediators, modulate inflammatory pathways and further exacerbate lung inflammation (5). Adding to a hyper-inflammatory state associated with the intrinsic CFTR defects (6,7), neutrophil responses to *P. aeruginosa* in the CF lung are both ineffective and excessive, further contributing to lung damage (8,9).

During chronic infection, *P. aeruginosa* evolves and genetically adapts to the host lung environment (10). *P. aeruginosa* isolates recovered from chronic "late" stage CF infections are genotypically and phenotypically distinct from those found in "early" stage infections, and commonly share phenotypes such as mucoidy, loss of motility or protease production (11,12). A notable example of this convergent evolution is the loss of LasR function, typically attributable to mutations in *lasR*, the gene encoding the major quorum sensing transcriptional regulator in *P. aeruginosa* (13–17). Loss of function *lasR* variants are found in at least one third of CF patients chronically infected with *P. aeruginosa* (15). Quorum sensing is a bacterial communication system that allows the coordinated expression of hundreds of *P. aeruginosa* genes, including many that encode exoproducts and virulence factors (18–20).

Although loss of LasR function leads to the attenuation of bacterial virulence in models of acute infection (12,21,22), chronic infections with *lasR* mutants in CF patients have been associated with accelerated decline in lung function (15) and increased markers of inflammation (23). To understand the impact of *P. aeruginosa lasR* mutants on host-pathogen interactions and on the inflammatory responses relevant to CF lung disease, our group previously demonstrated that *lasR* variants elicited an enhanced pro-inflammatory cytokine response in AEC due to a loss of cytokine degradation by LasR-regulated proteases, leading to greater neutrophil recruitment *in vitro*. *lasR* variants also caused exaggerated neutrophilic inflammation and immunopathology in a murine model of sub-acute airway infection (23).

Adhesion molecules, such as cell surface intercellular adhesion molecule 1 (ICAM-1), play an important role in lung inflammation (24). Membrane bound ICAM-1, expressed on endothelial and epithelial cells, is a ligand to β2 integrins on leukocytes and is involved in neutrophil

migration, adhesion, and other functions (25–28). Although the role of epithelial ICAM-1 is less well established than endothelial ICAM-1, which functions as the major adhesion receptor for leukocyte rolling-adhesion and transendothelial migration (28), studies suggest that airway epithelial ICAM-1 likely plays an important role in lung inflammation. Epithelial ICAM-1 mediates neutrophil adhesion and retention in the respiratory compartment, and contributes to lung inflammation in the setting of pulmonary infection and endotoxin-induced injury (26,29–33). In fact, epithelial cells express low levels of ICAM-1 unless infected or stimulated by inflammatory cytokines (34,35) or bacterial products including *P. aeruginosa* secreted products (31,36,37). Hubeau *et al* have also reported that AEC in the human CF lung over-express ICAM-1 compared to non-CF tissues, and ICAM-1 surface epithelial expression is associated with spatially adjacent neutrophil accumulation (38).

Since airway epithelial ICAM-1 expression is upregulated in *P. aeruginosa* infection, is a feature of CF lung disease and mediates neutrophilic inflammation in the lung, this led us to investigate the effect of *lasR* mutants on membrane bound ICAM-1 (mICAM-1) in AEC and its contribution to neutrophilic inflammation *in vitro* and *in vivo*.

2.4 Material and methods

Ethics statement

All experiments using human neutrophils were approved by the Research Ethics Board of the McGill University Health Centre (protocol 14–169), with informed written consent obtained from all subjects. All animal experiments were carried out with approval from the Animal Care Committee of the RI MUHC (AUP #2015–7586).

Bacterial strains, plasmids and growth conditions

All bacterial strains used in this study are described in detail in S2.1 Table. Primer sequences and plasmids are listed in S2.2 and S2.3 Tables respectively. To generate the constructs for inducible protease expression, the *lasA*, *aprA* and *prpL* coding sequences were amplified by PCR from the PAO1 genome using primers *lasA*-GWB5-RBS, *lasA*-GWB2, *aprA*-GWB5-RBS, *aprA*-GWB2, *prpL*-GWB5-RBS and *prpL*-GWB2 pairs respectively. The PCR products were recombined into pDONR221P5P2 using BP clonase II to generate the entry vectors pENTR-*lasA*, pENTR-*prpL* and pENTR-*aprA*. The constructed entry vectors pENTR-*lasA*, pENTR-*prpL*and pENTR-*aprA* were each recombined with the vector pJJH187 and the destination vector miniCTX2.1-Tc-GW using LR Clonase II Plus (Invitrogen) to generate the arabinose inducible constructs pEXP-*lasA*, pEXP-*prpL* and pEXP-*aprA*. The individual

expression vectors were subsequently integrated into the genome of the Late strain as previously described (23). Complemented strains were selected on LB agar containing 50 μg/ml tetracycline. Protease expression was induced with 1% (w/v) L-arabinose (ACROS Organics) added to the growth media.

P. aeruginosa filtrate preparation

Bacteria were grown overnight in 5 mL LB medium (BD Difco), washed twice in sterile phosphate-buffered saline (PBS) and the cell pellets were resuspended at an OD_{600} of 0.05 in synthetic CF medium (SCFM), which was developed to resemble the nutrient composition in CF sputum (39). 5 mL planktonic cultures were incubated at 37°C for 24h, with shaking at 250 rpm, then centrifuged for 5 min at 5000 rpm to pellet cells. The supernatants were filtered with 0.22 μm cellulose acetate filters (Fisher Scientific) to generate sterile cell-free filtrates. The remaining cell pellets were resuspended in PBS to measure the OD_{600} for estimation of the cell biomass. Filtrates were first normalized to the OD_{600} of the pellet by dilution in SCFM and then stored at -20°C until use. As control, we note that the normalization of each filtrate to the OD_{600} or total protein content of the pellet were equivalent. Each filtrate aliquot was discarded after one freeze-thaw cycle. Where indicated, filtrates were heat-inactivated for 10 min at 95°C.

Airway epithelial cell culture conditions and stimulation with *P. aeruginosa* filtrates

Immortalized human airway epithelial cells (BEAS-2B) were cultured in cell culture-grade plates in DMEM (Wisent) supplemented with 10% heat-inactivated fetal bovine serum (FBS, Wisent), penicillin and streptomycin (Wisent) at 37°C with 5% CO_2. Once 80–90% confluent, cells were seeded with 150,000 cells/well into 12- well tissue culture plates (Sarstedt) for flow cytometry experiments, or with 37,500 cells per well in 48-well tissue culture plates (Sarstedt) for neutrophil adhesion assays. Cells were seeded 48 h prior to stimulation with filtrates, and 24 h before stimulation, the culture medium was changed to starvation media (DMEM containing penicillin, streptomycin and 0.5% heat-inactivated FBS). BEAS-2Bs were stimulated with 30 μL *P. aeruginosa* filtrate (in 1 mL total volume) for flow cytometry experiments or 7.5 μL filtrate (in 250 μL total volume) for neutrophil adhesion assays for a duration of 24 h in fresh starvation media at 37°C with 5% CO_2. Equal volumes of SCFM were used as a negative control and a final concentration of 20 ng/mL TNF-α (BioLegend) was used as a positive control for ICAM-1 induction and neutrophil binding.

mICAM-1 measurement

Following stimulation with *P. aeruginosa* filtrates, the supernatants of BEAS-2B cultures were collected and 500 µL cold Accutase (STEMCELL Technologies) was added to each well and incubated at room temperature for 10 min to detach cells. The BEAS-2B cell suspensions were then added to their respective supernatants of the same well and centrifuged at 2000 rpm. The cells were resuspended in FACS buffer (PBS+1% heat-inactivated FBS), stained with 1:1000 Fixable Viability Dye eFluor 780 (eBioscience) for 25 min on ice, then with 1:50 FITC-conjugated anti-human ICAM-1 antibody or IgG_1-FITC isotype control (R&D Systems) for 30 min on ice, followed by fixation with 0.5% PFA for 10 min at room temperature. Cells were analyzed with a LSR II flow cytometer (BD Biosciences) and results were analyzed using FlowJo (BD Biosciences). For our analysis, debris (low FSC-A/SSC-A), doublets (higher SSC-A than SSC-H) and dead cells (high eFluor 780) were excluded. For each condition, the results were calculated by subtracting the median fluorescence intensity (MFI) of the isotype control from the corresponding sample's ICAM-1 MFI.

Protease activity measurements of *P. aeruginosa* filtrates

Total protease activity in filtrates was measured using the Hide-Remazol Brilliant Blue assay as previously described (40). Caseinolytic activity in filtrates was assessed by spotting 30 µL of filtrates on sterile 6mm paper disk placed on skim milk 1.5% agar plates as previously described (41) and the zone of clearance (diameter minus the 6mm filter) was measured after 16 h incubation at 37°C. Elastolytic activity in filtrates was measured by Elastin-Congo Red (ECR) assay, as previously described in detail (23).

Recombinant human ICAM-1 (rhICAM-1) degradation assay

To measure the ICAM-1 degradation by *P. aeruginosa* secreted proteases *in vitro*, 25 µL of 10 µg/mL (250 ng) rhICAM-1 (Peprotech) was incubated with 5 µL *P. aeruginosa* filtrate or PBS (negative control) for 24 h at 37°C, shaking at 200 rpm. The samples were then diluted in 4X loading buffer containing DTT, incubated at 95°C for 5 min, then stored at -20°C until quantification of rhICAM-1 by Western Blotting. 20 µL of each rhICAM-1 degradation sample was loaded onto 4–20% Mini-PROTEAN gels (Bio-Rad), separated by SDS-PAGE and then transferred onto PVDF membranes. The blots were blocked in 5% (w/v) skim milk prior to incubation with polyclonal anti-rhICAM-1 antibody (500-P287, Peprotech) overnight at 4°C. The protein bands were detected with anti-rabbit IgG DyLight 800 4X PEG conjugated secondary antibody (Cell Signaling Technology), imaged with the Odyssey imaging system

(Li-Cor Biosciences) and quantified using the Odyssey V3.0 software (Li-Cor Biosciences). Results are shown as % band density compared to the negative control (rhICAM-1 incubated with PBS control) on the respective blot. Full blots are provided in S2.1 Spreadsheet.

Neutrophil adhesion assay

Primary human neutrophils were isolated from 5 mL whole blood collected from healthy volunteer donors using the EasySep Direct Human Neutrophil Isolation Kit (Stemcell) according to the manufacturer's instructions in phenol red-free RPMI-1640 with 1% heat-inactivated donor serum, and included incubation in RBC lysis buffer (Stemcell) for 10 min. Neutrophils were stained with 1 μM calcein-AM for 30 min in the dark at room temperature, then washed twice with media and filtered through a 40 μm nylon cell strainer cap (Fisherbrand). BEAS-2B cells were first stimulated with 30 μL *P. aeruginosa* filtrates for 24h, and after removal of the filtrate-containing media, BEAS-2B cells were co-incubated with $4x10^5$ neutrophils in phenol red-free DMEM supplemented with 1% heat-inactivated donor serum for 2 h at 37°C with 5% CO_2. Neutrophils were then removed and BEAS-2B cells were washed three times with media to remove non-adherent neutrophils. For control experiments, $4x10^5$ neutrophils were stained and co-incubated with AEC as described above or incubated in wells containing media without AEC for 2h, then washed as described above. Adherent neutrophils were counted in a blinded manner using three representative fields of view per well obtained by laser scanning confocal microscopy (10X objective, Zeiss LSM700). Statistical analysis was performed using the average number of neutrophils per field of view (1.64 mm^2) for each individual well.

Subacute murine *P. aeruginosa* airway infection

Mice were infected with *P. aeruginosa* embedded in agar beads to generate a subacute non-lethal airway infections, as previously described (23). Briefly, bacterial suspensions were mixed at 1:1 (v/v) in 2% LB and 3% molten agar with continuous stirring into mineral oil to generate bacteria embedded agar beads. Sterile PBS LB agar beads were used as a negative control. Adult male C57BL/6 mice (6 to 9 weeks old, Charles River) were infected by non-surgical intratracheal injection of 50 μL bead suspension containing ~$5*10^5$ CFU/mouse. The mice were sacrificed at 2 or 4 days post infection (p.i). After cardiac puncture, the lungs were perfused by PBS injection into the vena cava to remove blood leukocytes prior to harvest. Perfused lungs were then lavaged with 4 x 0.5 mL ice-cold PBS through an intra-tracheal catheter for collection of the bronchoalveolar fluid (BALF). To measure the pulmonary

bacterial load, lungs were harvested, homogenized and serially diluted for viable CFU counts on LB agar plates.

Immune cell counts in lung homogenates and bronchoalveolar fluid (BALF)

For lung homogenates, perfused and lavaged lungs were placed in RPMI, minced, digested with 150 U/mL collagenase (Sigma-Aldrich) for 1 h at 37°C, then homogenized through a 16G needle. Cell suspensions were then filtered through a 100 μm cell strainer (BD Biosciences) and red blood cells were lysed with 0.2% (w/v) NaCl. The remaining cells were washed, resuspended in RPMI and enumerated using a Z1 cell counter (Beckmann-Coulter). Single cell suspensions were stained with Fixable Viability Dye eFluor780 (1:1000, eBioscience), blocked with anti-murine CD16/CD32 (1:100, eBioscience) then surface stained with eFluor610-conjugated anti-murine CD45 (1:40, 30-F11, eBioscience), FITC-conjugated anti-mouse CD11c (1:200, N418, eBioscience) and eFluor710-conjugated anti-murine Ly6G (1:160, 1A8, eBioscience). Cells were fixed with Cytofix (BD) and analyzed by flow cytometry using a LSR II Fortessa X-20 (BD Biosciences) and FlowJo 10.0.7 software (BD Biosciences). Neutrophils were defined as single, live, CD45+, Ly6G high and CD11c- cells, and total neutrophil counts were calculated by multiplying the proportion of neutrophils by the total number of live cells. For the BALF, cells were spun down at 1000 rpm for 10 min, resuspended in PBS and counted by hemocytometer. For immune cell counts, cells collected from the BALF were loaded onto Shandon Cytoslides (Thermo Fisher), air-dried, stained with Shandon Kwik-Diff (Thermo Fisher) and analyzed by light microscopy to obtain average neutrophil, monocyte/macrophage and lymphocyte counts.

Lung histopathology and ICAM-1 immunofluorescence

Perfused and lavaged lungs were inflated, fixed overnight with 10% formalin phosphate solution and sectioned in 5 μM thick slices. For histopathology, paraffin-embedded lung sections were stained with H&E and images were acquired using an Olympus BX51 microscope fitted with an Olympus DP70 CCD camera. For immunofluorescence, lung sections were stained with an anti-mouse ICAM-1 primary antibody (1:1000, eBioscience, YN1/1.7.4) and OmniMap anti-rat HRP (Ventana). All slides were processed using a Ventana DISCOVERY ULTRA automated slide preparation system (Roche) at the same time. The lung sections were imaged by laser scanning confocal microscopy (20x objective, Zeiss LSM700) at Ex 488 nm/Em 518 nm to visualize the autofluorescence of the lung tissues, and Ex 542 nm/Em 568 nm to visualize the ICAM-1 signal. All lung sections were imaged using identical

confocal microscopy settings. Seven representative fields of view containing at least one airway cross-section were randomly selected per lung and imaged in a blinded manner.

Image analyses to quantify airway epithelial ICAM-1 expression were performed in two independent manners. First, the airway epithelial ICAM-1 expression of each airway was scored by visual assessment from 1 (no signal) to 10 (very strong) in a blinded manner by two independent reviewers. Second, ICAM-1 fluorescence intensity was quantified within the airway epithelium based on a manually designated region of interest (ROI) using the Icy software (V2.0.3.0, Institut Pasteur) (42). The total fluorescence intensity of each ROI above a set threshold (defined by ICAM-1 negative regions in PBS lungs) was measured and normalized to the ROI surface area (in pixels).

P. aeruginosa colony morphology

Bacteria were grown on LB agar for 16h. The presence of a metallic sheen caused by the accumulation of 4-hydroxy-2-heptylquinoline, which has previously been linked to loss of LasR function (16), was assessed visually.

N-3-oxo-dodecanoyl-homoserine lactone (3-oxo-C12-HSL) measurement

Production of the LasR autoinducer 3-oxo-C12-HSL was measured as previously described (43,44). Briefly, bacterial strains were grown in LB medium + 50 mM MOPS for 16h. 3-oxo-C12-HSL levels were quantified using the bioassay strain E. coli DH5α expressing pJN105L and pSC11.

Statistical analyses

All results are shown as mean ± SD or SEM (as indicated), unless otherwise stated in the figure legends. Statistical analyses between two groups were performed using an unpaired two-tailed t-test or Mann-Whitney test as appropriate. Analyses between three or more groups were performed using a one-way ANOVA and Sidak's multiple comparisons test. Correlation between two measurements were estimated by linear regression and statistical analysis was conducted using Pearson's correlation analysis. Proportions within two groups were compared by Chi-Square test. Statistical analyses were done in Graphpad Prism 8.3.0 (GraphPad Software).

2.5 Results

Stimulation with LasR-deficient variants induces higher mICAM-1 levels in AECs than wild-type *P. aeruginosa*

In order to compare the AEC mICAM-1 responses to secreted factors from loss-of-function *lasR* mutant and wild-type strains, we first stimulated BEAS-2B cells with filtrates of a *P. aeruginosa* clinical isolate isolated from early CF infection ("Early") and its isogenic *lasR* mutant, and measured cell surface mICAM-1 levels by flow cytometry. We observed a 2.7-fold increase in mICAM-1 levels in cells stimulated with the *lasR* mutant filtrates compared to the wild-type filtrates (Fig 2.1A). Of note, stimulation with TNF-α was used as a positive control for mICAM-1 induction in every experiment (S2.1A Fig) and stimulation with SCFM medium, which was used as a negative control, did not induce significantly greater mICAM-1 expression than starvation media alone (S2.1B Fig).

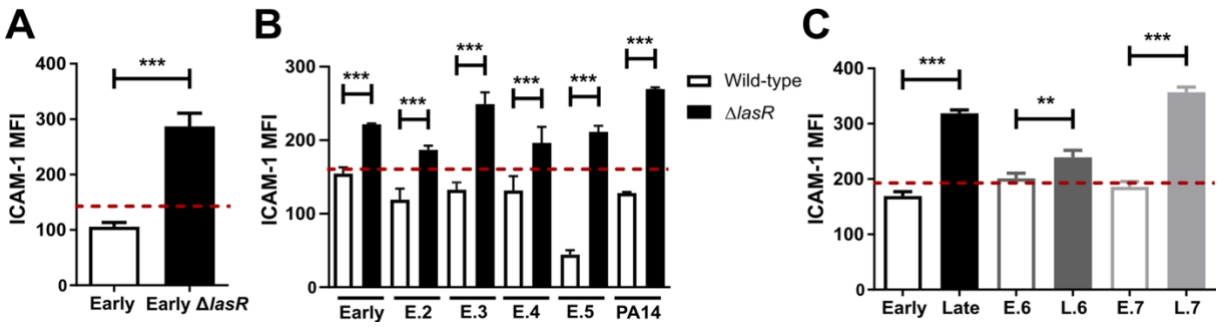

Fig 2.1. LasR deficient variants induce increased levels of mICAM-1 in AEC.

BEAS-2B cells were stimulated for 24h with 30 μL sterile filtrates of (A) the Early clinical isolate and its isogenic lasR mutant, (B) five "early" clinical isolates or PA14 wild-type and their isogenic *lasR* mutants or (C) three "early" clinical isolates paired with their clonally-related "late" isolates (Early/Late, E6/L6, E7/L7). mICAM-1 levels (MFI) were measured by flow cytometry, with SCFM (media) serving as negative control (-dashed line). Results are shown as the mean ± SD of one representative experiment (from ≥ 2 independent experiments, each with biological triplicates). *P < 0.05; **P < 0.01; ***P < 0.001.

To validate that the increased mICAM-1 response was attributable to the loss of LasR function in multiple *P. aeruginosa* strain backgrounds, we then stimulated AEC with filtrates from five other pairs of wild-type and isogenic *lasR* mutant strains, including four "early" clinical isolates (E.2 to E.5) and the common *P. aeruginosa* reference strain PA14. Stimulation with all *lasR* mutant filtrates induced mICAM-1 levels to a greater degree than their wild-type

parental filtrates, ranging from a 1.4- to a 4.7-fold increase in mICAM-1 levels (Fig 2.1B). Furthermore, all mICAM-1 flow cytometry measurements were gated on live cells, and the cell viability ranged from 86.4% to 96.4% in different conditions (S2.1C Fig). We therefore conclude that these modest differences in cell viability were unlikely to be sufficient to explain the magnitude of mICAM-1 reduction observed in wild-type filtrate-stimulated AEC.

Since loss-of-function *lasR* mutations are commonly found in *P. aeruginosa* clinical isolates recovered during late stage CF infections, we next compared several "early" infection LasR-competent clinical isolates to their clonally related, "late" infection LasR-deficient isolates (characterized by low protease production, low 3-oxo-C12 HSL autoinducer levels and metallic colony sheen) (16) recovered from the same patients, namely the Early/Late, E.6/L.6 and E.7/L.7 paired isolates as characterized in S2.4 Table. We observed a similar pattern in mICAM-1 response, with stimulation by all "late" isolates eliciting a higher mICAM-1 response (Fig 2.1C). Both the Late and L.7 filtrate resulted in 1.9-fold greater mICAM-1 levels compared to their clonally related "early" isolates, but the difference in mICAM-1 levels was more modest (1.2-fold) with the E.6 - L.6 pair. The variability observed across the different "early-late" pairs was not surprising since "late" isolates harbour numerous genetic and phenotypic differences compared to their clonally related "early" isolates. Furthermore, different *lasR* mutations have varying effects on LasR function, and the LasR regulon can vary across different strain backgrounds (45). These results thus indicated that loss-of-function *lasR* variants, both genetically engineered and naturally occurring ones, elicited higher mICAM-1 responses in human AEC than their respective wild-type counterparts, but that the magnitude of this phenotype varied depending on the *P. aeruginosa* strain background. Since the *P. aeruginosa* blue-green pigment pyocyanin can stimulate ICAM-1 expression (36) and is typically a LasR-controlled secreted secondary metabolite, we also noted that pyocyanin production was significantly decreased in the Early Δ*lasR* and Late strains compared to the Early strain (S2.1D Fig), thus indicating that the mICAM-1 expression in *lasR* mutant-stimulated AEC was unlikely to be attributable to increased pyocyanin levels.

Increased mICAM-1 levels on *lasR* mutant-stimulated AEC correlate with decreased caseinolytic and elastolytic activity in *lasR* mutant filtrates

In nearly all wild-type stimulation conditions, we also noted that mICAM-1 levels were below those observed in media control conditions (Figs 2.1A-1C and 2.2A), raising the possibility that mICAM-1 might be degraded or downregulated by wild-type filtrates. To start

investigating this hypothesis, we heat-treated wild-type and *lasR* mutant filtrates prior to stimulation to inactivate heat labile bacterial exoproducts, which include secreted proteases. As shown in Fig 2.2A, heat inactivation of wild-type filtrates restored mICAM-1 to levels above those seen with non-heat treated *lasR* mutant filtrates, indicating that LasR-regulated heat-labile compound(s) present in wild-type filtrates degraded or down-regulated mICAM-1. We also noted that heat inactivation in both wild-type and *lasR* mutant filtrates led to a 1.8- and 1.2-fold increase in mICAM-1 levels compared to their respective non-heat-treated filtrates (Fig 2.2A), suggesting the concurrent presence of heat-stable compound(s) that either induced ICAM-1 production or prevented its degradation in both wild-type and *lasR* mutant filtrates.

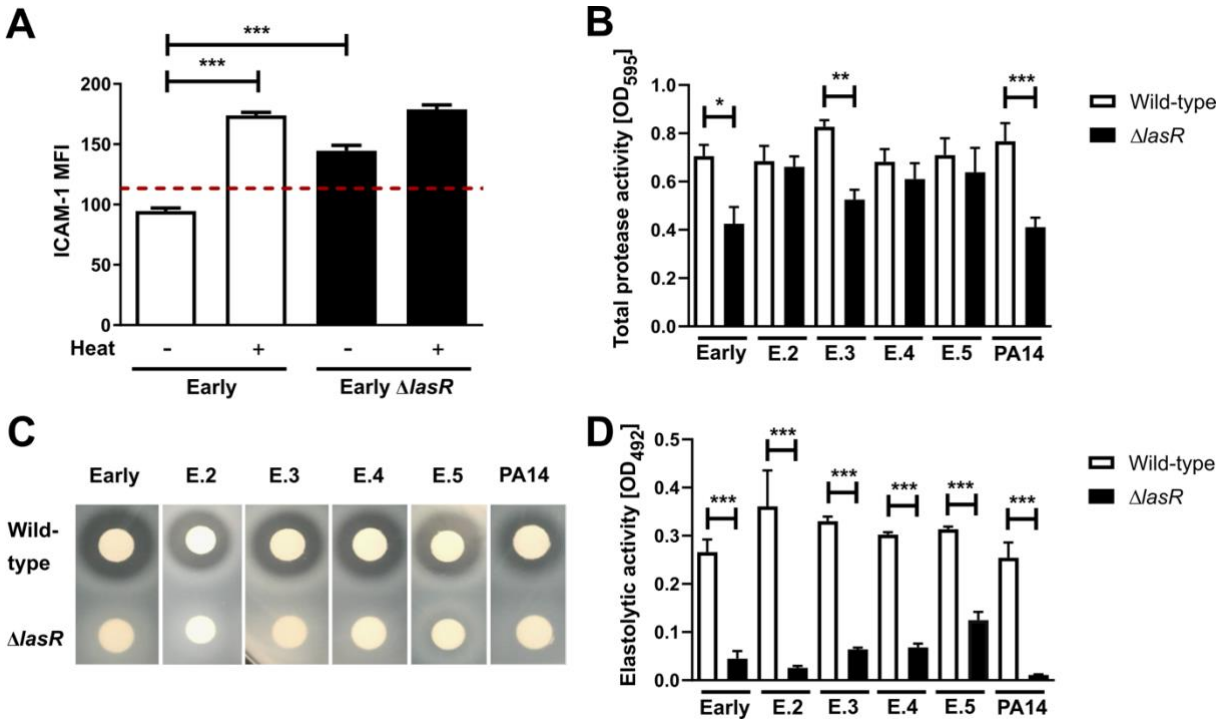

Fig 2.2. Induction of mICAM-1 is associated with reduced caseinolytic and elastolytic activity in *lasR* mutant filtrates.

BEAS-2B cells were stimulated for 24h with 30 µL filtrates of (A) the Early and isogenic Early Δ*lasR* mutant (+/- heat inactivation). mICAM-1 levels (MFI) were measured by flow cytometry, with SCFM (media) serving as negative control (—dashed line). Protease activity in wild-type and *lasR* mutant filtrates was characterized for (B) total protease activity using the Hide-Remazol Brilliant Blue assay, (C) for caseinolytic activity using the clearance zone diameter on skim milk agar and (D) for elastolytic activity using the Elastin-Congo Red assay. Results for (A) are shown as mean ± SD of one representative experiment (from ≥ 2 independent experiments, each with biological triplicates). Results for (B) and (D) are shown as mean ± SEM, with pooled data (n ≥ 4 biological replicates from two independent

experiments). Results for (C) are representative of ≥ 2 independent experiments in biological duplicates. *P < 0.05; **P < 0.01; ***P < 0.001.

LasR regulates the expression of several secreted proteases such as AprA, LasA, LasB and type IV protease (T4P) that can degrade components of host defenses and immunity (23,46–48), some of which have been shown to be heat-labile (23,49). Therefore, we hypothesized that the loss of mICAM-1 protein signal upon stimulation with wild-type filtrates was due to the activity of these proteases, and sought to characterize the proteolytic activity in wild-type and *lasR* mutant filtrates. We measured protease activity in several manners, with a Hide Blue degradation assay for total protease activity, skim milk plates for caseinolytic activity and Elastin-Congo Red assay for elastolytic activity. Although the total protease activity only showed differences in three (Early, E.3, PA14) out of the six pairs (Fig 2.2B), caseinolytic (Fig 2.2C) and elastolytic activity (Fig 2.2D) were highly reduced (at least by 68%) or undetectable in all *lasR* mutants compared to parental wild-type strains. We also confirmed both caseinolytic and elastolytic activities to be heat-labile (S2.2A and S2.2B Fig). These results therefore indicated that there was a significant loss in caseinolytic and elastolytic activities among all *lasR* mutants tested. We further observed a negative correlation between the filtrates' protease activity and ICAM-1 induction on AEC, with caseinolytic protease activity showing a stronger correlation (R^2= 0.76) than elastolytic protease activity (R^2 = 0.66) (S2.2C and S2.2D Fig).

LasR-regulated proteases degrade mICAM-1

To test the contribution of the different LasR-regulated proteases on mICAM-1, we measured the effect of PAO1-V, an invasive *P. aeruginosa* isolate, and its single (*lasA, lasB, aprA*), double (*lasA/lasB*) and triple (*lasA/lasB/aprA*) protease mutants on mICAM-1 levels by flow cytometry. We observed a modest increase (1.3- to 1.4-fold) in mICAM-1 levels upon stimulation with filtrates from the Δ*lasA*, Δ*lasB* and Δ*lasA* Δ*lasB* strains (compared to wild-type) as well as a more pronounced increase (1.6- and 1.8-fold) upon stimulation with the Δ*aprA* and triple mutant, respectively (Fig 2.3A), suggesting that AprA might have the greatest effect on ICAM-1 levels in this strain background. The caseinolytic activity of the protease mutants further confirmed the relative contribution of each protease in the PAO1-V strain background, as loss of AprA caused the greatest reduction in caseinolytic activity among the three proteases, while loss of all three LasB/LasB/AprA completely abrogated all caseinolytic

activity (S2.3A Fig). Not surprisingly, elastolytic activity was nearly undetectable in the *lasB* and triple protease mutant (S2.3B Fig).

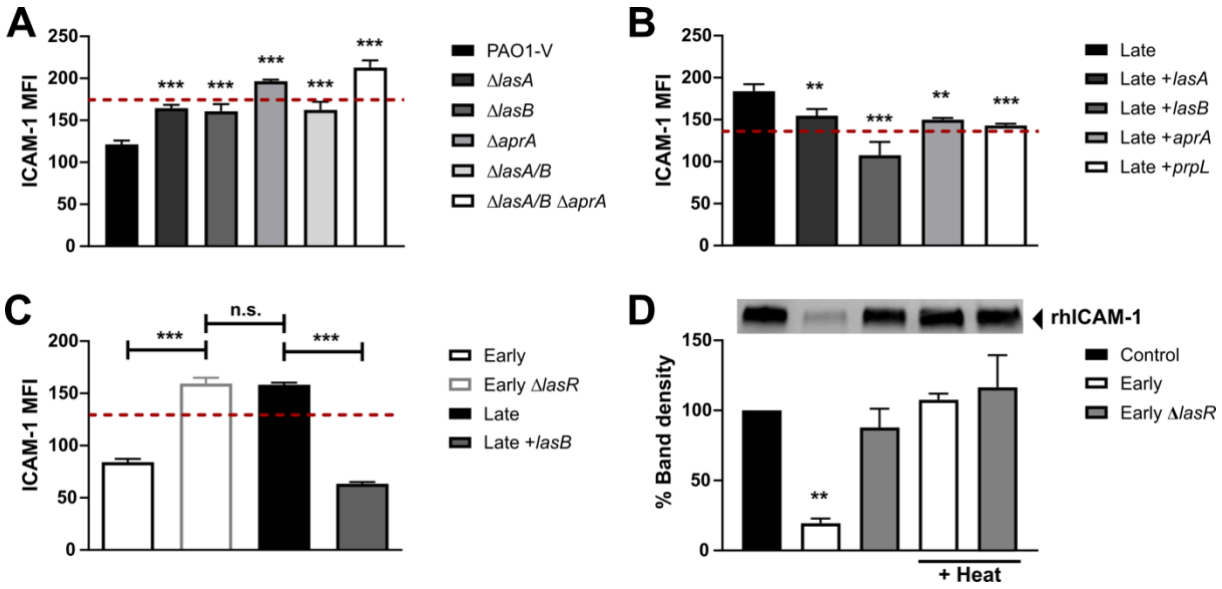

Fig 2.3. LasR-regulated proteases degrade ICAM-1.

BEAS-2B cells were stimulated for 24h with 30 µL filtrates of (A) PAO1-V and its isogenic protease mutants of *lasA*, *lasB* and *aprA*, (B) the Late isolate and complemented strains Late +*lasA*, Late +*lasB*, Late +*aprA* or Late +*prpL* (T4P) or (C) Early, Early Δ*lasR*, Late, Late +*lasB*. mICAM-1 levels were measured by flow cytometry, with SCFM (media) serving as negative control (—dashed line). (D) *in vitro* degradation of recombinant human ICAM-1 (rhICAM-1) by *P. aeruginosa* filtrate. In each sample, 250 ng rhICAM-1 was incubated with 5 µL filtrates of the Early and Early Δ*lasR* strains (+/- heat inactivation) or PBS control for 24h, and the remaining intact rhICAM-1 following degradation was quantified by Western Blotting. Results in (A), (B) and (C) are shown as mean ± SD from one representative experiment (from ≥ 2 independent experiments, each with biological triplicates). Results in (D) are displayed as a representative Western Blot and quantification of the % band density compared to the PBS control condition (n ≥ 3 biological replicates from two independent experiments). Different lanes were cropped from the same blot and imaged at the same exposure. Full blots can be found in the S2.1 Spreadsheet. *P < 0.05; **P < 0.01; ***P < 0.001.

We further investigated the contribution of individual proteases by genetically complementing the Late (LasR-deficient) strain with the *lasA*, *lasB*, *aprA* or *prpL* (T4P) genes under control of an arabinose-inducible promoter to generate the Late +*lasA*, Late +*lasB*, Late +*aprA* and Late +*prpL* constructs (S2.1 Table). We confirmed that caseinolytic activity was increased upon

complementation with the +*lasB*, +*aprA* and +*prpL* constructs (S2.3C Fig) and that elastolytic activity, which is mostly attributed to LasB, was only restored upon complementation with the +*lasB* construct (S2.3D Fig). Complementation with any of the four proteases resulted in decreased mICAM-1 levels compared to stimulation with the parental Late strain filtrate, with the greatest reduction in mICAM-1 levels (1.7-fold) observed with the Late +*lasB* strain (Fig 2.3B). Notably, *lasB* complementation of the Late isolate was sufficient to restore mICAM-1 levels to those observed in AECs stimulated with wild-type filtrates (Fig 2.3C).

To examine whether the decreased ICAM-1 levels induced by wild-type filtrates were due to direct degradation of ICAM-1, we incubated recombinant human ICAM-1 (rhICAM-1) with Early and Early Δ*lasR* filtrates and measured the *in vitro* rhICAM-1 degradation by Western blotting. Incubation with the Early, but not the Early Δ*lasR* filtrate, resulted in a significant reduction (81% decrease) in detectable and thus intact rhICAM compared to the PBS control (Fig 2.3D). We also confirmed that *in vitro* rhICAM-1 degradation was abrogated upon heat-inactivation of filtrates (Fig 2.3D), and reduced upon loss of one or more LasR-regulated proteases (S2.3E Fig). These results suggested that several LasR-regulated proteases present in wild-type filtrates can degrade rhICAM-1, the individual contribution of which might be strain-dependent.

Neutrophil binding to AEC is increased upon stimulation with *lasR* mutant filtrates

Next, we sought to characterize the functional consequences of the increased mICAM-1 responses in AEC stimulated with mutant *lasR* filtrates. Since mICAM-1 is involved in neutrophil adhesion to endothelial and epithelial cells (28,34,50), we hypothesized that AEC stimulated with *lasR* mutant filtrates will bind more neutrophils than AEC stimulated with wild-type filtrates. To test this, we quantified the adhesion of primary human neutrophils to AECs pre-stimulated with bacterial filtrates by confocal microscopy, and observed that significantly higher numbers of neutrophils adhered to AEC stimulated with *lasR* mutant filtrates (both Early Δ*lasR* and Late) compared to wild-type filtrate (5.5- and 8.6-fold increase respectively) or media control (Fig 2.4A and 2.4B). We also confirmed that neutrophil binding was specific to AEC, as control experiments using wells without AEC showed no adherent neutrophils (S2.3F Fig).

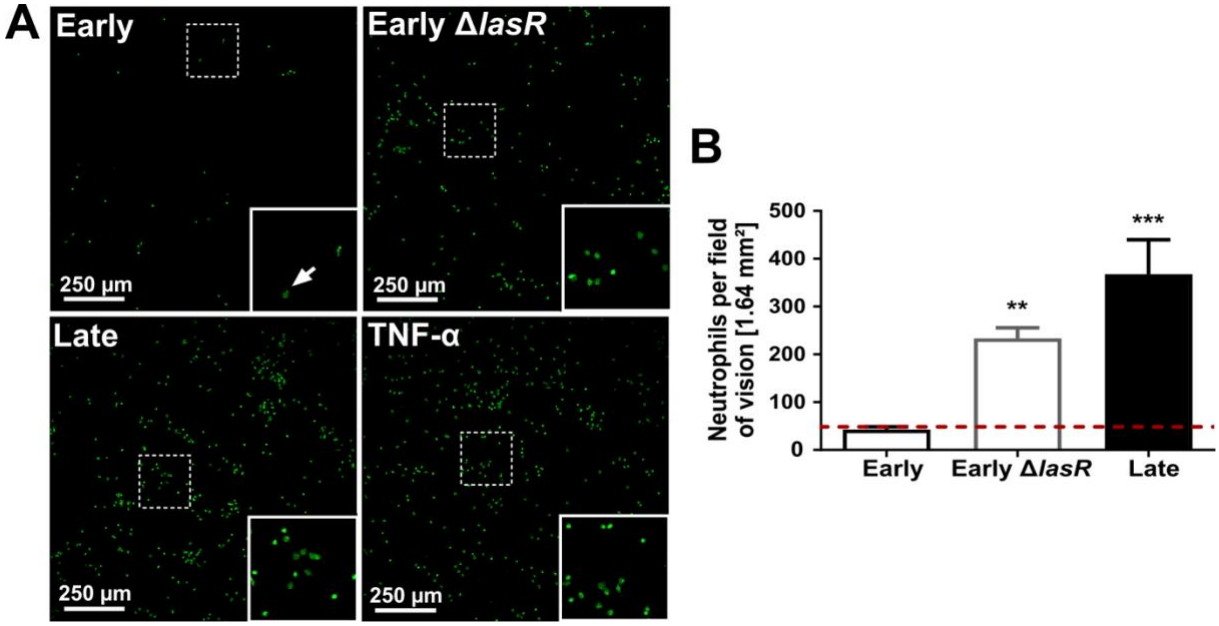

Fig 2.4. Neutrophil adhesion is increased in AEC stimulated with *lasR* mutant filtrates.
BEAS-2B cells were pre-stimulated with 30 µL filtrates of Early, Early Δ*lasR* and Late strains, then co-incubated with calcein-stained primary neutrophils (green). 20 ng/mL TNF-α served as positive control and SCFM served as negative control (—dashed line). Adherent neutrophils were visualized by confocal microscopy (10X objective) in (A) and quantified in (B). Results are shown as mean ± SD from one representative experiment (from 2 independent experiments, each with 3 biological replicates). *P < 0.05; **P < 0.01; ***P < 0.001.

The *lasR* mutant induces greater bronchial ICAM-1 levels and neutrophilic lung infiltration in a subacute murine lung infection model

We previously reported that *lasR* mutants induced a hyperinflammatory phenotype with higher levels of pro-inflammatory cytokines IL-6 and IL-8, greater neutrophilic inflammation and increased immunopathology compared to wild-type strains in a murine model of subacute lung infection (23). In this well-established model, bacteria are embedded in agar beads and inoculated endotracheally, causing a non-lethal airway-centric infection that persist and is associated with neutrophilic inflammation. Our observations of ICAM-1 modulation *in vitro* therefore led us to ask whether *lasR* mutant infections were also associated with increased airway ICAM-1 expression *in vivo*. We infected C57BL/6 mice with wild-type or *lasR* mutant bacteria and analyzed the airway epithelial ICAM-1 expression by immunofluorescence, with confocal microscopy imaging of airway cross sections on whole lung thin sections (S2.4A Fig). We analyzed mice at 2 and 4 days post-infection (p.i) and confirmed that both infection groups harboured equivalent bacterial burden at all time points (S2.4C Fig).

Although ICAM-1 can be expressed by multiple cell types in the lung, including endothelial and alveolar epithelial cells, we focused on the ICAM-1 expression of the bronchial epithelium where we observed a strong induction in expression with *P. aeruginosa* infection, whereas ICAM-1 expression in the alveolar compartment remained constant in all conditions and time points (Fig 2.5A, area surrounding airways). To quantify ICAM-1 expression, we first developed an automated image analysis method to measure ICAM-1 signals across multiple airway cross-sections per lung section, and to normalize the total ICAM-1 fluorescence of each airway epithelial cross- section to its surface area (as outlined in S2.4A Fig). As highlighted in Figs 2.5A and S2.4B, bronchial ICAM-1 expression was largely restricted to the apical (luminal) side of the bronchial epithelium. We validated our automated ICAM-1 quantification method using a conventional semi-quantitative scoring system, and given the very good correlation between the two methods ($R^2 = 0.84$, S2.4D Fig), we proceeded with the automated approach. The median ICAM-1 expression of all airways was significantly (3.2-fold) higher in *lasR* mutant infected mice compared to wild-type infected mice (Fig 2.5B). Analysis of pooled lung sections demonstrated a 2.9-fold higher median ICAM-1 airway signal in *lasR* mutant infected mice compared to wild-type infected mice at 2 days p.i, and consistently low (or undetectable) levels of ICAM-1 in PBS control mice (Fig 2.5C).

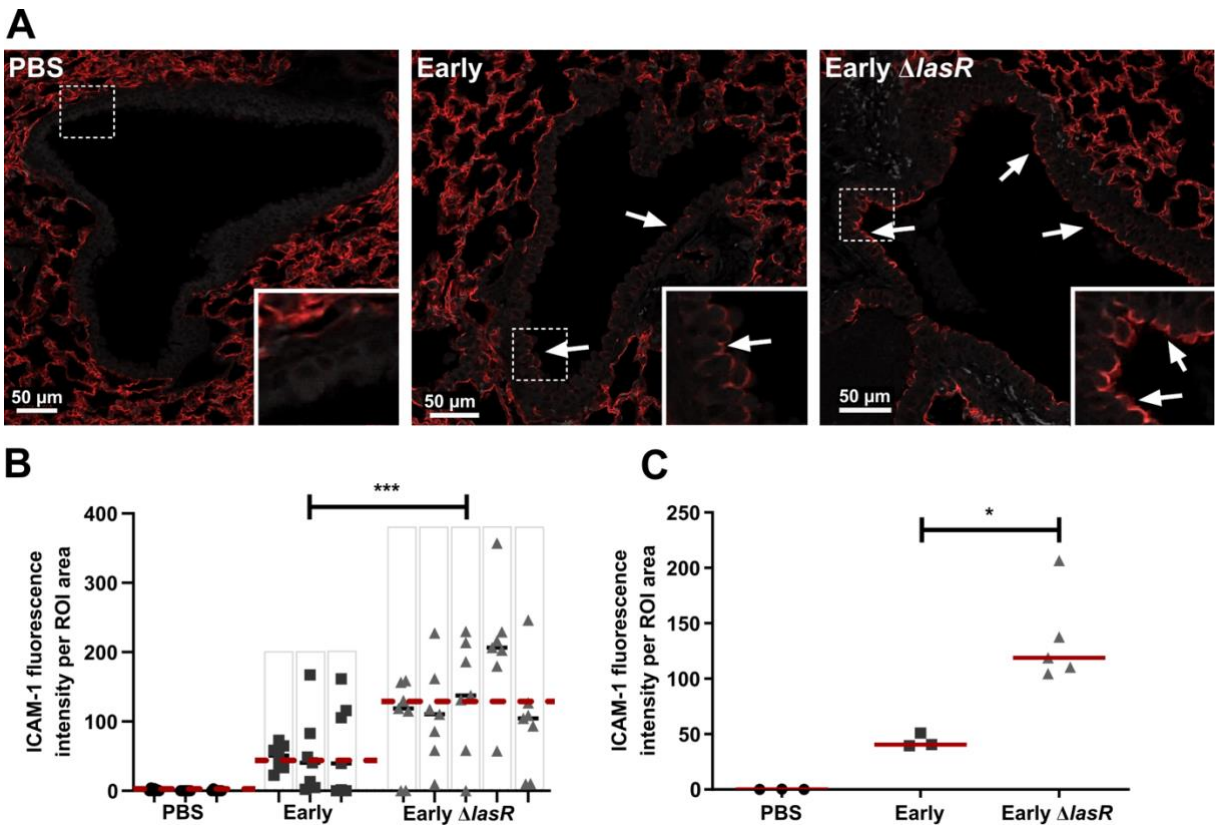

Fig 2.5. *lasR* mutant infected mice display increased airway epithelial ICAM-1 expression.

Mice were infected with Early, Early Δ*lasR* or PBS embedded agar beads and lungs were harvested at 2 days p.i. for ICAM-1 immunofluorescence (shown as red). (A) Images shown are representative of airway cross-sections displaying the median ICAM fluorescence scores of each infection group. Images were taken with a 20X objective, inset boxes are digital magnification of the bronchial epithelium and the white arrows point to regions of high ICAM-1 expression localized to the apical epithelial surface (luminal side). The green autofluorescence (Ex 488/ Em 518, shown as grey) was imaged to visualize the tissue structure. (B) ICAM-1 total fluorescence normalized to the airway surface area (ROI) in every image, with results shown as median within each lung (black line) and median within each group (— dashed line), each dot corresponding to one distinct airway, and columns corresponding to one distinct mouse lung. (C) Median normalized ICAM-1 fluorescence, with results shown as medians using data pooled from 7 randomly selected airways per lung, and each dot corresponding to one mouse ($n \geq 3$ mice per condition). *$P < 0.05$; **$P < 0.01$; ***$P < 0.001$.

We also noted considerable heterogeneity in airway mICAM-1 expression within the same mouse lung (each mouse with its individual airway data points is represented in columns, Fig 2.5B) in both infection groups. This anatomically heterogeneous pattern was not surprising given that we used an airway infection model where agar bead embedded bacteria are entrapped within airway lumens and cause foci of infection rather than a diffuse infection throughout the lung (51). As a result, lung regions in closest proximity to bacteria-containing beads displayed the greatest host responses to infection while more distant regions remained relatively normal, a pattern observed in other studies using a similar infection model (26,51). By 4 days p.i, the majority of airways showed little to no mICAM-1 expression, and no significant differences were detected in the two infection groups (S4E Fig). While the proportion of ICAM-1 negative airways (i.e. airways with ICAM-1 signal comparable to PBS control) was not significantly different across both infection groups at 2 days p.i. (81% vs 91%, $p = 0.251$), we observed a trend towards a higher percentage of ICAM-1-positive airways in *lasR* mutant-infected mice at 4 days p.i. compared to wild-type-infected mice (40% vs 18%, $p = 0.057$, S2.4F Fig). Together, these results thus suggested that *lasR* mutants were associated with increased airway ICAM-1 induction both *in vitro* and *in vivo*.

Next, we measured neutrophil counts in the lung homogenates and bronchoalveolar lavage fluid (BALF) to determine whether the increased ICAM-1 response to *lasR* mutant infections at 2 days p.i was also associated with increased lung neutrophilic infiltration. H&E staining of Early and Early Δ*lasR*-infected mouse lungs revealed that peri-bronchial and parenchymal inflammation in Early Δ*lasR*-infected mice was more extensive than in Early-infected or PBS control mice (Fig 2.6A). We note that the H&E lung sections could not be accurately assessed for intraluminal airway inflammation because the mouse airways were flushed with PBS for BALF collection prior to fixation. Both total lung neutrophil counts (1.6-fold increase, $p = 0.006$) and percentage of neutrophils (68% vs. 53%, $p = 0.033$) were significantly elevated in *lasR* mutant compared to wild-type infected mice (Fig 2.6B and 2.6C). We also noted no significant differences in the BALF analyses at day 2 p.i. (S2.5A and S2.5B Fig), although our previous studies using the same agar bead infection model showed that, by day 4 p.i, Early Δ*lasR*-infected mice displayed 25-fold greater BALF neutrophil counts compared to Early-infected mice ($8.6x10^5$ vs $3.4x10^4$) (23). Furthermore, our previous studies also reported greater BALF protein and more severe lung histopathology scores in Early Δ*lasR*-infected mice at day 4 p.i, confirming the presence of immunopathology in association with increased lung inflammation (23). These results suggested that *lasR* mutants induced an early enhanced airway epithelial mICAM-1 response *in vivo* at 2 days p.i. which subsides by 4 days p.i. and are associated with increased neutrophil lung inflammation. Given that the bacterial burden in both Early and Early Δ*lasR* strains remained equivalent from the time of infection until day 4 p.i, the differences in ICAM-1 and inflammatory responses most likely resulted from differences in pathogen-host interactions rather than bacterial burden.

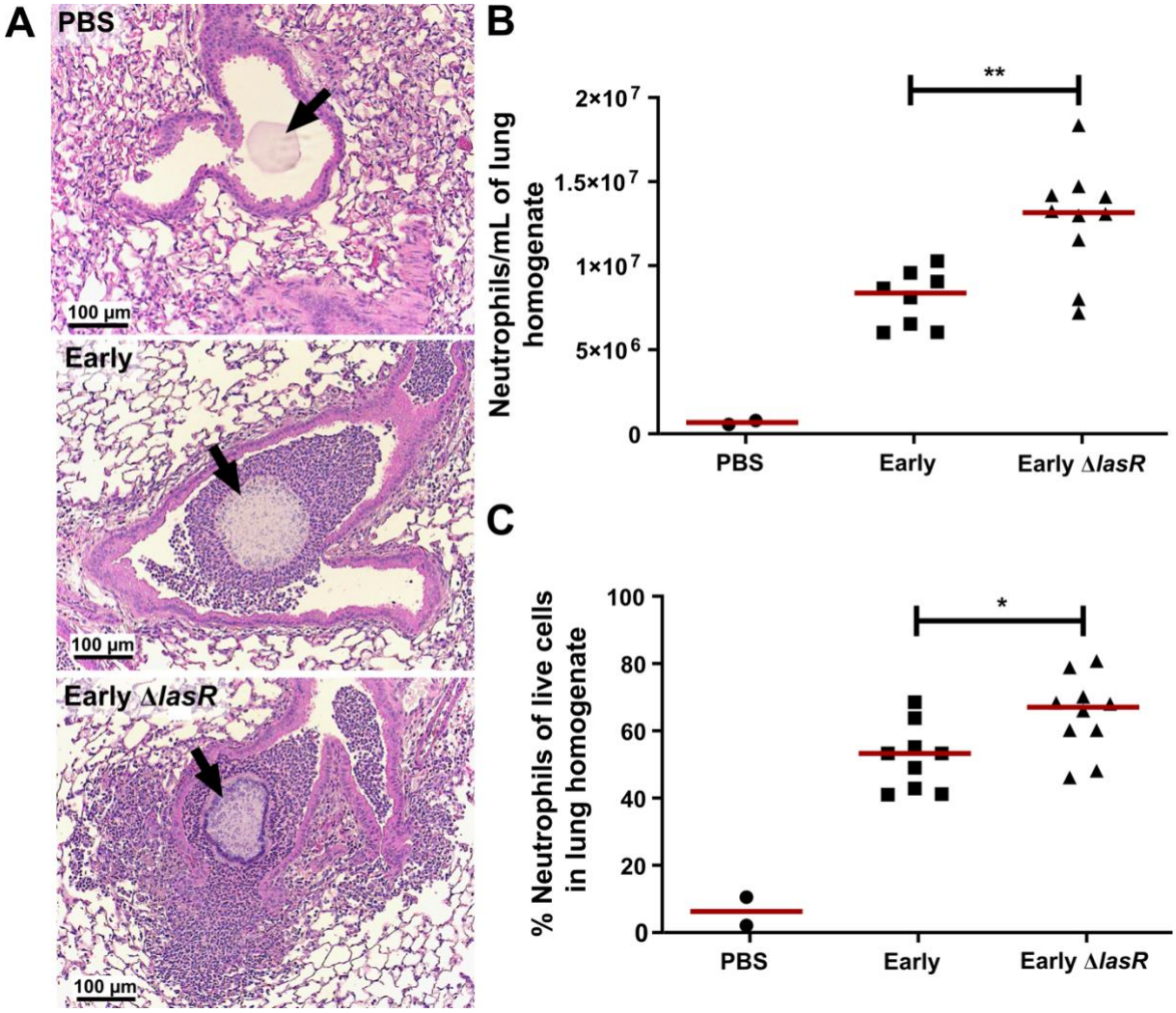

Fig 2.6. *lasR* mutant induces greater pulmonary neutrophilic inflammation than wild-type infection.

Mice were infected with Early, Early Δ*lasR* or PBS embedded agar beads and lungs were harvested at 2 days p.i. for lung histopathology and immune cell counts. (A) Representative images of H&E stained lung sections (10X objective), demonstrating airway cross-sections and surrounding peri-bronchial tissues. Lung homogenates were analyzed by flow cytometry for enumeration of (B) total neutrophils (CD45+, Ly6G high, CD11c-) and (C) the percentage of neutrophils among all live single cells. Results are shown as medians, with each dot representing one mouse. *P < 0.05; **P < 0.01.

2.6 Discussion

Loss-of-function *lasR* mutants are common in chronic CF infections (13,52), and are associated with more severe lung disease (15) and increased markers of inflammation (23) in CF patients. They cause dysregulated bacterial-host interactions through multiple mechanisms

(23,46,53–55) that likely contribute to their propensity to cause greater pathology in chronic infection. Our lab has previously shown that *lasR* mutant infections caused an increased pro-inflammatory cytokine and chemokine response in airway epithelial cells, and an exaggerated neutrophilic inflammation and lung immunopathology *in vivo* (23). In this study, we showed that loss-of-function *lasR* mutants also induced increased mICAM-1 levels on AEC compared to wild-type strains in cell culture models, and this effect facilitated neutrophil adhesion. We also found that *lasR* mutant infected mice showed increased airway epithelial ICAM-1 expression and neutrophilic lung inflammation compared to wild-type infected mice in a model of subacute airway infection. Our findings thus provide new insights into the intricate interplay between LasR-regulated proteases and airway ICAM-1 expression. As *P. aeruginosa* adapts to the CF lung and *lasR* variants emerge, these bacterial-host interactions and their effects in modulating lung inflammation change over the course of chronic infections.

Loss-of-function *lasR* mutations can emerge under laboratory conditions (16,56,57) and in human infections (58,59). They are highly prevalent in chronic CF infections, as previously reported by our group and others (13,15,23,60), and numerous genomic studies of longitudinally collected *P. aeruginosa* clinical strains indicate that the *lasR* gene is under strong positive selection, with evidence of convergent evolution and pathoadaptation to the CF host (10,13,14,61–63). Several studies have reported that loss-of-function *lasR* mutants have increased fitness in conditions such as low oxygen (64,65), denitrification (66), high cell density (67) and growth on certain amino acids (16,68). It is therefore plausible that loss of LasR function confers a growth or survival advantage in such conditions relevant to the CF lung environment. We thus surmise that the exaggerated neutrophilic inflammation is a consequence rather than the selection pressure that drives the emergence of loss-of-function *lasR* variants in the CF lung.

Our results also demonstrated that the enhanced mICAM-1 response was primarily attributable to the loss of LasR-regulated proteases that degraded ICAM-1, findings which are consistent with previous reports by our group and others that LasR-regulated proteases can degrade mediators of the innate immune system and the complement system (23,46–48,54,69). Furthermore, proteolytic cleavage of mICAM-1 by host-proteases such as neutrophil elastase and cathepsin G has been described (70,71), and degradation by bacterial proteases has been considered a potential mechanism of bacterial virulence (72). While our previous findings suggested a key role for LasB in the degradation of IL-6 and IL-8 (23), we now observed that

several LasR-regulated proteases, primarily LasB, AprA and T4P can degrade mICAM-1, and that their contributions likely vary depending on strain specific expression and secretion levels of each protease. The proteolytic activity of distinct proteases can also show interdependence, as LasA requires activation through proteolytic cleavage by LasB, and T4P function is significantly increased upon proteolytic cleavage by LasB and AprA (73,74).

P. aeruginosa can modulate ICAM-1 expression through other mechanisms. *P. aeruginosa* and other gram-negative bacterial lipopolysaccharide (LPS) can induce ICAM-1 expression in epithelial and other cell types (37,75,76). Although LPS expression or structures may vary across *P. aeruginosa* clinical strains, we doubt that this variable had a major effect on the ICAM-1 induction by the Early and Early Δ*lasR* strains since heat-inactivated filtrates of both strains, which contain heat-stable compounds such as LPS, stimulated mICAM-1 to comparable levels (Fig 2.2A). The *P. aeruginosa* type III effector ExoU also induces cleavage of mICAM-1 to soluble ICAM-1, but through a host cyclooxygenase-dependent pathway (77,78). We note that the effect of *P. aeruginosa* ExoU on mICAM-1 does not explain our results since ExoU secretion requires an active type III secretion system (79) and is likely negligible in the cell-free *P. aeruginosa* filtrates used in our *in vitro* experimental system. Finally, Look *et al*. have reported that phenazines (such as pyocyanin) secreted by *P. aeruginosa* also induce ICAM-1 expression in AEC (36). However, these secondary metabolites are unlikely to account for the increased ICAM-1 response to our *lasR* mutant strains which are pyocyanin deficient (S2.1D Fig).

Our results support an important role for airway epithelial mICAM-1 responses in neutrophil adhesion. As an adhesion molecule expressed on the apical surface of epithelial cells (27,37), mICAM-1 allows immune cells, notably neutrophils, to bind to the airway epithelial surface, an interaction that promotes transepithelial migration and thus recruitment of inflammatory cells (26,30). It also facilitates neutrophil-mediated clearance of pulmonary pathogens through yet unclear mechanisms (25,26). We recognize that other adhesion molecules such as vascular cell adhesion molecule 1 (VCAM-1) also contribute to neutrophil adhesion to AEC. For example, VCAM-1 basal expression in AEC is low but upregulated in response to pro-inflammatory cytokine and respiratory syncytial virus (80–82). This is consistent with our observation that neutrophil adhesion to AEC stimulated with Late filtrates is greater than Early Δ*lasR* filtrates despite similar mICAM-1 levels in both conditions, indicating that mICAM-1 is not the sole adhesion factor involved.

LasR regulates the expression of many secreted proteins and small molecules. We thus recognize that loss-of-function *lasR* variants likely modulate host inflammatory responses through additional pathways. For example, LasR-regulated secreted molecules such as pyocyanin and rhamnolipids can cause cell death, dampen immune cell function and trigger inflammation (83–85). LasR-regulated proteases can degrade a broad range of host proteins that mediate lung inflammation, from cytokines such as IL-6, IL-8, MCP-1 and IFN-γ (23,48,69,86) to protease-activated receptors such as PAR2 (87,88), as well as flagellin monomers, a well-established pathogen-associated molecular pattern (89,90). Although the ability of LasR-regulated proteases to target host immune and inflammatory mediators has typically been considered as a mechanism of immune evasion in the context of acute infections, we propose that the loss of such activity contributes in fact to the hyper-inflammation and immunopathology observed in the setting of subacute or chronic infections.

In our *in vivo* infection model, we observed that *lasR* mutant infections were associated with higher pulmonary neutrophil counts by flow cytometry and peri-bronchial inflammation by immunohistopathology. While BALF neutrophil counts did not differ significantly at 2 days p.i., we have previously reported that they were significantly increased at 4 days p.i. in Early Δ*lasR*-infected mice (23). This suggests that neutrophil recruitment into the airways likely lags and manifests later than in the peri-bronchial compartments. Although we cannot directly infer the causal contribution of airway ICAM-1 to the pulmonary neutrophilic inflammation in our *in vivo* model, the association between the two is consistent with our *in vitro* neutrophil adhesion data.

The role of airway epithelial mICAM-1 in lung inflammation during infection is emerging but complex and incompletely understood. Previous studies have also suggested that airway epithelial mICAM-1 expression significantly affects neutrophil recruitment to the lungs *in vivo* and *in vitro* (26,34). For example, in a model of subacute *H. influenzae* lung infection, Humlicek *et al* demonstrated a marked reduction of leukocyte recruitment upon intratracheal instillation of anti-ICAM-1 blocking antibody which predominantly targets epithelial cells of the lungs (26). Studies have reported that basal mICAM-1 expression is minimal in the airway epithelium in human and rodent lung tissues and cell cultures, but induced in states of inflammation and infection (29,38,82). This stands in contrast to alveolar epithelial cells which show high constitutive expression levels of mICAM-1 in the absence of infection, as we and

others observed in mice, rats and humans (33,91). Induction of mICAM-1 expression in AEC has been observed with infection by *H. influenzae*, *C. pneumoniae*, *Pneumocystis carinii* (26,29–31) or *P. aeruginosa* (36) as seen in our study, either directly in response to bacterial products, or indirectly in response to inflammatory cytokines such as TNF-α (82,92). Epithelial ICAM-1 thus promotes neutrophil recruitment and retention to the airway compartment (24,26), a response that may aid in pathogen clearance during infection but also exacerbates inflammation-mediated pathology. Our study thus demonstrates that loss-of-function *lasR* mutants induce greater mICAM-1 expression and neutrophil adhesion to human airway epithelial cells *in vitro*. We also observed that *lasR* mutant infections elicit greater ICAM-1 expression in the bronchial epithelium and greater lung inflammation in murine infections, but this association remains to be mechanistically proven *in vivo*.

In conclusion, we report on a novel mechanism through which *P. aeruginosa* modulates innate immune and inflammatory responses in the host lung, and how loss of LasR function, a common patho-adaptation during chronic CF infections, enhances neutrophilic inflammation. Additionally, modulation of airway epithelial mICAM-1 expression may also have other implications through its function as the major entry receptor of human rhinoviruses (HRV) (93). For example, stimulation of AEC with *H. influenzae*, which also induces mICAM-1 expression, leads to increased susceptibility to HRV-infection (94). Whether AEC stimulated with *P. aeruginosa lasR* mutants are more susceptible to HRV infection remains to be determined. HRV infections are common in CF patients and may be linked to pulmonary exacerbations (95), an important determinant of lung function decline in CF patients. Whether CF patients chronically infected with *P. aeruginosa lasR* mutants are more susceptible to HRV infection as a result of enhanced airway mICAM-1 levels is an intriguing hypothesis to be explored.

2.7 Supporting information

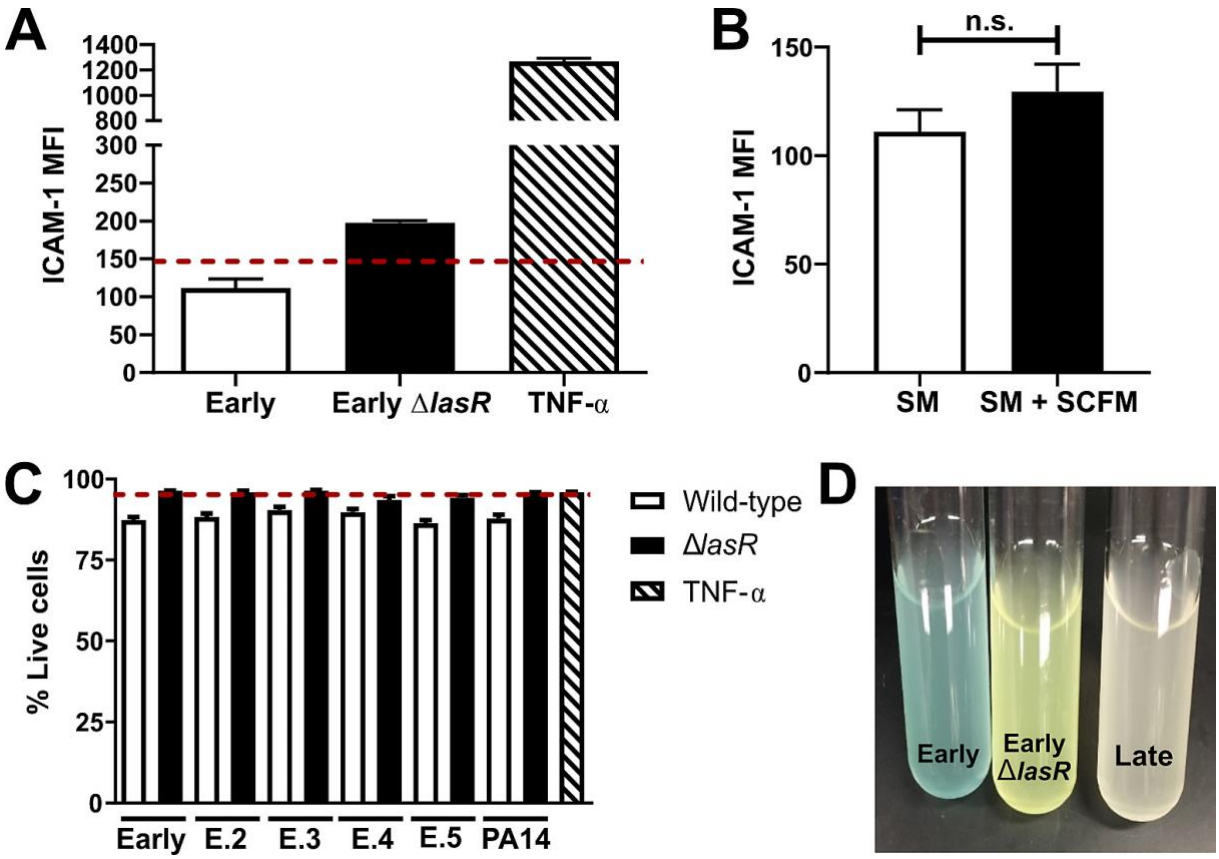

S2.1 Fig. Controls for mICAM-1 induction and AEC viability.

BEAS-2B cells were stimulated for 24h with (A) 30 µL filtrate of the Early or Early Δ*lasR* strain or 20 ng/mL TNF-α; (B) starvation media (SM) +/- 30 µL SCFM medium; (C) 30 µL filtrates from six pairs of wild-type clinical isolates and isogenic *lasR* mutant. In (A) and (C), SCFM served as negative control (—dashed line) and 20 ng/mL TNF-α as positive control. (A+B) mICAM-1 levels were measured by flow cytometry and (B) AEC viability following filtrate stimulation was measured as the percentage of live cells (low eFluor 780) among all single cells by flow cytometry. The results are shown as mean ± SD of one representative experiment (from ≥ 2 independent experiments, each with biological triplicates). (D) Representative bacterial cultures of the Early, Early Δ*lasR* and Late strains, with pyocyanin (blue-green pigment) production only evident with the Early strain. Cultures were grown in SCFM, as used for filtrate production. **P* < 0.05; ***P* < 0.01; ****P* < 0.001.

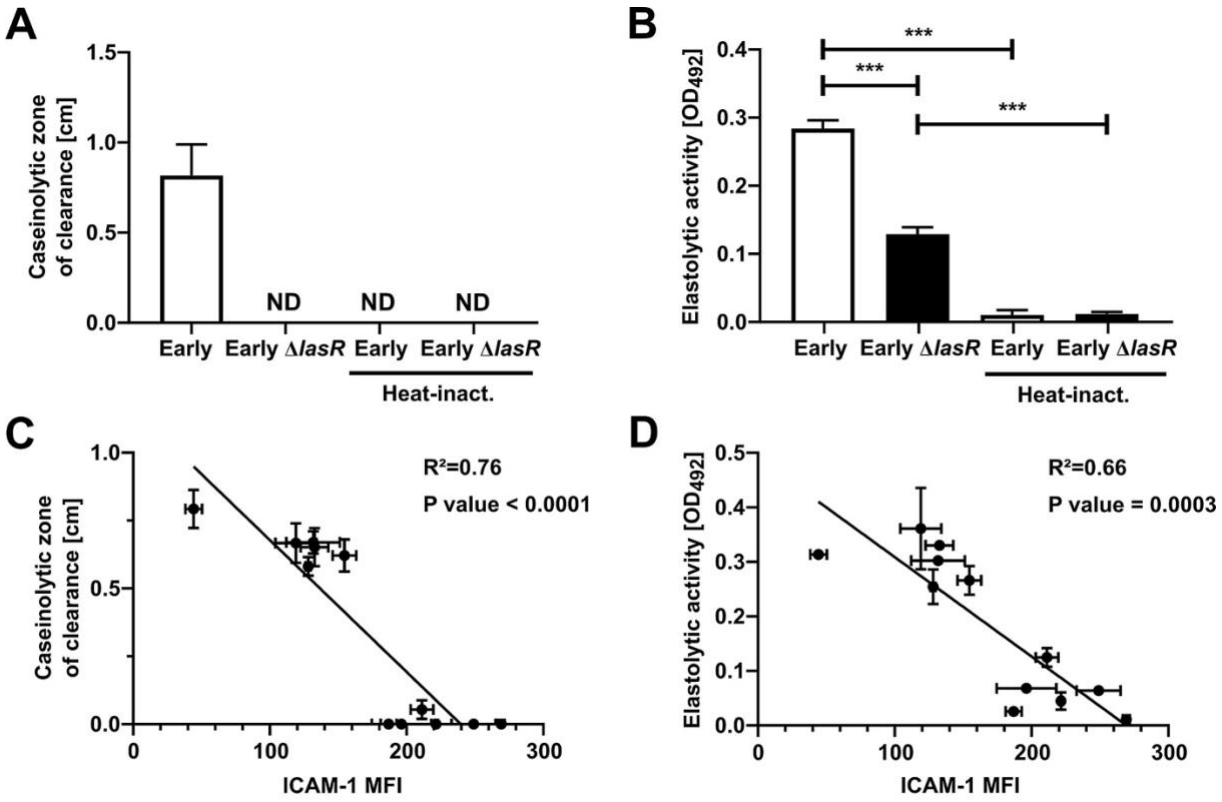

S2.2 Fig. Secreted protease activity in *P. aeruginosa* filtrates is heat-labile and negatively correlated with mICAM-1 levels in filtrate-stimulated AEC.

(A) Caseinolytic activity in Early and Early Δ*lasR* filtrates (+/- heat treatment) was measured on skim milk agar plates. (B) Elastolytic activity in Early and Early Δ*lasR* filtrates (+/- heat treatment) was measured by Elastin-Congo Red assay. Correlation between (C) caseinolytic or (D) elastolytic activity of different *P. aeruginosa filtrates* and mICAM-1 levels on AEC stimulated with the respective filtrates. Results in (A) and (B) are shown as mean +SEM and are representative of ≥ 2 independent experiments, each with biological duplicates. In (C) and (D), each data point represents one wild-type or *lasR* mutant strain, with the X value displaying the mean ±SD ICAM-1 induction in one representative experiment (in biological triplicates) and the Y value displaying the mean ± SEM (C) caseinolytic or (D) elastolytic activity (two independent experiments, each with biological duplicates). The trendlines in (C) and (D) were calculated by linear regression. ND = not detectable. **P* < 0.05; ***P* < 0.01; ****P* < 0.001.

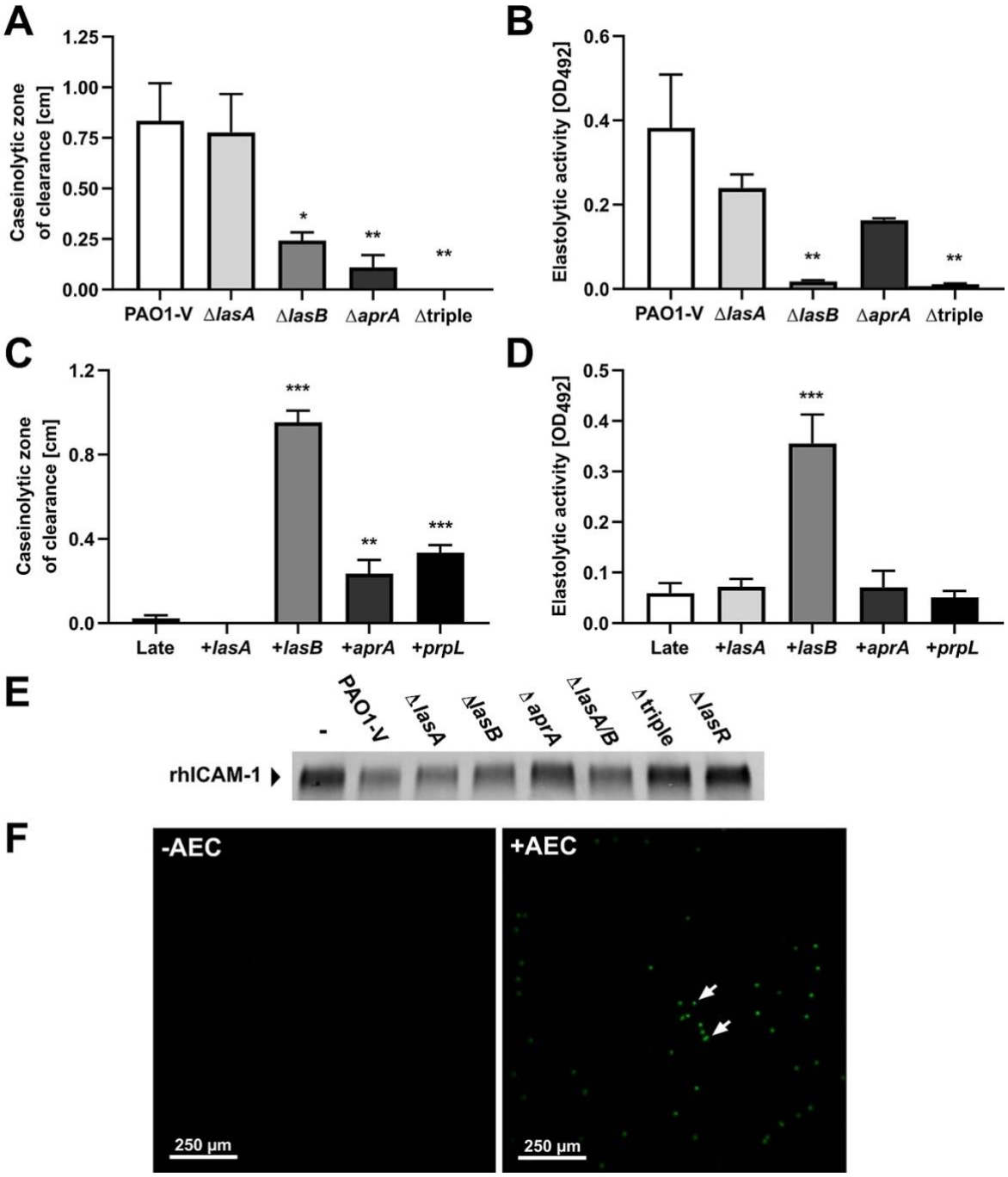

S2.3 Fig. Controls for secreted protease mutants and complementation.

Caseinolytic (A+C) and elastolytic (B+D) activity of (A+B) PAO1-V and its isogenic protease mutants of *lasA, lasB* and *aprA* or (C+D) the Late strain complemented with *lasA, lasB, aprA* or *prpL* (T4P) was measured on skim milk agar plates and by Elastin-Congo Red assay, respectively. (E) rhICAM-1 was quantified by Western Blotting with a polyclonal anti rhICAM-1 antibody, following incubation for 24h with PBS (- control) or filtrates of PAO1-V and its isogenic protease mutants as indicated. (F) Adhesion of calcein-stained human primary neutrophils (green) after 2h of incubation in wells with or without AEC

was analyzed by confocal imaging. Results in (A-D) are shown as mean ± SEM, with pooled data (n ≥ 3 biological replicates from ≥ 2 independent experiments). Results in (G) are representative of 2 independent experiments. Results in (F) are representative of 2 independent experiments. *$P < 0.05$; **$P < 0.01$; ***$P < 0.001$.

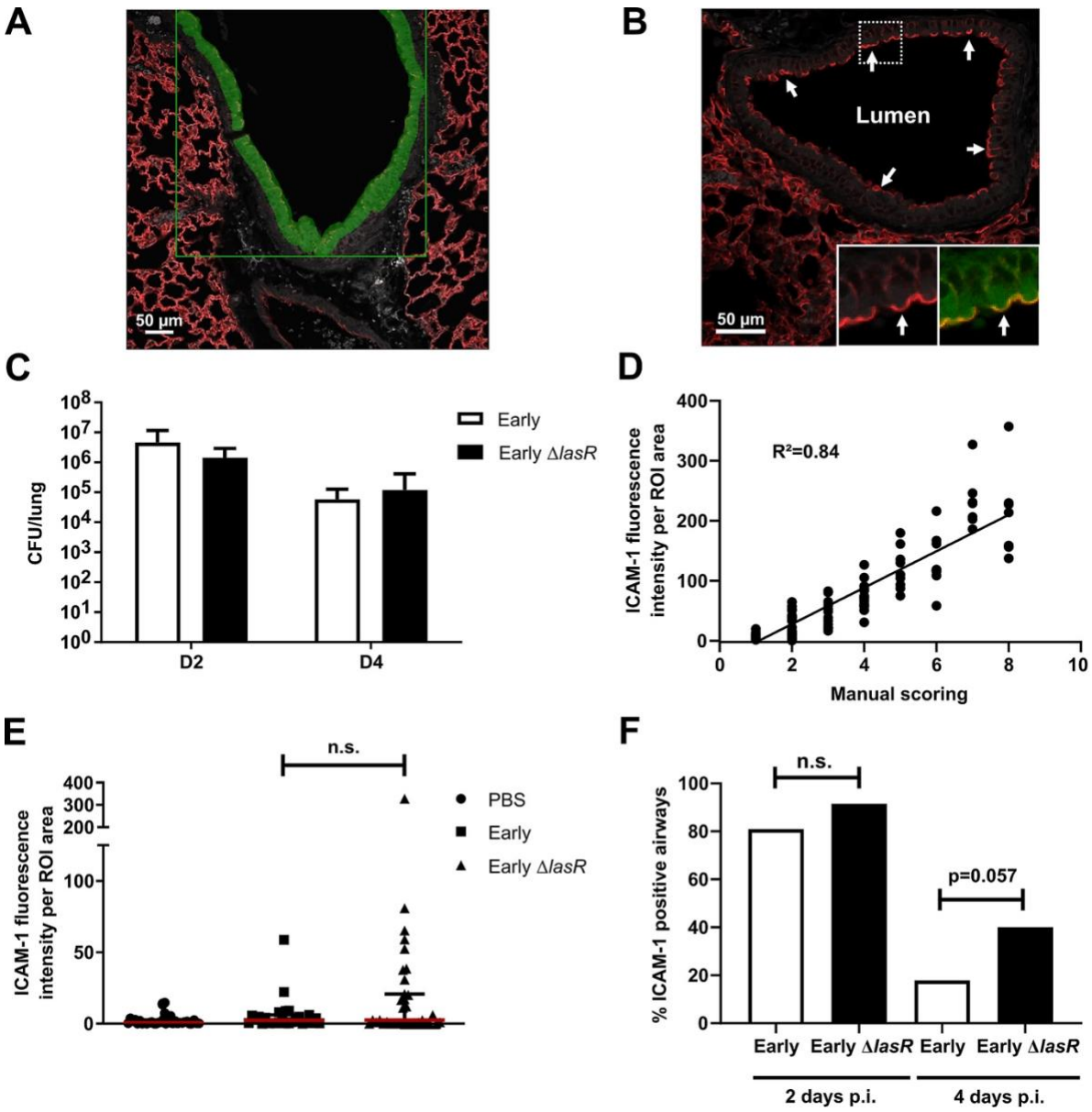

S2.4 Fig. ICAM-1 immunofluorescence and bacterial burden in mouse infection model. (A) Representative image of the region of interest (ROI, green area) manually drawn to define the airway epithelium on mouse lung sections. (B) Representative image of an airway cross-section (20X objective, with digital magnification in the inset box) displaying high bronchial ICAM-1 expression (red) localized to the apical side the bronchial epithelium facing the lumen (arrows). The autofluorescence of the tissue was imaged in the green channel (Ex 488/ Em 518) and is shown both in grey (to better highlight the ICAM-1 signal) or green. (C) Total lung

bacterial burden at 2 and 4 days p.i, in mice infected with the Early or Early Δ*lasR* strain. Results are pooled from two independent experiments. (D) Correlation between manual and automated scoring of the airway epithelial mICAM-1 fluorescence intensity. Each dot represents one distinct airway section analyzed. (E) ICAM-1 fluorescence intensity per ROI area in mice infected with the Early, Early Δ*lasR* or PBS control. Each dot represents one airway section. (F) Percentage of ICAM-1 positive airways in mice infected with the Early or Early Δ*lasR* strain at 2 and 4 days p.i. Results are shown as mean ± SEM (C), median ± IQR (E) or percentages (F). **P* < 0.05; ***P* < 0.01; ****P* < 0.001; n.s. *P* ≥ 0.05.

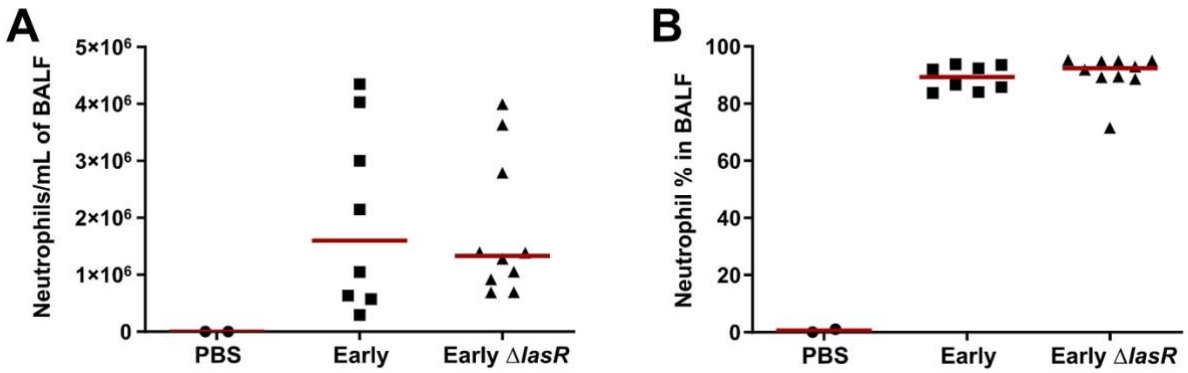

S2.5 Fig. Neutrophilic inflammation in mouse BALF.

C57BL/6 mice were infected with the Early, Early Δ*lasR* or PBS control and sacrificed at 2 days p.i. (A) In BALF, the proportion of neutrophils was determined by Kwik-Diff staining. (B) Total BALF neutrophil counts, calculated by multiplying the proportion of neutrophils by the total number of live cells. Results are shown as medians (n = 2 mice in the control group, n ≥ 8 mice in infected groups). **P* < 0.05; ***P* < 0.01; ****P* < 0.001.

Strains	Genotype and relevant phenotypic characteristics	Reference
Early	"AMT0023-30" early infection clinical CF isolate with wild-type *lasR* Additional information in Table S2.4	(13)
Early Δ*lasR*	Early isolate with *lasR*::Gm^R	(16)
Late	"AMT0023-34" late infection clinical CF isolate clonally related to Early with loss-of-function *lasR* mutation Additional information in Table S2.4	(13)
Late +*lasA*	Late isolate with integrated attCTX::miniCTX2.1-Tc-GW-araC-pBAD::*lasA*, Tc^R, resulting in arabinose-inducible *lasA* expression	This study

Late +*lasB*	Late isolate with integrated attCTX::miniCTX2.1-Tc-GW-araC-pBAD::*lasB*, Tc^R, resulting in arabinose-inducible *lasB* expression	(23)
Late +*aprA*	Late isolate with integrated attCTX::miniCTX2.1-Tc-GW-araC-pBAD::*aprA*, Tc^R, resulting in arabinose-inducible *aprA* expression	This study
Late +*prpL*	Late isolate with integrated attCTX::miniCTX2.1-Tc-GW-araC-pBAD::*prpL*, Tc^R, resulting in arabinose-inducible *prpL* expression	This study
E.2	"CF215" early infection CF clinical isolate with wild-type *lasR*	(16)
E.2 Δ*lasR*	E.4 with *lasR*::Gm^R	(16)
E.3	"CF3-0.8" early infection CF clinical isolate with wild-type *lasR*	(16)
E.3 Δ*lasR*	E.5 with *lasR*::Gm^R	(16)
E.4	"CF6-1" early infection CF clinical isolate with wild-type *lasR*	(16)
E.4 Δ*lasR*	E.6 with *lasR*::Gm^R	(16)
E.5	"CF716" early infection CF clinical isolate with wild-type *lasR*	(16)
E.5 Δ*lasR*	E.7 with *lasR*::Gm^R	(16)
E.6	"c5198d" early infection clinical CF isolate with wild-type *lasR*. RAPD genotype A173. Additional information in Table S2.4	This study
L.6	"D3010c" late infection clinical CF isolate clonally related to E.6 with loss-of-function *lasR* mutation. RAPD genotype A173. Additional information in Table S2.4	This study
E.7	"AMT0020-1" early infection clinical CF isolate with wild-type *lasR*. Additional information in Table S2.4	(23)
L.7	"AMT0020-84" Late infection clinical CF isolate clonally related to E.7. Additional information in Table S2.4	(23)
PA14	Reference strain, isolated from a burn wound infection, wild-type *lasR*	(96)
PA14 Δ*lasR*	PA14 with *lasR*::Gm^R	(97)
PAO1-V	Invasive *P. aeruginosa* isolate with wild-type *lasR*	(98)
PAO1-V Δ*lasA*	PAO1-V with *lasA*ΩGm^R	(98, 99)

PAO1-V Δ*lasB*	PAO1-V with Δ*lasB* deletion	(23)
PAO1-V Δ*aprA*	PAO1-V with Δ*aprA* deletion	(98, 99)
PAO1-V Δ*lasA* Δ*lasB*	PAO1-V with *lasA*ΩGm^R and *lasB*ΩSm^R	(98, 99)
PAO1-V Δtriple	PAO1-V with *lasA*ΩGm^R, *lasB*ΩSm^R, Δ*aprA*	(98, 99)
PAO1-V Δ*lasR*	PAO1-V with *lasR*::Gm^R	(23)
E. coli DH5α (pJN105L, pSC11)	3-oxo-C12-HSL bioassay strain	Ajai Dandekar (U Washington)

S2.1 Table. Strains used in this study.

Primer	Primer Sequence
***lasA*-GWB5-RBS**	GGGGACAACTTTGTATACAAAAGTTGCCAGAGGAGGATATTC ATGCAGCACAAAAGATCCCGC
***lasA*-GWB2**	GGGGACCACTTTGTACAAGAAAGCTGGGTATCAGAGCGCCAG GCCGGG
***aprA*-GWB5-RBS**	GGGGACAACTTTGTATACAAAAGTTGCCAGAGGAGGATATTC ATGTCCAGCAATTCTCTTG
***aprA*-GWB2**	GGGGACCACTTTGTACAAGAAAGCTGGGTATCAGACGACGAT GTCGGCCT
***prpL*-GWB5-RBS**	GGGGACAACTTTGTATACAAAAGTTGCCAGAGGAGGATATTC ATGCATAAGAGAACGTACCTGAAT
***prpL*-GWB2**	GGGGACCACTTTGTACAAGAAAGCTGGGTATCAGGGCGCGAA GTAGCG

S2.2 Table. Primers used in this study.

Plasmid	Description	Source or Reference
pDONR221P5P2	Multisite Gateway donor vector with attP5 and attP2 recombination sites, Cm^R, Km^R	Invitrogen
pJJH187	pDONR221P5P2 with an attL-flanked, 1192-bp fragment encoding the araC repressor and the pBAD promoter, Km^R	(100)
miniCTX2.1-GW	miniCTX2.1-Tc with a Gateway destination cloning site, Tc^R	J J Harrison

pENTR-*lasA*	pDONR221P5P2 containing the entire *lasA* ORF fragment (1257 bp), Cm^R, Km^R	This Study
pENTR-*prpL*	pDONR221P5P2 containing the entire *prpL* ORF fragment (1389 bp), Cm^R, Km^R	This Study
pENTR-*aprA*	pDONR221P5P2 containing the entire *aprA* ORF fragment (1483 bp), Cm^R, Km^R	This Study
pEXP-*lasA*	miniCTX2.1-Tc-GW-araC-pBAD::*lasA*, Tc^R	This Study
pEXP-*prpL*	miniCTX2.1-Tc-GW-araC-pBAD::*prpL*, Tc^R	This Study
pEXP-*aprA*	miniCTX2.1-Tc-GW-araC-pBAD::*aprA*, Tc^R	This Study

S2.3 Table. Plasmids used in this study.

Strains	Time interval	*lasR* genotype	Protease activity	Metallic sheen	3-oxo-C12-HSL level
Early	-	Wild-type	Elastolytic ++ Caseinolytic ++	Yes	++
Late	7.5 years	1 bp deletion at position 147	Elastolytic +/- Caseinolytic -	No	-
E.6	-	Wild-type	Elastolytic ++ Caseinolytic ++	Yes	+
L.6	15 years	T75K missense mutation	Elastolytic - Caseinolytic -	No	-
E.7	-	Wild-type	Elastolytic ++ Caseinolytic ++	Yes	++
L.7	16 years	NA	Elastolytic - Caseinolytic -	No	-

S2.4 Table. Characteristics of paired clonally related early and late infection isolates.
Low protease production, the presence of a metallic sheen and low 3-oxo-C12-HSL signal level are characteristic phenotypes of LasR-deficient strains. NA not available.

2.8 Acknowledgments

We would like to thank S. Fleiszig and J. A. Hobden for providing the PAO1-V, PAO1-V Δ*lasA*, PAO1-V Δ*aprA*, PAO1-V Δ*lasA/B* and PAO1-V Δ*lasA/B* Δ*aprA* strains. The Gateway miniCTX2.1 vector was provided by J. J. Harrison and the E. coli DH5α (pJN105L, pSC11) bioassay strain was obtained from A. A. Dandekar. We acknowledge D. P. Speert, James

Slosnik and J. L. Burns for providing the *P. aeruginosa* clinical isolates. We would also like to thank C. Hupperetz for his technical support with the filtrates.

2.9 References

1. Ratjen F, Bell SC, Rowe SM, Goss CH, Quittner AL, Bush A. Cystic fibrosis. Nature reviews Disease primers. 2015;1:15010.
2. Folkesson A, Jelsbak L, Yang L, Johansen HK, Ciofu O, Hoiby N, et al. Adaptation of Pseudomonas aeruginosa to the cystic fibrosis airway: an evolutionary perspective. Nature reviews Microbiology. 2012;10(12):841–51.
3. Lynch SV, Bruce KD. The cystic fibrosis airway microbiome. Cold Spring Harbor perspectives in medicine. 2013;3(3):a009738.
4. Kosorok MR, Zeng L, West SE, Rock MJ, Splaingard ML, Laxova A, et al. Acceleration of lung disease in children with cystic fibrosis after Pseudomonas aeruginosa acquisition. Pediatric pulmonology. 2001;32(4):277–87.
5. Lin CK, Kazmierczak BI. Inflammation: A Double-Edged Sword in the Response to Pseudomonas aeruginosa Infection. Journal of innate immunity. 2017;9(3):250–61.
6. Rosen BH, Evans TIA, Moll SR, Gray JS, Liang B, Sun X, et al. Infection Is Not Required for Mucoinflammatory Lung Disease in CFTR-Knockout Ferrets. American journal of respiratory and critical care medicine. 2018;197(10):1308–18.
7. Paemka L, McCullagh BN, Abou Alaiwa MH, Stoltz DA, Dong Q, Randak CO, et al. Monocyte derived macrophages from CF pigs exhibit increased inflammatory responses at birth. Journal of cystic fibrosis: official journal of the European Cystic Fibrosis Society. 2017;16(4):471–4.
8. Konstan MW, Berger M. Current understanding of the inflammatory process in cystic fibrosis: onset and etiology. Pediatric pulmonology. 1997;24(2):137–42; discussion 59–61.
9. Cantin AM, Hartl D, Konstan MW, Chmiel JF. Inflammation in cystic fibrosis lung disease: Pathogenesis and therapy. Journal of cystic fibrosis: official journal of the European Cystic Fibrosis Society. 2015;14(4):419–30.
10. Winstanley C O'Brien S, Brockhurst MA. Pseudomonas aeruginosa Evolutionary Adaptation and Diversification in Cystic Fibrosis Chronic Lung Infections. Trends in microbiology. 2016;24(5):327–37.
11. Faure E, Kwong K, Nguyen D. Pseudomonas aeruginosa in Chronic Lung Infections: How to Adapt Within the Host? Frontiers in immunology. 2018;9:2416.

12. Lorè NI, Cigana C, De Fino I, Riva C, Juhas M, Schwager S, et al. Cystic fibrosis-niche adaptation of Pseudomonas aeruginosa reduces virulence in multiple infection hosts. PloS one. 2012;7(4):e35648.
13. Smith EE, Buckley DG, Wu Z, Saenphimmachak C, Hoffman LR, D'Argenio DA, et al. Genetic adaptation by Pseudomonas aeruginosa to the airways of cystic fibrosis patients. Proceedings of the National Academy of Sciences of the United States of America. 2006;103(22):8487–92.
14. Marvig RL, Sommer LM, Molin S, Johansen HK. Convergent evolution and adaptation of Pseudomonas aeruginosa within patients with cystic fibrosis. Nature genetics. 2015;47(1):57–64.
15. Hoffman LR, Kulasekara HD, Emerson J, Houston LS, Burns JL, Ramsey BW, et al. Pseudomonas aeruginosa lasR mutants are associated with cystic fibrosis lung disease progression. Journal of cystic fibrosis: official journal of the European Cystic Fibrosis Society. 2009;8(1):66–70.
16. D'Argenio DA, Wu M, Hoffman LR, Kulasekara HD, Déziel E, Smith EE, et al. Growth phenotypes of Pseudomonas aeruginosa lasR mutants adapted to the airways of cystic fibrosis patients. Molecular microbiology. 2007;64(2):512–33.
17. Bjarnsholt T, Jensen P, Jakobsen TH, Phipps R, Nielsen AK, Rybtke MT, et al. Quorum sensing and virulence of Pseudomonas aeruginosa during lung infection of cystic fibrosis patients. PloS one. 2010;5(4):e10115.
18. Schuster M, Lostroh CP, Ogi T, Greenberg EP. Identification, timing, and signal specificity of Pseudomonas aeruginosa quorum-controlled genes: a transcriptome analysis. Journal of bacteriology. 2003;185(7):2066–79.
19. Wagner VE, Bushnell D, Passador L, Brooks AI, Iglewski BH. Microarray analysis of Pseudomonas aeruginosa quorum-sensing regulons: effects of growth phase and environment. Journal of bacteriology. 2003;185(7):2080–95.
20. Schuster M, Greenberg EP. A network of networks: quorum-sensing gene regulation in Pseudomonas aeruginosa. International journal of medical microbiology: IJMM. 2006;296(2–3):73–81.
21. Lelong E, Marchetti A, Simon M, Burns JL, van Delden C, Köhler T, et al. Evolution of Pseudomonas aeruginosa virulence in infected patients revealed in a Dictyostelium discoideum host model. Clinical microbiology and infection: the official publication of the European Society of Clinical Microbiology and Infectious Diseases. 2011;17(9):1415–20.

22. Lesprit P, Faurisson F, Join-Lambert O, Roudot-Thoraval F, Foglino M, Vissuzaine C, et al. Role of the quorum-sensing system in experimental pneumonia due to Pseudomonas aeruginosa in rats. American journal of respiratory and critical care medicine. 2003;167(11):1478–82.
23. LaFayette SL, Houle D, Beaudoin T, Wojewodka G, Radzioch D, Hoffman LR, et al. Cystic fibrosis-adapted Pseudomonas aeruginosa quorum sensing lasR mutants cause hyperinflammatory responses. Science advances. 2015;1(6).
24. Beck-Schimmer B, Schimmer RC, Pasch T. The airway compartment: chambers of secrets. News in physiological sciences: an international journal of physiology produced jointly by the International Union of Physiological Sciences and the American Physiological Society. 2004;19:129–32.
25. Schnitzler N, Haase G, Podbielski A, Lütticken R, Schweizer KG. A co-stimulatory signal through ICAM-beta2 integrin-binding potentiates neutrophil phagocytosis. Nature medicine. 1999;5(2):231–5.
26. Humlicek AL, Pang L, Look DC. Modulation of airway inflammation and bacterial clearance by epithelial cell ICAM-1. American journal of physiology Lung cellular and molecular physiology. 2004;287(3):L598–607.
27. Sumagin R, Robin AZ, Nusrat A, Parkos CA. Transmigrated neutrophils in the intestinal lumen engage ICAM-1 to regulate the epithelial barrier and neutrophil recruitment. Mucosal immunology. 2014;7(4):905–15.
28. Lawson C, Wolf S. ICAM-1 signaling in endothelial cells. Pharmacological reports: PR. 2009;61(1):22–32.
29. Yu ML, Limper AH. Pneumocystis carinii induces ICAM-1 expression in lung epithelial cells through a TNF-alpha-mediated mechanism. The American journal of physiology. 1997;273(6):L1103–11.
30. Jahn HU, Krüll M, Wuppermann FN, Klucken AC, Rosseau S, Seybold J, et al. Infection and activation of airway epithelial cells by Chlamydia pneumoniae. The Journal of infectious diseases. 2000;182(6):1678–87.
31. Frick AG, Joseph TD, Pang L, Rabe AM, St Geme JW 3rd, Look DC. Haemophilus influenzae stimulates ICAM-1 expression on respiratory epithelial cells. Journal of immunology (Baltimore, Md: 1950). 2000;164(8):4185–96.
32. Beck-Schimmer B, Madjdpour C, Kneller S, Ziegler U, Pasch T, Wüthrich RP, et al. Role of alveolar epithelial ICAM-1 in lipopolysaccharide-induced lung inflammation. The European respiratory journal. 2002;19(6):1142–50.

33. Burns AR, Takei F, Doerschuk CM. Quantitation of ICAM-1 expression in mouse lung during pneumonia. Journal of immunology (Baltimore, Md: 1950). 1994;153(7):3189–98.
34. Tosi MF, Stark JM, Hamedani A, Smith CW, Gruenert DC, Huang YT. Intercellular adhesion molecule-1 (ICAM-1)-dependent and ICAM-1-independent adhesive interactions between polymorphonuclear leukocytes and human airway epithelial cells infected with parainfluenza virus type 2. Journal of immunology (Baltimore, Md: 1950). 1992;149(10):3345–9.
35. Look DC, Rapp SR, Keller BT, Holtzman MJ. Selective induction of intercellular adhesion molecule-1 by interferon-gamma in human airway epithelial cells. The American journal of physiology. 1992;263(1 Pt 1):L79–87.
36. Look DC, Stoll LL, Romig SA, Humlicek A, Britigan BE, Denning GM. Pyocyanin and its precursor phenazine-1-carboxylic acid increase IL-8 and intercellular adhesion molecule-1 expression in human airway epithelial cells by oxidant-dependent mechanisms. Journal of immunology (Baltimore, Md: 1950). 2005;175(6):4017–23.
37. Madjdpour C, Oertli B, Ziegler U, Bonvini JM, Pasch T, Beck-Schimmer B. Lipopolysaccharide induces functional ICAM-1 expression in rat alveolar epithelial cells in vitro. American journal of physiology Lung cellular and molecular physiology. 2000;278(3):L572–9.
38. Hubeau C, Lorenzato M, Couetil JP, Hubert D, Dusser D, Puchelle E, et al. Quantitative analysis of inflammatory cells infiltrating the cystic fibrosis airway mucosa. Clinical & Experimental Immunology. 2001;124(1):69–76.
39. Palmer KL, Aye LM, Whiteley M. Nutritional cues control Pseudomonas aeruginosa multicellular behavior in cystic fibrosis sputum. Journal of bacteriology. 2007;189(22):8079–87.
40. Woods DE, Schaffer MS, Rabin HR, Campbell GD, Sokol PA. Phenotypic comparison of Pseudomonas aeruginosa strains isolated from a variety of clinical sites. Journal of clinical microbiology. 1986;24(2):260–4.
41. Bjorn MJ, Sokol PA, Iglewski BH. Influence of iron on yields of extracellular products in Pseudomonas aeruginosa cultures. Journal of bacteriology. 1979;138(1):193–200.
42. de Chaumont F, Dallongeville S, Chenouard N, Hervé N, Pop S, Provoost T, et al. Icy: an open bioimage informatics platform for extended reproducible research. Nature methods. 2012;9(7):690–6.

43. Sappington KJ, Dandekar AA, Oinuma K, Greenberg EP. Reversible signal binding by the Pseudomonas aeruginosa quorum-sensing signal receptor LasR. mBio. 2011;2(1):e00011–11.
44. Lee JH, Lequette Y, Greenberg EP. Activity of purified QscR, a Pseudomonas aeruginosa orphan quorum-sensing transcription factor. Molecular microbiology. 2006;59(2):602–9.
45. Chugani S, Kim BS, Phattarasukol S, Brittnacher MJ, Choi SH, Harwood CS, et al. Strain-dependent diversity in the Pseudomonas aeruginosa quorum-sensing regulon. Proceedings of the National Academy of Sciences of the United States of America. 2012;109(41):E2823–31.
46. Sorensen M, Kantorek J, Byrnes L, Boutin S, Mall MA, Lasitschka F, et al. Pseudomonas aeruginosa Modulates the Antiviral Response of Bronchial Epithelial Cells. Frontiers in immunology. 2020;11:96.
47. Laarman AJ, Bardoel BW, Ruyken M, Fernie J, Milder FJ, van Strijp JA, et al. Pseudomonas aeruginosa alkaline protease blocks complement activation via the classical and lectin pathways. Journal of immunology (Baltimore, Md: 1950). 2012;188(1):386–93.
48. Leidal KG, Munson KL, Johnson MC, Denning GM. Metalloproteases from Pseudomonas aeruginosa degrade human RANTES, MCP-1, and ENA-78. Journal of interferon & cytokine research: the official journal of the International Society for Interferon and Cytokine Research. 2003;23(6):307–18.
49. Park SJ, Kim SK, So YI, Park HY, Li XH, Yeom DH, et al. Protease IV, a quorum sensing-dependent protease of Pseudomonas aeruginosa modulates insect innate immunity. Molecular microbiology. 2014;94(6):1298–314.
50. Sumagin R, Brazil JC, Nava P, Nishio H, Alam A, Luissint AC, et al. Neutrophil interactions with epithelial-expressed ICAM-1 enhances intestinal mucosal wound healing. Mucosal immunology. 2016;9(5):1151–62.
51. Facchini M, De Fino I, Riva C, Bragonzi A. Long term chronic Pseudomonas aeruginosa airway infection in mice. Journal of visualized experiments: JoVE. 2014(85).
52. Jiricny N, Molin S, Foster K, Diggle SP, Scanlan PD, Ghoul M, et al. Loss of social behaviours in populations of Pseudomonas aeruginosa infecting lungs of patients with cystic fibrosis. PloS one. 2014;9(1):e83124.
53. Skopelja-Gardner S, Theprungsirikul J, Lewis KA, Hammond JH, Carlson KM, Hazlett HF, et al. Regulation of Pseudomonas aeruginosa-Mediated Neutrophil Extracellular Traps. Frontiers in immunology. 2019;10(1670).

54. Alcorn JF, Wright JR. Degradation of pulmonary surfactant protein D by Pseudomonas aeruginosa elastase abrogates innate immune function. The Journal of biological chemistry. 2004;279(29):30871–9.
55. Maillé É, Ruffin M, Adam D, Messaoud H, Lafayette SL, McKay G, et al. Quorum Sensing Down-Regulation Counteracts the Negative Impact of Pseudomonas aeruginosa on CFTR Channel Expression, Function and Rescue in Human Airway Epithelial Cells. Frontiers in cellular and infection microbiology. 2017;7:470.
56. Köhler T, Buckling A, van Delden C. Cooperation and virulence of clinical Pseudomonas aeruginosa populations. Proceedings of the National Academy of Sciences of the United States of America. 2009;106(15):6339–44.
57. Sandoz KM, Mitzimberg SM, Schuster M. Social cheating in Pseudomonas aeruginosa quorum sensing. Proceedings of the National Academy of Sciences of the United States of America. 2007;104(40):15876–81.
58. Hammond JH, Hebert WP, Naimie A, Ray K, Van Gelder RD, DiGiandomenico A, et al. Environmentally Endemic Pseudomonas aeruginosa Strains with Mutations in lasR Are Associated with Increased Disease Severity in Corneal Ulcers. mSphere. 2016;1(5).
59. Dénervaud V, TuQuoc P, Blanc D, Favre-Bonté S, Krishnapillai V, Reimmann C, et al. Characterization of cell-to-cell signaling-deficient Pseudomonas aeruginosa strains colonizing intubated patients. Journal of clinical microbiology. 2004;42(2):554–62.
60. Ciofu O, Johansen HK, Aanaes K, Wassermann T, Alhede M, von Buchwald C, et al. P. aeruginosa in the paranasal sinuses and transplanted lungs have similar adaptive mutations as isolates from chronically infected CF lungs. Journal of cystic fibrosis: official journal of the European Cystic Fibrosis Society. 2013;12(6):729–36.
61. Nguyen D, Singh PK. Evolving stealth: genetic adaptation of Pseudomonas aeruginosa during cystic fibrosis infections. Proceedings of the National Academy of Sciences of the United States of America. 2006;103(22):8305–6.
62. Damkiær S, Yang L, Molin S, Jelsbak L. Evolutionary remodeling of global regulatory networks during long-term bacterial adaptation to human hosts. Proceedings of the National Academy of Sciences of the United States of America. 2013;110(19):7766–71.
63. Dettman JR, Kassen R. Evolutionary Genomics of Niche-Specific Adaptation to the Cystic Fibrosis Lung in Pseudomonas aeruginosa. Molecular biology and evolution. 2021;38(2):663–75.
64. Clay ME, Hammond JH, Zhong F, Chen X, Kowalski CH, Lee AJ, et al. Pseudomonas aeruginosa lasR mutant fitness in microoxia is supported by an Anr-regulated oxygen-

binding hemerythrin. Proceedings of the National Academy of Sciences of the United States of America. 2020;117(6):3167–73.

65. Hammond JH, Dolben EF, Smith TJ, Bhuju S, Hogan DA. Links between Anr and Quorum Sensing in Pseudomonas aeruginosa Biofilms. Journal of bacteriology. 2015;197(17):2810–20.
66. Toyofuku M, Nomura N, Fujii T, Takaya N, Maseda H, Sawada I, et al. Quorum sensing regulates denitrification in Pseudomonas aeruginosa PAO1. Journal of bacteriology. 2007;189(13):4969–72.
67. Heurlier K, Dénervaud V, Haenni M, Guy L, Krishnapillai V, Haas D. Quorum-sensing-negative (lasR) mutants of Pseudomonas aeruginosa avoid cell lysis and death. Journal of bacteriology. 2005;187(14):4875–83.
68. Hoffman LR, Richardson AR, Houston LS, Kulasekara HD, Martens-Habbena W, Klausen M, et al. Nutrient availability as a mechanism for selection of antibiotic tolerant Pseudomonas aeruginosa within the CF airway. PLoS pathogens. 2010;6(1):e1000712.
69. Horvat RT, Parmely MJ. Pseudomonas aeruginosa alkaline protease degrades human gamma interferon and inhibits its bioactivity. Infection and immunity. 1988;56(11):2925–32.
70. Champagne B, Tremblay P, Cantin A, St Pierre Y. Proteolytic cleavage of ICAM-1 by human neutrophil elastase. Journal of immunology (Baltimore, Md: 1950). 1998;161(11):6398–405.
71. Robledo O, Papaioannou A, Ochietti B, Beauchemin C, Legault D, Cantin A, et al. ICAM-1 isoforms: specific activity and sensitivity to cleavage by leukocyte elastase and cathepsin G. European journal of immunology. 2003;33(5):1351–60.
72. Tada H, Sugawara S, Nemoto E, Imamura T, Potempa J, Travis J, et al. Proteolysis of ICAM-1 on human oral epithelial cells by gingipains. Journal of dental research. 2003;82(10):796–801.
73. Kessler E, Safrin M, Gustin JK, Ohman DE. Elastase and the LasA protease of Pseudomonas aeruginosa are secreted with their propeptides. The Journal of biological chemistry. 1998;273(46):30225–31.
74. Oh J, Li XH, Kim SK, Lee JH. Post-secretional activation of Protease IV by quorum sensing in Pseudomonas aeruginosa. Scientific reports. 2017;7(1):4416.
75. Perfetto B, Donnarumma G, Criscuolo D, Paoletti I, Grimaldi E, Tufano MA, et al. Bacterial components induce cytokine and intercellular adhesion molecules-1 and activate transcription factors in dermal fibroblasts. Research in microbiology. 2003;154(5):337–44.

76. Beck-Schimmer B, Schimmer RC, Warner RL, Schmal H, Nordblom G, Flory CM, et al. Expression of lung vascular and airway ICAM-1 after exposure to bacterial lipopolysaccharide. American journal of respiratory cell and molecular biology. 1997;17(3):344–52.
77. Lins RX, de Assis MC, Mallet de Lima CD, Freitas C, Maciel Plotkowski MC, Saliba AM. ExoU modulates soluble and membrane-bound ICAM-1 in Pseudomonas aeruginosa-infected endothelial cells. Microbes and infection. 2010;12(2):154–61.
78. Grenier D, Bodet C. Streptococcus suis stimulates ICAM-1 shedding from microvascular endothelial cells. FEMS immunology and medical microbiology. 2008;54(2):271–6.
79. Galle M, Carpentier I, Beyaert R. Structure and function of the Type III secretion system of Pseudomonas aeruginosa. Current protein & peptide science. 2012;13(8):831–42.
80. Wang SZ, Hallsworth PG, Dowling KD, Alpers JH, Bowden JJ, Forsyth KD. Adhesion molecule expression on epithelial cells infected with respiratory syncytial virus. The European respiratory journal. 2000;15(2):358–66.
81. Sabatini F, Silvestri M, Sale R, Serpero L, Di Blasi P, Rossi GA. Cytokine release and adhesion molecule expression by stimulated human bronchial epithelial cells are downregulated by salmeterol. Respiratory medicine. 2003;97(9):1052–60. pmid:14509560
82. Atsuta J, Sterbinsky SA, Plitt J, Schwiebert LM, Bochner BS, Schleimer RP. Phenotyping and cytokine regulation of the BEAS-2B human bronchial epithelial cell: demonstration of inducible expression of the adhesion molecules VCAM-1 and ICAM-1. American journal of respiratory cell and molecular biology. 1997;17(5):571–82.
83. Rada B, Leto TL. Pyocyanin effects on respiratory epithelium: relevance in Pseudomonas aeruginosa airway infections. Trends in microbiology. 2013;21(2):73–81.
84. Bianchi SM, Prince LR, McPhillips K, Allen L, Marriott HM, Taylor GW, et al. Impairment of apoptotic cell engulfment by pyocyanin, a toxic metabolite of Pseudomonas aeruginosa. American journal of respiratory and critical care medicine. 2008;177(1):35–43.
85. Jensen P, Bjarnsholt T, Phipps R, Rasmussen TB, Calum H, Christoffersen L, et al. Rapid necrotic killing of polymorphonuclear leukocytes is caused by quorum-sensing-controlled production of rhamnolipid by Pseudomonas aeruginosa. Microbiology (Reading, England). 2007;153(Pt 5):1329–38.
86. Horvat RT, Clabaugh M, Duval-Jobe C, Parmely MJ. Inactivation of human gamma interferon by Pseudomonas aeruginosa proteases: elastase augments the effects of alkaline

protease despite the presence of alpha 2-macroglobulin. Infection and immunity. 1989;57(6):1668–74.

87. Moraes TJ, Martin R, Plumb JD, Vachon E, Cameron CM, Danesh A, et al. Role of PAR2 in murine pulmonary pseudomonal infection. American journal of physiology Lung cellular and molecular physiology. 2008;294(2):L368–77.
88. Kida Y, Higashimoto Y, Inoue H, Shimizu T, Kuwano K. A novel secreted protease from Pseudomonas aeruginosa activates NF-kappaB through protease-activated receptors. Cellular microbiology. 2008;10(7):1491–504.
89. Casilag F, Lorenz A, Krueger J, Klawonn F, Weiss S, Häussler S. The LasB Elastase of Pseudomonas aeruginosa Acts in Concert with Alkaline Protease AprA To Prevent Flagellin-Mediated Immune Recognition. Infection and immunity. 2016;84(1):162–71.
90. Bardoel BW, van der Ent S, Pel MJ, Tommassen J, Pieterse CM, van Kessel KP, et al. Pseudomonas evades immune recognition of flagellin in both mammals and plants. PLoS pathogens. 2011;7(8):e1002206.
91. Kasper M, Koslowski R, Luther T, Schuh D, Müller M, Wenzel KW. Immunohistochemical evidence for loss of ICAM-1 by alveolar epithelial cells in pulmonary fibrosis. Histochemistry and cell biology. 1995;104(5):397–405.
92. Chan SC, Shum DK, Tipoe GL, Mak JC, Leung ET, Ip MS. Upregulation of ICAM-1 expression in bronchial epithelial cells by airway secretions in bronchiectasis. Respiratory medicine. 2008;102(2):287–98.
93. Tomassini JE, Graham D, DeWitt CM, Lineberger DW, Rodkey JA, Colonno RJ. cDNA cloning reveals that the major group rhinovirus receptor on HeLa cells is intercellular adhesion molecule 1. Proceedings of the National Academy of Sciences of the United States of America. 1989;86(13):4907–11.
94. Gulraiz F, Bellinghausen C, Bruggeman CA, Stassen FR. Haemophilus influenzae increases the susceptibility and inflammatory response of airway epithelial cells to viral infections. FASEB journal: official publication of the Federation of American Societies for Experimental Biology. 2015;29(3):849–58.
95. Goffard A, Lambert V, Salleron J, Herwegh S, Engelmann I, Pinel C, et al. Virus and cystic fibrosis: rhinoviruses are associated with exacerbations in adult patients. Journal of clinical virology: the official publication of the Pan American Society for Clinical Virology. 2014;60(2):147–53. pmid:24637203.

96. Rahme LG, Stevens EJ, Wolfort SF, Shao J, Tompkins RG, Ausubel FM. Common virulence factors for bacterial pathogenicity in plants and animals. Science (New York, NY). 1995;268(5219):1899-902.
97. Déziel E, Lépine F, Milot S, He J, Mindrinos MN, Tompkins RG, et al. Analysis of Pseudomonas aeruginosa 4-hydroxy-2-alkylquinolines (HAQs) reveals a role for 4-hydroxy-2-heptylquinoline in cell-to-cell communication. Proceedings of the National Academy of Sciences of the United States of America. 2004;101(5):1339-44.
98. Hobden JA. Pseudomonas aeruginosa proteases and corneal virulence. DNA and cell biology. 2002;21(5-6):391-6.
99. Cowell BA, Twining SS, Hobden JA, Kwong MSF, Fleiszig SMJ. Mutation of lasA and lasB reduces Pseudomonas aeruginosa invasion of epithelial cells. Microbiology (Reading, England). 2003;149(Pt 8):2291-9.
100. Khakimova M, Ahlgren HG, Harrison JJ, English AM, Nguyen D. The stringent response controls catalases in Pseudomonas aeruginosa and is required for hydrogen peroxide and antibiotic tolerance. Journal of bacteriology. 2013;195(9):2011-20.

Preamble to Chapter 3

Together, *P.a.*-associated lung pathology and bacterial persistence represent the biggest challenges in the treatment of chronic *P.a.* infections in CF patients. While we explored the inflammatory consequences of a common adaptation observed in *P.a.* isolates from chronic infections in chapter 2, we sought to explore another aspect of *P.a.* pathogenesis in chapter 3. *P.a.* employs a multitude of mechanisms, including biofilm formation and antibiotic resistance, that account for its considerable persistence during chronic infection stages. Another potential mechanism is intracellular *P.a.* survival within AEC, which would potentially allow for increased antibiotic tolerance and immune evasion. For instance, intracellular *P.a.* within the airway epithelium may function as a reservoir during antibiotic eradication therapy. However, the long-term intracellular survival of *P.a.* remains poorly understood as most infection models focus on internalization and short-term intracellular survival. We thus sought to establish a robust model of long-term intracellular *P.a.* survival within AEC that would allow us to identify bacterial factors facilitating intracellular *P.a.* survival.

Chapter 3: A Model of Intracellular Persistence of *Pseudomonas aeruginosa* in Airway Epithelial Cells

Julien K. Malet[1]*, Lisa C. Hennemann[1,2]*, Elizabeth M.-L. Hua[2], Emmanuel Faure[3,4], Valerie Waters[5], Simon Rousseau[1] and Dao Nguyen[1,2,6]

*Contributed equally

[1]Meakins Christie Laboratories, Research Institute of the McGill University Health Centre, Montreal, Quebec, Canada

[2]Department of Microbiology and Immunology, McGill University, Montreal, Quebec, Canada

[3]Univ. Lille, U1019-UMR 9017-CIIL-Center for Infection and Immunity of Lille, F-59000 Lille, France

[4]CHU Lille, Service Universitaire de Maladies Infectieuses, F-59000 Lille, France

[5]Division of Infectious Diseases, Department of Pediatrics, The Hospital for Sick Children, University of Toronto, Toronto, CA, Canada

[6]Department of Medicine, McGill University, Montreal, Quebec, Canada

Cellular Microbiology, vol. 2022, Article ID 5431666, 14 pages, 2022.

3.1 Abstract

Pseudomonas aeruginosa (*P.a.*) is a major human pathogen capable of causing chronic infections in hosts with weakened barrier functions and host defenses, most notably airway infections commonly observed in individuals with the genetic disorder cystic fibrosis (CF). While mainly described as an extracellular pathogen, previous *in vitro* studies have described the molecular events leading to *P.a.* internalization in diverse epithelial cell types. However, the long-term fate of intracellular *P.a.* remains largely unknown. Here, we developed a model allowing for a better understanding of long-term (up to 120 h) intracellular bacterial survival in the airway epithelial cell line BEAS-2B. Using a tobramycin protection assay, we characterized the internalization, long-term intracellular survival, and cytotoxicity of the lab strain PAO1, as well as clinical CF isolates, and conducted analyses at the single-cell level using confocal microscopy and flow cytometry techniques. We observed that infection at low multiplicity of infection allows for intracellular survival up to 120 h post-infection without causing significant host cytotoxicity. Finally, infection with clinical isolates revealed significant strain-to-strain heterogeneity in intracellular survival, including a high persistence phenotype associated with bacterial replication within host cells. Future studies using this model will further elucidate the host and bacterial mechanisms that promote *P. aeruginosa* intracellular persistence in airway epithelial cells, a potentially unrecognized bacterial reservoir during chronic infections.

3.2 Introduction

Many bacteria can survive within the intracellular host environment where they escape immune recognition, clearance by extracellular host defenses, and many antibiotics. While the intracellular lifestyle of obligate intracellular pathogens (e.g., *Chlamydia* and *Rickettsia* species) and facultative intracellular pathogens (e.g., *Listeria monocytogenes* and *Salmonella enterica*) has been extensively studied, the capacity for intracellular residence of other bacteria classically known as extracellular pathogens is less well appreciated. Several bacterial pathogens, such as *Staphylococcus aureus* and *Escherichia coli*, can invade, survive, and in some cases replicate within host cells. By adopting an intracellular lifestyle, their evasion of host defenses and antimicrobial therapy likely contributes to their ability to cause infections that persist or recur after antibiotic treatment (1, 2). For example, uropathogenic *Escherichia coli* can persist within bladder epithelial cells for several weeks in murine models of urinary tract infections (3, 4), and its intracellular form has been detected in urinary samples of patients with recurrent urinary tract infections

(5, 6). *Staphylococcus aureus* can invade different cell types, including phagocytes, epithelial, and endothelial cells *in vitro* (7–9), and its intracellular residence in nonphagocytic cells has been linked to chronic rhinosinusitis, osteomyelitis, and mastitis (10–13). Not only are intracellular bacteria able to survive during antibiotic treatment, as many antibiotics show limited penetration and/or activity inside host cells, but intracellular bacteria may also serve as a reservoir for reinfection of surrounding tissue, thus contributing to the establishment of difficult to eradicate chronic infections (11, 14, 15).

Pseudomonas aeruginosa (*P.a.*) is an opportunistic gram-negative bacterium, primarily known as an extracellular pathogen capable of causing a wide spectrum of human infections. Notably, *P.a.* colonizes mucosal and external epithelial surfaces in hosts with impaired barrier functions and host defenses, causing chronic or subacute infections of different organs and tissues such as the cornea, soft tissue wounds, and airways (16). Chronic *P.a.* airway infections are common in individuals with cystic fibrosis (CF) who carry mutations in the cystic fibrosis transmembrane conductance regulator (CFTR) gene, and in whom defects in mucociliary clearance and mucosal host immunity lead to impaired bacterial clearance (17). Within respiratory secretions found in the airway lumen (18–21), *P.a.* can form biofilm microcolonies refractory to antibacterial killing and immune clearance (22, 23). *P.a.* also subverts host immunity through a wide range of mechanisms (24), such as bacterial type 3 secretion system (T3SS)-mediated host cell killing (25), proteolytic degradation of proinflammatory and immune mediators (26–28), and exopolysaccharide overproduction (29). While these host and antimicrobial evasion mechanisms have been extensively studied, the intracellular lifestyle of *P.a.* within airway epithelial cells and its potential contribution to the persistence of *P.a.* infections have been largely overlooked.

Previous *in vitro* studies have demonstrated *P.a.*'s ability to invade different epithelial and endothelial cell types. *P.a.* binds to the epithelium through interactions of bacterial adhesins (e.g., flagellum, type IV pilus, and LecA) (30–33) or other surface molecules (e.g., outer membrane porins and lipopolysaccharides) (34, 35) with host cell surface binding motifs (glycosphingolipid Gb3, N-glycosylated receptors, or heparan sulfate proteoglycans) (31, 32). *P.a.*'s entry is an actin-dependent process which requires Rho family GTPases (Rho, Cdc42, or Rak1) for cytoskeletal remodeling (36, 37). Recruitment of the host cell endocytic machinery is mediated by several signal transduction pathways, notably the phosphatidylinositol 3-kinase (PI3K)/PIP3/Akt pathway (30, 31, 38, 39), but also through

activation of different tyrosine kinases, such as Src, Abl, and Fyn (37, 40, 41). Studies examining the fate of intracellular *P.a*. (42–46) have primarily focused on short-term survival (typically 3 h to 8 h post-infection (p.i.)) and were performed in different epithelial cell types. Intracellular *P.a.* was described by the Fleiszig group to reside in nonapoptotic blebs, namely large cytosolic compartments generated by the detachment of host membranes from the cytoskeletal cortex (42, 43, 45, 47, 48). Others observed intracellular *P.a.* in cytosolic dense aggregates called pod-like compartments similar to those formed by *E. coli* in bladder cells (44, 49) or in membrane-bound intracellular vesicles (39, 50).

Remarkably, the long-term fate of intracellular *P.a.* within epithelial cells is largely unknown. Garcia-Medina et al. assessed the long-term intracellular survival of the lab strain PAO1 in mouse tracheal epithelial cells and reported *P.a.* persistence without loss of host cell viability up to 72 h p.i (44). More recently, Penaranda et al. assessed the intracellular survival of *P.a.* in the human 5637 bladder cell line and also observed bacterial survival up to 48 h p.i. without significant host cell death despite upregulation of the NF-κB signaling pathway (50). Interestingly, results from several studies also suggest that the intracellular survival of *P.a.* clinical isolates may differ from laboratory strains such as PAO1 (50–53).

In order to better understand the intracellular persistence of *P.a.*, we developed a model of *P.a.* infection in airway epithelial cells that allowed the study of long-term (up to 120 h) intracellular bacterial survival. We characterized the infection kinetics with measurements of intracellular bacterial burden by viable bacterial counts and host cell cytotoxicity. For studies at the single-cell level, we validated analyses by flow cytometry, cell sorting, and confocal microscopy. Using this model, we also assessed several *P.a.* clinical isolates and demonstrated significant heterogeneity in the intracellular survival phenotype, including a high persistence phenotype.

3.3 Material and Methods

Bacterial Strains and Growth Conditions

Bacterial strains used in this study are listed in Supplementary Table S3.1. Bacterial strains were streaked from frozen stocks onto LB agar (BD Difco) (Wisent, 800-015) or LB agar containing 250 μg/mL carbenicillin (for PAO1-mCherry) and incubated overnight at 37°C. Isolated colonies were then inoculated in 5 mL of liquid LB media or LB media containing 250 μg/mL carbenicillin and incubated overnight at 37°C with shaking at 250 r.p.m. After 2

washes with sterile PBS (#311-010, Wisent), the bacterial cell pellets were resuspended in 5 mL of PBS to an optical density, equivalent to ~10^9 CFU/mL. The initial dilution in PBS was followed by serial dilution in Dulbecco's modified Eagle's medium (DMEM, #319-005-CL, Wisent) supplemented with 10% heat-inactivated fetal bovine serum (FBS, #080-150, Wisent) to reach the desired multiplicity of infection (MOI).

Airway Epithelial Cell Culture Conditions and *P.a.* Infection

Immortalized human bronchial epithelial cells (BEAS-2B) were grown in DMEM supplemented with 10% heat-inactivated FBS and 50 IU/50 μg/mL penicillin/streptomycin (#450-200, Wisent) at 37°C with 5% CO_2. Once ~90% confluent, BEAS-2B cells were harvested and seeded at a density of 200,000 cells/mL (100,000 cells/well) in DMEM supplemented with 10% FBS in 24-well tissue culture plates (#83.3922, Sarstedt) in the absence of antibiotics. After seeding, plates were incubated for 24 hours at 37°C prior to infection. The medium was then replaced by 500 μL of bacterial suspension at the required MOI in DMEM supplemented with 10% FBS (no antibiotics) and mixed by gentle shaking in a cross-wise manner. Plates were then centrifuged at 700 r.p.m. for 3 min to allow for bacterial adherence. After 4-h incubation at 37°C with 5% CO_2 for the internalization phase, tobramycin (#32986-56-4, Sigma-Aldrich) was added to each well to a final concentration of 100 μg/mL for 15 min (or until the end of infection when using clinical isolates) before harvesting for the $T = 4-$h time point. For later time points, the media was replaced by fresh DMEM (with 10% FBS) containing variable concentrations of tobramycin (25 μg/mL unless specified otherwise) for maintenance until cell harvest. For cell harvest, culture supernatants were first collected. Cells were then washed with PBS and lysed with 0.5% Triton X-100 (#9002-93-1, Sigma-Aldrich) in sterile PBS. Lysed cells were serially diluted in sterile PBS and plated on LB agar plates for bacterial growth. After overnight incubation at 37°C, CFU were counted to determine the viable intracellular bacterial load. Culture supernatants were also plated on LB agar plates to confirm the absence of extracellular bacteria in the cell culture media.

Cytotoxicity Assay

Epithelial cell viability was assessed using the lactate dehydrogenase (LDH) release/cytotoxicity assay, with measurement of LDH released by damaged cells into the culture supernatant and LDH in cell lysates as a measure of intact cell biomass (LDH assay kit, #11644793001, Sigma-Aldrich) according to the manufacturer's instructions. LDH concentrations were measured by absorbance at 492 nm (with reference wavelength subtraction

at 690 nm), and cytotoxicity was expressed as the ratio of released LDH (in the supernatant) to total LDH (in the supernatant + cell lysate). To estimate the AEC biomass, we established a LDH standard curve using 10-fold dilution of BEAS-2B cells (from 1,000,000 cells to 5,000 cells) spun down, lysed with 0.5% Triton X-100 and used for LDH determination.

Flow Cytometry Analyses

Confluent BEAS-2B cells were harvested, seeded at a density of 200,000 cells/mL (200,000 cells/well) in DMEM supplemented with 10% FBS in 12-well tissue culture plates (#83.3921, Sarstedt), and infected with *P.a.* as described above. At the indicated time points following infection, culture supernatants were first collected to recover cells that had detached during the infection. Adherent cells were gently washed with PBS and incubated for 3 min at RT in PBS containing 1 mM EDTA (#60-00-4, Sigma-Aldrich) and 1 mM EGTA (#E4378, Sigma) to detach cells before harvesting by gentle pipetting. Cell suspensions were then pooled with their respective supernatants, centrifuged (2000 r.p.m for 5 min), and transferred to 96-well round-bottom plates (#82.1582, Sarstedt). Cells were then stained with 1 : 1000 Fixable Viability Dye eFluor 780 (FVD eF780, #65-0865-14, eBioscience) in PBS for 30 min on ice, followed by a wash with FACS buffer (PBS+0.5% FBS) and fixation in 0.5% PFA (#554655, BD Biosciences) for 10 minutes at RT. For cell sorting experiments, cells remained unfixed. Cells were then resuspended in FACS buffer for downstream analyses.

Stained cells were analyzed with an LSR II flow cytometer (BD Biosciences) and results were analyzed using FlowJo (BD Biosciences). Debris (low FSC-A, low SSC-A), doublets (SSC-A > SSC-H), and dead cells (high FVD eF780) were excluded. The gating for mCherry-positive cells was then defined for each experiment by exclusion of BEAS-2B cells infected with the nonfluorescent isogenic PAO1 strain (negative control) and restricting the false-positive mCherry signal to <0.5%. The proportion of dead cells was estimated as the percentage of dead cells among all single cells (after excluding debris and doublets).

Fluorescence-Activated Cell Sorting

For cell sorting, stained cells were resuspended at 5,000,000 cells/mL of FACS buffer before sorting using a BD FACSAria Fusion Cell Sorter (BD Biosciences). In order to validate the viability, plasmid expression, and amount of intracellular bacteria in mCherry-neg, mCherry-low, and mCherry-high populations, 10 and 100 cells for each population were sorted in 100 μL

of lysis buffer (0.5% Triton X-100 in PBS) in a 96-well plate format at room temperature and processed for cell sorting validation.

To measure viable intracellular bacteria, sorted cells were lysed in 100 μL 0.5% Triton X-100 in PBS through vigorous pipetting. 45 μL of lysate were then plated on one regular LB agar plate and one LB agar plate containing 250 μg/mL carbenicillin, each. Plates were incubated overnight at 37°C, and CFU counts were enumerated the next day.

Detection of Intracellular *P.a.* by Immunofluorescence

BEAS-2B cells were seeded on uncoated sterile 15 mm or 12 mm round microscopy-grade borosilicate glass coverslips (0.13 to 0.17 mm thick, #12-545-80P or #22-031-145P, Fisherbrand) placed in 24-well plates and infected as described above (100.000 cells/well). At defined time points, cells were gently washed with PBS before fixation in 1% PFA for 15 min. Cells were then washed twice in PBS and blocked for 20 min at RT in staining solution (PBS+1% Bovine Serum Albumin (#A7906, Sigma-Aldrich) +1% goat serum (#G9023, Sigma-Aldrich)). Extracellular *P.a.* was first stained with a polyclonal anti-*P.a.* rabbit antibody (1:1000 dilution in staining solution, Abcam ab68538) for 45 min and counterstained for 30 min with an Alexa Fluor 647-conjugated antirabbit secondary goat antibody (1: 500 dilution, #A21-244, Life Technologies). Cells were then permeabilized with 0.2% Triton X-100 for 10 min, blocked, stained for both intracellular and extracellular *P.a.* (total *P.a.* stain) with the same polyclonal anti-*P.a*. rabbit antibody (1: 1000 dilution, Abcam ab68538) for 45 min, and counterstained for 30 min with an Alexa Fluor 488-conjugated antirabbit secondary goat antibody (1 : 500 dilution, #A11-008, Life Technologies) as well as DAPI nuclear stain (#LSD1306, Invitrogen) and TRITC-conjugated phalloidin (#5783, R&D) to stain the actin cytoskeleton. Samples were then mounted on glass coverslips using Fluoromount-G (#50-187-88, Thermo Fisher Scientific). Extracellular *P.a.*was thus double stained by the extracellular and the total *P.a.* stains, while intracellular *P.a.*was single stained by the total *P.a.* stain.

Confocal Microscopy and Image Analysis

Samples were imaged with a Zeiss LSM700 confocal microscope equipped with 405 nm, 488 nm, 543 nm, and 633 nm lasers for the DAPI, AF488, TRITC, and AF647 channels, respectively. For each coverslip, 16 to 100 fields of view were randomly acquired (based on DAPI staining for focusing) with a 40× or 63× oil immersion objective for imaging of a minimum of 1000 (up to 9000) epithelial cells from at least 2 independent experiments. Z-

stacks covering approximately 10-μm depth of the sample were acquired for maximum intensity Z-projection images. For each individual experiment, acquisition (including laser power, electronic gain, and background) and processing (fluorescence threshold) parameters were optimized for detection of host cells and bacteria using infected AEC and extracellular bacteria controls and kept constant for acquisition of all images. Intracellular bacteria were defined as a single green (Alexa Fluor 488) fluorescent signal at least 4 pixels in size (equivalent to approximately 500 nm) on maximum intensity Z-projection, located within the limits of the actin cytoskeleton (phalloidin staining). If any signal bigger than 2 pixels was also observed in the red channel (Alexa Fluor 647), the bacteria was considered as double positive and thus extracellular. For each image, the percentage of AEC harboring intracellular bacteria as well as the number of intracellular bacteria per AEC were reported. All images were randomly and manually analyzed by 2 blinded readers using ImageJ (54) software. Maximum intensity Z-projection images used for analysis are available at https://omero.med.ualberta.ca/webclient/?show=dataset-1152.

Automated analyses of confocal images (maximum intensity Z-projection) were also performed using a customized pipeline in Icy software (55) for counting of intracellular bacteria in eukaryotic cells (Icy analysis pipeline and script available as Supplementary methods and at https://omero.med.ualberta.ca/webclient/?show=dataset-1152). Eukaryotic cell segmentation was performed by active contouring of the cell nuclei using the actin signal as boundary. Identification of intracellular bacteria was based on spot detection (scale 2 parameter ≅3 pixel-sized objects) analysis performed on both red (extracellular stain) and green (total stain) channels, followed by colocalization analysis of the detected spots. Spots detected in the green channel that were not colocalized with spots in the red channel were considered as intracellular bacteria, while those that colocalized in both channels were considered extracellular bacteria. Correlation analysis of automated counts vs. manual counts was performed using a random subset of images (n=29) from one representative experiment.

Statistical Analysis

Results are shown as mean ± SD unless stated otherwise. Statistical analyses between 2 or more categorical groups were performed using a 2-way ANOVA followed by Tukey's multiple comparisons test. Correlation analyses were done using the Pearson's correlation coefficient. A P value ≤0.05 was considered statistically significant, *P < 0.05, **P < 0.01, and ***P <

0.001. All analyses were done using the GraphPad Prism 7.0a (GraphPad Software, San Diego).

3.4 Results

Development of an *In Vitro* Model of *P. aeruginosa* Long-Term Intracellular Survival in Human Airway Epithelial Cells

We sought to develop and validate a model of infection which optimized both bacterial survival and host cell viability for a period up to 120 h p.i. Airway epithelial cells (AECs) were first incubated for 4 h with *P.a.* to allow bacterial adhesion and uptake during an initial internalization phase, followed by an intracellular persistence phase where AEC were treated with tobramycin and maintained in tobramycin-containing culture medium. Tobramycin and other aminoglycosides, such as gentamicin, are cell impermeable antibiotics that kill extracellular bacteria while sparing intracellular ones and have thus been extensively used for the study of intracellular bacteria including *P.a.* (44–46, 48, 56). In an initial experiment, we observed that the intracellular bacterial burden at 4 h p.i. was 9.5-fold higher in BEAS-2B compared to CFBE-*wt* cells grown in submerged cultures, two commonly used immortalized human epithelial cell line of bronchial origin (average of 3.5×10^4 vs. 3.7×10^3 CFU/well for BEAS-2B and CFBE-*wt*, respectively, Figure S3.1A-B), suggesting greater bacterial internalization in BEAS-2B cells. We thus chose to use BEAS-2B cells (57) for our model as this AEC cell line readily internalized *P.a.*

We then characterized the intracellular infection kinetics using different bacterial inoculum corresponding to a multiplicity of infection (MOI) of 0.1, 1, and 10 by assessing the intracellular bacterial burden by viable colony forming unit (CFU) count after AEC lysis and cytotoxicity by measurement of lactate dehydrogenase (LDH) release into the media. We observed that bacterial internalization (CFU count at T=4 h) was relatively proportional to the MOI, with a 7-fold increase in internalization from MOI 0.1 to 1 and a 5-fold increase from MOI 1 to 10 (Figure 3.1A). After initial entry in BEAS-2B, the viable intracellular bacterial burden declined over time, with infections at MOI 10 resulting in the most rapid decline over 48 h from 1.9×10^5 CFU/well to 3.3×10^2 CFU/well, which led to near eradication of intracellular *P.a.* by 120 h p.i. In contrast, infections with MOI 1 and 0.1 resulted in only a modest decline in viable intracellular bacterial burden and allowed for significant bacterial persistence at 120 h p.i (Figure 3.1A and S3.1C). Notably, concomitant measurements of LDH release revealed that the marked reduction in intracellular CFU counts in cells infected at MOI

10 was associated with very high cytotoxicity (98% at 24 h to 94% at 120 h p.i) compared to MOI 1 (25.3% at 24 h and 17.4% at 120 h p.i) and 0.1 (4.9% at 24 h and 11.2% at 120 h p.i) (Figure 3.1B and Figure S3.1D). These results thus indicate that infection at low MOIs of 1 and 0.1 allow for long-term intracellular persistence of *P.a.* within AEC, whereas infection at MOI 10 results in a rapid decline in intracellular bacterial counts likely attributable to extensive host cell death. We noted that the modest reduction in cell death estimates between 48 h and 120 h in AEC infected at MOI 10 (from 99.0% to 94.3%) and MOI 1 (from 26.6% to 17.4%) were likely attributable to AEC proliferation during the course of the experiment. Indeed, using total LDH as a quantitative estimate of AEC biomass (Figure S3.1F), we observed an average of 2.3-fold increase in AEC biomass over 5 days for all conditions except for AEC infected at MOI 10 where AEC biomass first declined significantly between 4 h and 24 h (Figure S3.1E).

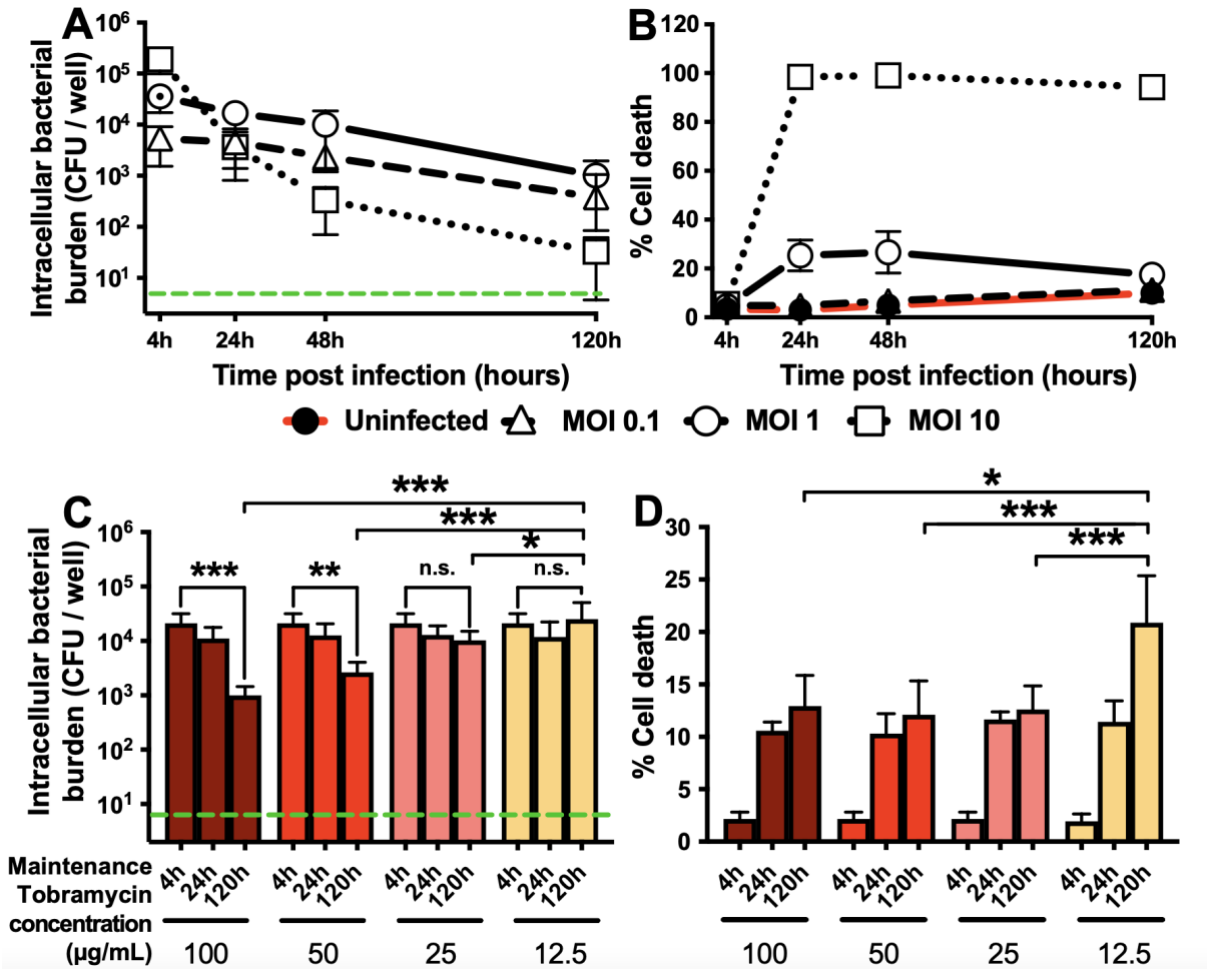

Figure 3.1

Intracellular *P.a.* survival in an airway epithelial cell infection model. (A) Intracellular bacterial burden and (B) cytotoxicity after infection with different MOI. (C) Intracellular bacterial burden and (D) cytotoxicity at different maintenance concentrations of tobramycin.

For all experiments, BEAS-2B cells were infected with *P.a.* strain PAO1 at MOI 1, unless stated otherwise. After 4 h p.i., extracellular bacteria were first killed with 100 µg/mL tobramycin × 15 min for all experiments. For (A) and (B), AEC cultures were then maintained in 100 µg/mL tobramycin for the remainder of the experiment, while the tobramycin maintenance concentrations ranged from 12.5 to 100 µg/mL for (C) and (D) as indicated. The intracellular bacterial burden was measured by viable CFU count (detection limit shown as green dashed line), and cytotoxicity was measured by LDH release assay. Results shown are from data pooled from ≥4 biological replicates (≥2 independent experiments). *P < 0.05; **P < 0.01; ***P < 0.001.

Following the initial internalization phase, *P.a.*-infected AEC were briefly treated with tobramycin at a bactericidal concentration (100 μg/mL for 15 min) to eliminate the remaining extracellular bacteria. For the subsequent intracellular persistence phase, AEC were then maintained in culture medium containing tobramycin to inhibit any extracellular replication of bacteria released from AEC and thus avoid host cell reinfection or bacterial overgrowth in the cell culture medium. Although aminoglycosides cannot permeate cell membranes due to their anionic nature, they can still slowly accumulate intracellularly by fluid-phase endocytosis at high concentrations (58–60), a process which can influence survival of intracellular bacteria. We therefore compared the effect of different "maintenance" tobramycin concentrations (100, 50, 25, and 12.5 μg/mL) on the infection kinetics. We observed that the tobramycin concentration did not affect intracellular bacterial counts at 24 h (Figure 3.1C). However, by 120 h, 100 and 50 μg/mL tobramycin were associated with 21- and 8-fold decrease in intracellular CFU count compared to 4 h, respectively, while 25 and 12.5 μg/mL tobramycin were not. Although the highest intracellular bacterial burden at 120 h p.i was observed with 12.5 μg/mL tobramycin, this low maintenance concentration of tobramycin also led to a significant increase of cell death, likely due to breakthrough growth of extracellular bacteria causing cell death (Figure 3.1D and Figure S3.1G). These results showed that the long-term survival of intracellular bacteria and AEC viability were optimal with PAO1 infection at a MOI 1 and maintenance of AEC with 25 μg/mL tobramycin.

Flow Cytometry Analysis to Assess Intracellular Infection at the Single-Cell Level

Measurement of intracellular bacterial burden by viable CFU counts allows assessment of bacterial survival in AEC on a population level but lacks resolution at the single-cell level. In order to measure both the percentage of infected AEC and the bacterial burden in individual

AEC, we analyzed AEC infected with a fluorescently tagged mCherry-PAO1 strain by flow cytometry. After infection with mCherry-PAO1 using the model described above, AEC harvested at different time points were stained with fixable viability dye and analyzed for mCherry fluorescence. A gating strategy (shown in Figure S3.2A-C) was set using an isogenic nonfluorescent *P.a.* strain to allow for a false-positive rate of mCherry(+) AEC of <=0.5% (Figure 3.2A). We observed that 9.1% of live AEC harbored intracellular *P.a.* at 4 h p.i, a rate which decreased to 6.6% and 6.2% at 24 h and 120 h, p.i, respectively (Figure 3.2C; data from all independent experiments are shown in Figure S3.2D-G)). We also found more cell death among AEC exposed to *P.a.* compared to uninfected AEC (10.6% vs. 5.9% at 4 h p.i, 19.7% vs. 4.3 at 24 h p.i, and 14.5% vs. 3.2 at 120 h p.i, respectively), with cell death peaking at 24 h p.i (Figure 3.2D). These results were consistent with the cytotoxicity assessment by LDH release assay (Figure 3.1B).

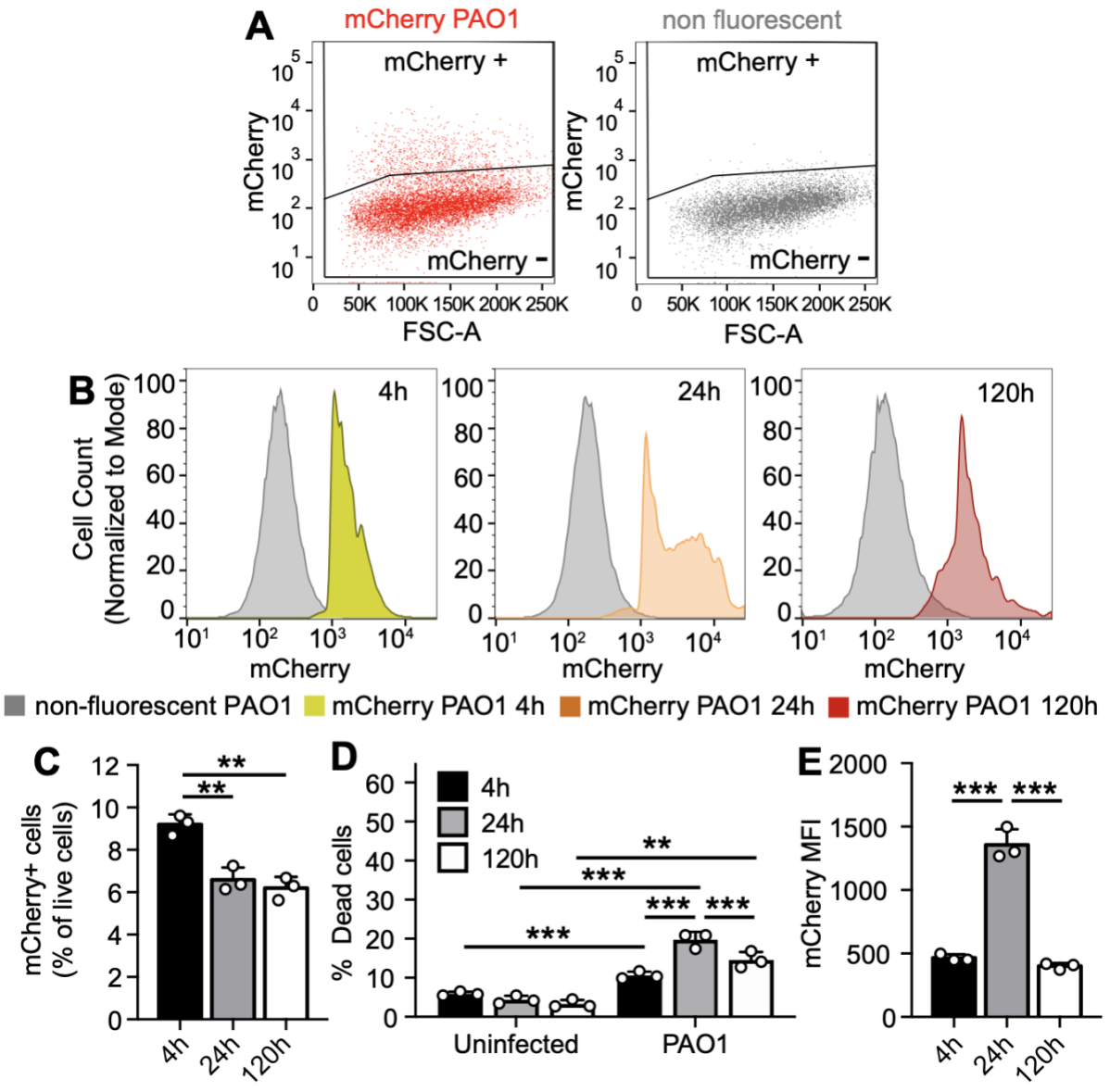

Figure 3.2

Analysis of *P.a.*-infected AEC by flow cytometry. (A) Gating strategy based on mCherry fluorescence intensity and forward scatter area (FSC-A) to detect mCherry(+)-infected AEC, with exclusion of mCherry(-) noninfected AEC using control samples infected with nonfluorescent PAO1. (B) mCherry fluorescence histograms of the AEC populations at different time points after infection with nonfluorescent PAO1 (whole population, grey) or mCherry PAO1 (mCherry(+) population only, colored) as indicated. Quantification of the proportion of (C) mCherry(+) AEC among all live AEC or (D) dead (FVD+) AEC among all AEC. (E) mCherry median fluorescence intensity (MFI) of the mCherry(+) AEC population at different time points after infection. The mCherry MFI of cells infected with nonfluorescent PAO1 was subtracted from the MFI of mCherry(+) cells to account for day-to-day variability in fluorescence. For all experiments, BEAS-2B cells were infected at MOI 1, except for

uninfected (UI) controls. ≥20,000 cells were analyzed in each sample. For (A) and (B), representative scatter plots and histograms are shown. For (C), (D), and (E), results shown are from biological triplicates from one representative experiment of 3 independent ones (data from all 3 independent experiments are shown in Figure S3.2). *P < 0.05; **P < 0.01; ***P < 0.001.

In order to confirm that mCherry(+) cells harbored live bacteria and that mCherry(-) cells did not, we sorted live AEC cells infected with mCherry-PAO1 at 24 h p.i into 3 different populations based on their mCherry fluorescence: mCherry negative, mCherry low, and mCherry high as shown in Figure S3.2H. Those AEC populations were sorted into sterile lysis buffer in pools of 10 or 100 cells per well for subsequent plating and CFU counts. No viable bacteria were recovered from mCherry-negative AEC lysates, compared to an average of 81 CFU/100 cells in mCherry-high populations and 12 CFU/100 cells in mCherry-low populations (Figure S3.2I). These results thus validated that most AEC from the mCherry-high populations likely harbored viable intracellular bacteria, while some cells from mCherry-low populations likely did not, and no cells from the mCherry-negative population did. Since the mCherry fluorescence histograms of mCherry-PAO1-infected AEC at 24 h p.i (Figure 3.2B and S3.2G) displayed a bimodal distribution, we also sought to confirm that intracellular bacteria did not lose fluorescence due to a loss of the mCherry expression plasmid. AEC lysates from the mCherry(+) populations were thus simultaneously plated for viable CFU counts on media without antibiotics and media containing carbenicillin for selection of the mCherry plasmid, and plate counts on both media showed good correlation (r=0.87, Figure S3.2J), indicating that plasmid loss was not a significant concern.

Confocal Microscopy Imaging of *P. aeruginosa*-Infected Airway Epithelial Cells

To further validate the proportion of AEC harboring intracellular *P.a.* estimated by flow cytometry and determine the intracellular bacterial burden at the single-cell level, we assessed for *P.a.* in infected AEC by immunofluorescence and confocal microscopy, with differential staining of extracellular and intracellular *P.a*. At different time points, infected AEC were fixed, and extracellular bacteria were first stained with a polyclonal anti-*P.a.* antibody (AF647, red). AEC were then permeabilized and stained again with the same polyclonal anti-*P.a.* antibody (AF488, green), resulting in differential staining of extracellular and intracellular bacteria (total *P.a.* staining) (Figures 3.3A and 3.3B and Figure S3.3A). Intracellular *P.a.*was thus identified by their single green signal, while extracellular *P.a.*was double stained

red/green. The validation of the extracellular staining was performed on bacteria spun down on coverslips without AEC and stained as previously described (Figure S3.3B). The absence of fluorescence spillover was assessed using single-stained infected AEC (Figure S3.3C).

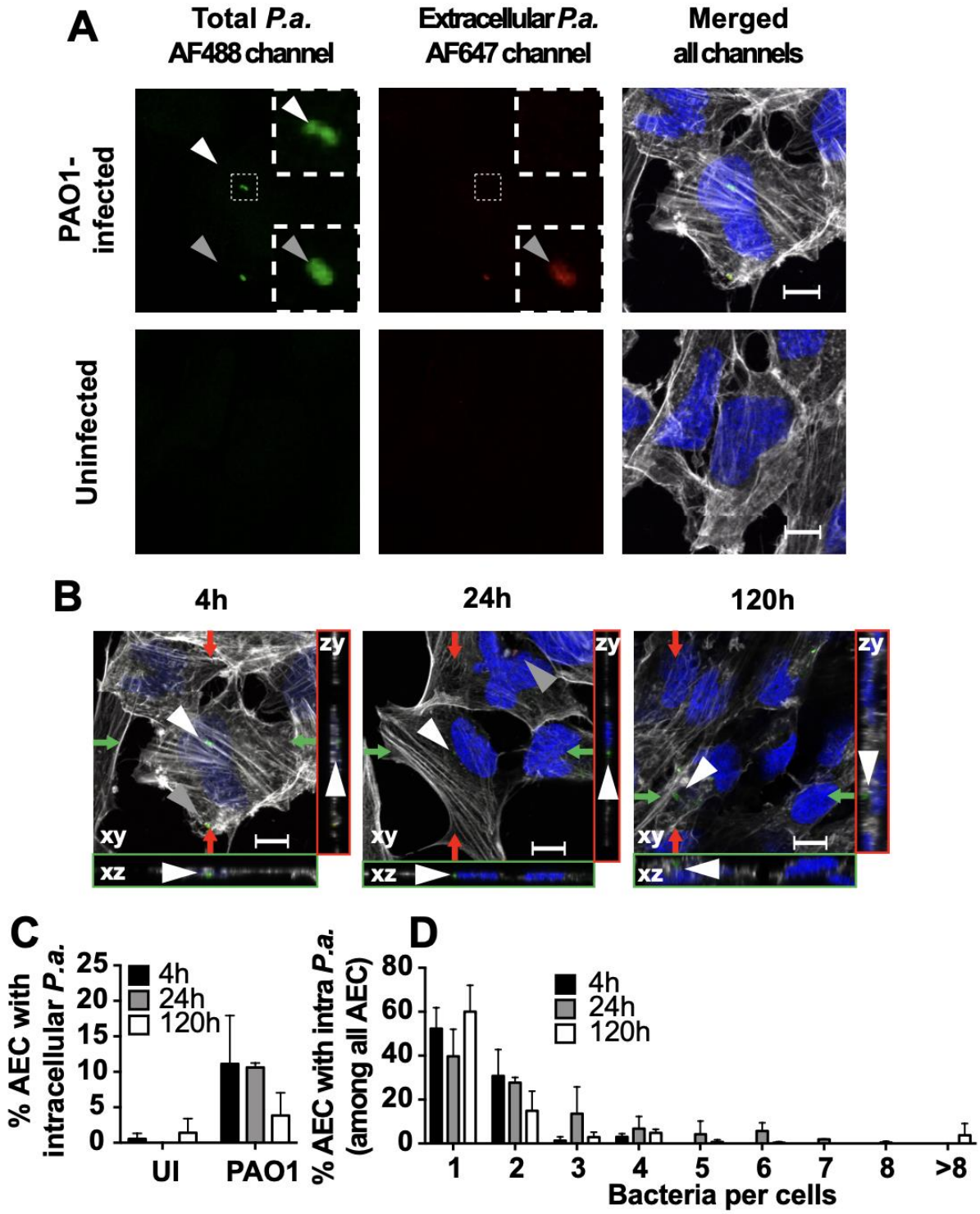

Figure 3.3

Detection of intracellular *P.a.* by confocal microscopy. (A) Z-projection images (AF488, AF647, and merged channels) to distinguish extracellular from intracellular bacteria in AEC at

4 h p.i or uninfected negative controls. (B) Z-projection and orthogonal views (merged channels) to localize bacteria at different time points. Green and red arrows denote the plane of cut for the and plane projections, respectively. Extracellular *P.a.* (gray arrowhead) was double-stained by the total (AF488 green) and extracellular (AF647 red) stains, while intracellular *P.a.* (white arrowhead) was single stained with the total (green) stain. The actin cytoskeleton was stained with phalloidin (grey) and the AEC nuclei with DAPI (blue). (C) The percentage of AEC harboring intracellular *P.a.* signals among all AEC. (D) The percentage of AEC harboring a given number of intracellular *P.a.* per AEC at different time points (among all AEC with intracellular *P.a.*). For all experiments, BEAS-2B cells were infected with PAO1 at MOI 1, and confocal microscopy images were analyzed manually. For (A) and (B), representative images are shown, with scale bar = 2 μm. Results in (C) and (D) shown are from pooled data (≥ 1000 cells or ≥ 16 fields of view per conditions) from 2 independent experiments.

We first analyzed the confocal microscopy images manually and estimated the percentage of infected AEC harboring intracellular *P.a.* to be 11.1% (±6.8%) at 4 h p.i and 10.6% (±0.6%) at 24 h p.i, decreasing to 3.8% (±3.1%) at 120 h p.i (Figure 3.3C). While these results were generally consistent with the flow cytometry results, small differences were noted between the different methods (11.1% vs. 9.1% at 4 h p.i, 10.6% vs. 6.6 at 24 h p.i, and 3.8% vs. 6.2% at 120 h p.i for confocal vs. flow cytometry, respectively). The bacterial burden per cell peaked at 24 h p.i (median number of bacteria per cell of 2 compared to 1 at 4 h) before decreasing at 120 h p.i (1 bacteria per cell) (Figure 3.3D). At 4 h p.i, 52% of infected cells harbored a single intracellular bacterium and less than 18% had more than two intracellular bacteria, consistent with the low MOI of 1. By 24 h p.i, 32.6% had 3 or more intracellular bacteria, possibly indicating intracellular bacterial proliferation within the first 24 h in some cells. We noted a small number of intracellular bacteria-like signal (less than 1.5%) in uninfected AEC, likely representing false-positive signals due to nonspecific binding of the secondary antibody (Figure S3.3A), as cultures of the AEC revealed no viable bacteria. We further validated the manual counts using an automated custom image analysis pipeline and found the two methods to be well correlated (r=0.906, Figure S3.3D).

P. aeruginosa Clinical Isolates Display Different Intracellular Infection Kinetics

Here, we sought to compare the long-term intracellular survival and cytotoxicity of *P.a.* clinical isolates collected from CF children (listed in supplemental Table S3.1-S3.2, (61)). The four

clinical isolates displayed a range of bacterial phenotypes (e.g., mucoidy, protease and pyocyanin production, flagellar, and pilus-mediated motility (Table S3.2)). All were susceptible to tobramycin, and none displayed any growth defects in LB or DMEM medium (S3.4D-E). The bacterial burden at 4 h p.i was relatively similar in the four clinical isolates (range 1.2 to 4.2 x 10^4 CFU/well in BEAS-2B and 0.7 to 3.7 x 10^3 in CFBE-*wt*, Figure S3.1A), suggesting comparable internalization rates. However, we observed different infection kinetics over time (Figures 3.4A and 3.4B and Figure S3.4A). The lab strain PAO1 and 2 out of 4 clinical isolates (CI455 and CI565) persisted until 120 h p.i. (an average of 47 to 474 CFU per well were recovered at 120 h p.i.) but showed a gradual decline in intracellular bacterial burden over time. The isolate CI581 displayed the most rapid decline in intracellular bacterial burden with no detectable viable bacteria in most replicates at 120 h p.i. In contrast, the isolate CI180 displayed on average a 5.7-fold increase in intracellular bacterial counts over time, from 4.2 x 10^4 CFU/well at 4 h p.i and 6.0 x 10^4 CFU/well at 24 h p.i to 1.6 x 10^5 CFU/well at 120 h p.i, suggesting probable replication of intracellular bacteria given that cell death remained constant between 24 h and 120 h p.i. We also observed that the different clinical isolates induced variable degrees of cytotoxicity over time (Figure 3.4C and Figure S3.4B-C). The CI180 and CI565 induced relatively limited cytotoxicity to a degree comparable to the lab strain PAO1. Conversely, CI581, which was associated with the lowest intracellular bacterial counts at 120 h p.i, caused the greatest cytotoxicity at 24 h, 48 h, and 120 h p.i. (which impaired further merasurement by confocal imaging of this strain, Figure S3.3E-F). Our results thus reveal that different *P.a*. isolates have divergent infection outcomes in AEC across a spectrum, from high cytotoxicity/low intracellular persistence (e.g., CI581) to low cytotoxicity/high persistence (e.g., CI180). Given the high persistence phenotype of CI180, we examined AEC infected with this clinical isolate by confocal imaging, with differential staining of *P.a.* as done with PAO1 (Figure 3.4D). We observed an increase in the proportion of AEC harboring intracellular bacteria, from 11% at 4 h p.i. to 25% at 24 h p.i. (Figure 3.4E), as well as an increase of the number of intracellular bacteria per AEC (median of 2 at 4 h p.i. vs. 3 at 24 h p.i.). Notably, at 24 h p.i, 27% AEC harbored 5 or more bacteria, including 8% AEC having 8 or more bacteria, compared to 2% with >=5 bacteria and none with >=8 bacteria at 4 h (Figure 3.4F), thus further supporting the notion that CI180 can replicate within AEC in our model.

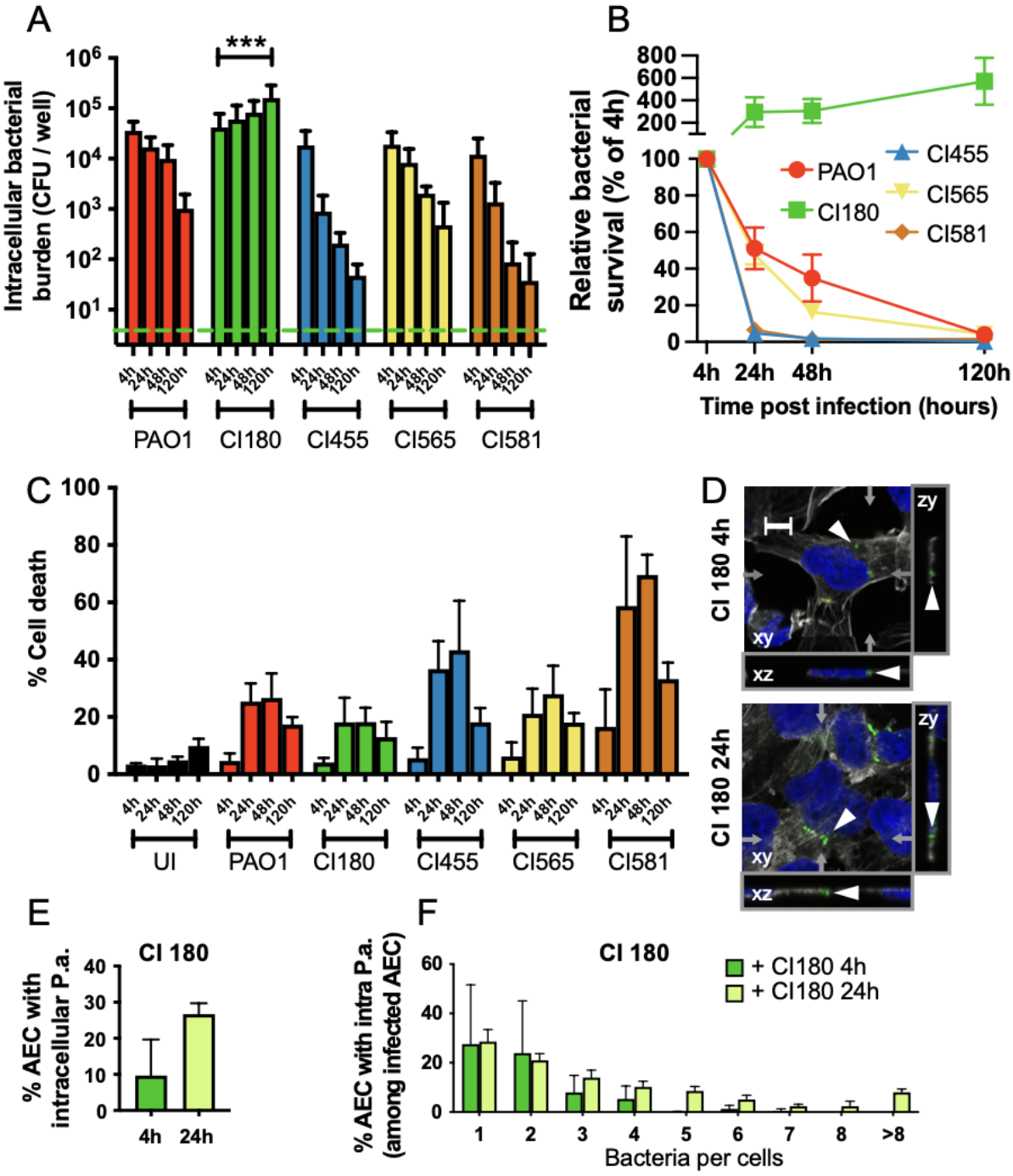

Figure 3.4

Intracellular infection kinetics and cytotoxicity of CF clinical isolates. (A) Intracellular bacterial burden, (B) relative bacterial survival, and (C) cytotoxicity over time following infection with PAO1 or clinical isolates CI180, CI455, CI565, or CI581. (D) Detection and 3D localization of intracellular *P.a.* (white arrowhead) by confocal microscopy, with evidence of clustered intracellular bacteria in AEC infected with CI180 at 24 h p.i. In AEC infected with CI180, (E) the percentage of AEC harboring intracellular *P.a.* signals among all AEC and (F) the percentage of AEC harboring a given number of bacteria per AEC at different time points (among all AEC with intracellular *P.a.*). For all experiments, BEAS-2B cells were infected

with at MOI 1, except for uninfected (UI) controls. The intracellular bacterial burden was measured by viable CFU count (detection limit shown as green dashed line), and the relative bacterial survival was calculated as the intracellular bacterial burden at the indicate time normalized to the 4 h counts. The cytotoxicity was measured by LDH release assay. Confocal microscopy images were analyzed manually. Results in (A), (B), and (C) are from pooled data (≥ 6 biological replicates) from ≥3 independent experiments. Results in (B) are depicted as mean ± SEM. For (D), images representative of 3 independent experiments are shown, with scale bar = 2 μm. For (E) and (F), results are from pooled data (≥ 8 fields of view per condition) from 3 independent experiments. *P < 0.05; **P < 0.01; ***P < 0.001.

3.5 Discussion

Although *P.a.* is widely known as an extracellular pathogen, many studies have demonstrated its ability to invade and survive in different models of epithelia, such as the cornea (48, 53, 62), skin (63), respiratory (31, 44), and urinary tract (50). Bacterial survival within epithelial cells could serve as a mechanism of evasion from the immune system, extracellular host defenses, or antibiotic therapies and thus contribute to the persistent and chronic nature of *P.a.* infections. Given that most studies to date have focused on the invasion process and short-term survival of *P.a.* within epithelial cells, our understanding of the intracellular survival kinetics during long-term infection remains limited. In this study, we described an *in vitro* model of *P.a.* infection in human airway epithelial cells. Using the BEAS-2B cell line in a tobramycin protection assay, we optimized the model for intracellular bacterial persistence and demonstrated bacterial survival for up to 5 days p.i. Flow cytometry and confocal microscopy analyses allowed us to study the infection kinetics at the single-cell level, demonstrating that at low MOI, a small but reproducible proportion of AEC (~10% at 4 h p.i) internalize *P.a.*, and intracellular *P.a.* can persist for up to 5 days p.i, without causing significant host cell death. Finally, infection with different *P.a.* strains revealed that CF clinical isolates were highly heterogeneous in their ability to survive intracellularly, with CI180 providing an example of a strain with a high intracellular persistence phenotype.

P.a. has been shown to invade several epithelial cell types including the polarized kidney MDCK cells (30), corneal cells (62), and intestinal Caco-2 cells (64), as well as respiratory cells such as A549 (46, 65) and polarized AEC (47, 51). For our study, we selected BEAS-2B cells, an AEC line widely used to study host cell signaling and inflammatory responses to *P.a.* and its secreted or surface molecules (66–69). Previous studies using live cell video

microscopy by the Fleiszig group have observed that *P.a.* can survive and replicate within epithelial cells in nonapoptotic membrane blebs (42, 43, 45, 47). The formation of blebs is dependent on a functional T3SS and the adenylate cyclase activity of the effector proteins ExoY (45) or the ADP-ribosyltransferase activity of ExoS (42, 48), while intravesicular bacterial survival requires ExoS to avoid vesicle acidification (45, 56) or to inhibit autophagy (46). In our model, we have not observed bleb-like structures by confocal microscopy, possibly due the specific cell line or lower MOI (1 rather than 10 or 100) used in our study or the fixation method which can collapse such structures (47).

We recognize that our current model with submerged BEAS-2B cells presents some limitations. This immortalized cell line may differ from polarized primary airway epithelial cells through display of mesenchymal-like properties (70) and thus mimic a nonpolarized or damaged epithelium (71). Those properties are known to favor bacterial engulfment through an increased display of molecular patterns associated with bacterial invasion (31, 72, 73). We indeed observed that bacterial internalization was 4 to 27-fold increased in BEAS-2B when compared to CFBE-*wt* cells, another commonly used bronchial epithelial cell line previously used to study AEC-*P.a.* interactions and internalization (51, 52). The use of BEAS-2B cells thus facilitates the study of intracellular *P.a.* over time and at the single-cell level, as these are relatively rare events. Our model will therefore benefit from further validation using AEC grown at the air liquid interface, since polarization and the formation of tight junctions may influence bacterial invasion, cytotoxicity, and other host cell responses (30, 31, 69, 74).

Our model was developed to study the long-term fate of intracellular bacteria under conditions that did not cause extensive host cell death with the lab strain PAO1. The MOI of 1 results in a low frequency of AEC harboring intracellular bacteria but achieves long-term infection (up to 5 days). In contrast, the use of high MOI (such as MOI 10) results in higher rates of bacterial internalization but causes significant cytotoxicity by 24 h p.i and thus precludes any study of the long-term fate of intracellular bacteria. Gentamicin protection assays have been widely used to study intracellular *P.a.* at drug concentrations ranging from 50 to 200 μg/mL (44, 62, 75). We chose to use tobramycin, a chemically related aminoglycoside, for its clinical relevance in the treatment of CF lung infection (76). While aminoglycosides (such as gentamicin and tobramycin) are impermeable to eukaryotic cells, they are slowly taken up by endocytosis over time (59), and high concentrations can impact intracellular bacterial survival and growth (58, 60). We thus observed that reducing the maintenance concentration of

tobramycin to 25 μg/mL enhanced the long-term survival of intracellular PAO1. However, the maintenance concentration was kept at 100 μg/mL during infection with CF clinical isolates to avoid growth of extracellular bacterial in *P.a.*, strains which may have varying tobramycin susceptibility.

Studies focused on long-term survival (beyond 24 h p.i) of *P.a.* in epithelial cells are scarce and have typically only assessed the intracellular bacterial burden by CFU counts (44, 51, 52, 62, 75). Our flow cytometry and confocal microscopy analyses provided complementary approaches to estimate the percentage of infected host cells and intracellular bacterial burden at the single-cell level. Flow cytometry allowed us to analyze a large number of AEC (~50,000 cells) and was likely more selective for detection of live (metabolically active) bacteria which express mCherry fluorescence, but this method lacked the resolution to assess the number of intracellular bacteria per cell. We also recognize that flow cytometry cannot distinguish cell surface-associated bacteria from intracellular bacteria, and that a very small proportion of mCherry(+) AEC may be false-positive since our gating for mCherry(+) cells was set by our negative control to tolerate up to 0.5% false-positive fluorescence signal. Conversely, confocal microscopy was low throughput, and antibody staining of intracellular *P.a.* could not distinguish live from dead bacteria, but it provided high-resolution images that permitted confident 3D localization and counting of intracellular bacteria. We did note small differences (2 to 4%) in the proportion of *P.a.*-infected AEC estimated by confocal microscopy compared to flow cytometry, which were likely due to the different methods for bacterial detection (mCherry expression vs. antibody labeling). However, results from both methods were consistent in estimating that ~10% of AEC harbor intracellular PAO1 at 4 h p.i, with comparable trends indicating a decrease in the proportion of PAO1-infected AEC at 24 h and 120 h p.i. While it remains to be determined whether this decline was due to bacterial clearance by the host or host cell death induced by intracellular *P.a.*, we also noted that AEC proliferation during the experiment contributed to the declining estimates of the proportion of *P.a.*-infected AEC.

We then compared the intracellular survival kinetics and cytotoxicity of different *P.a.* clinical isolates from CF airway infections. While their initial intracellular bacterial burdens suggested relatively comparable rates of internalization, there were significant differences in long-term intracellular survival and cytotoxicity. We observed a high intracellular persistence phenotype in CI180, while the other strains did not persist, and CI581 was the most cytotoxic strain.

Fleiszig et al. had previously reported an inverse correlation between cytotoxicity and intracellular invasion of MDCK kidney epithelial cells upon testing of *P.a*. isolates from corneal infections, but the study did not examine time points beyond 3 h p.i (53). More recent studies assessed a few CF clinical isolates for intracellular bacterial survival and cytotoxicity up until 24 h p.i in immortalized airway epithelial cells and described clinical isolates with a persistent intracellular infection phenotype reminiscent of what we observed with CI180 (51, 52). Using a model of bladder epithelial cell infection, Penaranda et al. also observed a comparable intracellular persistence in certain *P.a.* clinical isolates originating from urinary tract infections (50). The bacterial functions that might contribute to strain-specific intracellular persistence are likely numerous but remain incompletely understood. These include mechanisms that directly enhance bacterial survival and/or replication, such as the ability to metabolically adapt to the intracellular host milieu (50, 52), or indirectly modulate host cell viability or responses, such as the expression of the T3SS, effectors proteins, and other secreted cytotoxic factors (42, 45, 48, 56, 77–79). The ability of certain clinical isolates to successfully persist in AEC raises the possibility that these host-adapted *P.a.* strains harbor phenotypic characteristics that promote their ability to cause chronic human infections. Our model would enable future mechanistic studies to understand the host-pathogen interactions and bacterial factors involved in long-term intracellular persistence of *P.a.* in airway epithelial cells.

3.6 Supplemental methods

Bacterial growth conditions

To compare the growth kinetics of the different *P.a* clinical isolates, bacterial strains were streaked from frozen stocks onto LB (BD Difco) agar (Wisent, 800-015) and incubated overnight at 37°C. Isolated colonies were then inoculated in 5 mL of liquid LB medium and incubated at 37°C with shaking at 250 r.p.m. until $OD_{600} \cong 0.8\text{-}1$. Bacterial cultures were then diluted in 200 µL LB (OD_{600}= 0.05) in triplicates and incubated in a 96-wells plate at 37°C with shaking (Cytation 5 plate reader, Agilent).

CFBE-*wt* airway epithelial cell culture conditions.

The immortalized human bronchial epithelial CFBE-*wt* cell line originated from the cystic fibrosis CFBE41o- parental cells (80), which carries the ΔF508/ΔF508 CFTR mutations and is stably transduced with *wt*-Cftr to express wild-type CFTR (81). The experiments were performed in a similar fashion to BEAS-2B cells, except for the use of collagen-coated plates

and EMEM culture medium. Prior to AEC seeding, 24-well plates were first coated for at least 2h at 37°C h with a Purecol solution of type 1 collagen at 40 µg/mL (Advanced Biomatrix, #5005), followed by removal of the coating solution. Plates were either used immediately for seeding, or stored at 4°C (max 2 weeks) until use. The coated plates were seeded with CFBE-*wt* cells at a density of 200.000 cells/mL (100.000 cells/well), grown using EMEM medium (#320-005, Wisent) supplemented with 10% FBS and 50 IU/50 µg/mL penicillin/streptomycin (#450-200, Wisent) at 37°C with 5% CO_2.

Automated confocal image analysis

The automated image analysis was performed using a custom protocol for Icy (55). The following files are available at https://omero.med.ualberta.ca/webclient/?show=dataset-1152 :

Icy pipeline	Graphic description of the custom Icy protocol.
Icy automated image analysis.protocol	Custom ICY protocol for detection of bacteria using wavelet spot detector blocks, with distinction of extracellular from intracellular bacteria using the resulting ROI list and the colocalization studio block. This protocol can be run using ICY Version 2.3.0.0 and the test_image included in the supporting information.
Icy test_image	Representative confocal image of an infected BEAS-2B displaying intracellular bacteria as well as extracellular bacteria used with the icy protocol included.

3.7 Supplementary Figures and Tables

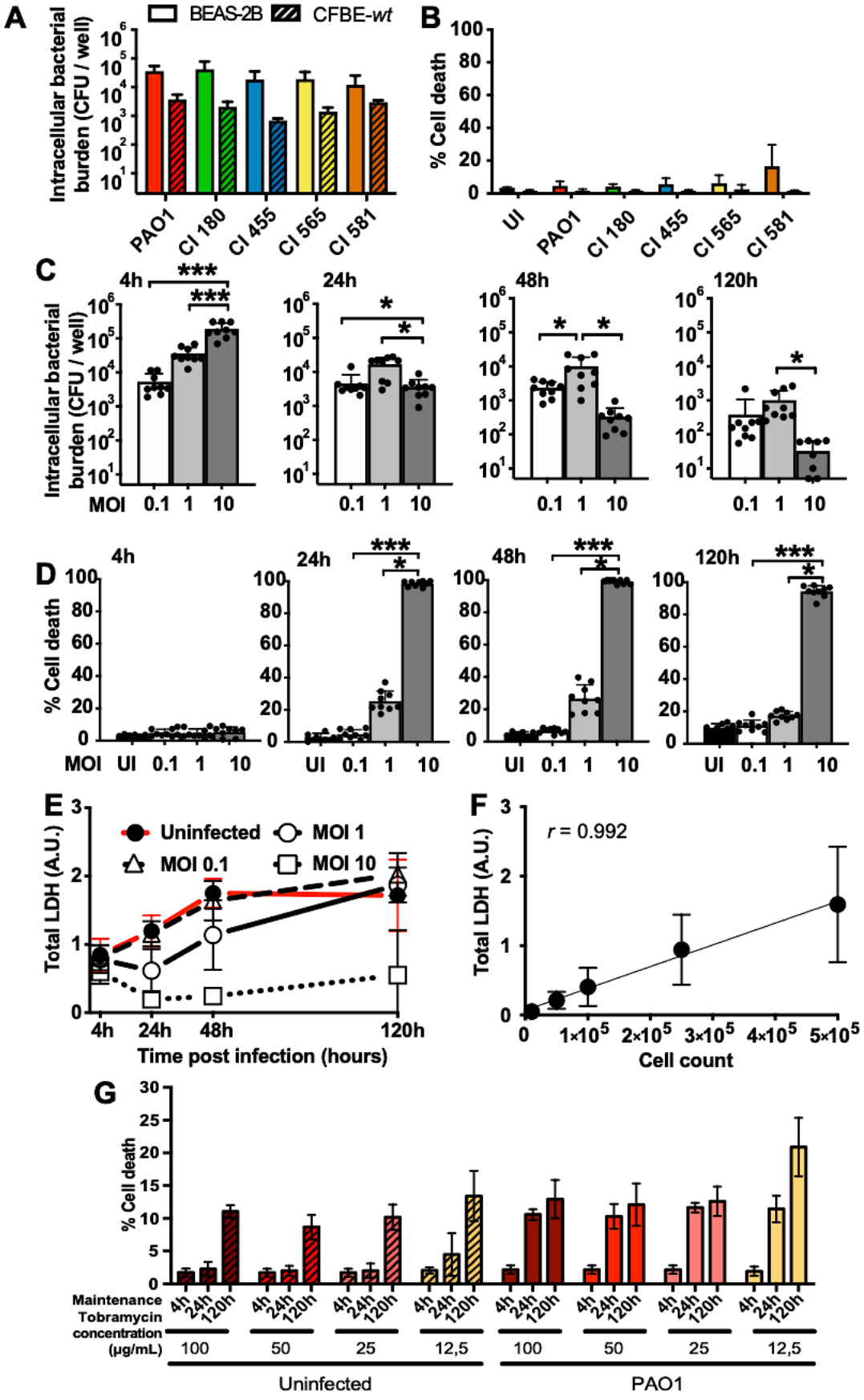

Figure S3.1. Effect of different AEC lines, MOI and tobramycin maintenance concentrations.

(A) Intracellular bacterial burden and (B) cytotoxicity at 4h p.i. in BEAS-2B and CFBE-*wt* AEC. (C) Intracellular bacterial burden and (D) cytotoxicity at different timepoints in BEAS-2B cells infected with PAO1 at different MOI. (E) The total AEC biomass over time following infection at different MOI, estimated by the total LDH content (absorbance units at 490nm) from the culture supernatants and lysates combined. (F) Linear correlation between BEAS-2B cell counts and total LDH content as an estimate for AEC biomass. (G) Cytotoxicity in BEAS-2B infected with PAO1 at different MOI or uninfected controls, upon maintenance with different concentrations of tobramycin. The intracellular bacterial burden was measured by viable CFU count (detection limit shown as dashed line) and cytotoxicity was measured by LDH release assay. Results shown are from data (≥ 4 biological replicates) from ≥ 2 independent experiments.

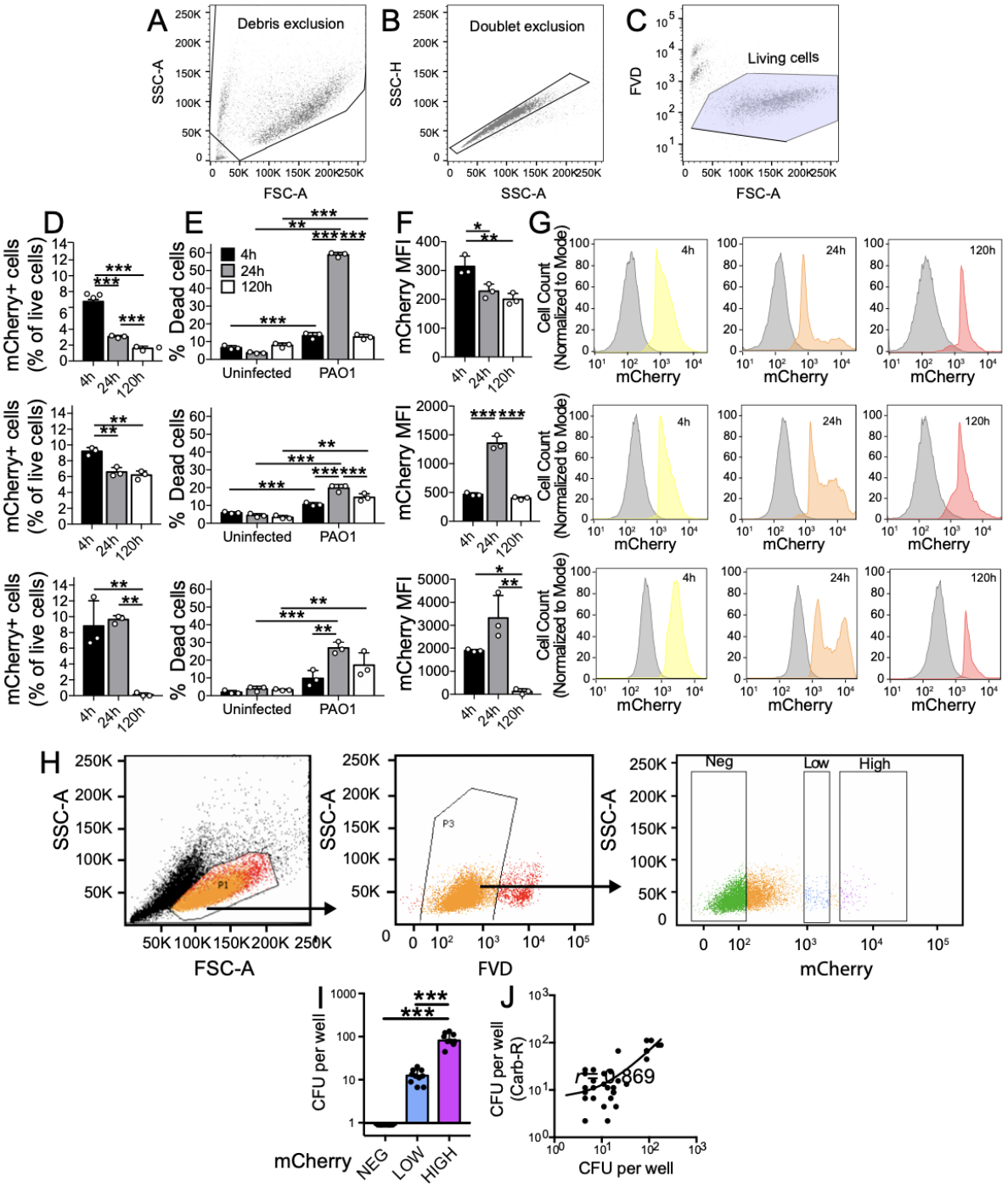

Figure S3.2. Flow cytometry analysis for detection of mCherry (+) AEC and cell sorting to validate mCherry fluorescence. The initial gating strategy included (A) exclusion of cell debris based of forward (FSC-A) and side (SSC-A) scatter area, (B) exclusion of doublets based of side scatter area (SSC-A) and height (SSC-H), and (C) selection of live cells based on fixable viability dye (FVD) staining. Quantification of the percentage of (D) mCherry(+) AEC among all live cells, (E) dead cells among all AEC, (F) mCherry median fluorescence intensity (MFI) of mCherry(+) cells, (G) mCherry fluorescence histograms of AEC populations at different time points after infection with non-fluorescent PAO1 (whole population, grey) or mCherry

PAO1 (mCherry(+) population only, colored). Each panel across one row for D to G represents one independent experiment (each with biological triplicates). (H) Gating strategy for AEC infected with mCherry PAO1, with sorting of cells no (mCherry Neg), low (mCherry Low) or high (mCherry High) mCherry fluorescence. (I) Quantification of intracellular bacterial burden in AEC sorted as mCherry Neg, Low or High to validate mCherry fluorescence. Viable CFU counts were measured per sorting well, which contained 100 cells per well, with data pooled from n=10 wells per condition. The CFU detection threshold is depicted as a black line. (J) Correlation between intracellular bacterial burden of AEC by viable CFU counts on selective media (with Carbenicilin) v.s. non-selective media to assess the mCherry (carbenicillin - resistant) plasmid stability. Viable CFU counts were measured per sorting well, which contained 10 or 100 cells per well, with data from n≥20 wells. The displayed trendline was calculated using a linear regression analysis. For H, I and J, BEAS-2B cells were infected with mCherry PAO1 at MOI 1 and analyzed at 24h p.i.

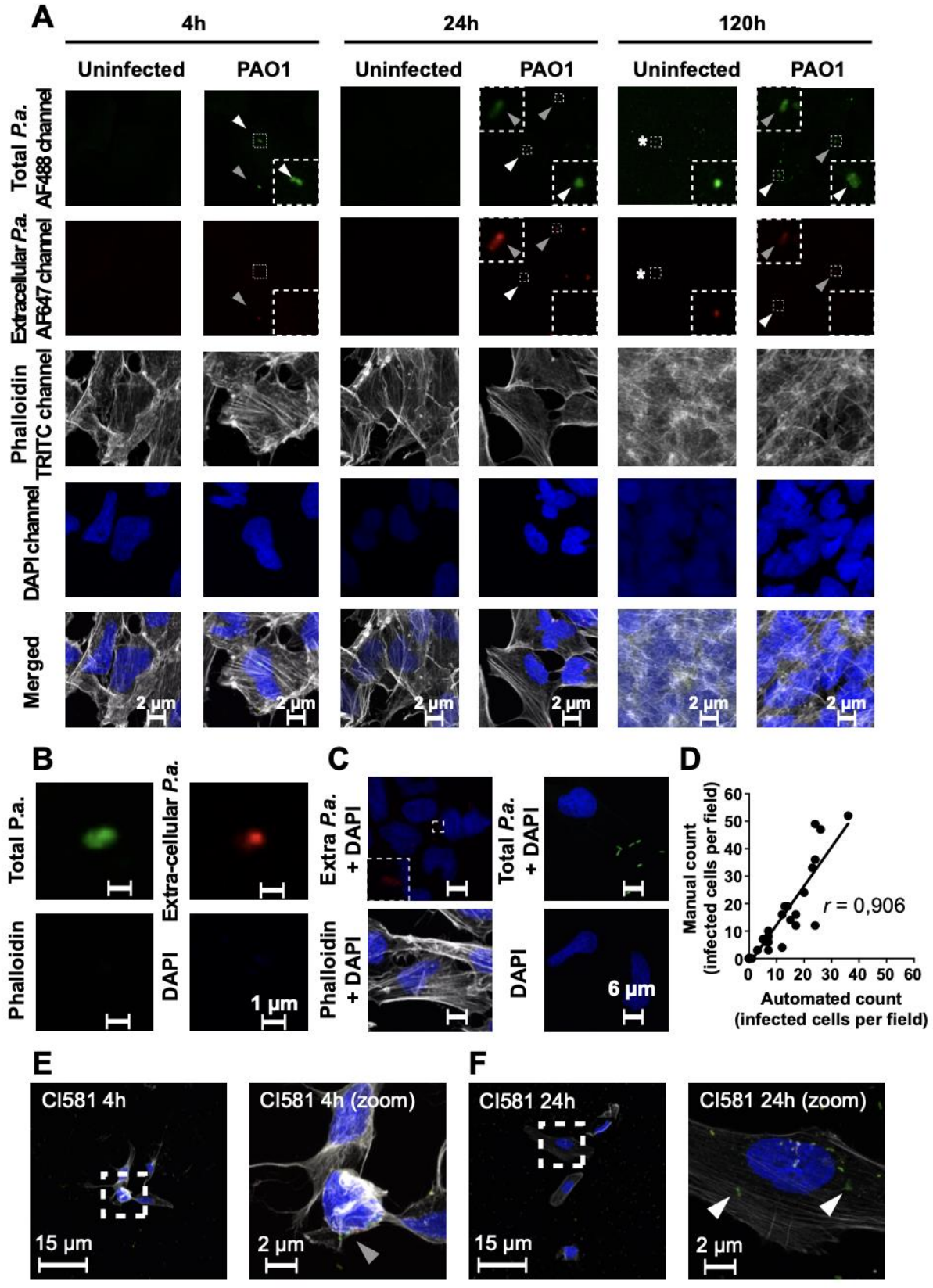

Figure S3.3. Confocal microscopy imaging of infected AEC and controls. Confocal images of (A) AEC infected with PAO1 and uninfected controls at different time points, with *indicating false-positive signals in uninfected controls. (B) Controls with PAO1 cells grown on coverslips without AEC, stained as in (A). Split-channel images (A-B) and merged channel

images (A only) are displayed. (C) Controls with infected AEC stained as indicated. For C, images shown are merged from all four channels and indicate no crossover fluorescence. (D) Correlation between manual and automated counts of AEC with intracellular bacterial signals, with each data point representing one field of view. Confocal images (merged from all channels) of AEC infected with clinical isolate CI581 at (E) 4h p.i and (F) 24h p.i, with the zoomed image corresponding to the inset visualized at low magnification, with extracellular *P.a.* (grey arrowhead) and intracellular *P.a.* (white arrowhead) indicated. For all experiments, BEAS-2B cells were infected at MOI 1, and (unless stated otherwise) stained for extracellular *P.a.* (red), total *P.a.* (green), AEC nuclei were stained with DAPI (blue) and the actin cytoskeleton with phalloidin (grey).

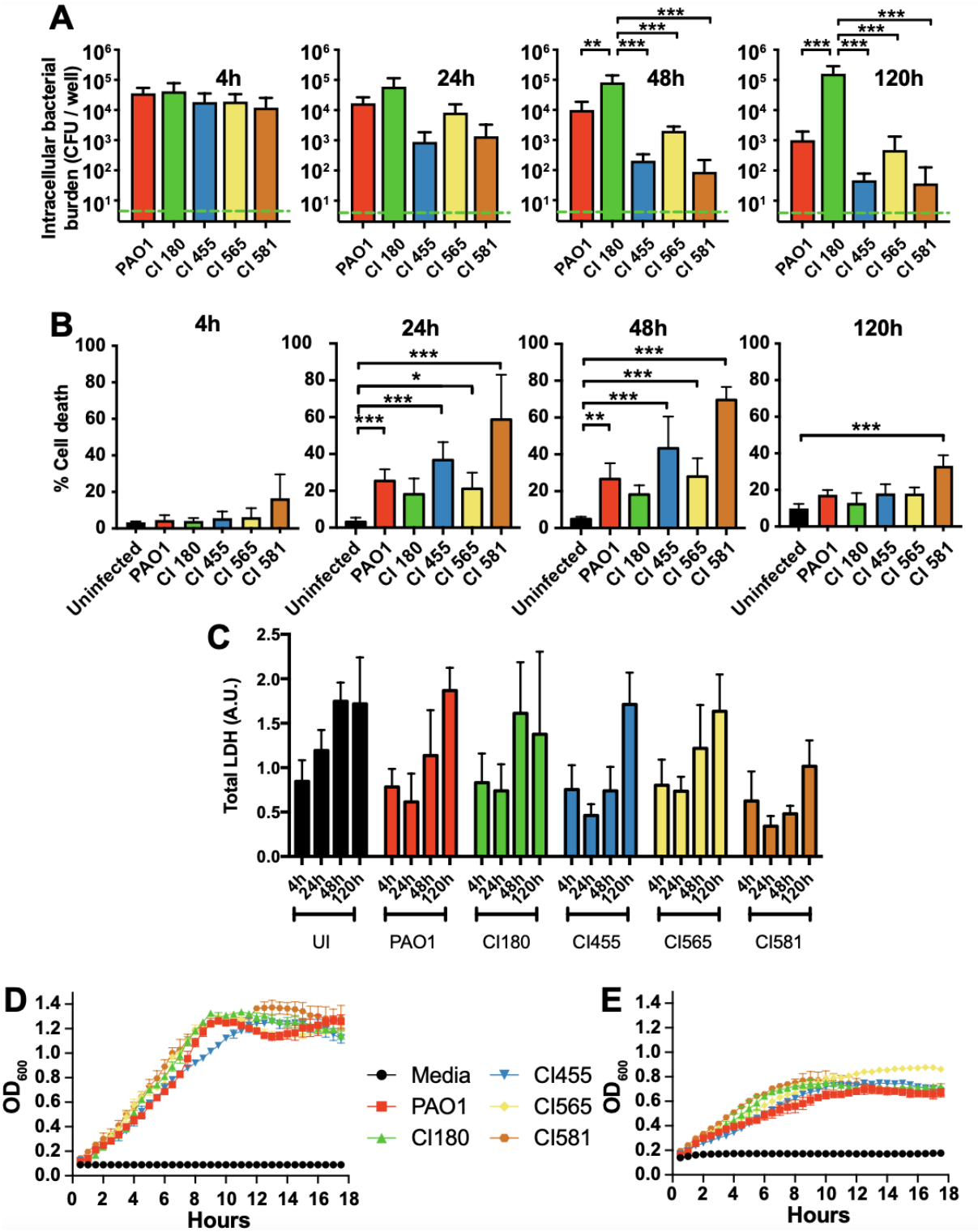

Figure S3.4. Intracellular infection kinetics, cytotoxicity and growth curve of CF clinical isolates. (A) Intracellular bacterial burden, (B) cytotoxicity and (C) total AEC biomass (estimated by total LDH) over time in BEAS-2B. Growth curves of PAO1 and clinical isolates in (D) LB or (E) DMEM medium. For all experiments, cells were infected with PAO1 or clinical isolates CI180, CI455, CI565 or CI581 at MOI 1. The CFU detection limited is shown

as a black dashed line. Results shown are pooled data (≥ 6 biological replicates) from ≥ 2 independent experiments. *P < 0.05; **P < 0.01; ***P < 0.001.

Strains	**Relevant information**	**Reference**	**DN#**
PAO1	Reference PAO1 (MPAO1) strain from Manoil lab.	(82)	DN145
PAO1-mCherry	PAO1 carrying the pMKB1, Cb^R.	(83)	DN894
CI 180	Clinical isolate from cystic fibrosis patient.	(61)	DN515
CI 455	Clinical isolate from cystic fibrosis patient.	(61)	DN615
CI 565	Clinical isolate from cystic fibrosis patient.	(61)	DN638
CI 581	Clinical isolate from cystic fibrosis patient.	(61)	DN619
Plasmid			
pMKB1	plasmid encoding a constitutively expressed mCherry, Cb^R.	(84)	DN814

Supplemental Table S3.1. Strains and plasmids used in this study.

Cb^R carbenecillin resistance.

Strains	**PAO1**	**CI 180**	**CI 455**	**CI 565**	**CI 581**
Mucoid	-	-	-	+	-
Secreted Protease	+	+	+	+	+
Swimming motility	+	+	+	-	+
Twitching motility	+	+	+	-	+
Pyocyanin	+	+	+	+	-
Tobramycin MIC (μg/mL)	≤ 2	≤ 2	≤ 2	≤ 2	≤ 2

Supplemental Table S3.2. Phenotypic characteristics of PAO1 and the *P.a.* clinical isolates. Mucoid phenotype (alginate overproduction) was assessed qualitatively by colony morphology on YEM agar medium; Total protease production was assessed by the presence of

a zone of clearance with bacterial growth on skim milk agar plate; Swimming motility was assessed by measuring the zone of bacterial growth after stab inoculation in 0.3% soft agar; Twitching motility was assessed by measuring the zone of bacterial adhesion at the agar-plastic interface after stab inoculation in 1% agar; Pyocyanin production was assessed qualitatively. Clinical isolates phenotypes were originally described in a previous study (61).

3.8 Acknowledgments

This study was supported by research funding from the Cystic Fibrosis Canada (559985 to D.N) and the US Cystic Fibrosis Foundation (NGUYEN21I0 to D.N), salary support from the Fonds de Recherche du Quebec Santé (D.N), and scholarships from the Fonds de Recherche du Quebec Santé (to K.J.M), the Reseau en Santé Respiratoire (to K.J.M and L.H), and the Deutscher Akademischer Austauschdienst (to L.H). We thank the Immunophenotyping Platform at the Research Institute of the McGill University Health Centre (RI-MUHC) for their assistance with the cell sorting. We thank Sam Moskowitz for providing the mCherry (pMKB1) plasmid.

3.9 References

1. Anderson GG, Dodson KW, Hooton TM, Hultgren SJ. Intracellular bacterial communities of uropathogenic Escherichia coli in urinary tract pathogenesis. Trends Microbiol. 2004;12(9):424-30.
2. Peyrusson F, Varet H, Nguyen TK, Legendre R, Sismeiro O, Coppee JY, et al. Intracellular Staphylococcus aureus persisters upon antibiotic exposure. Nat Commun. 2020;11(1):2200.
3. Hunstad DA, Justice SS. Intracellular lifestyles and immune evasion strategies of uropathogenic Escherichia coli. Annu Rev Microbiol. 2010;64:203-21.
4. Mysorekar IU, Hultgren SJ. Mechanisms of uropathogenic Escherichia coli persistence and eradication from the urinary tract. Proc Natl Acad Sci U S A. 2006;103(38):14170-5.
5. Martinez-Figueroa C, Cortes-Sarabia K, Del Carmen Alarcon-Romero L, Catalan-Najera HG, Martinez-Alarcon M, Vences-Velazquez A. Observation of intracellular bacterial communities in urinary sediment using brightfield microscopy; a case report. BMC Urol. 2020;20(1):89.
6. Rosen DA, Hooton TM, Stamm WE, Humphrey PA, Hultgren SJ. Detection of intracellular bacterial communities in human urinary tract infection. PLoS Med. 2007;4(12):e329.
7. Rollin G, Tan X, Tros F, Dupuis M, Nassif X, Charbit A, et al. Intracellular Survival of Staphylococcus aureus in Endothelial Cells: A Matter of Growth or Persistence. Front Microbiol. 2017;8:1354.

8. Strobel M, Pfortner H, Tuchscherr L, Volker U, Schmidt F, Kramko N, et al. Post-invasion events after infection with Staphylococcus aureus are strongly dependent on both the host cell type and the infecting S. aureus strain. Clin Microbiol Infect. 2016;22(9):799-809.
9. Vozza EG, Mulcahy ME, McLoughlin RM. Making the Most of the Host; Targeting the Autophagy Pathway Facilitates Staphylococcus aureus Intracellular Survival in Neutrophils. Front Immunol. 2021;12:667387.
10. Almeida RA, Matthews KR, Cifrian E, Guidry AJ, Oliver SP. Staphylococcus aureus invasion of bovine mammary epithelial cells. J Dairy Sci. 1996;79(6):1021-6.
11. Clement S, Vaudaux P, Francois P, Schrenzel J, Huggler E, Kampf S, et al. Evidence of an intracellular reservoir in the nasal mucosa of patients with recurrent Staphylococcus aureus rhinosinusitis. J Infect Dis. 2005;192(6):1023-8.
12. Ellington JK, Harris M, Webb L, Smith B, Smith T, Tan K, et al. Intracellular Staphylococcus aureus. A mechanism for the indolence of osteomyelitis. J Bone Joint Surg Br. 2003;85(6):918-21.
13. Reilly SS, Hudson MC, Kellam JF, Ramp WK. In vivo internalization of Staphylococcus aureus by embryonic chick osteoblasts. Bone. 2000;26(1):63-70.
14. Duraiswamy S, Chee JLY, Chen S, Yang E, Lees K, Chen SL. Purification of Intracellular Bacterial Communities during Experimental Urinary Tract Infection Reveals an Abundant and Viable Bacterial Reservoir. Infect Immun. 2018;86(4).
15. Scott VCS, Haake DA, Churchill BM, Justice SS, Kim J-H. Intracellular Bacterial Communities: A Potential Etiology for Chronic Lower Urinary Tract Symptoms. Urology. 2015;86(3):425-31.
16. Morin CD, Deziel E, Gauthier J, Levesque RC, Lau GW. An Organ System-Based Synopsis of Pseudomonas aeruginosa Virulence. Virulence. 2021;12(1):1469-507.
17. Shteinberg M, Haq IJ, Polineni D, Davies JC. Cystic fibrosis. Lancet. 2021;397(10290):2195-211.
18. Baltimore RS, Christie CD, Smith GJ. Immunohistopathologic localization of Pseudomonas aeruginosa in lungs from patients with cystic fibrosis. Implications for the pathogenesis of progressive lung deterioration. Am Rev Respir Dis. 1989;140(6):1650-61.
19. Bjarnsholt T, Jensen PO, Fiandaca MJ, Pedersen J, Hansen CR, Andersen CB, et al. Pseudomonas aeruginosa biofilms in the respiratory tract of cystic fibrosis patients. Pediatr Pulmonol. 2009;44(6):547-58.
20. Potts SB, Roggli VL, Spock A. Immunohistologic quantification of Pseudomonas aeruginosa in the tracheobronchial tree from patients with cystic fibrosis. Pediatr Pathol Lab Med. 1995;15(5):707-21.

21. Singh PK, Schaefer AL, Parsek MR, Moninger TO, Welsh MJ, Greenberg EP. Quorum-sensing signals indicate that cystic fibrosis lungs are infected with bacterial biofilms. Nature. 2000;407(6805):762-4.
22. Ciofu O, Tolker-Nielsen T. Tolerance and Resistance of Pseudomonas aeruginosa Biofilms to Antimicrobial Agents-How P. aeruginosa Can Escape Antibiotics. Front Microbiol. 2019;10:913.
23. Maurice NM, Bedi B, Sadikot RT. Pseudomonas aeruginosa Biofilms: Host Response and Clinical Implications in Lung Infections. Am J Respir Cell Mol Biol. 2018;58(4):428-39.
24. Faure E, Kwong K, Nguyen D. Pseudomonas aeruginosa in Chronic Lung Infections: How to Adapt Within the Host? Front Immunol. 2018;9:2416.
25. Sun Y, Karmakar M, Taylor PR, Rietsch A, Pearlman E. ExoS and ExoT ADP ribosyltransferase activities mediate Pseudomonas aeruginosa keratitis by promoting neutrophil apoptosis and bacterial survival. J Immunol. 2012;188(4):1884-95.
26. Bastaert F, Kheir S, Saint-Criq V, Villeret B, Dang PM, El-Benna J, et al. Pseudomonas aeruginosa LasB Subverts Alveolar Macrophage Activity by Interfering With Bacterial Killing Through Downregulation of Innate Immune Defense, Reactive Oxygen Species Generation, and Complement Activation. Front Immunol. 2018;9:1675.
27. Leidal KG, Munson KL, Johnson MC, Denning GM. Metalloproteases from Pseudomonas aeruginosa degrade human RANTES, MCP-1, and ENA-78. J Interferon Cytokine Res. 2003;23(6):307-18.
28. Saint-Criq V, Villeret B, Bastaert F, Kheir S, Hatton A, Cazes A, et al. Pseudomonas aeruginosa LasB protease impairs innate immunity in mice and humans by targeting a lung epithelial cystic fibrosis transmembrane regulator-IL-6-antimicrobial-repair pathway. Thorax. 2018;73(1):49-61.
29. Gunn JS, Bakaletz LO, Wozniak DJ. What's on the Outside Matters: The Role of the Extracellular Polymeric Substance of Gram-negative Biofilms in Evading Host Immunity and as a Target for Therapeutic Intervention. J Biol Chem. 2016;291(24):12538-46.
30. Bucior I, Mostov K, Engel JN. Pseudomonas aeruginosa-mediated damage requires distinct receptors at the apical and basolateral surfaces of the polarized epithelium. Infect Immun. 2010;78(3):939-53.
31. Bucior I, Pielage JF, Engel JN. Pseudomonas aeruginosa pili and flagella mediate distinct binding and signaling events at the apical and basolateral surface of airway epithelium. PLoS Pathog. 2012;8(4):e1002616.
32. Eierhoff T, Bastian B, Thuenauer R, Madl J, Audfray A, Aigal S, et al. A lipid zipper triggers bacterial invasion. Proc Natl Acad Sci U S A. 2014;111(35):12895-900.

33. Heiniger RW, Winther-Larsen HC, Pickles RJ, Koomey M, Wolfgang MC. Infection of human mucosal tissue by Pseudomonas aeruginosa requires sequential and mutually dependent virulence factors and a novel pilus-associated adhesin. Cell Microbiol. 2010;12(8):1158-73.
34. Azghani AO, Idell S, Bains M, Hancock RE. Pseudomonas aeruginosa outer membrane protein F is an adhesin in bacterial binding to lung epithelial cells in culture. Microb Pathog. 2002;33(3):109-14.
35. Zaidi TS, Fleiszig SM, Preston MJ, Goldberg JB, Pier GB. Lipopolysaccharide outer core is a ligand for corneal cell binding and ingestion of Pseudomonas aeruginosa. Invest Ophthalmol Vis Sci. 1996;37(6):976-86.
36. Kazmierczak BI, Jou TS, Mostov K, Engel JN. Rho GTPase activity modulates Pseudomonas aeruginosa internalization by epithelial cells. Cell Microbiol. 2001;3(2):85-98.
37. Pielage JF, Powell KR, Kalman D, Engel JN. RNAi Screen Reveals an Abl Kinase-Dependent Host Cell Pathway Involved in Pseudomonas aeruginosa Internalization. PLOS Pathogens. 2008;4(3):e1000031.
38. Kierbel A, Gassama-Diagne A, Mostov K, Engel JN. The phosphoinositol-3-kinase-protein kinase B/Akt pathway is critical for Pseudomonas aeruginosa strain PAK internalization. Mol Biol Cell. 2005;16(5):2577-85.
39. Lepanto P, Bryant DM, Rossello J, Datta A, Mostov KE, Kierbel A. Pseudomonas aeruginosa interacts with epithelial cells rapidly forming aggregates that are internalized by a Lyn-dependent mechanism. Cell Microbiol. 2011;13(8):1212-22.
40. Esen M, Grassme H, Riethmuller J, Riehle A, Fassbender K, Gulbins E. Invasion of human epithelial cells by Pseudomonas aeruginosa involves src-like tyrosine kinases p60Src and p59Fyn. Infect Immun. 2001;69(1):281-7.
41. Evans DJ, Kuo TC, Kwong M, Van R, Fleiszig SM. Mutation of csk, encoding the C-terminal Src kinase, reduces Pseudomonas aeruginosa internalization by mammalian cells and enhances bacterial cytotoxicity. Microb Pathog. 2002;33(3):135-43.
42. Angus AA, Evans DJ, Barbieri JT, Fleiszig SM. The ADP-ribosylation domain of Pseudomonas aeruginosa ExoS is required for membrane bleb niche formation and bacterial survival within epithelial cells. Infect Immun. 2010;78(11):4500-10.
43. Angus AA, Lee AA, Augustin DK, Lee EJ, Evans DJ, Fleiszig SM. Pseudomonas aeruginosa induces membrane blebs in epithelial cells, which are utilized as a niche for intracellular replication and motility. Infect Immun. 2008;76(5):1992-2001.
44. Garcia-Medina R, Dunne WM, Singh PK, Brody SL. Pseudomonas aeruginosa acquires biofilm-like properties within airway epithelial cells. Infect Immun. 2005;73(12):8298-305.
45. Hritonenko V, Mun JJ, Tam C, Simon NC, Barbieri JT, Evans DJ, et al. Adenylate cyclase activity of Pseudomonas aeruginosa ExoY can mediate bleb-niche formation in epithelial cells and contributes to virulence. Microb Pathog. 2011;51(5):305-12.

46. Rao L, De La Rosa I, Xu Y, Sha Y, Bhattacharya A, Holtzman MJ, et al. Pseudomonas aeruginosa survives in epithelia by ExoS-mediated inhibition of autophagy and mTOR. EMBO reports. 2021;22(2):e50613.
47. Jolly AL, Takawira D, Oke OO, Whiteside SA, Chang SW, Wen ER, et al. Pseudomonas aeruginosa-induced bleb-niche formation in epithelial cells is independent of actinomyosin contraction and enhanced by loss of cystic fibrosis transmembrane-conductance regulator osmoregulatory function. mBio. 2015;6(2):e02533.
48. Kroken AR, Chen CK, Evans DJ, Yahr TL, Fleiszig SMJ. The Impact of ExoS on Pseudomonas aeruginosa Internalization by Epithelial Cells Is Independent of fleQ and Correlates with Bistability of Type Three Secretion System Gene Expression. mBio. 2018;9(3).
49. Anderson GG, Palermo JJ, Schilling JD, Roth R, Heuser J, Hultgren SJ. Intracellular bacterial biofilm-like pods in urinary tract infections. Science. 2003;301(5629):105-7.
50. Penaranda C, Chumbler NM, Hung DT. Dual transcriptional analysis reveals adaptation of host and pathogen to intracellular survival of Pseudomonas aeruginosa associated with urinary tract infection. PLoS Pathog. 2021;17(4):e1009534.
51. Darling KE, Dewar A, Evans TJ. Role of the cystic fibrosis transmembrane conductance regulator in internalization of Pseudomonas aeruginosa by polarized respiratory epithelial cells. Cell Microbiol. 2004;6(6):521-33.
52. Del Mar Cendra M, Torrents E. Differential adaptability between reference strains and clinical isolates of Pseudomonas aeruginosa into the lung epithelium intracellular lifestyle. Virulence. 2020;11(1):862-76.
53. Fleiszig SM, Zaidi TS, Preston MJ, Grout M, Evans DJ, Pier GB. Relationship between cytotoxicity and corneal epithelial cell invasion by clinical isolates of Pseudomonas aeruginosa. Infect Immun. 1996;64(6):2288-94.
54. Schindelin J, Arganda-Carreras I, Frise E, Kaynig V, Longair M, Pietzsch T, et al. Fiji: an open-source platform for biological-image analysis. Nat Methods. 2012;9(7):676-82.
55. de Chaumont F, Dallongeville S, Chenouard N, Hervé N, Pop S, Provoost T, et al. Icy: an open bioimage informatics platform for extended reproducible research. Nat Methods. 2012;9(7):690-6.
56. Heimer SR, Evans DJ, Stern ME, Barbieri JT, Yahr T, Fleiszig SM. Pseudomonas aeruginosa utilizes the type III secreted toxin ExoS to avoid acidified compartments within epithelial cells. PLoS One. 2013;8(9):e73111.
57. Reddel RR, Ke Y, Gerwin BI, McMenamin MG, Lechner JF, Su RT, et al. Transformation of human bronchial epithelial cells by infection with SV40 or adenovirus-12 SV40 hybrid virus, or transfection via strontium phosphate coprecipitation with a plasmid containing SV40 early region genes. Cancer Res. 1988;48(7):1904-9.

58. Kortebi M, Milohanic E, Mitchell G, Pechoux C, Prevost MC, Cossart P, et al. Listeria monocytogenes switches from dissemination to persistence by adopting a vacuolar lifestyle in epithelial cells. PLoS Pathog. 2017;13(11):e1006734.
59. Takano M, Ohishi Y, Okuda M, Yasuhara M, Hori R. Transport of gentamicin and fluid-phase endocytosis markers in the LLC-PK1 kidney epithelial cell line. Journal of Pharmacology and Experimental Therapeutics. 1994;268(2):669-74.
60. VanCleave TT, Pulsifer AR, Connor MG, Warawa JM, Lawrenz MB. Impact of Gentamicin Concentration and Exposure Time on Intracellular Yersinia pestis. Front Cell Infect Microbiol. 2017;7:505.
61. Vidya P, Smith L, Beaudoin T, Yau YC, Clark S, Coburn B, et al. Chronic infection phenotypes of Pseudomonas aeruginosa are associated with failure of eradication in children with cystic fibrosis. Eur J Clin Microbiol Infect Dis. 2016;35(1):67-74.
62. Fleiszig SM, Zaidi TS, Pier GB. Pseudomonas aeruginosa invasion of and multiplication within corneal epithelial cells in vitro. Infect Immun. 1995;63(10):4072-7.
63. Alves PM, Al-Badi E, Withycombe C, Jones PM, Purdy KJ, Maddocks SE. Interaction between Staphylococcus aureus and Pseudomonas aeruginosa is beneficial for colonisation and pathogenicity in a mixed biofilm. Pathog Dis. 2018;76(1).
64. Pereira SH, Cervante MP, Bentzmann S, Plotkowski MC. Pseudomonas aeruginosa entry into Caco-2 cells is enhanced in repairing wounded monolayers. Microb Pathog. 1997;23(4):249-55.
65. Chi E, Mehl T, Nunn D, Lory S. Interaction of Pseudomonas aeruginosa with A549 pneumocyte cells. Infect Immun. 1991;59(3):822-8.
66. Hennemann LC, LaFayette SL, Malet JK, Bortolotti P, Yang T, McKay GA, et al. LasR-deficient Pseudomonas aeruginosa variants increase airway epithelial mICAM-1 expression and enhance neutrophilic lung inflammation. PLoS Pathog. 2021;17(3):e1009375.
67. LaFayette SL, Houle D, Beaudoin T, Wojewodka G, Radzioch D, Hoffman LR, et al. Cystic fibrosis-adapted Pseudomonas aeruginosa quorum sensing lasR mutants cause hyperinflammatory responses. Sci Adv. 2015;1(6).
68. Liu W, Sun T, Wang Y. Integrin αvβ6 mediates epithelial-mesenchymal transition in human bronchial epithelial cells induced by lipopolysaccharides of Pseudomonas aeruginosa via TGF-β1-Smad2/3 signaling pathway. Folia Microbiol (Praha). 2020;65(2):329-38.
69. Plotkowski MC, Brandão BA, de Assis MC, Feliciano LF, Raymond B, Freitas C, et al. Lipid body mobilization in the ExoU-induced release of inflammatory mediators by airway epithelial cells. Microb Pathog. 2008;45(1):30-7.
70. Han X, Na T, Wu T, Yuan BZ. Human lung epithelial BEAS-2B cells exhibit characteristics of mesenchymal stem cells. PLoS One. 2020;15(1):e0227174.

71. Stewart CE, Torr EE, Mohd Jamili NH, Bosquillon C, Sayers I. Evaluation of differentiated human bronchial epithelial cell culture systems for asthma research. J Allergy (Cairo). 2012;2012:943982.
72. Kierbel A, Gassama-Diagne A, Rocha C, Radoshevich L, Olson J, Mostov K, et al. Pseudomonas aeruginosa exploits a PIP3-dependent pathway to transform apical into basolateral membrane. J Cell Biol. 2007;177(1):21-7.
73. Plotkowski MC, de Bentzmann S, Pereira SH, Zahm JM, Bajolet-Laudinat O, Roger P, et al. Pseudomonas aeruginosa internalization by human epithelial respiratory cells depends on cell differentiation, polarity, and junctional complex integrity. Am J Respir Cell Mol Biol. 1999;20(5):880-90.
74. Kazmierczak BI, Mostov K, Engel JN. Epithelial cell polarity alters Rho-GTPase responses to Pseudomonas aeruginosa. Mol Biol Cell. 2004;15(2):411-9.
75. Ha U, Jin S. Growth phase-dependent invasion of Pseudomonas aeruginosa and its survival within HeLa cells. Infect Immun. 2001;69(7):4398-406.
76. Ratjen F, Brockhaus F, Angyalosi G. Aminoglycoside therapy against Pseudomonas aeruginosa in cystic fibrosis: a review. J Cyst Fibros. 2009;8(6):361-9.
77. Finck-Barbancon V, Goranson J, Zhu L, Sawa T, Wiener-Kronish JP, Fleiszig SM, et al. ExoU expression by Pseudomonas aeruginosa correlates with acute cytotoxicity and epithelial injury. Mol Microbiol. 1997;25(3):547-57.
78. O'Malley YQ, Abdalla MY, McCormick ML, Reszka KJ, Denning GM, Britigan BE. Subcellular localization of Pseudomonas pyocyanin cytotoxicity in human lung epithelial cells. Am J Physiol Lung Cell Mol Physiol. 2003;284(2):L420-30.
79. Shafikhani SH, Morales C, Engel J. The Pseudomonas aeruginosa type III secreted toxin ExoT is necessary and sufficient to induce apoptosis in epithelial cells. Cell Microbiol. 2008;10(4):994-1007.
80. Kunzelmann K, Schwiebert EM, Zeitlin PL, Kuo WL, Stanton BA, Gruenert DC. An immortalized cystic fibrosis tracheal epithelial cell line homozygous for the delta F508 CFTR mutation. Am J Respir Cell Mol Biol. 1993;8(5):522-9.
81. Bebok Z, Collawn JF, Wakefield J, Parker W, Li Y, Varga K, et al. Failure of cAMP agonists to activate rescued deltaF508 CFTR in CFBE41o- airway epithelial monolayers. J Physiol. 2005;569(Pt 2):601-15.
82. Jacobs MA, Alwood A, Thaipisuttikul I, Spencer D, Haugen E, Ernst S, et al. Comprehensive transposon mutant library of Pseudomonas aeruginosa. Proc Natl Acad Sci U S A. 2003;100(24):14339-44.
83. Tekwa EW, Nguyen D, Juncker D, Loreau M, Gonzalez A. Patchiness in a microhabitat chip affects evolutionary dynamics of bacterial cooperation. Lab Chip. 2015;15(18):3723-9.

84. Brannon MK, Davis JM, Mathias JR, Hall CJ, Emerson JC, Crosier PS, et al. Pseudomonas aeruginosa Type III secretion system interacts with phagocytes to modulate systemic infection of zebrafish embryos. Cell Microbiol. 2009;11(5):755-68.

Preamble to Chapter 4

Having established a robust long-term model of intracellular *P.a.* survival within AEC in chapter 3, we next sought to gain a deeper understanding of the "hyper-proliferator" phenotype observed in CI180 and identify potential underlying bacterial factors that mediate this phenotype. Bacterial factors promoting intracellular survival were of particular interest as they may be attractive future treatment targets in order to improve bacterial antibiotic eradication regimens. We thus decided to screen a larger subset of clinical isolates, allowing us to identify the loss of T3SS as an important bacterial phenotype that promotes intracellular survival, and to observe evidence of specific strains capable of high intracellular proliferation.

Chapter 4: Loss of type 3 secretion system function facilitates intracellular *Pseudomonas aeruginosa* survival and proliferation within airway epithelial cells, *Manuscript in preparation*

Lisa C. Hennemann[1,2], Julien K. Malet[1], Elizabeth M.-L. Hua[2], Sumaiya Jusab[2], Angela Nelson[2], Damien Adam[3,4], Emmanuelle Brochiero[3,4], Valerie Waters[5], Simon Rousseau[1] and Dao Nguyen[1,2,6]

[1]Meakins Christie Laboratories, Research Institute of the McGill University Health Centre, Montreal, Quebec, Canada

[2]Department of Microbiology and Immunology, McGill University, Montreal, Quebec, Canada

[3] Centre de recherche du Centre Hospitalier de l'Université de Montréal (CRCHUM), Montréal, Québec, Canada

[4] Département de médecine, Université de Montréal, Montréal, Québec, Canada

[5]Division of Infectious Diseases, Department of Pediatrics, The Hospital for Sick Children, University of Toronto, Toronto, CA, Canada

[6]Department of Medicine, McGill University, Montreal, Quebec, Canada

4.1 Abstract

While a combination of mucosal defense defects in the Cystic Fibrosis (CF) lung allows for the colonization by a range of opportunistic pathogens, the Gram-negative bacterium *Pseudomonas aeruginosa* (*P.a.*) is typically of particular concern due to its ability to establish chronic infections that are unresponsive to antibiotic treatment and are generally associated with excessive lung inflammation and tissue destruction. There are diverse factors accounting for *P.a.*'s persistence in the CF lung, including antibiotic resistance, biofilm formation and a downregulation of bacterial factors that are typically recognized by the host immune system. However, an additional potential persistence mechanism, intracellular bacterial survival within the airway epithelium, is often overlooked despite proof of intracellular *P.a.* both *in vitro* and in rodent infection models. Here, we explored the ability of a collection of clinical *P.a.* isolates to survive intracellularly within airway epithelial cells (AEC) for 24h post infection. We identified loss of type 3 secretions system (T3SS) function as a major determinant of bacterial intracellular survival and observed increased intracellular survival and proliferation in naturally occurring and engineered T3SS-deficient isolates in different strain backgrounds. Using both flow cytometry and confocal imaging, we determined that this increased proliferation of T3SS-deficient isolates was largely driven by a small subpopulation of infected cells harboring a high bacterial burden. These findings may offer additional insights into why chronic infection isolates, which are likely to be T3SS-deficient, are able to persist in the presence of antibiotics and immune cells. Future studies could elucidate the underlying mechanism and whether other phenotypes associated with chronic infection isolates further potentiate intracellular bacterial survival.

4.2 Introduction

Pseudomonas aeruginosa (*P.a.*) is an opportunistic Gram-negative pathogen well known to cause chronic infections such as chronic airway, wound or urinary infections, in individuals with defects in mucosal host defenses. In individuals with the genetic disease Cystic Fibrosis (CF), chronic airway *P.a.* infections, which persist despite antibiotic treatments and are nearly impossible to eradicate, are commonly observed and are associated with accelerated decline in lung function, increased symptoms and mortality (1, 2). Impaired mucociliary clearance and mucosal host defenses, as well as the ability for *P.a.* to form biofilms in airway mucus, resist antibiotics and evade host immunity, are all well-established host and bacterial factors that contribute to bacterial colonization and persistence in the CF airways (3-5).

In this study, we examined the intracellular lifestyle of *P.a.*, a potential bacterial evasion mechanism that has been largely overlooked, yet may contribute to the persistent nature of chronic *P.a.* infections. Although *P.a.* is traditionally considered an extracellular pathogen, several groups have established over the last three decades that *P.a.* can invade different epithelial cell types ranging from corneal and bladder to airway epithelial cells (AEC) (6-13). While the occurrence of, and the mechanisms involved in the intracellular lifestyle of *P.a.* remain incompletely understood, intracellular *P.a.* within epithelial cells may represent an unrecognized bacterial reservoir protected from immune cells and the action of extracellular host defenses. Intracellular bacteria are also shielded from cell-impermeable antibiotics such as tobramycin (14), and subpopulations of intracellular bacteria may become tolerant to cell-permeable antibiotics such as fluoroquinolones (10).

Multiple bacteria widely regarded as extracellular pathogens, such as *Staphylococcus aureus* and *Escherichia coli*, can survive inside host cells. The intracellular lifestyle of *S. aureus* and uropathogenic *E. coli* (UPEC) is increasingly recognized as a clinically relevant bacterial reservoir that survives antibiotic treatment and contributes to the persistent nature of chronic infections (15-17). Intracellular UPEC within bladder epithelial cells has been demonstrated in samples from UTI patients (16, 18) and is the likely bacterial reservoir responsible for relapsing infections, refractory to prolonged antibiotic therapy and caused by the same persistent bacterial strains (19, 20). While less frequent than UPEC infections, *P.a.* may also form intracellular reservoirs within bladder epithelial cells (7). Similarly, intracellular *S. aureus* has been observed both in non-phagocytic and phagocytic cells *in vitro* (21-23) and has been linked to chronic rhinosinusitis in patients (24).

In the intracellular *P.a.* field, several studies have looked at defined mutants of different bacterial virulence factors in a limited number of strain backgrounds in order to examine their contribution to bacterial internalization and/or survival, largely within a very limited infection time frame (6, 25-30). Particularly initial internalization has been extensively studied in different epithelial cell types, highlighting the involvement of bacterial factors such as the flagellum, pili, lipopolysaccharide outer core, the lectin LecA and the type 3 secretion system (T3SS) (6, 8, 25, 26, 31), as well as host factors including small GTPases, Src family kinases, the actin cytoskeleton and lipid raft membrane domains, among others (32-36). However, few have examined the intracellular lifestyle of clinical isolates (7, 33, 37, 38). Additionally, the scarce number of studies that have examined clinical strain survival are largely descriptive and

do not dissect the causes of the survival heterogeneity in greater detail (7, 33, 37). Using our newly established model of intracellular long-term survival (39), which had previously allowed us to identify a non-cytotoxic clinical isolate displaying high intracellular survival across 120h, we sought to investigate which bacterial factors may be major determinants of intracellular survival among a collection of clinical isolates.

In this study, we tested a large collection of CF clinical isolates and observed significant strain-to-strain heterogeneity in their intracellular survival in AEC, a phenotype strongly determined by each strain's cytotoxicity and T3SS status. Genetically engineered T3SS mutants in 4 clinical and one lab strain background, all of which were originally T3SS(+) ExoS(+), demonstrated that loss of T3SS injectisome function alone was sufficient to allow for intracellular strain survival, whereas T3SS effector mutants that retained injectisome function were unable to survive intracellularly despite being non-cytotoxic. Lastly, we determined that the increased survival of T3SS-deficient strains was driven by a sub-population of hyper-infected cells that was not observed among wild-type-infected cells, which likely account for the majority of the intracellular bacterial burden.

4.3 Material and methods:

Bacterial strains, mutant construction and culture conditions:

All bacterial strains and plasmids used in this study are described in supplementary table S4.1. Bacteria were streaked onto LB (BD Difco) agar (Wisent) plates to single colonies from glycerol stocks stored at -80C. Agar plates were then incubated overnight at 37°C and used to inoculate 5 mL LB media for overnight growth at 37°C with shaking at 250 rpm. After ~16h growth, stationary phase bacteria were used for subsequent experiments. To generate mCherry-tagged strains, the respective strains were transformed with pMKB1::mCherry via electroporation for constitutive mCherry expression, and cultured in LB media containing 250 μg/mL carbenicillin (PhytoTechnology Laboratories) for selection prior to infection experiments.

T3SS (*exsA* and *exoS*) unmarked deletion mutants were generated by two-step allelic replacement using the suicide vector pEX18-Gm containing Δ*exsA* and Δ*exoS* deletion constructs (40, 41). Briefly, following mating of SM10 *E. coli* donor cells containing the pEX18-Gm constructs with the recipient parental *P.a.* strain, merodiploids were selected on 10 μg/mL chloramphenicol and 50 μg/mL gentamicin (Wisent Bioproducts). Deletion mutants

were selected by counter-selection on 15% sucrose (42) and were confirmed by PCR. All PCR primer sequences used are provided in supplementary Table S4.2. Phenotypic loss of function was assessed by Western blotting as described below.

T3SS secretion:

In order to assess T3SS secretion by clinical strains or T3SS deletion mutants, overnight cultures were washed and adjusted to OD_{600}=0.2 in 5 mL of either LB (non-inducing media) or LB supplemented with 20 mM $MgCl_2$ and 5 mM EGTA (T3SS-inducing media). After 3h of growth (37°C, shaking at 250 rpm), cells were pelleted by centrifugation (12000 rpm x 5 min), bacterial supernatants were collected and mixed to a final concentration of 10% trichloroacetic acid (Sigma Aldrich) to precipitate proteins. Following overnight incubation at 4°C, supernatant proteins were pelleted by centrifugation (12000 rpm x 15 min at 4°C), washed twice with acetone (Sigma Aldrich), air-dried and resuspended in Tris-HCl (pH 8.8). Protein concentrations were assessed by BCA assay (Thermo Scientific) according to the manufacturer's instructions. Protein samples were then mixed with 4x loading buffer containing DTT, boiled at 95°C for 5 min and stored at -20°C until analysis.

Secretion of T3SS proteins

ExoS and PcrV were assessed by Western blotting as follows. 1 μg of protein per sample was loaded onto pre-cast 4-20% Mini-PROTEAN gels (Bio-Rad) for SDS-PAGE and subsequently transferred onto activated PVDF membranes (Bio-Rad). Membranes were then blocked with 5% skim milk for 45 min prior to overnight incubation at 4°C with 1:5000 rabbit anti-ExoS (Dr. Arne Rietsch) and/or 1:500 human anti-PcrV (AstraZeneca) (43) antibodies diluted in 5% skim milk. Following washing with TBS-T (Tris-buffered saline supplemented with 0.1% Tween 20), membranes were incubated with 1:5000 donkey anti-human IgG DyLight 680 (Invitrogen) and/or 1:5000 anti-rabbit IgG DyLight 800 4X PEG conjugated (Cell Signaling Technology) secondary antibody for 1h at room temperature. Protein bands were imaged with an Odyssey imaging system (Li-Cor Biosciences) and assessed for the presence or absence of PcrV and ExoS bands. Strains were determined to be T3SS-negative by two blinded examiners if no T3SS bands were observed in two independent experiments. For some experiments, duplicate SDS-PAGEs with the same amounts of the same samples were simultaneously processed for Western blotting and Coomassie staining. Coomassie-stained gels were analyzed using an Aplegen Omega Lum G Gel Documentation System.

Bronchial epithelial cell culture conditions:

Immortalized human bronchial epithelial cells (BEAS-2B) were maintained in DMEM (Wisent) supplemented with 10% fetal bovine serum (FBS, Wisent), penicillin and streptomycin (P/S, Wisent) at 37°C in 5% CO_2. Primary human bronchial epithelial cells from healthy (i.e. non-CF) donors were obtained from the CRCHUM's Respiratory Cell and Tissue Biobank of the Respiratory Health Research Network of Québec with informed written consent prior to enrolment (protocol #08.063). Submerged primary cells were maintained in BEBM (Lonza) supplemented with BEGM (except for gentamicin and retinoic acid, Lonza), 10% FBS and P/S and were grown at 37°C in 5% CO_2. Primary cells were grown to an approximate cell density of 200,000-600,000 cells/mL in cell culture-grade 24 well plates (Sarstedt) for infection, while BEAS-2B cells were seeded into fresh 24 well plates 24h prior to infection at 100,000 cells/well.

***P.a.* infection assay:**

BEAS-2B cells were infected with *P.a.* and processed for colony forming units (CFU), lactate dehydrogenase (LDH) release assay and other downstream assays as previously described (39). Briefly, BEAS-2B cells were infected with *P.a.* strains at a multiplicity of infection (MOI) of 1, spun down for 3 minutes at 700 rpm, and after 4h of infection, extracellular bacteria were killed through the addition of 100 μg/mL tobramycin (Sigma Aldrich), a cell impermeable antibiotic. BEAS-2B cells containing intracellular bacteria were maintained in the presence of 100 μg/mL tobramycin for up to 120h. To measure intracellular bacteria at different time points, host cells were lysed using 0.5% Triton X-100, and viable bacterial counts were measured by serial dilution and plating for CFU counts. *P.a.* cytotoxicity to epithelial cells was assessed by LDH release assay (Roche) in BEAS-2B cell lysates and culture supernatants as previously done (39).

Flow cytometry analyses:

BEAS-2B cells were processed and stained for flow cytometry as previously described (39). Briefly, BEAS-2B cells were infected with mCherry-expressing *P.a.* strains as described above. At varying time points post infection, cells were stained with fixable viability dye eFluor 780 (eBiosciences) and fixed in 0.5% PFA. Cell fluorescence was assessed on a Fortessa LSR-II flow cytometer (BD Biosciences) and results were analyzed using FlowJo (BD Biosciences). For the mCherry gating, fluorescence-minus-one samples infected with the corresponding non-fluorescent strain and stained/fixed in the same manner were used. The false-positive threshold

in the uninfected sample was set to ≤ 0.5% and the same gating was applied to all samples. The % of mCherry-positive cells in samples infected with the corresponding non-mCherry strain was subtracted from the % of mCherry-positive cells in samples infected with mCherry-expressing strains in order to account for the varying presence of auto-fluorescent cells upon infection with different strains.

Immunofluorescence and confocal microscopy imaging:

100,000 BEAS-2B cells were seeded onto sterile 12mm glass cover slips (22293232P, Fisherbrand) inside cell culture-grade 24 well plates (Sarstedt). BEAS-2B cells were infected with *P.a.* as described above. Fixation and staining for total/extracellular *P.a.* was conducted as previously described (39). Briefly, cells were fixed in 1% PFA followed by incubation with 1:1000 diluted primary (rabbit anti-*P.a*., Abcam ab68538) and 1:500 diluted secondary (AF647-conjugated anti-rabbit, #A21-244, Life technologies) antibody for staining of extracellular *P.a*. Cells were then permeabilized with 0.2% Triton X-100 and stained again for *P.a*. with the same primary antibody (rabbit anti-*P.a*., Abcam ab68538), followed by a secondary antibody conjugated to a different fluorophore (AF488-conjugated anti-rabbit, #A11-008, Life technologies). Simultaneously, cellular actin (TRITC-conjugated phalloidin, 1:250, #5783, R&D) and nuclei (DAPI, 1:1000, #LSD1306, Invitrogen) were stained. Samples were mounted on microscopic slides and analyzed on a Zeiss LSM700 confocal fluorescence microscope.

Image acquisition and analysis:

Stained coverslips were imaged by confocal microscopy using a Zeiss LSM 700 microscope with a 405nm, 488nm, 555nm and 639nm laser channels. The following objectives were used: EC plan-neofluor 40x/0.9 Pol M27 and plan-apochromat 63x/1.40 oil DIC M27 oil-immersion objective. Z-stacks were collected in 8 or 12 bit mode with a minimum of 2-line averaging and a resolution of minimum 1024x1024 pixels. Images were exported as czi files then processed and using ImageJ (Version 2.1) for image transformation and rendering or ICY (version 2.4.2.0) for automated detection of eukaryotic cells and bacteria (based on method described (39)). For colocalization analysis, maximum intensity projections were created for all channel and a correlation-based method was used to determine the Manders coefficient (44).

4.4 Results

T3SS-deficient clinical *P.a.* isolates display increased intracellular survival within AEC. Previous studies on the intracellular lifestyle of *P.a.* in epithelial cells have largely focused on initial internalization steps (25, 34, 36, 45) and early stages (≤12h) of intracellular survival (27-30). Studies have typically tested one *P.a.* strain at a time (e.g. PAO1, PAK), and few have reported on the heterogeneity of the intracellular lifestyle across different strains (37, 39). Here, we sought to investigate the heterogeneity in intracellular survival in a collection of 28 *P.a.* clinical isolates recovered from CF sputum (Supp. Table S4.1). We only tested ExoS+ isolates and excluded ExoU+ isolates since ExoU-mediated toxicity has previously been demonstrated to be incompatible with intracellular survival within epithelial cells (46).

We used a model of long-term infection of the airway epithelium where we measured the viable intracellular bacterial burden and cytotoxicity in AEC infected with the different *P.a.* isolates. We first examined the relationship between intracellular bacterial burden at 24h post-infection (p.i) and AEC cytotoxicity for each *P.a.* isolate and noted significant heterogeneity across the 28 isolates, with CFU counts ranging from undetectable (<10 CFU/mL) to $4.4x10^5$ CFU/mL and cytotoxicity ranging from 3.5% to 54.4% (Fig 4.1A). Since intracellular bacterial counts at 24h p.i are not only a measure of intracellular survival, but also affected by internalization rates, we then looked at bacterial survival at 24h p.i, namely the 24h CFU counts normalized by the initial CFU counts at 4h. Interestingly, we now noted that a small subset of isolates with high intracellular survival (≥100%) displayed low to no cytotoxicity, while those with low survival (<100%) caused varying degrees of cytotoxicity (Fig. 4.1B).

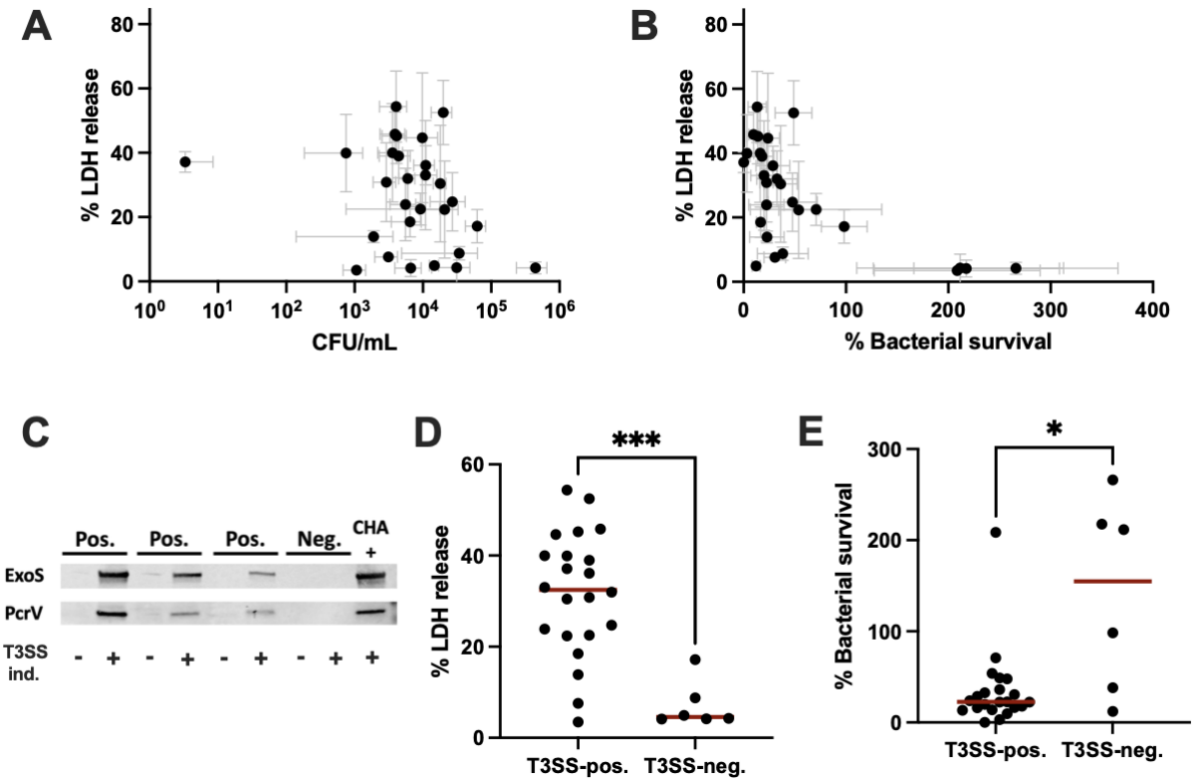

Fig. 4.1: T3SS-deficient clinical *P. aeruginosa* isolates display increased intracellular survival. BEAS-2B cells were infected with 28 clinical *P.a.* isolates from CF lung infections at MOI 1 for 4h. Extracellular bacteria were then cleared through the addition of tobramycin, cells were maintained in the presence of extracellular tobramycin for 24h. Time points to assess intracellular viable CFU counts and cytotoxicity (by LDH release assay) were taken at 4h and 24h. Cytotoxicity at 24h p.i. was plotted against **(A)** viable CFU counts at 24h p.i. and **(B)** intracellular bacterial survival. Bacterial survival ((24h CFU counts/4h CFU counts) x100) was expressed as a percentage for each strain. Clinical strains were assessed for their ability to secrete T3SS components (PcrV, ExoS) into surrounding growth media under T3SS-inducing (+) or non-inducing (-) conditions. Secreted protein was precipitated and 1 µg protein was loaded per sample. Secretion was assessed by Western blotting and strains were grouped into T3SS-positive and negative isolates, as shown in a representative Western blot in **(C)**. The average **(D)** cytotoxicity and **(E)** intracellular survival per strain at 24h are displayed for each group, where each dot represents one clinical isolate. Data points in **(A)** and **(B)** represent the mean ± SD values for each isolate, where each isolate was assessed in two independent experiments conducted in biological triplicates. **(D)** and **(E)** display the underlying data from **(B)** stratified by T3SS-secretion status. The median per group is displayed as a red line.

Since the *P.a.* T3SS is a well-established driver of epithelial cell cytotoxicity (47) and its activity is known to vary across CF clinical isolates, we assessed the T3SS activity of all clinical isolates under T3SS-inducing conditions (low Ca^{2+} (48)) by Western blot, probing for extracellular ExoS (effector) and PcrV (translocon). Representative Western blots for T3SS positive or negative strains are shown in Fig. 4.1C. The ExoS antibody was first validated using the reference strain PA14 which encodes for ExoT and ExoU but not ExoS, indicating specificity for ExoS despite the high sequence homology between ExoS and ExoT (Supp Fig. S4.1A) (49). The clinical isolate CHA, an ExoS+ *gacS* mutant which has a hyperactive T3SS (50), was used as a positive control and its isogenic *exsA* mutant was used as a negative control for both the PcrV and ExoS antibodies (Supp. Fig. S4.1A). Furthermore, three representative T3SS(-) and three T3SS(+) isolate samples analyzed simultaneously by Western Blotting and Coomassie staining showed similar protein patterns, thus excluding the possibility that the absence of T3SS bands was due to insufficient protein loading (Supp. Fig. S4.1B).

When grouped according to their T3SS status, T3SS(-) isolates, as expected, induced significantly less cytotoxicity than T3SS(+) isolates (32.5% vs 4.6%, p=0.0005, Fig. 4.1D). Notably, intracellular survival was higher in T3SS(-) compared to T3SS(+) isolates (155% vs 22.5%, p=0.0203, Fig. 4.1E), with all but one T3SS(+) isolate demonstrating low intracellular survival (< 71%). We also noted one outlier T3SS(+) isolate associated with low cytotoxicity (3.5%) and high intracellular survival (208%). Interestingly, T3SS(-) isolates were heterogeneous in their ability to survive intracellularly (range 13.1% to 266%), suggesting that bacterial factor(s) other than the T3SS may be involved.

Loss of T3SS function promotes intracellular bacterial survival in different strain backgrounds. In order to investigate the contribution of T3SS deficiency to *P.a.* intracellular survival, we deleted the T3SS transcriptional activator gene *exsA* from one lab strain PAO1-F (51) and 4 clinical isolates, all of whom were T3SS(+). Loss of ExsA function abolishes expression of the T3SS, resulting in a loss of T3SS-mediated cytotoxicity (52-54) and naturally occurring mutations in the *exsA* gene have been reported in CF clinical isolates (55-57). At 4 h p.i., both wild-type and *exsA* mutant strains appeared to be non-cytotoxic. However, by 24 h p.i., cells infected by wild-type stains displayed varying degrees of cytotoxicity with >19% LDH release, whereas *exsA* mutant strains were non-cytotoxic and induced <4% LDH release (Fig. 4.2A). The intracellular bacterial load at 4 h p.i ranged from $1.5x10^4$ to $4.3x10^5$ CFU/mL, with no clear distinction between the wild-type strains and *exsA* mutants. In contrast, the

intracellular CFU counts at 24 h p.i diverged into two non-overlapping clusters of wild-type strains and *exsA* mutants (range 1.2x10^3 to 1.7x10^4 CFU/mL and 3.9x10^4 to 2.6x10^5 CFU/mL respectively) (Fig. 4.2C).

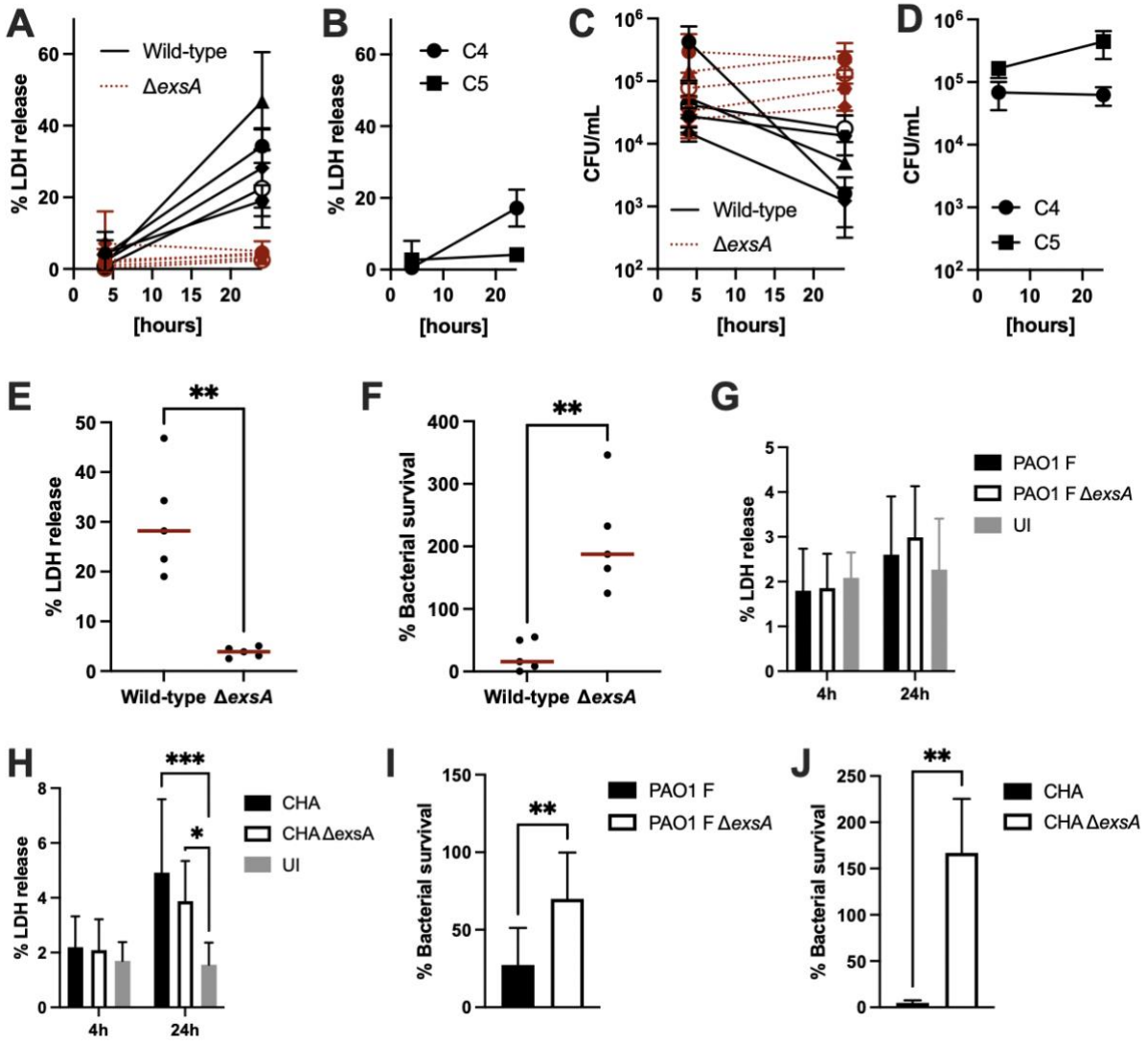

Fig. 4.2: T3SS loss-of-function is sufficient to allow *P. aeruginosa* to survive intracellularly within an airway epithelial cell line as well as human primary bronchial epithelial cells. BEAS-2B cells **(A-F)** or submerged human primary bronchial epithelial cells **(G-J)** were infected with a lab strain (PAO1 F) or four clinical isolates (CHA, C1-3) and their isogenic *exsA* mutants at MOI 1. Alternatively, cells were infected with naturally occurring T3SS-deficient isolates C4 or C5. At 4h p.i., extracellular bacteria were killed through the addition of tobramycin. Intracellular bacteria were maintained in the presence of extracellular tobramycin for the entire duration of the experiment. Samples were taken at 4h and 24h p.i. to assess cytotoxicity via LDH release assay **(A+B, E, G+H)**, intracellular viable CFU counts in CFU/mL **(C+D)** and the percentage of intracellular bacterial survival, which is a measure of

CFU counts at 24h in relation to CFU counts at 4h p.i. **(F, I+J)**. Each data point in **(E+F)** represents the average LDH release/bacterial survival at 24h p.i. for one out of the five wild-type or *exsA* mutant strains shown in **(A+C)**. Averages were calculated from ≥ 2 independent experiments in biological triplicates. Red bars designate the median for each group. All other panels show the mean ± SD from ≥ 2 independent experiments in biological triplicates (BEAS-2B experiments) or quadruplicates/quintuplicates (primary cell experiments).

To account for differences in internalization rates across different strains, we calculated the intracellular survival (as done for Fig. 4.1E) for each strain. Upon comparing wild-type strains to their isogenic *exsA* mutants, we found that *exsA* mutants displayed significantly higher intracellular survival compared to their wild-type counterparts (Fig. 4.2F, 188% vs 16% p=0.0079), which was associated with significantly lower cytotoxicity induced by *exsA* mutants at 24h p.i. (Fig. 4.2E), as previously observed for the naturally occurring T3SS-deficient strains (Fig. 1D). Interestingly, all 5 *exsA* mutants showed intracellular survival over 100%, potentially indicating intracellular proliferation. Notably, similar results were observed with the clinical isolates C4 and C5, two naturally occurring T3SS(-) strains which displayed 17.2% and 4.2% LDH release at 24h p.i., respectively (Fig. 4.2B). Intracellular CFU counts for C4 and C5 at 24h p.i. were $6.2x10^4$ and $4.4x10^5$ CFU/mL (Fig. 4.2D), with an intracellular survival of 98% and 266%, respectively. Taken together, our results indicate that loss of T3SS activity leads to reduced cytotoxicity and promotes intracellular survival within airway epithelial cells across genetically and phenotypically diverse *P.a.* strains.

Since BEAS-2B are an immortalized airway epithelial cell line (58, 59), we sought to validate our findings in primary human (non-CF) airway epithelial cells. Submerged primary human bronchial epithelial cells were infected with two pairs of wild-type strains, the PAO1 F lab strain and the CHA clinical isolate, and their respective isogenic *exsA* mutants. Surprisingly, infection with both PAO1 and CHA resulted in very modest cytotoxicity (Fig 4.2G/H), suggesting that primary cells are less susceptible to T3SS-induced cell death than BEAS-2B cells. Despite this absence of cytotoxicity, both *exsA* mutants displayed greater intracellular survival than their parental strains (Fig. 4.2I+J, 27% vs 70% p=0.005 for PAO1, 5% vs 167% p=0.0012 for CHA), even if the magnitude of difference varied based on the *P.a.* strain background and the airway epithelial cell type.

The increased intracellular survival of T3SS-deficient strains is not due to a lack of effector-mediated cytotoxicity. Since loss of T3SS activity led to increased intracellular survival and reduced cytotoxicity, we sought to determine which component of the T3SS mediated this effect. We tested knockouts of the major T3SS components, namely mutants of *exsA* (transcriptional activator), *popB* (translocon), *pscD* (needle) and *exoSTY* (all T3SS effectors) in the PAO1 F background. Their T3SS secretion activity was first validated by detecting extracellular ExoS and PcrV under T3SS-inducing low calcium conditions and confirming that both the wild-type strain and the *popB* mutant secreted ExoS and PcrV, while the *exsA* and *pscD* mutants did not, and the *exoSTY* mutant only lacked ExoS as expected (Fig 4.3A). We note that detection of ExoS and PcrV in the *popB* mutant is not surprising as translocon function is crucial for translocation of effectors across host membranes, but dispensable in culture media (60). As shown in Fig 4.3B, all four mutants were impaired for cytotoxicity at 24 h p.i. compared to the wild-type strain, indicating that all examined components of the T3SS (needle, translocon, effectors) are required for T3SS-mediated cytotoxicity (Fig. 4.3B). Surprisingly, despite causing low cytotoxicity like the other three T3SS mutants, the *exoSTY* mutant did not maintain a high intracellular bacterial burden over time, in contrast to the other three T3SS mutants (Fig. 4.3C).

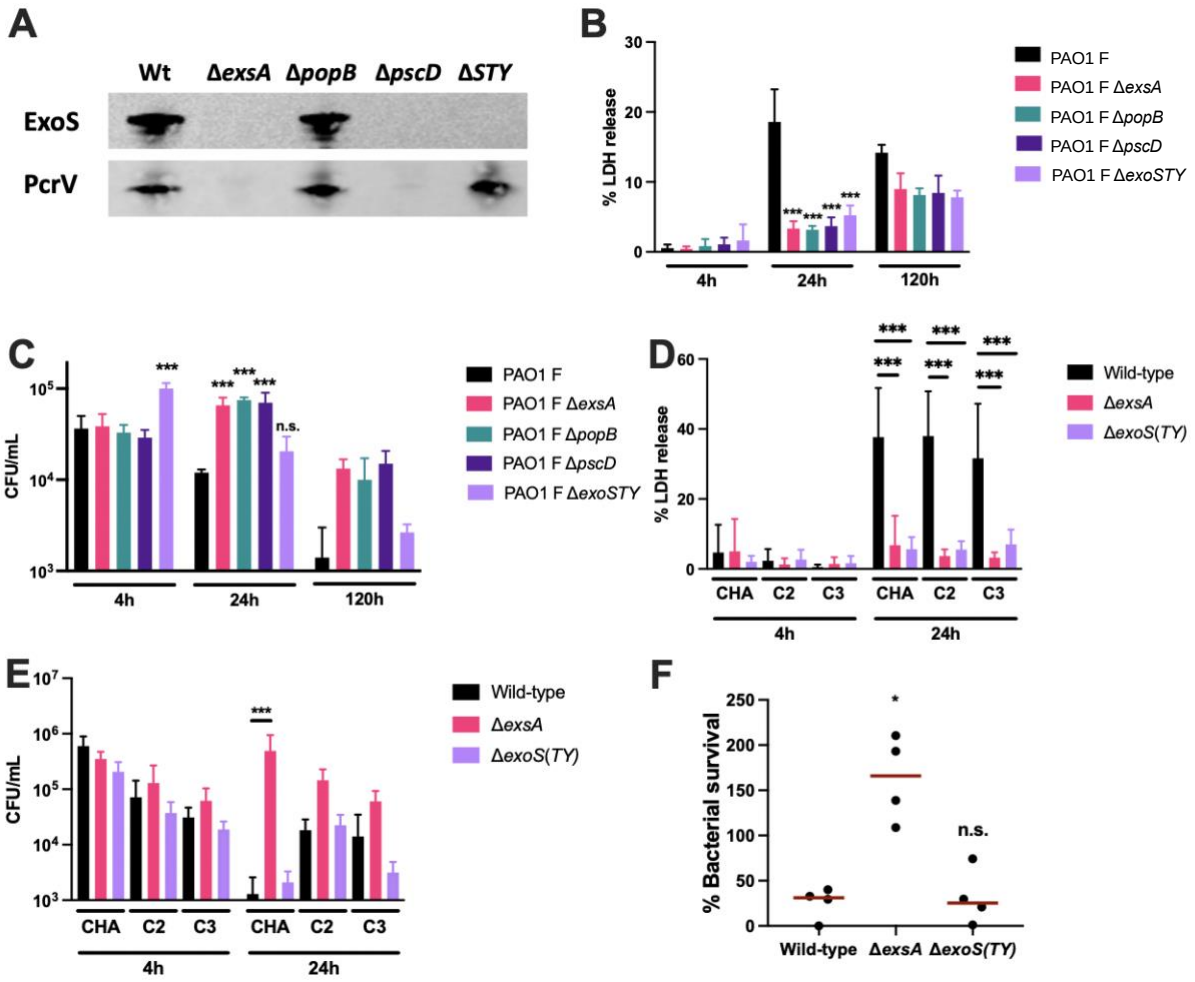

Fig. 4.3: Loss of T3SS effector-mediated cytotoxicity does not allow for intracellular bacterial survival. (A) T3SS mutant strains (Δ*exsA*, Δ*popB*, Δ*pscD*, Δ*exoSTY*) in the PAO1 F background were assessed for their ability to secrete T3SS components (PcrV, ExoS) into surrounding growth media under T3SS-inducing conditions. Secretion was assessed by Western blotting, 1 µg precipitated supernatant protein was loaded per sample. **(B-F)** BEAS-2B cells were infected with the lab strain PAO1 F, the clinical strains CHA, C2 and C3 or their isogenic T3SS mutants (Δ*exsA*, Δ*popB*, Δ*pscD*, Δ*exoS* (C2/C3), Δ*exoSTY* (PAO1 F/CHA)) at MOI 1. **(B+D)** Cytotoxicity (by LDH release assay) and **(C+E)** intracellular viable CFU counts were assessed at different time points. The percentage of intracellular bacterial survival **(F)** was calculated as the percentage of CFU counts at 24h relative to 4h CFU counts, where each data point represents the average for a different strain background (PAO1 F, CHA, C2, C3). All data is based on ≥ 3 independent experiments in biological triplicates and is shown as mean ± SD, with the exception of **(F)**, where red bars show the median.

To validate these results in other genetic backgrounds, we tested the clinical isolates CHA, C2 and C3, their isogenic *exsA* mutants, and the *exoSTY* (CHA) or *exoS* (C2/C3) mutants. Similarly, both *exsA* and effector (*exoSTY* or *exoS*) mutants were minimally cytotoxic compared to their parental wild-type strains (Fig. 4.3D), but only the *exsA* mutants displayed increased CFU counts compared to the parental strain at 24h p.i. (Fig. 4.3E). Upon pooling the data for all four strain backgrounds and comparing their bacterial survival (which normalizes for initial internalization rates), we clearly observed that intracellular survival was enhanced in the *exsA* mutants (31% vs 166% survival in wild-type vs Δ*exsA*, p=0.037) while survival of the *exoSTY* effector mutants was similar to the wild-type strains (Fig. 4.3F). Together, these results indicated that loss of effector-mediated cytotoxicity was not sufficient to allow for intracellular survival of *P.a.*, while the loss of either needle or translocon function was. Intracellular bacterial survival was thus enhanced in injectisome-deficient mutants (where either needle or translocon function was impaired), but not effector-deficient mutants. We did note that the intracellular bacterial burden of the PAO1 F *exoSTY* mutant at 4h p.i., was higher than the wild-type strain. Since this was not observed in the other *exoSTY* mutants, we did not further investigate this observation as it was beyond the main focus of this study.

Increased intracellular survival is linked to enhanced intracellular proliferation of T3SS-deficient strains. Next, we sought to analyze the infection dynamics at a single-cell level by flow cytometry. We infected AEC with mCherry-tagged PAO1-F and its T3SS mutants (*exsA*, *popB*, *pscD*, *exoSTY*) and analyzed for mCherry(+) AEC. The mCherry(+) gating was first set using uninfected AEC controls, allowing for a false positive threshold of 0.5%, then applied to all samples (Fig. 4.4A). The complete gating strategy is shown in Supp. Fig S4.2. Using the well-established fixable viability dye eFluor 780 to assess the cytotoxicity of the different strains, we observed similar results as with the LDH release assay (Fig. 4.3B), where the wild-type strain was the only strain that caused significant cytotoxicity (compared to an uninfected control) at 4h and 24h p.i. (Fig. 4.4B).

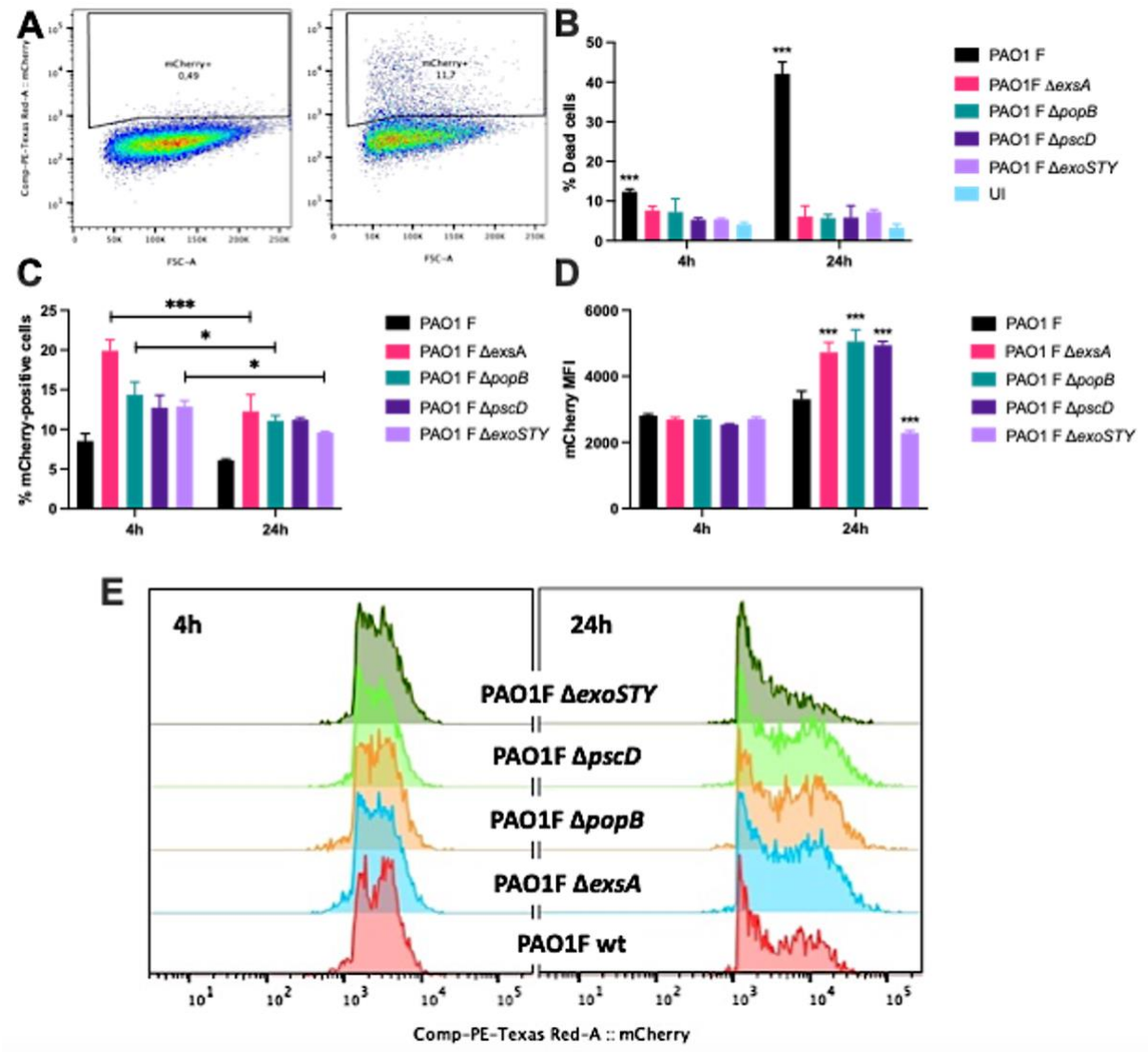

Fig. 4.4: Increased intracellular bacterial proliferation of *exsA*, *popB* and *pscD*, but not *exoSTY* mutant. BEAS-2B cells were infected with mCherry-expressing PAO1 F or its isogenic T3SS mutants at MOI 1 for up to 24h. Extracellular bacteria were killed through the addition of tobramycin at 4h p.i. and cells were maintained in the presence of extracellular tobramycin for the entire duration of the experiment. **(A)** The mCherry-positive gate was set using an uninfected control (left) and applied to all samples within the same time point (representative mCherry-positive infected sample on the right). **(B)** Dead cells were defined as fixable viability dye eFluor 780-positive cells and are displayed as a percentage. The percentage of infected cells **(C)** and mCherry median fluorescence intensity within the mCherry-positive gate **(D)** are shown. **(E)** displays representative mCherry fluorescence spectra for each strain for both time points. All results are from 1 representative of 3 independent experiments conducted in biological triplicates. The data is displayed as mean ± SD.

Using mCherry(+) cells as an indication of AEC infected with intracellular *P.a*., we noted that all T3SS mutants displayed a greater percentage of infected cells compared to the wild-type-infected cells at 4h p.i., indicating that T3SS mutants may be internalized more efficiently than their wild-type counterpart (Fig. 4.4C). However, when comparing the percentage of infected cells within strains between 4 h and 24 h, we only observed a moderate decline in the *exsA*, *popB* and *exoSTY* mutant infected cells at 4 h vs 24 h p.i (Fig. 4.4C). This suggests that a difference in the percentage of infected cells is unlikely to account for the diverging CFU counts of wt/Δ*exoSTY* and Δ*exsA*/Δ*popB*/Δ*pscD* strains from 4h to 24h p.i. we observed in Fig. 4.3C. The observed differential intracellular survival of wild-type and T3SS mutant strains is thus likely attributable to a factor other than the percentage of infected cells. Next, we examined the median mCherry fluorescence intensity within the mCherry(+) cell populations as a proxy for the intracellular bacterial burden. While there was no difference between the five strains at 4 h p.i., the MFI at 24 h p.i. was significantly higher in *exsA*, *popB* and *pscD* mutant-infected AEC compared to wild-type or *exoSTY* mutant-infected cells, indicating an increased bacterial burden of Δ*exsA*/Δ*popB*/Δ*pscD* per cell at this time point (Fig. 4.4D). We further noted the appearance of a high fluorescence subpopulation upon comparison of the mCherry fluorescence histograms of AEC infected with each of the five strains at 24 h p.i. compared to 4 h p.i. (Fig 4.4E). While the fluorescence histograms are identical for all *P.a*. strains at 4 h p.i., a second high fluorescence population apparent at 24 h p.i., is more pronounced in the *exsA*, *popB* and *pscD* mutant-infected cells than in the wild-type or *exoSTY* mutant-infected cells. This population of highly infected cells is likely the consequence of bacterial proliferation as additional internalization of extracellular bacteria after 4 h is impossible due to the presence of extracellular tobramycin and due to the fact that no such population was observed at 4 h p.i.

We validated these results with the clinical strains C2 and C3 and their isogenic *exsA* mutants. As observed with the PAO1 F-derived mutants, the C2 and C3 *exsA* mutants were less cytotoxic than their parental strain at 24 h p.i. (Supp Fig. S4.3A and S4.3B) and infected a greater percentage of infected cells at 4 h p.i., but this difference was variable by 24h p.i. (Supp. Fig. S4.3C and S4.3D), suggesting that differences in the percentage of infected AEC were not sufficient to explain the high intracellular CFU counts at 24 h p.i observed in Fig. 4.3E. The *exsA* mutant-infected cells also displayed an increased mCherry MFI at 24h p.i. (Supp Fig. S4.3E and S4.3F) as well as a more pronounced high fluorescence second peak compared to wild-type-infected AEC (Supp. Fig S4.3G and S4.3H).

Together, these results suggest that the increased intracellular survival of *exsA* and injectisome mutants is primarily driven by an increased ability to proliferate intracellularly in a sub-population of infected AEC.

Confocal imaging reveals a sub-population of highly infected cells among cells infected with injectisome- or ExsA-deficient strains 24h p.i. We next performed confocal microscopy imaging to directly localize intracellular bacteria at the single AEC level. Samples were stained with both AF647 (red)-conjugated anti-*P.a*. antibody before and AF488 (green)-conjugated anti-*P.a*. antibody after permeabilization of AEC, resulting in double-stained extracellular bacteria, and single-stained (green) intracellular bacteria. As shown in Fig. 4.5, cells infected with both CHA and PAO1 F strain panels at 4h p.i. typically exhibit only 1-3 intracellular bacteria, and few extracellular (yellow) bacteria are visible both adherent to the coverslip as well as eukaryotic cells. This is likely attributable to the fact that the extracellular bacteria were killed with tobramycin just prior to fixation, but not enough time has passed for the dead bacteria to disintegrate. By 24h p.i., cells harboring 1-3 intracellular bacteria were still observed in all conditions. Interestingly, we noted highly infected AEC, as exemplified by the PAO1 F Δ*popB*-infected and CHA Δ*exsA*-infected cells in Fig. 4.5, but not with the wild-type CHA and to a lesser extent for the wild-type PAO1 F infection. This subpopulation of AEC harboring ≥5 bacteria per cell at 24h p.i. likely corresponds to the high fluorescence subpopulations observed by flow cytometry, and may represent a subset of infected AEC in which injectisome- and ExsA-deficient strains successfully proliferate in.

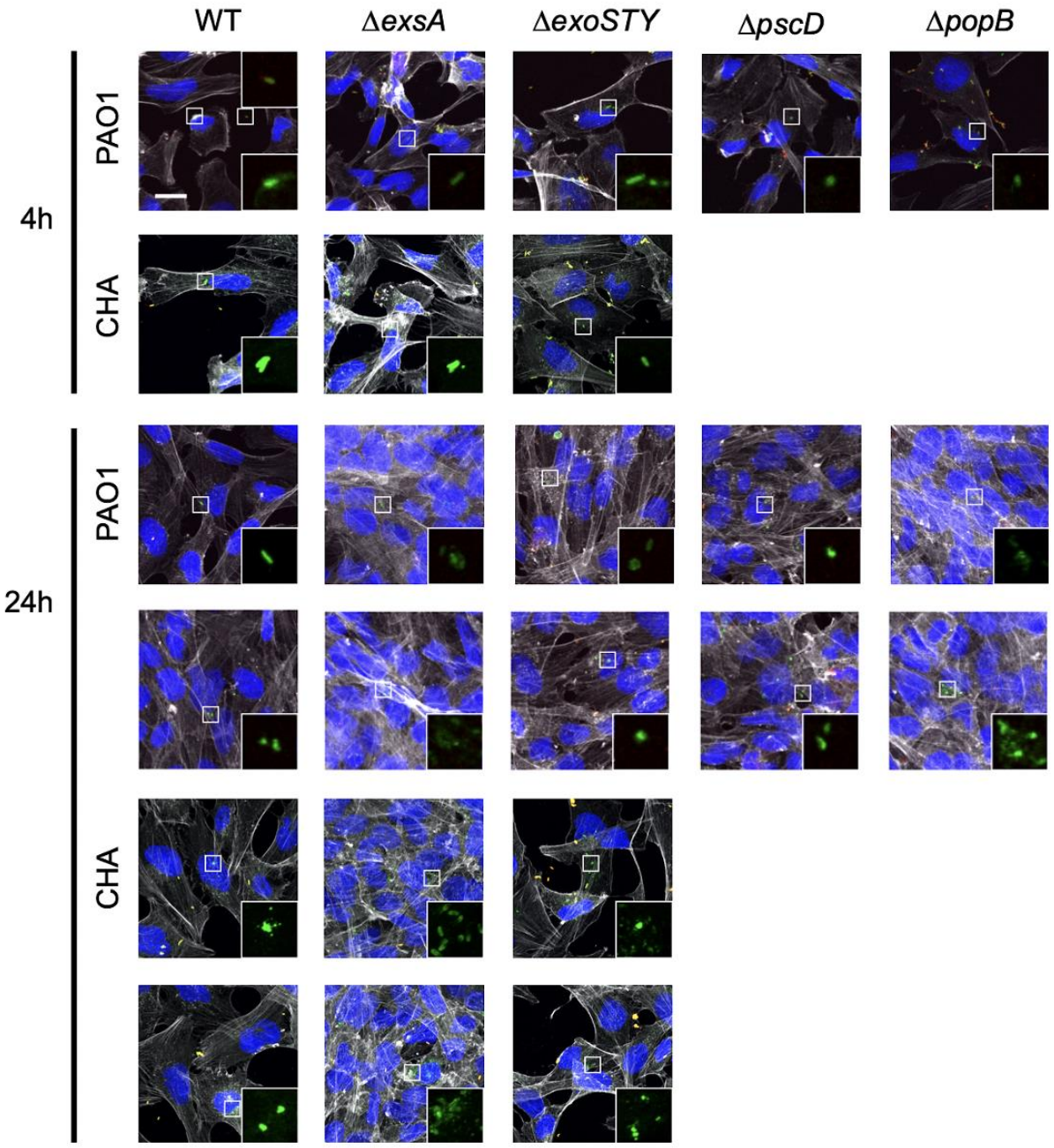

Fig. 4.5: Evidence of intracellular proliferation at 24h p.i. in injectisome- and ExsA-deficient strains as measured by confocal microscopy. BEAS-2B cells were infected with either PAO1 F or CHA and their isogenic *exsA*, *exoSTY*, *pscD* or *popB* mutants for 24h at MOI 1. Time points were taken at 4h and 24h p.i., cells were fixed on coverslips and stained prior to permeabilization (anti-*P.a.* – red) and post permeabilization (anti-*P.a.* – green, DAPI – blue, phalloidin – grey). Double-staining of extracellular (yellow), but not intracellular (green) bacteria allows for the distinguishment of intracellular bacteria. Confocal imaging was conducted using a 40X or 63X objective, the size of the ruler is 10 μm. Images are representative of ≥ 2 independent experiments with ≥ 3 randomly selected areas imaged per

slide. One representative image is shown for all 4h conditions and 2 representative images are shown for the 24h conditions.

4.5 Discussion

In this study, we sought to examine the intracellular survival of a collection of 28 CF clinical isolates and establish the role of the T3SS in determining their long-term intracellular survival within AEC. We demonstrated that a deficiency in T3SS activity, both in naturally occurring clinical isolates as well as in genetically engineered mutants, promotes intracellular survival. Interestingly, complete loss of T3SS effector activity and low cytotoxicity were not sufficient to confer this intracellular survival phenotype.

We have recently validated our intracellular infection model (39), which was developed specifically to study the long-term fate of intracellular *P.a.* in airway epithelial cells and has several characteristics that differentiate our study from previous ones. First, most studies have predominantly focused on initial invasion and early intracellular survival, typically up to 12 h p.i. (6, 9, 25-28, 30, 61), and rarely up to 24h (10, 37), while we focused on the longer-term infection kinetics from 4 h to 24 h and up to 120 h p.i. Second, we used a low infection inoculum (MOI 1) rather than MOI 10 to 50 (9, 10, 61-63), as we have previously established that low MOI infections were compatible with a model of chronic infection, whereas high MOI infection (MOI 10) results in excessive cytotoxicity by 24h p.i. (39). Lastly, our study focused on airway epithelial cells and used the BEAS-2B immortalized cell line as well as primary human bronchial epithelial cells.

Our model does present, however, several limitations. First, aminoglycoside-resistant strains are not compatible with our intracellular infection assay. This has restricted our ability to test chronic infection isolates, many of which are resistant to aminoglycosides, and thus has limited our identification of T3SS-deficient clinical isolates. Second, we recognize that BEAS-2B are an immortalized cell line which does not recapitulate certain physiological features of the airway epithelium. Since the limited availability, complex culture conditions and significant biological variability of primary human cells precluded their use as a primary source of epithelial cells, we only used the latter to validate our study's key findings. While some studies suggest that *P.a.* uptake into or survival within CF AEC may be altered (33, 64), examining the effect of CFTR dysfunction was beyond the scope of our study. Furthermore, CFTR expression is highly reduced in non-polarized, submerged epithelial cells (65) and comparisons

for CF vs non-CF cell lines present many limitations. As such, we chose to focus on AEC expressing wild-type CFTR in our study but recognize that the intracellular survival of *P.a* may be different in CF AEC.

Our results indirectly suggest that T3SS injectisome activity may limit intracellular survival, and possibly intracellular proliferation in an effector-independent manner. While the exact mechanism of these interactions remains unclear, several explanations are possible. The injectisome activity may directly or indirectly cause the death of host cells harboring intracellular *P.a*. It could also induce an antibacterial host response leading to killing of intracellular *P.a*. Epithelial cells could sense both components of the T3SS injectisome as well as non-T3SS components injected into the host cell cytosol via the T3SS, resulting in inflammasome activation (66-68). The pore formation by the injectisome complex across compartment membranes may also be sensed by the host as a danger signal and initiate an anti-bacterial host response (69). Lastly, it has been suggested that T3SS(+) *P.a.* can escape from bacteria-containing vacuoles into the cytosol, while T3SS(-) mutants are trapped inside vacuoles (30). While bacterial replication inside the cytosol might occur, the host cytosol is also a hostile environment for bacteria, where cytosolic bacteria and the process of vacuolar escape are readily sensed and induce antibacterial defense mechanisms (70-72). For example, damaged vacuoles expose glycans which are recognized by galectin-8, and host sensing of bacterial LPS via RNF213 activates guanylate-binding protein signaling platforms, both resulting in antibacterial autophagy (73, 74). Other innate antibacterial defense mechanisms in the cytosol of epithelial cells include the formation of septin cages that limit bacterial proliferation and spread, and the expression of bactericidal compounds like apolipoprotein L (75-78). In fact, septin cages have been detected around T3SS-proficient cytosolic bacteria at 4h p.i. in a HeLa cell infection model (76). While bacterial evasion mechanisms from cytosolic defenses remain incompletely understood even for professional intracellular pathogens, numerous bacterial factors are likely required to combat the multi-layered host defenses (79, 80). It is thus conceivable that a primarily extracellular pathogen such as *P.a.* may not be equipped for long-term survival in the host cytosol and a strictly vacuolar localization may be beneficial for reservoir formation. However, while the literature suggests a strictly vacuolar localization of T3SS-deficient bacteria, the bacterial localization throughout the extended time course in our infection model remains to be established.

Although we did not obtain direct evidence of bacterial intracellular replication, both the flow cytometry and confocal microscopy data were consistent with this notion. The appearance of a high mCherry fluorescence subpopulation by flow cytometry, as well as the evidence of epithelial cells harboring up to 10+ bacteria at 24h p.i. but not 4h p.i., are highly suggestive of intracellular bacterial replication in a small subpopulation of *P.a.*- infected epithelial cells. These highly infected subpopulations were more abundant in the *exsA* or injectisome mutants, particularly the CHA Δ*exsA* strain, compared to wild-type strains or effector mutants. Notably, these hyper-infected cells were morphologically normal without rounding or other cytoskeletal deformation to suggest major cellular stress, suggesting that the absence of injectisome activity may allow intracellular *P.a.* to be tolerated by its host cell. The mechanism(s) underlying the heterogenous fate of *P.a.*-infected AEC remains unknown. We speculate that this may be determined by heterogeneous expression or activity of either host or bacterial responses. For example, T3SS expression is heterogeneous in bacterial populations even under T3SS-inducing conditions (81). As a consequence, a subpopulation of wild-type *P.a.* that encodes for a functional T3SS may be phenotypically T3SS-deficient and survive intracellularly. Future studies of the underlying mechanisms, for instance by analyzing the differential transcriptional host response of cells harboring wild-type and T3SS-deficient bacteria, or by investigating the potential differential intracellular localization of the strains, may be very insightful.

We do note that our results do not align with certain previous observations in the literature. Our findings, which suggest that loss of T3SS injectisome function promotes intracellular bacterial survival through an effector-independent mechanism, stands in contrast to reports indicating that ExoS-dependent T3SS function is necessary for *P.a.* intracellular survival. Previous studies observed that the T3SS effector ExoS inhibits both autophagy and lytic host cell death and promotes bacterial escape into the cytosol, which allows for greater bacterial proliferation compared to a vacuolar localization (9, 30, 82). Penaranda et al, on the other hand, found no differences in bacterial internalization or intracellular survival in wild-type and *exsA* mutant bacteria in an intracellular infection model with bladder epithelial cells (7), while Kroken et al reported that the effect of ExoS on host cell death and intracellular replication differs between corneal epithelial cells and HeLa cells (82). These divergent results could be explained by several factors that influence the fate of intracellular bacteria: cells from distinct epithelial sources differ in their susceptibility to cell death and permissiveness to intracellular bacterial replication (37, 39, 82); *P.a.* strains, even within the same lineage (e.g. PAO1) are phenotypically heterogeneous in their cytotoxicity and intracellular survival phenotype, as our

results demonstrate. Furthermore, even epithelial cells infected with a single wild-type strain may in fact be heterogeneous due to differential gene regulation that is highly dependent on environmental factors. Kumar et al. recently reported that infection with wild-type *P.a*. led to distinct subpopulations with high and low T3SS expression, and vacuolar T3SS(-) subpopulations displayed biofilm-like properties and increased drug tolerance compared to their cytosolic counterparts, and could thus contribute to *P.a.* long-term intracellular survival (10).

Loss of T3SS function is a very common adaptation of *P.a.* during chronic CF infections, as it is observed in 82-96% of chronic infection isolates, but only in 51% acute infections and 10% of environmental isolates, although these percentages may vary in different study populations (83-85). To our knowledge, no studies have examined whether T3SS-deficient variants arise in other chronic *P.a.* infections. In contrast, loss of T3SS function appears uncommon in acute infection settings such as *P.a.* hospital-acquired pneumonia and sepsis (85-87). T3SS-deficiency may be caused by loss of function *exsA* mutations or indirectly via downregulation of T3SS gene expression through the Gac/Rsm pathways or altered c-di-GMP levels (56, 88, 89). While the ability of *P.a.* to persist within the CF airways is clearly multifactorial, the emergence of T3SS-deficient strains with enhanced intracellular survival may facilitate the establishment of an intracellular reservoir which contributes to the persistent and recurrent nature of chronic *P.a*. infections. While most previous studies focused on one or few strains (9, 30, 82), we conducted the most comprehensive study of CF clinical isolates to date, which included both naturally occurring T3SS-deficient isolates as well as genetically engineered T3SS mutants in several clinical strain backgrounds. Our data highlight how the fate of intracellular *P.a.* differs across clinical isolates, and the contribution of the T3SS is influenced by *P.a.* genetic backgrounds. Some T3SS(+) isolates (e.g. PAO1-F and C2) displayed greater intracellular survival than others, and not all naturally occurring T3SS-deficient strains survive intracellularly, likely as the result of other *P.a.* factors involved in bacterial survival or other host-bacterial interactions.

In summary, this study provides novel insights into the heterogeneous intracellular survival of clinically relevant *P.a.* isolates and identifies loss of T3SS function as a driver of intracellular survival within AEC. This suggests that loss of T3SS function may contribute to the formation of an intracellular *P.a.* reservoir, which might have clinical implications in the context of *P.a.* eradication regimens.

4.6 Supplementary materials

Strain	Description	Source
PAO1 F	PAO1 variant, commonly used lab strain isolated from a wound infection	(51)
PAO1 F Δ*exsA*	Markerless in-frame deletion of *exsA* in PAO1 F	This study
PAO1 F Δ*exoSTY*	Markerless in-frame deletion of *exoS*, *exoT* and *exoY* in PAO1 F	(90)
PAO1 F Δ*pscD*	Markerless in-frame deletion of *pscD* in PAO1 F	(91)
PAO1 F Δ*popB*	Markerless in-frame deletion of *popB* in PAO1 F	(90)
CHA	Mucoid chronic infection isolate from CF sputum with hyperactive T3SS expression due to a mutation in *gacS*	(92)
CHA Δ*exoSTY*::Gm^R	Deletion of *exoS*, *exoT* and *exoY* in CHA	(93)
CHA Δ*exsA*::Gm^R	Insertion deletion of *exsA* that confers gentamicin resistance in CHA	(93)
C1	Initial infection clinical isolate from CF sputum with wild-type T3SS secretion of PcrV and ExoS; “SK7”	(94)
C1 Δ*exsA*	Markerless in-frame deletion of *exsA* gene in C1 (“SK7”)	This study
C2	Initial infection clinical isolate from CF sputum with wild-type T3SS secretion of PcrV and ExoS; “SK273”	(94)
C2 Δ*exsA*	Markerless in-frame deletion of *exsA* gene in C2 (“SK273”)	This study
C2 Δ*exoS*	Markerless in-frame deletion of *exoS* gene in C2 (“SK273”)	This study

C3	Initial infection clinical isolate from CF sputum with wild-type T3SS secretion of PcrV and ExoS; "SK455"	(94)
C3 Δ*exsA*	Markerless in-frame deletion of *exsA* gene in C3 ("SK455")	This study
C3 Δ*exoS*	Markerless in-frame deletion of *exoS* gene in C3 ("SK455")	This study
C4	Initial infection clinical isolate from CF sputum lacking T3SS activity; "SK180"	(94)
C5	Initial infection clinical isolate from CF sputum lacking T3SS activity; "SK298"	(94)
***E. coli* SM10 pEX18Gm::*exsA* deletion construct**	*E. coli* SM10 strain containing pEX18Gm plasmid used to generate in-frame markerless deletion of *exsA* in *P.a.*	Matthew Wolfgang (UNC Chapel Hill) (41)
***E. coli* SM10 pEX18Gm::*exoS* deletion construct**	*E. coli* SM10 strain containing pEX18Gm plasmid used to generate in-frame markerless deletion of *exoS* in *P.a.*	Matthew Wolfgang (UNC Chapel Hill) (40)
pMKB1::mCherry	Plasmid encoding a constitutively expressed mCherry, Cb^R.	(95)

Supplementary Table S4.1: Bacterial strains and plasmids used in this study.

Primer	Sequence	Source
***exsA*-forward**	3'-CGCTTCTCGGGAGTACTGCTT-5'	This study
***exsA*-reverse**	3'-TATGCCGTCGTTCAGGGAAGG-5'	This study
***exoS*-forward**	3'-GAGAAAAAGCTGGTGGATGGC-5'	This study
***exoS*-reverse**	3'-TGGTATCCAAGGCGAGCAAC-5'	This study

Supplementary Table S4.2: Sequences of primers used to validate successful deletion mutants.

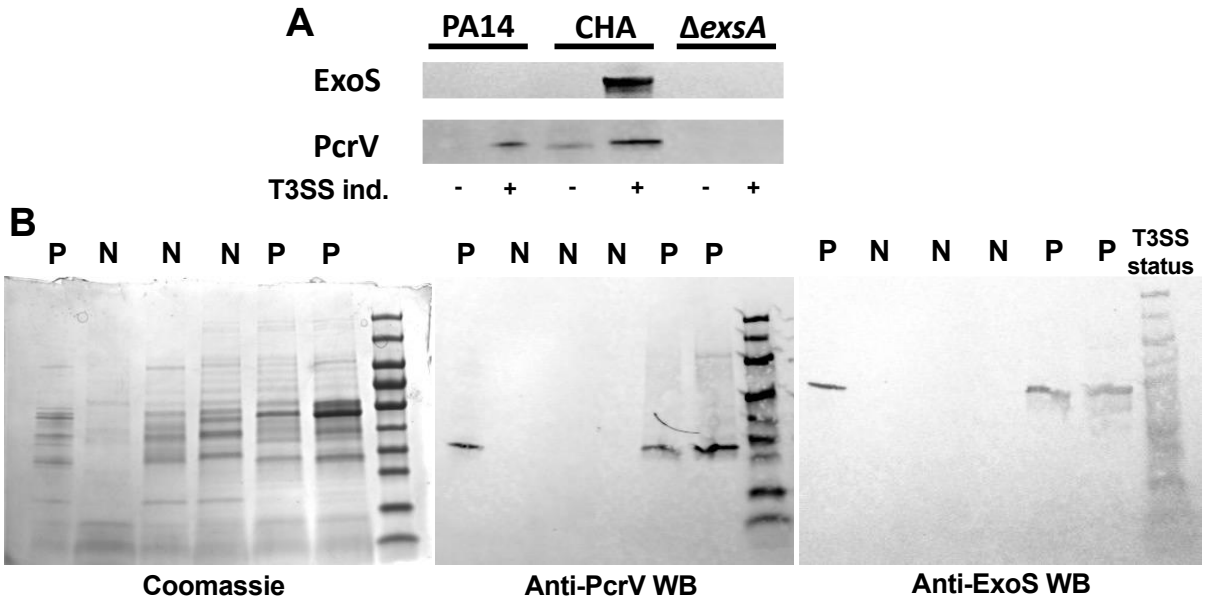

Supp. Fig. S4.1: Western Blot controls. Strains were grown under T3SS-inducing (A+B) or non-inducing (A) conditions. For (A), 1 μg precipitated supernatant protein was loaded for each sample and T3SS secretion was assessed by probing a Western Blot using anti-ExoS and anti-PcrV antibodies. Western blots for (B) were conducted in the same manner as described above, but a second SDS-PAGE using the same volumes of each sample was loaded and run at the same time as the SDS-PAGE meant for Western Blotting. This SDS-PAGE was then stained with Coomassie to assess total protein in the samples.

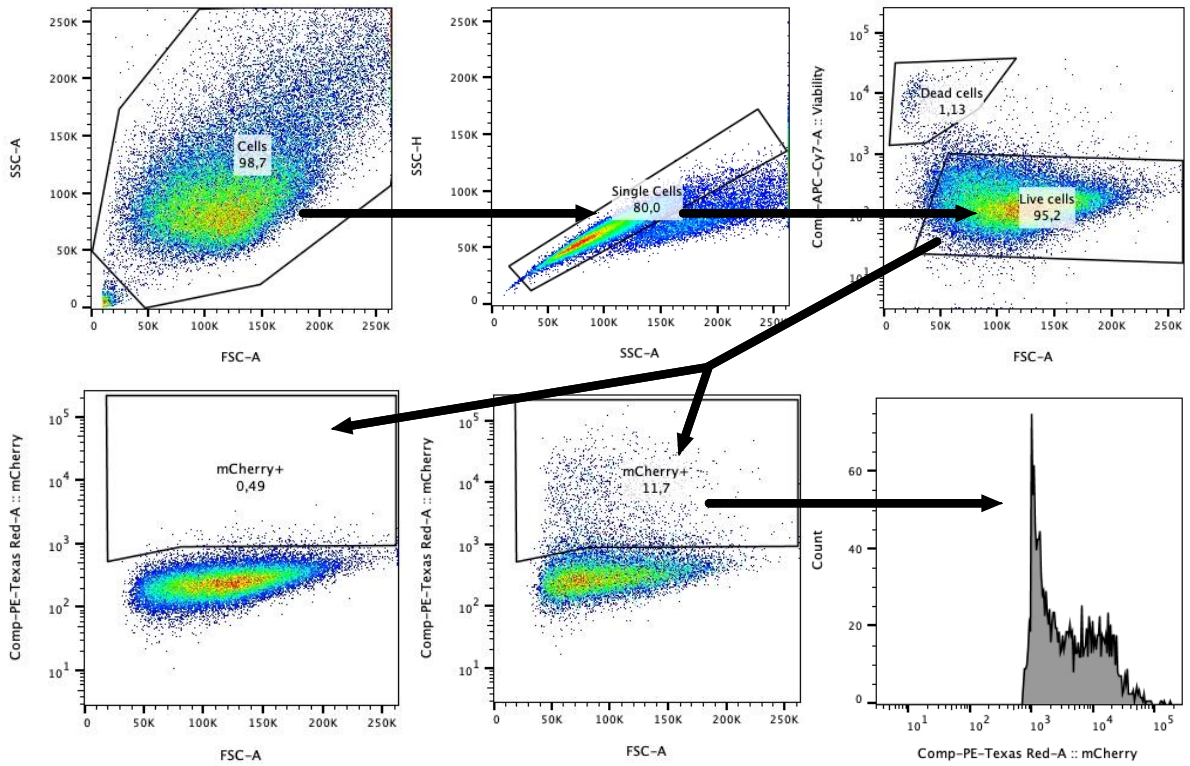

Supp. Fig. S4.2: Flow cytometry gating strategy. Debris (low FSC-A, low SSC-A) was gated out, after which single cells (proportional SSC-A to SSC-H) were gated on. Live cells (low fixable viability dye eFluor 780 staining) were gated on for further analysis, while dead cells (high fixable viability dye eFluor 780 staining) were gated on to quantify strain cytotoxicity. Within the live cell population, uninfected (non-fluorescent) cells were used as a negative control to set the mCherry-positive gate. Within samples infected with mCherry-expressing *P.a.* strains, mCherry frequency histograms of the cells within the mCherry-positive gate were used as a proxy for the bacterial burden per infected cell.

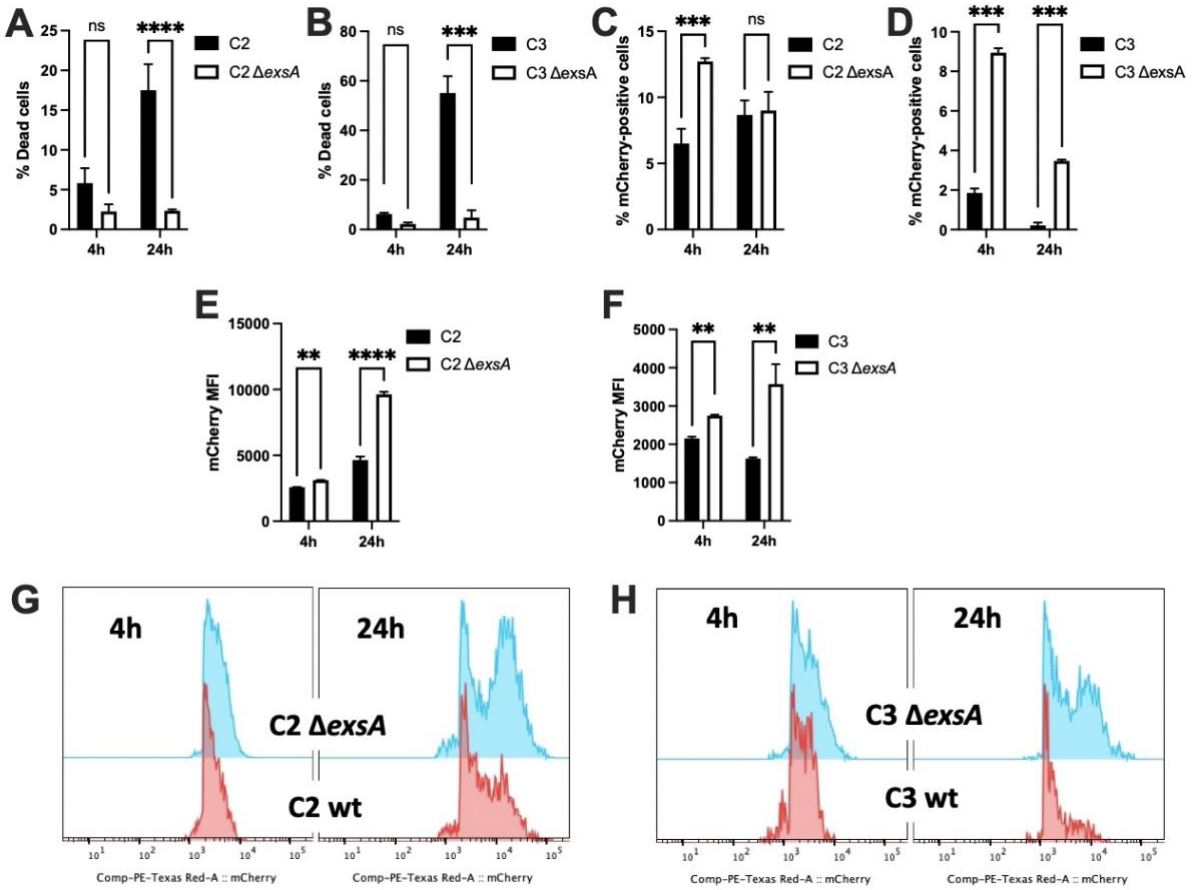

Supp. Fig. S4.3: Increased intracellular bacterial proliferation of *exsA* mutants vs wild-type strains. BEAS-2B cells were infected with mCherry-expressing clinical isolates C2 and C3 or their isogenic *exsA* mutants at MOI 1 for up to 24h. Extracellular bacteria were killed through the addition of tobramycin at 4h p.i. and cells were maintained in the presence of extracellular tobramycin for the entire duration of the experiment. **(A+B)** Dead cells were defined as fixable viability dye eFluor 780-positive cells and are displayed as a percentage. The percentage of infected cells **(C+D)** and mCherry median fluorescence intensity within the mCherry-positive gate **(E+F)** are shown. **(G+H)** display representative mCherry fluorescence spectra for each strain for both time points. All results are from 1 representative of 2 independent experiments conducted in biological triplicates. The data is displayed as mean ± SD.

4.7 Acknowledgements

We would like to acknowledge Drs. Jane Burns (Seattle Childrens'), David Speert and James Zlosnik (University of British Columbia) for providing the clinical isolates for this study. We would like to thank Dr. Arne Rietsch (Case Western Reserve University) for generously providing the PAO1 F wild-type, Δ*exoSTY*, Δ*popB* and Δ*pscD* strains as well as the ExoS

antibody, Drs. Bertrand Toussaint (CHU-Grenoble) and Emmanuel Faure (CHU-Lille) for the CHA wild-type and T3SS mutants, Dr. Antonio DiGiandomenico (AstraZeneca) for the PcrV antibody, Dr. Sam Moskowitz for the mCherry (pMKB1) plasmid and Dr. Matthew Wolfgang (University North Carolina) for the T3SS deletion plasmids that allowed us to engineer mutants in the clinical strains. The primary human AEC were available through the CRCHUM's Respiratory Cell and Tissue Biobank of the Respiratory Health Research Network of Québec.

4.8 References

1. Bhagirath AY, Li Y, Somayajula D, Dadashi M, Badr S, Duan K. Cystic fibrosis lung environment and Pseudomonas aeruginosa infection. BMC Pulm Med. 2016;16(1):174.

2. Kosorok MR, Zeng L, West SE, Rock MJ, Splaingard ML, Laxova A, et al. Acceleration of lung disease in children with cystic fibrosis after Pseudomonas aeruginosa acquisition. Pediatr Pulmonol. 2001;32(4):277-87.

3. Winstanley C, O'Brien S, Brockhurst MA. Pseudomonas aeruginosa Evolutionary Adaptation and Diversification in Cystic Fibrosis Chronic Lung Infections. Trends Microbiol. 2016;24(5):327-37.

4. Faure E, Kwong K, Nguyen D. Pseudomonas aeruginosa in Chronic Lung Infections: How to Adapt Within the Host? Frontiers in Immunology. 2018;9.

5. Ciofu O, Tolker-Nielsen T. Tolerance and Resistance of Pseudomonas aeruginosa Biofilms to Antimicrobial Agents—How P. aeruginosa Can Escape Antibiotics. Frontiers in Microbiology. 2019;10.

6. Fleiszig SM, Arora SK, Van R, Ramphal R. FlhA, a component of the flagellum assembly apparatus of Pseudomonas aeruginosa, plays a role in internalization by corneal epithelial cells. Infect Immun. 2001;69(8):4931-7.

7. Penaranda C, Chumbler NM, Hung DT. Dual transcriptional analysis reveals adaptation of host and pathogen to intracellular survival of Pseudomonas aeruginosa associated with urinary tract infection. PLoS Pathog. 2021;17(4):e1009534.

8. Ha U, Jin S. Growth phase-dependent invasion of Pseudomonas aeruginosa and its survival within HeLa cells. Infect Immun. 2001;69(7):4398-406.

9. Rao L, De La Rosa I, Xu Y, Sha Y, Bhattacharya A, Holtzman MJ, et al. Pseudomonas aeruginosa survives in epithelia by ExoS-mediated inhibition of autophagy and mTOR. EMBO Rep. 2021;22(2):e50613.

10. Kumar NG, Nieto V, Kroken AR, Jedel E, Grosser MR, Hallsten ME, et al. Pseudomonas aeruginosa can diversify after host cell invasion to establish multiple intracellular niches. bioRxiv. 2022:2022.10.07.511388.

11. Garcia-Medina R, Dunne WM, Singh PK, Brody SL. Pseudomonas aeruginosa Acquires Biofilm-Like Properties within Airway Epithelial Cells. Infection and Immunity. 2005;73(12):8298-305.

12. Esen M, Grassmé H, Riethmüller J, Riehle A, Fassbender K, Gulbins E. Invasion of human epithelial cells by Pseudomonas aeruginosa involves src-like tyrosine kinases p60Src and p59Fyn. Infect Immun. 2001;69(1):281-7.

13. Mittal R, Grati M, Gerring R, Blackwelder P, Yan D, Li JD, et al. In vitro interaction of Pseudomonas aeruginosa with human middle ear epithelial cells. PLoS One. 2014;9(3):e91885.

14. Bonventre PF, Hayes R, Imhoff J. Autoradiographic evidence for the impermeability of mouse peritoneal macrophages to tritiated streptomycin. J Bacteriol. 1967;93(1):445-50.

15. Peyrusson F, Varet H, Nguyen TK, Legendre R, Sismeiro O, Coppée J-Y, et al. Intracellular Staphylococcus aureus persisters upon antibiotic exposure. Nature Communications. 2020;11(1):2200.

16. Rosen DA, Hooton TM, Stamm WE, Humphrey PA, Hultgren SJ. Detection of intracellular bacterial communities in human urinary tract infection. PLoS Med. 2007;4(12):e329.

17. Mysorekar IU, Hultgren SJ. Mechanisms of uropathogenic Escherichia coli persistence and eradication from the urinary tract. Proceedings of the National Academy of Sciences. 2006;103(38):14170-5.

18. Martínez-Figueroa C, Cortés-Sarabia K, del Carmen Alarcón-Romero L, Catalán-Nájera HG, Martínez-Alarcón M, Vences-Velázquez A. Observation of intracellular bacterial communities in urinary sediment using brightfield microscopy; a case report. BMC Urology. 2020;20(1):89.

19. Scott VC, Haake DA, Churchill BM, Justice SS, Kim JH. Intracellular Bacterial Communities: A Potential Etiology for Chronic Lower Urinary Tract Symptoms. Urology. 2015;86(3):425-31.

20. Anderson GG, Dodson KW, Hooton TM, Hultgren SJ. Intracellular bacterial communities of uropathogenic Escherichia coli in urinary tract pathogenesis. Trends Microbiol. 2004;12(9):424-30.

21. Rollin G, Tan X, Tros F, Dupuis M, Nassif X, Charbit A, et al. Intracellular Survival of Staphylococcus aureus in Endothelial Cells: A Matter of Growth or Persistence. Front Microbiol. 2017;8:1354.

22. Strobel M, Pförtner H, Tuchscherr L, Völker U, Schmidt F, Kramko N, et al. Post-invasion events after infection with Staphylococcus aureus are strongly dependent on both the host cell type and the infecting S. aureus strain. Clinical Microbiology and Infection. 2016;22(9):799-809.

23. Vozza EG, Mulcahy ME, McLoughlin RM. Making the Most of the Host; Targeting the Autophagy Pathway Facilitates Staphylococcus aureus Intracellular Survival in Neutrophils. Frontiers in Immunology. 2021;12.

24. Clement S, Vaudaux P, Francois P, Schrenzel J, Huggler E, Kampf S, et al. Evidence of an intracellular reservoir in the nasal mucosa of patients with recurrent Staphylococcus aureus rhinosinusitis. J Infect Dis. 2005;192(6):1023-8.

25. Zaidi TS, Fleiszig SM, Preston MJ, Goldberg JB, Pier GB. Lipopolysaccharide outer core is a ligand for corneal cell binding and ingestion of Pseudomonas aeruginosa. Invest Ophthalmol Vis Sci. 1996;37(6):976-86.

26. Eierhoff T, Bastian B, Thuenauer R, Madl J, Audfray A, Aigal S, et al. A lipid zipper triggers bacterial invasion. Proceedings of the National Academy of Sciences. 2014;111(35):12895-900.

27. Evans D, Kuo T, Kwong M, Van R, Fleiszig S. Pseudomonas aeruginosa strains with lipopolysaccharide defects exhibit reduced intracellular viability after invasion of corneal epithelial cells. Exp Eye Res. 2002;75(6):635-43.

28. Hritonenko V, Evans DJ, Fleiszig SM. Translocon-independent intracellular replication by Pseudomonas aeruginosa requires the ADP-ribosylation domain of ExoS. Microbes Infect. 2012;14(15):1366-73.

29. Li X, He S, Zhou X, Ye Y, Tan S, Zhang S, et al. Lyn Delivers Bacteria to Lysosomes for Eradication through TLR2-Initiated Autophagy Related Phagocytosis. PLOS Pathogens. 2016;12(1):e1005363.

30. Heimer SR, Evans DJ, Stern ME, Barbieri JT, Yahr T, Fleiszig SM. Pseudomonas aeruginosa utilizes the type III secreted toxin ExoS to avoid acidified compartments within epithelial cells. PLoS One. 2013;8(9):e73111.

31. Comolli JC, Waite LL, Mostov KE, Engel JN. Pili binding to asialo-GM1 on epithelial cells can mediate cytotoxicity or bacterial internalization by Pseudomonas aeruginosa. Infect Immun. 1999;67(7):3207-14.

32. Fleiszig SM, Zaidi TS, Pier GB. Pseudomonas aeruginosa invasion of and multiplication within corneal epithelial cells in vitro. Infect Immun. 1995;63(10):4072-7.
33. Darling KE, Dewar A, Evans TJ. Role of the cystic fibrosis transmembrane conductance regulator in internalization of Pseudomonas aeruginosa by polarized respiratory epithelial cells. Cell Microbiol. 2004;6(6):521-33.
34. Zaas DW, Duncan MJ, Li G, Wright JR, Abraham SN. Pseudomonas invasion of type I pneumocytes is dependent on the expression and phosphorylation of caveolin-2. J Biol Chem. 2005;280(6):4864-72.
35. Lepanto P, Bryant DM, Rossello J, Datta A, Mostov KE, Kierbel A. Pseudomonas aeruginosa interacts with epithelial cells rapidly forming aggregates that are internalized by a Lyn-dependent mechanism. Cell Microbiol. 2011;13(8):1212-22.
36. Pielage JF, Powell KR, Kalman D, Engel JN. RNAi screen reveals an Abl kinase-dependent host cell pathway involved in Pseudomonas aeruginosa internalization. PLoS Pathog. 2008;4(3):e1000031.
37. Del Mar Cendra M, Torrents E. Differential adaptability between reference strains and clinical isolates of Pseudomonas aeruginosa into the lung epithelium intracellular lifestyle. Virulence. 2020;11(1):862-76.
38. Fleiszig SM, Zaidi TS, Preston MJ, Grout M, Evans DJ, Pier GB. Relationship between cytotoxicity and corneal epithelial cell invasion by clinical isolates of Pseudomonas aeruginosa. Infect Immun. 1996;64(6):2288-94.
39. Malet JK, Hennemann LC, Hua EML, Faure E, Waters V, Rousseau S, et al. A Model of Intracellular Persistence of Pseudomonas aeruginosa in Airway Epithelial Cells. Cellular Microbiology. 2022;2022:5431666.
40. Vance RE, Rietsch A, Mekalanos JJ. Role of the type III secreted exoenzymes S, T, and Y in systemic spread of Pseudomonas aeruginosa PAO1 in vivo. Infect Immun. 2005;73(3):1706-13.
41. Intile PJ, Balzer GJ, Wolfgang MC, Yahr TL. The RNA Helicase DeaD Stimulates ExsA Translation To Promote Expression of the Pseudomonas aeruginosa Type III Secretion System. Journal of Bacteriology. 2015;197(16):2664-74.
42. Hmelo LR, Borlee BR, Almblad H, Love ME, Randall TE, Tseng BS, et al. Precision-engineering the Pseudomonas aeruginosa genome with two-step allelic exchange. Nature Protocols. 2015;10(11):1820-41.

43. Warrener P, Varkey R, Bonnell JC, DiGiandomenico A, Camara M, Cook K, et al. A novel anti-PcrV antibody providing enhanced protection against Pseudomonas aeruginosa in multiple animal infection models. Antimicrob Agents Chemother. 2014;58(8):4384-91.
44. Lagache T, Sauvonnet N, Danglot L, Olivo-Marin JC. Statistical analysis of molecule colocalization in bioimaging. Cytometry A. 2015;87(6):568-79.
45. Evans DJ, Maltseva IA, Wu J, Fleiszig SM. Pseudomonas aeruginosa internalization by corneal epithelial cells involves MEK and ERK signal transduction proteins. FEMS Microbiol Lett. 2002;213(1):73-9.
46. Fleiszig SM, Wiener-Kronish JP, Miyazaki H, Vallas V, Mostov KE, Kanada D, et al. Pseudomonas aeruginosa-mediated cytotoxicity and invasion correlate with distinct genotypes at the loci encoding exoenzyme S. Infect Immun. 1997;65(2):579-86.
47. Lee VT, Smith RS, Tümmler B, Lory S. Activities of Pseudomonas aeruginosa effectors secreted by the Type III secretion system in vitro and during infection. Infect Immun. 2005;73(3):1695-705.
48. Vallis AJ, Yahr TL, Barbieri JT, Frank DW. Regulation of ExoS production and secretion by Pseudomonas aeruginosa in response to tissue culture conditions. Infect Immun. 1999;67(2):914-20.
49. Barbieri JT, Sun J. Pseudomonas aeruginosa ExoS and ExoT. Rev Physiol Biochem Pharmacol. 2004;152:79-92.
50. Sall KM, Casabona MG, Bordi C, Huber P, de Bentzmann S, Attrée I, et al. A gacS deletion in Pseudomonas aeruginosa cystic fibrosis isolate CHA shapes its virulence. PLoS One. 2014;9(4):e95936.
51. Bleves S, Soscia C, Nogueira-Orlandi P, Lazdunski A, Filloux A. Quorum sensing negatively controls type III secretion regulon expression in Pseudomonas aeruginosa PAO1. J Bacteriol. 2005;187(11):3898-902.
52. Hauser AR. The type III secretion system of Pseudomonas aeruginosa: infection by injection. Nat Rev Microbiol. 2009;7(9):654-65.
53. Dasgupta N, Ashare A, Hunninghake GW, Yahr TL. Transcriptional induction of the Pseudomonas aeruginosa type III secretion system by low Ca2+ and host cell contact proceeds through two distinct signaling pathways. Infect Immun. 2006;74(6):3334-41.
54. Anantharajah A, Buyck JM, Faure E, Glupczynski Y, Rodriguez-Villalobos H, De Vos D, et al. Correlation between cytotoxicity induced by Pseudomonas aeruginosa clinical isolates from acute infections and IL-1β secretion in a model of human THP-1 monocytes. Pathog Dis. 2015;73(7).

55. van Mansfeld R, de Been M, Paganelli F, Yang L, Bonten M, Willems R. Within-Host Evolution of the Dutch High-Prevalent Pseudomonas aeruginosa Clone ST406 during Chronic Colonization of a Patient with Cystic Fibrosis. PLoS One. 2016;11(6):e0158106.
56. Smith EE, Buckley DG, Wu Z, Saenphimmachak C, Hoffman LR, D'Argenio DA, et al. Genetic adaptation by Pseudomonas aeruginosa to the airways of cystic fibrosis patients. Proc Natl Acad Sci U S A. 2006;103(22):8487-92.
57. Camus L, Vandenesch F, Moreau K. From genotype to phenotype: adaptations of Pseudomonas aeruginosa to the cystic fibrosis environment. Microb Genom. 2021;7(3).
58. Han X, Na T, Wu T, Yuan BZ. Human lung epithelial BEAS-2B cells exhibit characteristics of mesenchymal stem cells. PLoS One. 2020;15(1):e0227174.
59. Reddel RR, Ke Y, Gerwin BI, McMenamin MG, Lechner JF, Su RT, et al. Transformation of human bronchial epithelial cells by infection with SV40 or adenovirus-12 SV40 hybrid virus, or transfection via strontium phosphate coprecipitation with a plasmid containing SV40 early region genes. Cancer Res. 1988;48(7):1904-9.
60. Goure J, Pastor A, Faudry E, Chabert J, Dessen A, Attree I. The V antigen of Pseudomonas aeruginosa is required for assembly of the functional PopB/PopD translocation pore in host cell membranes. Infect Immun. 2004;72(8):4741-50.
61. Sana TG, Baumann C, Merdes A, Soscia C, Rattei T, Hachani A, et al. Internalization of Pseudomonas aeruginosa Strain PAO1 into Epithelial Cells Is Promoted by Interaction of a T6SS Effector with the Microtubule Network. mBio. 2015;6(3):e00712-15.
62. Kierbel A, Gassama-Diagne A, Mostov K, Engel JN. The phosphoinositol-3-kinase-protein kinase B/Akt pathway is critical for Pseudomonas aeruginosa strain PAK internalization. Mol Biol Cell. 2005;16(5):2577-85.
63. Schaible B, McClean S, Selfridge A, Broquet A, Asehnoune K, Taylor CT, et al. Hypoxia Modulates Infection of Epithelial Cells by Pseudomonas aeruginosa. PLOS ONE. 2013;8(2):e56491.
64. Jolly AL, Takawira D, Oke OO, Whiteside SA, Chang SW, Wen ER, et al. Pseudomonas aeruginosa-induced bleb-niche formation in epithelial cells is independent of actinomyosin contraction and enhanced by loss of cystic fibrosis transmembrane-conductance regulator osmoregulatory function. mBio. 2015;6(2):e02533.
65. Bebök Z, Tousson A, Schwiebert LM, Venglarik CJ. Improved oxygenation promotes CFTR maturation and trafficking in MDCK monolayers. American Journal of Physiology-Cell Physiology. 2001;280(1):C135-C45.

66. Grandjean T, Boucher A, Thepaut M, Monlezun L, Guery B, Faudry E, et al. The human NAIP-NLRC4-inflammasome senses the Pseudomonas aeruginosa T3SS inner-rod protein. International Immunology. 2017;29(8):377-84.
67. Ince D, Sutterwala FS, Yahr TL. Secretion of Flagellar Proteins by the Pseudomonas aeruginosa Type III Secretion-Injectisome System. J Bacteriol. 2015;197(12):2003-11.
68. Zhao Y, Shao F. The NAIP-NLRC4 inflammasome in innate immune detection of bacterial flagellin and type III secretion apparatus. Immunol Rev. 2015;265(1):85-102.
69. Ellison CJ, Kukulski W, Boyle KB, Munro S, Randow F. Transbilayer Movement of Sphingomyelin Precedes Catastrophic Breakage of Enterobacteria-Containing Vacuoles. Curr Biol. 2020;30(15):2974-83.e6.
70. Randow F. How cells deploy ubiquitin and autophagy to defend their cytosol from bacterial invasion. Autophagy. 2011;7(3):304-9.
71. Randow F, MacMicking JD, James LC. Cellular self-defense: how cell-autonomous immunity protects against pathogens. Science. 2013;340(6133):701-6.
72. Radoshevich L, Dussurget O. Cytosolic Innate Immune Sensing and Signaling upon Infection. Front Microbiol. 2016;7:313.
73. Otten EG, Werner E, Crespillo-Casado A, Boyle KB, Dharamdasani V, Pathe C, et al. Ubiquitylation of lipopolysaccharide by RNF213 during bacterial infection. Nature. 2021;594(7861):111-6.
74. Thurston TL, Wandel MP, von Muhlinen N, Foeglein A, Randow F. Galectin 8 targets damaged vesicles for autophagy to defend cells against bacterial invasion. Nature. 2012;482(7385):414-8.
75. Mostowy S, Bonazzi M, Hamon MA, Tham TN, Mallet A, Lelek M, et al. Entrapment of intracytosolic bacteria by septin cage-like structures. Cell Host Microbe. 2010;8(5):433-44.
76. Krokowski S, Lobato-Márquez D, Chastanet A, Pereira PM, Angelis D, Galea D, et al. Septins Recognize and Entrap Dividing Bacterial Cells for Delivery to Lysosomes. Cell Host Microbe. 2018;24(6):866-74.e4.
77. Tretina K, Park ES, Maminska A, MacMicking JD. Interferon-induced guanylate-binding proteins: Guardians of host defense in health and disease. J Exp Med. 2019;216(3):482-500.
78. Gaudet RG, Zhu S, Halder A, Kim BH, Bradfield CJ, Huang S, et al. A human apolipoprotein L with detergent-like activity kills intracellular pathogens. Science. 2021;373(6552).

79. Wandel MP, Pathe C, Werner EI, Ellison CJ, Boyle KB, von der Malsburg A, et al. GBPs Inhibit Motility of Shigella flexneri but Are Targeted for Degradation by the Bacterial Ubiquitin Ligase IpaH9.8. Cell Host Microbe. 2017;22(4):507-18.e5.

80. Ogawa M, Yoshimori T, Suzuki T, Sagara H, Mizushima N, Sasakawa C. Escape of intracellular Shigella from autophagy. Science. 2005;307(5710):727-31.

81. Rietsch A, Mekalanos JJ. Metabolic regulation of type III secretion gene expression in Pseudomonas aeruginosa. Mol Microbiol. 2006;59(3):807-20.

82. Kroken AR, Gajenthra Kumar N, Yahr TL, Smith BE, Nieto V, Horneman H, et al. Exotoxin S secreted by internalized Pseudomonas aeruginosa delays lytic host cell death. PLoS Pathog. 2022;18(2):e1010306.

83. Jain M, Ramirez D, Seshadri R, Cullina JF, Powers CA, Schulert GS, et al. Type III secretion phenotypes of Pseudomonas aeruginosa strains change during infection of individuals with cystic fibrosis. J Clin Microbiol. 2004;42(11):5229-37.

84. Dacheux D, Toussaint B, Richard M, Brochier G, Croize J, Attree I. Pseudomonas aeruginosa cystic fibrosis isolates induce rapid, type III secretion-dependent, but ExoU-independent, oncosis of macrophages and polymorphonuclear neutrophils. Infect Immun. 2000;68(5):2916-24.

85. Roy-Burman A, Savel RH, Racine S, Swanson BL, Revadigar NS, Fujimoto J, et al. Type III Protein Secretion Is Associated with Death in Lower Respiratory and Systemic Pseudomonas aeruginosa Infections. The Journal of Infectious Diseases. 2001;183(12):1767-74.

86. Berthelot P, Attree I, Plésiat P, Chabert J, de Bentzmann S, Pozzetto B, et al. Genotypic and phenotypic analysis of type III secretion system in a cohort of Pseudomonas aeruginosa bacteremia isolates: evidence for a possible association between O serotypes and exo genes. J Infect Dis. 2003;188(4):512-8.

87. Wareham DW, Curtis MA. A genotypic and phenotypic comparison of type III secretion profiles of Pseudomonas aeruginosa cystic fibrosis and bacteremia isolates. International Journal of Medical Microbiology. 2007;297(4):227-34.

88. Wu W, Badrane H, Arora S, Baker HV, Jin S. MucA-mediated coordination of type III secretion and alginate synthesis in Pseudomonas aeruginosa. J Bacteriol. 2004;186(22):7575-85.

89. Williams McMackin EA, Djapgne L, Corley JM, Yahr TL. Fitting Pieces into the Puzzle of Pseudomonas aeruginosa Type III Secretion System Gene Expression. J Bacteriol. 2019;201(13).

90. Cisz M, Lee PC, Rietsch A. ExoS controls the cell contact-mediated switch to effector secretion in Pseudomonas aeruginosa. J Bacteriol. 2008;190(8):2726-38.

91. Sun Y, Karmakar M, Taylor PR, Rietsch A, Pearlman E. ExoS and ExoT ADP ribosyltransferase activities mediate Pseudomonas aeruginosa keratitis by promoting neutrophil apoptosis and bacterial survival. J Immunol. 2012;188(4):1884-95.

92. Toussaint B, Delicattree I, Vignais PM. Pseudomonas aeruginosa Contains an IHF-like Protein That Binds to the algD Promoter. Biochemical and Biophysical Research Communications. 1993;196(1):416-21.

93. Faure E, Mear J-B, Faure K, Normand S, Couturier-Maillard A, Grandjean T, et al. Pseudomonas aeruginosa Type-3 Secretion System Dampens Host Defense by Exploiting the NLRC4-coupled Inflammasome. American Journal of Respiratory and Critical Care Medicine. 2014;189(7):799-811.

94. Vidya P, Smith L, Beaudoin T, Yau YC, Clark S, Coburn B, et al. Chronic infection phenotypes of Pseudomonas aeruginosa are associated with failure of eradication in children with cystic fibrosis. Eur J Clin Microbiol Infect Dis. 2016;35(1):67-74.

95. Brannon MK, Davis JM, Mathias JR, Hall CJ, Emerson JC, Crosier PS, et al. Pseudomonas aeruginosa Type III secretion system interacts with phagocytes to modulate systemic infection of zebrafish embryos. Cell Microbiol. 2009;11(5):755-68.

Chapter 5: Discussion

5.1 Major findings

While *P.a.* adaptations to the CF airways over time are well documented, the implications of specific adaptations to lung disease pathology remain incompletely understood. Here, we sought to elucidate how two common *P.a.* adaptations, loss of LasR and T3SS function, affect *P.a.*-AEC interactions in terms of inflammation and intracellular bacterial survival. In chapter 2, we observed that loss of function of the quorum sensing transcriptional activator LasR was associated with increased mICAM-1 expression on AEC *in vitro* and *in vivo*. We further found that the observed increase in mICAM-1 expression was associated with increased neutrophil adhesion *in vitro* and with increased neutrophilic pulmonary inflammation *in vivo*. These observations were attributed to a lack of mICAM-1 degradation by LasR-regulated proteases upon stimulation with *lasR* mutant filtrates, resulting in overall higher mICAM-1 levels on AEC. Together, these results complement a growing body of literature showing that LasR-regulated proteases may facilitate immune evasion in early infection stages, but enhance deleterious inflammation during chronic infection stages (1-4).

In chapter 3, we sought to establish tools allowing us to explore the long-term survival of intracellular *P.a.* in AEC as most studies have primarily focused on bacterial internalization and early intracellular survival. Given the chronic nature of *P.a.* infections in the context of CF, we sought to establish an *in vitro* model that could model long-term intracellular bacterial survival within AEC, as would be expected to occur during periods of antibiotic treatment in the CF lung. Thus, we established a robust model of intracellular *P.a.* infection, which allows for the analysis of intracellular *P.a.*-host interactions both at the population and single cell level for up to 120h post-infection. Using this model, we observed heterogeneous intracellular survival phenotypes among a small set of clinical *P.a.* isolates.

Using the model established in chapter 3, we then screened a collection of 28 CF clinical isolates for their ability to survive intracellularly and observed that loss of T3SS function is a major driver of intracellular survival among clinical *P.a.* isolates. By testing genetically engineered T3SS mutants, we demonstrated that intracellular bacterial survival is likely limited by T3SS injectisome function, even in the absence of T3SS effector-mediated cytotoxicity. We further uncovered a "hyper-proliferator" phenotype in a subset of cells harboring T3SS-deficient bacteria, while this phenotype was not observed (or observed to a lesser extent) among cells infected with T3SS-positive strains. Our work represents the most extensive analysis of

clinical *P.a.* isolate intracellular survival within AEC to date and offers novel insights into how *P.a.* might adapt towards increased intracellular survival within the airway epithelium. This increased intracellular survival may thus be a bacterial evasion mechanism that contributes to *P.a.*'s ability to persist during antibiotic treatment.

5.2 LasR-regulated proteases: a double-edged sword

The quorum sensing transcriptional activator LasR is widely recognized for its role in regulating the expression of acute virulence factors, notably several secreted proteases which cause direct host damage and subvert host immunity in acute infections (1, 4-9). While the loss of LasR function often (although not always) results in impaired production of LasR-controlled acute virulence factors, the implication of this pathoadaptation on host-pathogen interactions and chronic disease pathology is less well recognized. Here, we discuss how (loss of) LasR function and LasR-regulated proteases affect host immunity, inflammation and tissue pathology in acute vs. chronic *P.a.* lung infection.

LasR-regulated proteases are among the key virulence factors employed by *P.a.* during acute infection stages and appear to have low substrate specificity, as demonstrated by the vast range of substrates degraded by LasR-regulated proteases (1, 4-9). LasB and AprA in particular have been demonstrated to cleave a variety of host proteins ranging from cytokines and chemokines to adhesion molecules, structural proteins and surfactants (1-3, 5, 10). Since LasR-regulated proteases can be deleterious to the host in a multitude of ways, one would expect that loss-of-function *lasR* variants lacking LasR-regulated proteases, which are highly prevalent among clinical isolates from chronic CF infections, would cause less severe lung disease. Surprisingly, CF patients infected with *lasR* variants show accelerated decline in lung function and increased IL-8 levels, a marker of neutrophilic inflammation, compared to patients infected with wild-type *lasR* strains (1, 11). Past and present studies in our lab have aimed at understanding the mechanisms that contribute to this apparent paradoxical outcome.

We propose that the interactions between LasR-regulated exoproducts and the host vary and have different implications to disease pathology and severity in acute vs. chronic infection settings (Fig. 5.1). In acute infections, *P.a.* is likely motile, expresses functional LasR and a large array of acute virulence factors, with LasR-regulated proteases causing direct tissue damage by degrading extracellular matrix proteins and cell junctions (5, 12). While host epithelial cells express pro-inflammatory surface receptors and produce high levels of pro-

inflammatory cytokines (e.g. IL-8, ENA78) upon stimulation by *P.a.*, LasR-regulated proteases can counteract these responses by directly degrading inflammatory and immune mediators (1, 4). LasR-mediated interactions thus dampen immune responses, allowing for immune evasion, bacterial proliferation and direct tissue damage. These deleterious interactions likely dominate during acute infection settings and explain the attenuated virulence of the *lasR* mutant observed in various acute infection models (13-15).

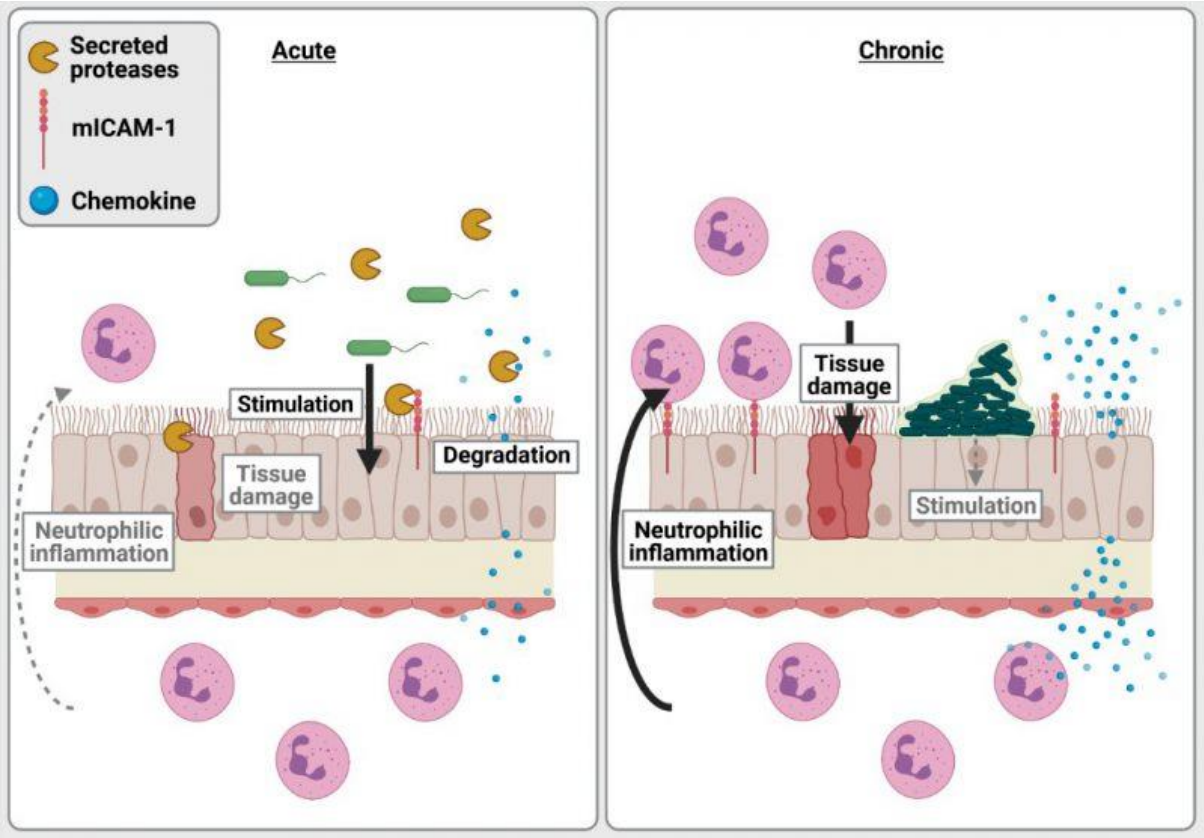

Figure 5.1: LasR-regulated proteases and neutrophilic inflammation in acute vs. chronic lung infection. Adapted from (16).

In contrast, *P.a.* in chronic CF infections grows as biofilm aggregates with cells encased and immobilized in an extracellular matrix, and undergoes extensive pathoadaptation to the CF lung environment (12, 17). CF-adapted *P.a.* strains are often non-motile, induce less cytotoxicity and frequently carry loss-of-function *lasR* variant alleles (11, 17, 18). Although LasR loss of function might dampen the direct tissue damage inflicted by LasR-regulated factors, our work indicates that protease-deficient *lasR* variants induce an exaggerated neutrophilic inflammation. Using a murine model of subacute lung infection with *P.a.* embedded in agar beads to approximate CF airway infections, we show that *lasR* variants induce higher levels of pro-inflammatory cytokines, increased airway

epithelial mICAM-1 expression as well as greater neutrophilic inflammation and lung pathology than wild-type infections. These results support our *in vitro* findings that the loss of secreted proteases in LasR-deficient variants induces a highly pro-inflammatory milieu, with accumulation of cytokines (e.g. IL-8, IL-6) and mICAM-1, leading to increased recruitment, transmigration and adhesion of neutrophils to the airway epithelium (1). We thus propose that in chronic infections such as those seen in CF airway infections, the loss of LasR-dependent secreted proteases fuels the exuberant and tissue-damaging neutrophilic inflammation.

LasR quorum sensing and LasR-regulated proteases are involved in complex interactions with host targets, with divergent implications on the pathogenesis of acute and chronic infections. While inhibitors of LasR and secreted proteases have been proposed as anti-virulence therapy for *P.a.* infections (19, 20), these therapies should be considered with caution, as they may further exacerbate inflammation and thus worsen the outcomes of chronic *P.a.* lung infections where excess neutrophils are major drivers of the disease pathology.

While we successfully demonstrated that increased mICAM-1 levels on AEC were caused by a lack of proteolytic degradation by LasR-regulated proteases, the exact contribution of the varying ICAM-1 levels to the observed neutrophil phenotypes remains to be elucidated in greater detail. It is possible that other adhesion molecules are affected by the stimulation with *P.a.* supernatants and that these molecules, along with the changes in ICAM-1 levels, modulate neutrophil adhesion. Other adhesion molecules involved in neutrophil adhesion to AEC, such as VCAM-1, may similarly be a target of proteolytic degradation by LasR-regulated proteases. Similarly, there may be a synergistic effect between higher ICAM-1 levels and greater secretion of pro-inflammatory molecules like IL-6 and IL-8 by AEC that may activate neutrophils and increase neutrophil adhesion (1). The exact contribution of ICAM-1 to this adhesion phenotype could be further investigated either by using ICAM-1 knock-out AEC or by pre-treating AEC with ICAM-1 neutralizing antibodies prior to supernatant stimulation. In a similar manner, we have demonstrated an association between increased ICAM-1 levels on the bronchial epithelium of mice infected with a *lasR* mutant strain and enhanced neutrophilic pulmonary inflammation, but causation remains to be shown. Pre-treatment with aerosolized ICAM-1 antibodies that would specifically target the lung epithelium and not the entire organism could definitively show the role of bronchial ICAM-1 in neutrophil recruitment and retention in this infection context.

5.3 Challenges and limitations of the intracellular *Pseudomonas aeruginosa* infection model

In this study, we established a model of chronic intracellular *P.a.* infections within AEC. Intracellular *P.a.* may be relevant not only in the context of pulmonary infections, but also in *P.a.* keratitis and UTIs (21-23). As a consequence, there is extensive literature on *P.a.*-corneal epithelial cell interactions (22-27). However, the results and methodology of these studies may not necessarily apply to AEC, as differences in bacterial intracellular survival have been observed across corneal and other types of epithelial cells (28). Furthermore, several studies investigated the internalization and survival of *P.a.* in epithelial cell lines (such as MDCK, HEK and HeLa) that are unlikely to be appropriate models for airway infections (29-31).

There are caveats and limitations to using immortalized epithelial cells. We chose to use a bronchial epithelial cell line rather than other respiratory epithelial cells such as the alveolar epithelial cell line A549 (32), since CF *P.a.* infections are typically observed in the conducting airways, whereas the respiratory airways are typically involved only in advanced infection stages (33). We primarily used BEAS-2B cells due to their high bacterial uptake and ease of culturing compared to another immortalized bronchial epithelial cell line or primary cells (34). However, we do recognize that BEAS-2B cells display increased replication rates compared to primary cells and cannot be polarized, both of which may affect host-microbe interactions. For instance, polarized AEC can express cilia, have a distinct apical and basolateral membrane and form tight junctions between neighboring cells, all of which may affect *P.a.* adherence, internalization and intracellular survival compared to submerged cells (35-37). In many ways, human primary AEC polarized at the air-liquid interface (ALI) represent the gold standard of *in vitro* infection models. However, primary cells also present limitations, such as significant experimental variability across donors and culture batches, limited access and supply of cells, potential microbial contamination, as well as lengthy procedures for polarization. As a consequence, human primary cells were not appropriate for screening large collections of bacterial strains, but were useful to validate key phenotypes in a more physiologically relevant model, as was done in chapter 4.

In addition to an *in vitro* model system, the development of an *in vivo* model would greatly advance the study of intracellular *P.a.*-host interactions in pulmonary infections. Although corneal infection models have successfully been established in mice and rats by the Fleiszig lab and a murine urinary tract infection model was recently published by the Hung lab (21, 22,

38, 39), animal models of *P.a.* chronic respiratory infections remain challenging, as discussed in detail in section 1.4.2.

Lastly, evidence of intracellular *P.a.* in human infected tissues still lacks in the literature. To address this knowledge gap, the Nguyen lab has recently analyzed human tissues from CF lung explants recovered at the time of lung transplantation (unpublished data). Using immunohistochemistry and immunofluorescence microscopy methods, intracellular *P.a.* was detected at a low bacterial burden per cell in a small population of ciliated AEC in sections of CF lung explant tissues from patients known to be chronically infected with *P.a.* prior to transplantation. Interestingly, intracellular *P.a.* was even detected by microscopy and culture of lysed tissues in one patient known for chronic *P.a.* infection but in whom sputum cultures were consistently negative for one year prior to transplantation. These data thus suggest that intracellular *P.a.* can be detected in the CF lung tissues, even in one instance where *P.a.* was no longer cultured from sputum cultures. The study of human CF lung explants could offer additional insights by comparing intracellular vs extracellular bacterial populations from the same sample or by establishing the 3D spatial distribution of bacteria using the MiPACT technique (40, 41). While these microscopy findings from the Nguyen lab represent the first evidence of intracellular *P.a.* in the CF bronchial epithelium, it is important to also recognize the limitations of this data. Microscopy analyses of CF lung explant tissues only offer a snapshot of end stage lung disease and do not provide insights into the dynamics of intracellular *P.a.* infections, the overall duration of bacterial persistence, or the contribution of intracellular *P.a.* to the persistent nature of chronic CF infections. Combining *in vitro* infection models using immortalized and primary AEC infections with *in vivo* pulmonary *P.a.* infections in animal models and human lung tissue analyses could provide a holistic approach to the study of intracellular *P.a.* within AEC.

5.4 *Pseudomonas aeruginosa* adaptations to the Cystic Fibrosis lung and their implications for intracellular survival

Intracellular *P.a.* within the bronchial epithelium of the CF lung may function as a reservoir, particularly during antibiotic eradication therapy using cell-impermeable antibiotics such as tobramycin. In this study, we observed significant heterogeneity in the ability of clinical isolates to survive intracellularly within AEC as well as in their cytotoxicity towards AEC, consistent with previous studies by our group and others that tested smaller collections of clinical CF isolates (34, 42). Although we observed that T3SS-deficient isolates showed

significantly elevated intracellular survival within AEC compared to T3SS-positive isolates, there was heterogeneity in intracellular survival among T3SS-deficient mutants from different strain backgrounds, ranging from 125% survival to 346% (Fig. 4.2), suggesting that additional bacterial factors likely contribute to the variability in survival across different *P.a.* strains. These results highlight the importance of testing defined mutants in different relevant strain backgrounds as phenotypes may be under- or overestimated if a single strain is tested.

Some studies suggest that T3SS-deficient strains display increased internalization into epithelial cells (26, 31), while our study demonstrates that T3SS-deficient strains show greater intracellular survival, and in some cases, proliferation within AEC compared to T3SS(+) isolates. These observations raise the question of whether T3SS-deficient strains commonly observed in chronic CF infections are more adapted towards an intracellular lifestyle, and contribute to the antibiotic refractory nature of chronic infections. Furthermore, the Fleiszig lab's finding that T3SS-deficient intracellular populations are refractory not only to cell-impermeable, but also cell-permeable antibiotic killing, may contribute to the phenotype we have observed (39). We thus speculate that loss of T3SS function may favor the survival of intracellular bacterial populations during periods of antibiotic treatment, leading to a fitness advantage for T3SS-deficient bacteria and their positive selection (43).

Here, we established that loss of T3SS function facilitates intracellular bacterial survival within AEC and that this phenotype was largely driven by a sub-population of AEC that permitted high intracellular bacterial proliferation of T3SS-negative strains, but was not observed in AEC infected with T3SS-positive strains. While some of these observations diverge from the literature (potential explanations are discussed in greater detail in chapter 4.5), future studies will be required to further examine the intracellular phenotype and gain a deeper understanding to explain how and why some of our observations differ from others. For example, an important future direction is to define the intracellular localization of T3SS-positive and -negative bacteria over time. The intracellular localization could be explored either by live cell imaging or at defined time points in fixed cells. Live cell imaging would offer the advantage of tracking single bacteria over time without the risk of missing important events between time points. Recombinant cell lines expressing fluorescently labelled markers of intracellular localization combined with fluorescence-tagged bacteria would enable the tracking and colocalization of the bacterial and host signals over time. However, the downside of live cell imaging is its very low throughput. On the other hand, imaging of fixed cells stained for intracellular localization

markers would be higher throughput, but may miss important dynamic events. A combination of both approaches where initial time points of interest are identified by live cell imaging and then confirmed by staining of fixed cells may be the most thorough and informative approach.

Bulk host RNA sequencing or dual host/pathogen RNA sequencing could also inform the next steps of this project. Host RNA sequencing could be used to explore the differential host response to T3SS-positive and -negative bacteria by extracting RNA from cells infected with the respective strains and sorted to enrich for those harboring intracellular bacteria. The Nguyen lab has taken the first steps towards establishing intracellular *P.a.* host RNA sequencing by optimizing the cell sorting methodology to recover cells harboring intracellular bacteria vs. uninfected cells from the same sample, the results of which are partly published in chapter 3. Follow up host RNA sequencing experiments could reveal which host cell death, antimicrobial defense or inflammatory pathways are upregulated by intracellular infection, offering insights into how the host cell restricts intracellular *P.a.* proliferation and whether the increased survival of T3SS-negative *P.a.* is due to a lack of detection by the host. Dual RNA sequencing would provide a powerful way to profile both host and bacterial transcriptomic responses but presents significant experimental hurdles, namely the isolation of sufficient bacterial RNA. While dual RNA sequencing has successfully been established for professional intracellular pathogens such as *S. enterica* Typhimurium (44), both the percentage of infected host cells as well as the bacterial burden per cell are significantly lower in AEC infected with *P.a.* compared to professional intracellular pathogens (34, 44, 45). As a consequence, additional bacterial RNA enrichment steps would likely be required. Follow-up studies will undoubtedly uncover new aspects of the complex intracellular *P.a.*/host interactions and will offer a deeper understanding of how T3SS-negative bacteria survive within AEC.

5.5 Conclusions

The clinical observation that patients infected with LasR-deficient strains display greater lung function decline (11) initially appeared paradoxical based on the presumed role of LasR in controlling bacterial virulence. However, a previous publication from our lab revealed that loss of LasR function was associated with increased IL-6 and IL-8 levels *in vitro* and *in vivo*, along with increased neutrophilic inflammation *in vivo*, which was attributed to a loss of proteolytic degradation by the LasR-regulated protease LasB (1). Here, we established that increased mICAM-1 levels on AEC also contributes to this phenotype, where higher IL-6 and IL-8 levels result in the recruitment and activation of neutrophils, while increased epithelial mICAM-1

levels may facilitate neutrophil transepithelial migration and neutrophil retention in the lung lumen. As a consequence, our findings extend a growing body of literature demonstrating the plethora of mechanisms by which LasR-regulated proteases interfere with innate immune signaling during acute infection stages. More importantly, our work highlights their implication in lung inflammation and disease pathogenesis when loss of key LasR-regulated virulence factors occurs during chronic infection stages. The excessive inflammation observed during chronic *P.a.* infection may not only be driven by the large bacterial abundance in the airways, but by the emergence of *P.a.* variants such as LasR-deficient variants.

Our model of long-term intracellular *P.a.* survival within AEC allowed us to screen a large collection of clinical *P.a.* isolates, to correlate intracellular survival with cytotoxicity and T3SS activity, and thus to identify loss of T3SS function as a major driver of intracellular survival among clinical isolates. These finding suggest that T3SS-deficient isolates, which are commonly recovered in chronic infections, could be more adapted towards an intracellular lifestyle. The implications are manifold: If *P.a.* adapts towards an increased ability to survive within AEC, this could be a mechanism which contributes to the persistent nature of *P.a.* chronic infection, in addition to biofilm formation and antibiotic resistance. While the loss of T3SS function is widely speculated to be a result of the antibody response to T3SS components, clearing T3SS-positive isolates (43), the enhanced intracellular survival of T3SS-deficient bacteria may represent an additional selective force. Finally, our data further raises questions regarding the potential use of T3SS-targeting antibodies (46-48). While these antibodies may enhance antibiotic eradication therapy efficacy during early infection stages by enhancing immune cell killing of *P.a.*, inhibiting the T3SS during intermittent infection stages may accelerate the transition to a chronic infection by facilitating the formation of an intracellular *P.a.* reservoir.

Together, our findings show how the loss of two key virulence factors that are important during acute infection stages yet dispensable during chronic infections, may paradoxically contribute to deleterious lung inflammation and ineffective pathogen clearance. Furthermore, our observations imply that targeting the LasR and T3S systems during chronic infection in which the infecting isolate still has a wild-type phenotype should be carefully considered, as it may have unintended negative consequences for the patient's lung function and may even impair antibiotic efficacy on *P.a.*

5.6 References

1. LaFayette SL, Houle D, Beaudoin T, Wojewodka G, Radzioch D, Hoffman LR, et al. Cystic fibrosis-adapted Pseudomonas aeruginosa quorum sensing lasR mutants cause hyperinflammatory responses. Sci Adv. 2015;1(6).

2. Sörensen M, Kantorek J, Byrnes L, Boutin S, Mall MA, Lasitschka F, et al. Pseudomonas aeruginosa Modulates the Antiviral Response of Bronchial Epithelial Cells. Frontiers in Immunology. 2020;11.

3. Laarman AJ, Bardoel BW, Ruyken M, Fernie J, Milder FJ, van Strijp JA, et al. Pseudomonas aeruginosa alkaline protease blocks complement activation via the classical and lectin pathways. J Immunol. 2012;188(1):386-93.

4. Leidal KG, Munson KL, Johnson MC, Denning GM. Metalloproteases from Pseudomonas aeruginosa degrade human RANTES, MCP-1, and ENA-78. J Interferon Cytokine Res. 2003;23(6):307-18.

5. Golovkine G, Faudry E, Bouillot S, Voulhoux R, Attrée I, Huber P. VE-cadherin cleavage by LasB protease from Pseudomonas aeruginosa facilitates type III secretion system toxicity in endothelial cells. PLoS Pathog. 2014;10(3):e1003939.

6. Yang J, Zhao H-L, Ran L-Y, Li C-Y, Zhang X-Y, Su H-N, et al. Mechanistic Insights into Elastin Degradation by Pseudolysin, the Major Virulence Factor of the Opportunistic Pathogen Pseudomonas aeruginosa. Scientific Reports. 2015;5(1):9936.

7. Li J, Ramezanpour M, Fong SA, Cooksley C, Murphy J, Suzuki M, et al. Pseudomonas aeruginosa Exoprotein-Induced Barrier Disruption Correlates With Elastase Activity and Marks Chronic Rhinosinusitis Severity. Frontiers in Cellular and Infection Microbiology. 2019;9.

8. Heck LW, Morihara K, McRae WB, Miller EJ. Specific cleavage of human type III and IV collagens by Pseudomonas aeruginosa elastase. Infect Immun. 1986;51(1):115-8.

9. Leduc D, Beaufort N, de Bentzmann S, Rousselle JC, Namane A, Chignard M, et al. The Pseudomonas aeruginosa LasB metalloproteinase regulates the human urokinase-type plasminogen activator receptor through domain-specific endoproteolysis. Infect Immun. 2007;75(8):3848-58.

10. Alcorn JF, Wright JR. Degradation of pulmonary surfactant protein D by Pseudomonas aeruginosa elastase abrogates innate immune function. J Biol Chem. 2004;279(29):30871-9.

11. Hoffman LR, Kulasekara HD, Emerson J, Houston LS, Burns JL, Ramsey BW, et al. Pseudomonas aeruginosa lasR mutants are associated with cystic fibrosis lung disease progression. J Cyst Fibros. 2009;8(1):66-70.

12. Folkesson A, Jelsbak L, Yang L, Johansen HK, Ciofu O, Høiby N, et al. Adaptation of Pseudomonas aeruginosa to the cystic fibrosis airway: an evolutionary perspective. Nat Rev Microbiol. 2012;10(12):841-51.

13. Lorè NI, Cigana C, De Fino I, Riva C, Juhas M, Schwager S, et al. Cystic fibrosis-niche adaptation of Pseudomonas aeruginosa reduces virulence in multiple infection hosts. PLoS One. 2012;7(4):e35648.

14. Lelong E, Marchetti A, Simon M, Burns JL, van Delden C, Köhler T, et al. Evolution of Pseudomonas aeruginosa virulence in infected patients revealed in a Dictyostelium discoideum host model. Clin Microbiol Infect. 2011;17(9):1415-20.

15. Lesprit P, Faurisson F, Join-Lambert O, Roudot-Thoraval F, Foglino M, Vissuzaine C, et al. Role of the quorum-sensing system in experimental pneumonia due to Pseudomonas aeruginosa in rats. Am J Respir Crit Care Med. 2003;167(11):1478-82.

16. Hennemann LC, Nguyen D. LasR-regulated proteases in acute vs. chronic lung infection: a double-edged sword. Microb Cell. 2021;8(7):161-3.

17. Faure E, Kwong K, Nguyen D. Pseudomonas aeruginosa in Chronic Lung Infections: How to Adapt Within the Host? Frontiers in Immunology. 2018;9.

18. Smith EE, Buckley DG, Wu Z, Saenphimmachak C, Hoffman LR, D'Argenio DA, et al. Genetic adaptation by Pseudomonas aeruginosa to the airways of cystic fibrosis patients. Proc Natl Acad Sci U S A. 2006;103(22):8487-92.

19. O'Brien KT, Noto JG, Nichols-O'Neill L, Perez LJ. Potent Irreversible Inhibitors of LasR Quorum Sensing in Pseudomonas aeruginosa. ACS Med Chem Lett. 2015;6(2):162-7.

20. O'Loughlin CT, Miller LC, Siryaporn A, Drescher K, Semmelhack MF, Bassler BL. A quorum-sensing inhibitor blocks Pseudomonas aeruginosa virulence and biofilm formation. Proceedings of the National Academy of Sciences. 2013;110(44):17981-6.

21. Penaranda C, Chumbler NM, Hung DT. Dual transcriptional analysis reveals adaptation of host and pathogen to intracellular survival of Pseudomonas aeruginosa associated with urinary tract infection. PLoS Pathog. 2021;17(4):e1009534.

22. Fleiszig SM, Zaidi TS, Fletcher EL, Preston MJ, Pier GB. Pseudomonas aeruginosa invades corneal epithelial cells during experimental infection. Infect Immun. 1994;62(8):3485-93.

23. Evans DJ, Maltseva IA, Wu J, Fleiszig SM. Pseudomonas aeruginosa internalization by corneal epithelial cells involves MEK and ERK signal transduction proteins. FEMS Microbiol Lett. 2002;213(1):73-9.

24. Fleiszig SM, Zaidi TS, Pier GB. Pseudomonas aeruginosa invasion of and multiplication within corneal epithelial cells in vitro. Infect Immun. 1995;63(10):4072-7.

25. Fleiszig SM, Zaidi TS, Preston MJ, Grout M, Evans DJ, Pier GB. Relationship between cytotoxicity and corneal epithelial cell invasion by clinical isolates of Pseudomonas aeruginosa. Infect Immun. 1996;64(6):2288-94.

26. Cowell BA, Chen DY, Frank DW, Vallis AJ, Fleiszig SM. ExoT of cytotoxic Pseudomonas aeruginosa prevents uptake by corneal epithelial cells. Infect Immun. 2000;68(1):403-6.

27. Zaidi TS, Fleiszig SM, Preston MJ, Goldberg JB, Pier GB. Lipopolysaccharide outer core is a ligand for corneal cell binding and ingestion of Pseudomonas aeruginosa. Invest Ophthalmol Vis Sci. 1996;37(6):976-86.

28. Kroken AR, Gajenthra Kumar N, Yahr TL, Smith BE, Nieto V, Horneman H, et al. Exotoxin S secreted by internalized Pseudomonas aeruginosa delays lytic host cell death. PLoS Pathog. 2022;18(2):e1010306.

29. Kierbel A, Gassama-Diagne A, Mostov K, Engel JN. The phosphoinositol-3-kinase-protein kinase B/Akt pathway is critical for Pseudomonas aeruginosa strain PAK internalization. Mol Biol Cell. 2005;16(5):2577-85.

30. Sana TG, Baumann C, Merdes A, Soscia C, Rattei T, Hachani A, et al. Internalization of Pseudomonas aeruginosa Strain PAO1 into Epithelial Cells Is Promoted by Interaction of a T6SS Effector with the Microtubule Network. mBio. 2015;6(3):e00712-15.

31. Ha U, Jin S. Growth phase-dependent invasion of Pseudomonas aeruginosa and its survival within HeLa cells. Infect Immun. 2001;69(7):4398-406.

32. Rao L, De La Rosa I, Xu Y, Sha Y, Bhattacharya A, Holtzman MJ, et al. Pseudomonas aeruginosa survives in epithelia by ExoS-mediated inhibition of autophagy and mTOR. EMBO Rep. 2021;22(2):e50613.

33. Moore JE, Mastoridis P. Clinical implications of Pseudomonas aeruginosa location in the lungs of patients with cystic fibrosis. Journal of Clinical Pharmacy and Therapeutics. 2017;42(3):259-67.

34. Malet JK, Hennemann LC, Hua EML, Faure E, Waters V, Rousseau S, et al. A Model of Intracellular Persistence of Pseudomonas aeruginosa in Airway Epithelial Cells. Cellular Microbiology. 2022;2022:5431666.

35. Kierbel A, Gassama-Diagne A, Rocha C, Radoshevich L, Olson J, Mostov K, et al. Pseudomonas aeruginosa exploits a PIP3-dependent pathway to transform apical into basolateral membrane. J Cell Biol. 2007;177(1):21-7.

36. Plotkowski MC, Chevillard M, Pierrot D, Altemayer D, Zahm JM, Colliot G, et al. Differential adhesion of Pseudomonas aeruginosa to human respiratory epithelial cells in primary culture. J Clin Invest. 1991;87(6):2018-28.

37. Plotkowski MC, de Bentzmann S, Pereira SH, Zahm JM, Bajolet-Laudinat O, Roger P, et al. Pseudomonas aeruginosa internalization by human epithelial respiratory cells depends on cell differentiation, polarity, and junctional complex integrity. Am J Respir Cell Mol Biol. 1999;20(5):880-90.

38. Tam C, Mun JJ, Evans DJ, Fleiszig SMJ. The Impact of Inoculation Parameters on the Pathogenesis of Contact Lens–Related Infectious Keratitis. Investigative Ophthalmology & Visual Science. 2010;51(6):3100-6.

39. Kumar NG, Nieto V, Kroken AR, Jedel E, Grosser MR, Hallsten ME, et al. Pseudomonas aeruginosa can diversify after host cell invasion to establish multiple intracellular niches. bioRxiv. 2022:2022.10.07.511388.

40. DePas WH, Starwalt-Lee R, Sambeek LV, Kumar SR, Gradinaru V, Newman DK. Exposing the Three-Dimensional Biogeography and Metabolic States of Pathogens in Cystic Fibrosis Sputum via Hydrogel Embedding, Clearing, and rRNA Labeling. mBio. 2016;7(5):e00796-16.

41. Dar D, Dar N, Cai L, Newman DK. Spatial transcriptomics of planktonic and sessile bacterial populations at single-cell resolution. Science. 2021;373(6556):eabi4882.

42. Del Mar Cendra M, Torrents E. Differential adaptability between reference strains and clinical isolates of Pseudomonas aeruginosa into the lung epithelium intracellular lifestyle. Virulence. 2020;11(1):862-76.

43. Jain M, Ramirez D, Seshadri R, Cullina JF, Powers CA, Schulert GS, et al. Type III secretion phenotypes of Pseudomonas aeruginosa strains change during infection of individuals with cystic fibrosis. J Clin Microbiol. 2004;42(11):5229-37.

44. Westermann AJ, Förstner KU, Amman F, Barquist L, Chao Y, Schulte LN, et al. Dual RNA-seq unveils noncoding RNA functions in host-pathogen interactions. Nature. 2016;529(7587):496-501.

45. Castanheira S, García-Del Portillo F. Salmonella Populations inside Host Cells. Front Cell Infect Microbiol. 2017;7:432.

46. Milla CE, Chmiel JF, Accurso FJ, VanDevanter DR, Konstan MW, Yarranton G, et al. Anti-PcrV antibody in cystic fibrosis: a novel approach targeting Pseudomonas aeruginosa airway infection. Pediatr Pulmonol. 2014;49(7):650-8.

47. Ali SO, Yu XQ, Robbie GJ, Wu Y, Shoemaker K, Yu L, et al. Phase 1 study of MEDI3902, an investigational anti-Pseudomonas aeruginosa PcrV and Psl bispecific human monoclonal antibody, in healthy adults. Clin Microbiol Infect. 2019;25(5):629.e1-.e6.

48. Warrener P, Varkey R, Bonnell JC, DiGiandomenico A, Camara M, Cook K, et al. A novel anti-PcrV antibody providing enhanced protection against Pseudomonas aeruginosa in multiple animal infection models. Antimicrob Agents Chemother. 2014;58(8):4384-91.